Exploring the cooperation and targetability of *CRLF2* and *HMGN1* in Down Syndrome Acute Lymphoblastic Leukaemia

Elyse Page

B.Sc (Advanced) Biochemistry and Genetics

A thesis submitted in fulfilment of the

Doctor of Philosophy Degree in Sciences

Department of Molecular and Cellular Biology

School of Biological Sciences

University of Adelaide, Australia

January 2021

This page has been intentionally left blank

Table of Contents

Abstract

Cytokine receptor like factor 2 (*CRLF2*) is dysregulated in approximately 50% of high-risk and 60% of Down Syndrome (DS) acute lymphoblastic leukaemia (ALL) patients. *CRLF2* is most commonly rearranged in DS-ALL patients via a 320 KB deletion in the pseudoautosomal region of the X/Y chromosome resulting in the *P2RY8-CRLF2* gene fusion, or can become mutated; *CRLF2* p.F232C. Dysregulation of *CRLF2* results in the upregulation of thymic stromal lymphopoietin receptor (TSLPR) and JAK/STAT, PI3K and Ras signalling pathways and is associated with poor survival outcomes. Constituents of these signalling pathways are targetable with small molecule inhibitors. The increased frequency of the *P2RY8-CRLF2* fusion in DS-ALL patients indicates a predisposition to the development of this fusion, however, the genetic basis is unknown and warrants further investigation.

Many groups have postulated the involvement of the high mobility nucleosome binding protein 1 (*HMGN1*) in DS-ALL, however, this body of work identifies its role and cooperation with *P2RY8-CRLF2.* Using *in vivo* and *in vitro* models, as well as novel CRISPR/Cas9 modelling, the role of *HMGN1* in the development, proliferation and persistence of *CRLF2* rearranged ALL is demonstrated here, for the first time.

The trisomy 21 human xenograft *HMGN1* knockout (KO) model presented here demonstrates that *HMGN1* KO in *CRLF2* p.F232C cells halts leukaemic progression in mice, reverses the leukaemic phenotype and increases murine survival outcomes. This indicates that *HMGN1* has driver potential in DS-ALL. Significantly, *HMGN1* overexpression occurs due to trisomy 21, suggesting DS patients who acquire *P2RY8-CRLF2* may not require a 'second hit' for leukaemic transformation.

Using *in vitro* Ba/F3 and unique CRISPR/Cas9-generated *P2RY8-CRLF2* models, the cooperation between *P2RY8-CRLF2* and *HMGN1* was also confirmed. Leukaemic transformation was achieved via the co-expression of *P2RY8-CRLF2* and *HMGN1* in Ba/F3 cells. To support this finding, modelling *HMGN1* overexpression prior to generating the endogenous *P2RY8-CRLF2* fusion with CRISPR/Cas9 increased the efficiency of fusion development.

The identification of *P2RY8-CRLF2* and *HMGN1* cooperation could positively affect the treatment of patients with DS-ALL, *CRLF2r* or +21 and lead to better treatment outcomes for patients who currently have poor overall survival. Furthermore, the mechanism of leukaemic transformation in *P2RY8-CRLF2* and *HMGN1* co-expressing cells was identified in both the Ba/F3 model and CRISPR *P2RY8-CRLF2* model via increased *CRLF2* expression and an upregulation of TSLPR, as well as JAK/STAT signalling and increased gene activation marks via HMGN1 nucleosome remodelling. A synergistic combination therapy comprising the JAK2 inhibitor, fedratinib, and de-methylase inhibitor, GSK-J4, was identified to target *P2RY8-CRLF2* and *HMGN1* co-expressing cells, however, *CRLF2* p.F232C cells were less sensitive to this therapy and activated different signalling pathways. Furthermore, also presented here, is an additional combination therapy of fedratinib and the MEK inhibitor, selumetinib, to synergistically target cells harbouring the aggressive *CRLF2* p.F232C mutation.

In summary, this thesis provides critical insight into the development and persistence of *CRLF2* rearranged DS-ALL. For the first time, the important role of *HMGN1* in the proliferation and survival of DS-ALL cells and cooperation with *P2RY8-CRLF2* for

increased cell signalling has been identified. These findings suggest HMGN1 is a potential target for a precision treatment approach in DS-ALL. Two synergistic combination therapies targeting *CRLF2* and/or *HMGN1* co-expressing cells, as well as an endogenous model of *P2RY8-CRLF2* that provides a clinically relevant tool for identification of cooperating genes have been produced. Together, this body of work describes the leukaemic potential of *HMGN1* and significant understanding of its cooperation with *P2RY8-CRLF2*. Findings from this thesis present an opportunity to reduce the toxicity DS-ALL patients experience from current treatment regimens and improve outcomes in this high-risk group of patients.

Declaration of originality

I certify that this work contains no material which has been accepted for the award of any other degree or diploma in my name, in any university or other tertiary institution and, to the best of my knowledge and belief, contains no material previously published or written by another person, except where due reference has been made in the text. In addition, I certify that no part of this work will, in the future, be used in a submission in my name, for any other degree or diploma in any university or other tertiary institution without the prior approval of the University of Adelaide and where applicable, any partner institution responsible for the joint-award of this degree.

I also give permission for the digital version of my thesis to be made available on the web, via the University's digital research repository, the Library Search and also through web search engines, unless permission has been granted by the University to restrict access for a period of time.

I acknowledge the support I have received for my research through the provision of an Australian Government Research Training Program Scholarship.

Elyse Chenae Page

February 2021

Acknowledgments

First and foremost, the biggest thank you goes to Professor Deb White. You gave me the most wonderful opportunity to start an M.Phil with your incredible lab when the program was just starting out. The journey to upgrading an M.Phil to a PhD was daunting but you were with me every step of the way and believed in me and my potential to become a great researcher. Deb, you are more than a supervisor and a mentor and I am so lucky to have had you as a role model throughout my PhD. You constantly inspire me and I wouldn't have achieved as much as I have in the last three and a half years without you as a supervisor. Dr Sue Heatley, thank you for being my go-to person in and out of the lab. You are always in my corner and pushing me to reach my goals and helping me to get there. I can't thank you enough for the support you have shown me, whether it be about my data or personal matters. And finally, Professor Paul Thomas, thank you for only ever being an email away and for being the CRISPR guru I needed to get through this PhD. A lot of CRISPR approaches were tried in the first 18 months of this project, so thank you for your patience and extensive knowledge.

Of course, the Melissa White Laboratory (MWL) is filled with amazing people, particularly the rest of the ALL team, Dr Barbara McClure, Dr Laura Eadie, Caitlin Schultz and Jacqui Rehn. Thank you all for your fabulous insights into my project, support and guidance along the way and for making ALL meetings feel like a female powerhouse. I'd like to thank Dr Tessa Sadras, while you weren't in the lab during my PhD, you were a big part of me choosing the MWL during my undergraduate placement. A big thank you to Verity Saunders for your amazing organisational skills and keeping the lab running so, so smoothly. Thank you for supporting me and of course, sharing your amazing recipes with me to let off my PhD stress through baking. To Bronwyn

Cambareri and Stephanie Arbon, this PhD wouldn't have been possible without the two of you and all of your behind the scenes work, so a big thank you to you both. To Randall Grose, a lot of flow cytometry is in this thesis and it wouldn't have been possible without your guidance in the Flow Core, and of course the long nights sorting or analysing were made all the better with the Flow Core music and disco lights. And to the MWL students – Nadia, Charlotte, Paniz, Michelle and Steph, a huge thank you for going through all of this with me, the late nights and weekends spent in the lab wouldn't have been the same without you guys. Without this PhD, I wouldn't have met one of my best friends, future Dr Caitlin Skinner. Thank you for doing your honours year with MWL, it was the best year of my PhD and our croissant dates always prepared me for the rest of the lab day!

A big thank you goes to my friends outside of the lab, I truly appreciate your support and letting me rant about science – your excitement is always genuine even though I'm speaking another language. This PhD wouldn't have been possible without my amazing family. Mum and Mick, Dad and Suzanne, and my brother, Ben. To my parents, thank you for instilling me with the work ethic and courage to begin this journey, teaching me to shoot for my dreams and for being my inspiration to do the amazing work that is leukaemia research. You are my biggest fans and the strongest support system.

And of course, I have saved the best 'til last. My soul mate and fiancée, (soon-to-be Dr) Andy Ung. You have been there for me throughout undergrad when I applied for my PhD, celebrated with me when my upgrade went through, listened to the endless practice talks, read my papers, and most importantly given me the love and confidence I needed to achieve great results over the last few years. I cannot thank you enough for

the unwavering support you have given me and ensuring my passion for my work stays strong. Thank you for always knowing when I get home if we need to order in churros, put on re-runs of my favourite TV series', or put a bottle of champagne in the fridge. Andy, you have made this PhD journey truly enjoyable and with all seriousness, the best few years of my life so far and I can't wait to continue my academic journey with you by my side.

Finally, thank you to you, the reader of this thesis. I hope that when you read this, you can feel the love, hard work and joy I have put into it.

Publications

Page EC, Heatley SL, Thomas PQ, White DL, 2021. Unique modelling of *P2RY8-CRLF2* using CRISPR/Cas9 reveals *HMGN1* as a predisposing factor in Down Syndrome Acute Lymphoblastic Leukemia. *Submitted to Journal Cellular and Molecular Medicine.*

Page EC, Heatley SL, Eadie LJ, McClure BJ, Yeung DT, Hughes TP, Thomas PQ, White DL, 2021. *HMGN1* is necessary for leukemic cell transformation and proliferation in *CRLF2* related Down Syndrome leukemia. *Submitted to Journal of Experimental Medicine.*

Page EC, White DL, 2020. Understanding the Role of Chromosome 21 for precision treatment in Down Syndrome Acute Lymphoblastic Leukaemia. *Journal of Alzheimer's Disease and Parkinsonism,* 11, 1.

Page EC, Heatley SL, Thomas PQ, White DL, 2020. Inducible Knockout of *HMGN1* in an *In Vivo* xenograft Model Reduces Down Syndrome Leukemic Burden and Increases Survival Outcomes. *Blood*, 136. Doi: 10.1182/blood-2020-138620

Page EC, Heatley S L, Yeung DT, Thomas PQ, & White DL, 2019. A novel role for *HMGN1* in Down Syndrome Acute Lymphoblastic Leukaemia. *Blood*, 134, 1462 – 1462. Doi: 10.1182/blood-2019-126244.

Page EC, Heatley SL, Yeung DT, Thomas PQ, White DL, 2018. Precision medicine approaches may be the future for *CRLF2* rearranged Down Syndrome Acute Lymphoblastic Leukaemia. *Cancer Letters,* 432, 69-74.

Conference Presentations

Dec 2020 American Society of Haematology, Orlando, CA, USA

Poster Presentation

Page EC, Heatley SL, Thomas PQ, White DL (2020). *Inducible knockout of HMGN1 in an in vivo xenograft model reduces Down Syndrome Leukaemic burden and increases survival outcomes*

Sep 2020 Precision Medicine Theme Seminar, Adelaide, SA, AUS

Oral Presentation

Page EC, Heatley SL, Thomas PQ, White DL (2020). *Using an in vivo CRISPR/Cas9 model to explore Down Syndrome Acute Lymphoblastic Leukaemia*

Jul 2020 HSANZ Blood Club, via zoom, Sydney NSW, AUS

Oral Presentation

Page EC, Heatley SL, Thomas PQ, White DL (2019). *Using an in vivo CRISPR/Cas9 model to explore Down Syndrome Acute Lymphoblastic Leukaemia*

July 2020 Adelaide University science postgraduate symposium: 3 Minute Thesis, Adelaide, SA, AUS

Oral Presentation

Page EC, Heatley SL, Thomas PQ, White DL (2019). *Leukaemia; a poisonous butterfly*

Mar 2020 New Directions in Leukaemia Research, Brisbane, QLD, AUS (postponed due to COVID-19)

Poster Presentation

Page EC, Heatley SL, Thomas PQ, White DL (2020). *Knockout of HMGN1 in vivo reduces CRLF2r Down Syndrome Acute Lymphoblastic Leukaemia burden*

Dec 2019 American Society of Haematology, Orlando, FL, USA

Poster Presentation

Page EC, Heatley SL, Yeung, DT, Thomas PQ, White DL (2019). *A novel role for HMGN1 in Down Syndrome Acute Lymphoblastic Leukaemia*

Oct 2019 SAHMRI Annual Scientific Meeting, Adelaide, SA, AUS

Oral Presentation

Page EC, Heatley SL, Thomas PQ, White DL (2019). *Down Syndrome Acute Lymphoblastic Leukaemia: An Inside Job*

July 2019 Cancer in S.A Translational Meeting, Adelaide, SA, AUS

Oral Presentation

Page EC, Heatley SL, Thomas PQ, White DL (2019). *Exploring the leukaemic potential of HMGN1 in CRLF2r Down Syndrome Acute Lymphoblastic Leukaemia*

July 2019 Adelaide University science postgraduate symposium: 3 Minute Thesis, Adelaide, SA, AUS

Oral Presentation

Page EC, Heatley SL, Thomas PQ, White DL (2019). *Down Syndrome Acute Lymphoblastic Leukaemia: An Inside Job*

June 2019 Australian Society for Medical Research (ASMR) SA Meeting, Adelaide, SA, AUS

Oral Presentation

Page EC, Heatley SL, Thomas PQ, White DL (2019). *Exploring the leukaemic potential of HMGN1 in CRLF2r Down Syndrome Acute Lymphoblastic Leukaemia*

June 2019 Australian and New Zealand Children's Haematology/Oncology Group, Christchurch, CAN, NZ

Oral Presentation

Page EC, Heatley SL, Thomas PQ, White DL (2019). *Exploring the leukaemic potential of HMGN1 in CRLF2r Down Syndrome Acute Lymphoblastic Leukaemia*

Oct 2018 SAHMRI Annual Scientific Meeting, Adelaide, SA, AUS

Poster Presentation

Page EC, Heatley SL, Thomas PQ, White DL (2018). *Targeted therapies for CRLF2 rearranged Down Syndrome Acute Lymphoblastic Leukaemia*.

July 2018 Adelaide University science postgraduate symposium, Adelaide, SA, AUS

Poster Presentation

Page EC, Heatley SL, Thomas PQ, White DL (2018). *Targeted therapies for CRLF2 rearranged Down Syndrome Acute Lymphoblastic Leukaemia*.

June 2018 Australian Society for Medical Research (ASMR) SA Meeting, Adelaide, SA, AUS

Oral Presentation

Page EC, Heatley SL, Thomas PQ, White DL (2018). *Precision medicine approaches may be the future for CRLF2 rearranged Down Syndrome Acute Lymphoblastic Leukaemia.*

Scholarships and Awards

3MT Finalist, Faculty of Science, 2020

Winner of the school of biological science 3MT and runner up in the Faculty of Science 3MT

Upgrade to PhD scholarship, Australian Government, 2018

Support for the educational and professional development of researchers undertaking a PhD through Australian higher education providers.

Chapter 1:

Introduction

Statement of Authorship

Title of Paper	Precision medicine approaches may be the future for *CRLF2* rearranged Down Syndrome Acute Lymphoblastic Leukaemia patients
Publication Status	☐ Published ☒ Accepted for Publication ☐ Submitted for Publication ☐ Unpublished and Unsubmitted work written in manuscript style
Publication Details	Page EC, Heatley SL, Yeung DT, Thomas PQ, White DL. Precision medicine approaches may be the future for *CRLF2* rearranged Down Syndrome Acute Lymphoblastic Leukaemia patients. *Cancer letters*. Sep 28 2018;432:69-74. doi:10.1016/j.canlet.2018.05.045

Principal Author

Name of Principal Author (Candidate)	Elyse Page		
Contribution to the Paper	Conducted literature review and wrote the manuscript		
Overall percentage (%)	95%		
Certification:	This paper reports on original research I conducted during the period of my Higher Degree by Research candidature and is not subject to any obligations or contractual agreements with a third party that would constrain its inclusion in this thesis. I am the primary author of this paper.		
Signature		Date	23/2/21

Co-Author Contributions

By signing the Statement of Authorship, each author certifies that:

i. the candidate's stated contribution to the publication is accurate (as detailed above);

ii. permission is granted for the candidate in include the publication in the thesis; and

iii. the sum of all co-author contributions is equal to 100% less the candidate's stated contribution.

Name of Co-Author	Susan Heatley		
Contribution to the Paper	Supervised, and edited the manuscript		
Signature		Date	23-2-21

Name of Co-Author	David Yeung		
Contribution to the Paper	Edited the manuscript		
Signature		Date	24 FEB 2021

Name of Co-Author	Paul Thomas		
Contribution to the Paper	Supervised, and edited the manuscript		
Signature		Date	24/2/2021

Name of Co-Author	Deborah White		
Contribution to the Paper	Supervised, and edited the manuscript		
Signature		Date	25/2/2021

Cancer Letters 432 (2018) 69–74

Contents lists available at ScienceDirect

Cancer Letters

journal homepage: www.elsevier.com/locate/canlet

Mini-review

Precision medicine approaches may be the future for *CRLF2* rearranged Down Syndrome Acute Lymphoblastic Leukaemia patients

Elyse C. Page[a,c], Susan L. Heatley[a,b,d,e], David T. Yeung[a,b,h], Paul Q. Thomas[a,b], Deborah L. White[a,b,c,d,e,f,g,*]

[a] Cancer Theme, South Australian Health & Medical Research Institute, Adelaide, SA, Australia
[b] Discipline of Medicine, University of Adelaide, Adelaide, SA, Australia
[c] School of Biological Sciences, University of Adelaide, Adelaide, SA, Australia
[d] Australian and New Zealand Children's Haematology/Oncology Group (ANZCHOG), Australia
[e] The Kids' Cancer Project, Australia
[f] Australian Genomic Health Alliance (AGHA), Australia
[g] Discipline of Paediatrics, University of Adelaide, Adelaide, SA, Australia
[h] Haematology Department, SA Pathology, Australia

ABSTRACT

Breakthrough studies over the past decade have uncovered unique gene fusions implicated in acute lymphoblastic leukaemia (ALL). The critical gene, cytokine receptor-like factor 2 (*CRLF2*), is rearranged in 5–16% of B-ALL, comprising 50% of Philadelphia-like ALL and cooperates with genomic lesions in the Jak, Mapk and Ras signalling pathways. Children with Down Syndrome (DS) have a predisposition to developing *CRLF2* rearranged-ALL which is observed in 60% of DS-ALL patients. These patients experience a poor survival outcome. Mutations of genes involved in epigenetic regulation are more prevalent in DS-ALL patients than non-DS ALL patients, highlighting the potential for alternative treatment strategies. DS-ALL patients also suffer greater treatment-related toxicity from current ALL treatment regimens compared to non-DS-ALL patients. An increased gene dosage of critical genes on chromosome 21 which have roles in purine synthesis and folate transport may contribute. As the genomic landscape of DS-ALL patients is different to non-DS-ALL patients, targeted therapies for individual lesions may improve outcomes. Therapeutically targeting each rearrangement with targeted or combination therapy that will perturb the transforming signalling pathways will likely improve the poor survival rates of this subset of patients.

1. Introduction to Down Syndrome Acute Lymphoblastic Leukaemia

Children with Down Syndrome (DS) have a 20-fold increased risk of developing acute lymphoblastic leukaemia (ALL); the most common paediatric cancer worldwide, and are 150 times more likely to develop acute myeloid leukaemia (AML) by the age of 5 years [1–3]. DS-ALL patients are grouped into a high-risk treatment category as they have poorer survival outcomes and experience higher treatment related toxicity compared to non-DS-ALL patients [2,4]. Common good-risk cytogenetic alterations (such as *ETV6-RUNX1*) present in non-DS-ALL patients do not frequently occur. Instead, higher-risk fusions that are often associated with a more aggressive leukaemic phenotype, including rearrangements of cytokine receptor like factor 2 (*CRLF2r*), are often observed [5,6]. This may contribute to the higher rate of relapse in DS-ALL compared to non-DS-ALL patients. A better understanding of the genomic landscape of DS-ALL patients will lead to the investigation of targeted therapies. ALL can be grouped into different subsets based on driving genomic lesions, and a current focus of treatment in ALL is the use of rationally selected tyrosine kinase inhibitors (TKI) and small molecule inhibitors in the setting of clinical trials [7]. The impact of these therapies has not been extensively studied in the context of DS-ALL, however, the successful implementation of such molecules in a precision medicine approach could potentially result in the reduction of toxic chemotherapeutic elements.

* Corresponding author. Cancer Theme, South Australian Health & Medical Research Institute, Adelaide, SA, Australia.
E-mail addresses: elyse.page@sahmri.com (E.C. Page), sue.heatley@sahmri.com (S.L. Heatley), david.yeung@adelaide.edu.au (D.T. Yeung), paul.thomas@adelaide.edu.au (P.Q. Thomas), deborah.white@sahmri.com (D.L. White).

https://doi.org/10.1016/j.canlet.2018.05.045
Received 2 March 2018; Received in revised form 16 May 2018; Accepted 28 May 2018
0304-3835/

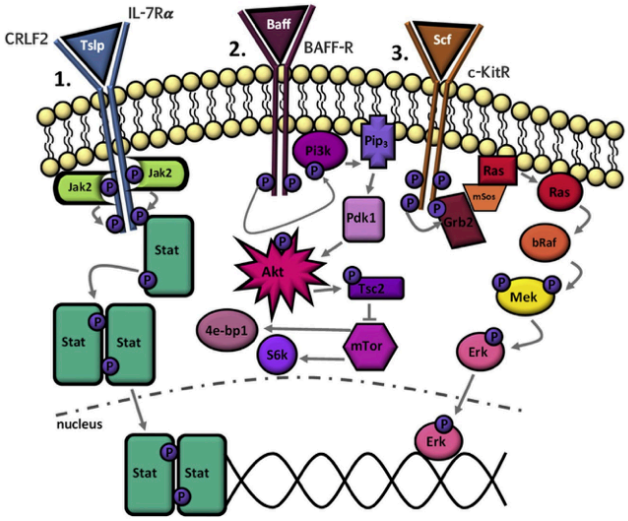

Fig. 1. 1) Thymic stromal lymphopoietin receptor signalling cascade where Crlf2 and the IL-7 receptor alpha chain (IL7rα) heterodimerise resulting in the functional receptor for thymic stromal lymphopoietin (Tslp) initiating the Jak/Stat pathway. 2) The phosphoinositide 3-kinase (Pi3k) signalling pathway initiated by B-cell activating factor binding (Baff) binding to its receptor. 3) The Ras signalling pathway activated by stem cell factor (Scf) binding to c-kit. All three pathways lead to the activation of transcription of FOXOs, Bcl-2, Cyclin D1, D2, D3 and Glut25 and play a role in B-cell survival, angiogenesis, proliferation and inflammation. P = phosphorylation. Adapted from Bibi et al. [26].

2. Current therapeutic strategies for DS-ALL

Children with DS-ALL are reported to experience greater treatment-related toxicities [2,8,9] and treatment is often adjusted to reflect this. Methotrexate (MTX) is a fundamental chemotherapeutic agent incorporated in high doses in nearly all ALL chemotherapy regimens. By inhibiting dihydrofolate reductase, it interferes with *de novo* thymidine synthesis, an essential building block for DNA replication. MTX can cause stomatitis and myelosuppression, which can be particularly severe in DS-ALL patients [10,11]. The exact mechanism for this is unclear, though the increased dosage of chromosome 21 genes involved in purine synthesis may contribute [8]. DS-ALL patients also experience folate depletion as a result of increased cystathionine β-synthase and overexpression of the reduced folate carrier (RFC) [12]. DS-ALL patients are more susceptible to infections, often due to MTX side effects and impaired B- and T-cell function, with infection a significant cause of treatment-related mortality [2,5,17].

Commonly, leucovorin (folinic acid) is administered as a rescue therapy for non-leukaemic cells by overcoming the block in dihydrofolate reductase. The recent children's' oncology group (COG) AALL1131 study reduced the dose of MTX and brought forward the schedule of leucovorin rescue, to tailor therapy specifically to reduce toxicity for DS-ALL patients. Doses of other drugs may also be attenuated for DS-ALL patients, and some physicians choose to augment anti-bacterial prophylaxis. All protocols (including the Tokyo children's cancer study group (TCCSG), Dutch children's oncology group (DCOG), United Kingdom (UK), Italian-German consortium (AIEOP-BFM), France Acute Lymphoblastic Leukaemia (FRALLE) and COG) decrease the high dosage of MTX, and most will attenuate other drugs, such as daunorubicin (UKALL and DCOG). A number of clinical studies are currently underway, either designed specifically for DS-ALL, or with separate cohort of DS-ALL patients with specifically tailored therapy, in order to preserve efficacy and reduce toxicity in this patient group (e.g. NCT03286634).

Many studies demonstrate that DS-ALL patients have a poorer therapeutic outcome compared to non-DS-ALL patients. Conversely, some reports suggest there is no difference in induction failure for DS-ALL patients compared to non-DS-ALL [5,9,13]. It is, however, agreed upon that DS-ALL patients do experience a higher rate of relapse and lower event free survival [5,11]. In the event of relapse DS-ALL patients, like their non-DS-ALL counterpart, undergo salvage therapy, proceeding to haematopoietic stem cell transplant (HSCT) if a second remission can be achieved [2]. Due to the complex treatment approaches to address the additional toxicities experienced by this cohort of patients, advances in precision medicine may allow for the investigation of a targeted therapy based on each patients karyotypic or molecular profile.

3. Biological and genomic features of DS-ALL

In DS-ALL, there is a decreased prevalence of both favourable (e.g. *ETV6-RUNX1*) and unfavourable chromosomal aberrations (e.g. *BCR-ABL1*) [5,6], suggesting that there may be a different driver(s) of leukaemogenesis in DS-ALL. Multiple studies have found that *CRLF2* is frequently overexpressed in DS-ALL cases [1,3,5,11,14–18]. *CRLF2* is commonly overexpressed via a 320 KB deletion in the pseudoautosomal region (PAR1) of the X or Y chromosome (Xp22.33 and Yp11.22), placing it downstream of the first non-coding exon of the G-protein coupled purinergic receptor (*P2RY8*) [15]. A translocation of *CRLF2* to chromosome 14, downstream of the Immunoglobulin heavy chain (*IGH*) enhancer elements also causes *CRLF2* overexpression. Upregulation of Crlf2, activates the Janus Kinase (Jak) and signal transducer and activator of transcription (Stat) signalling pathway. The genes amplified from this pathway include *FOXOs, Bcl-2, Cyclin D1, D2, D3 and Glut25*, which are implicated in B-cell survival, angiogenesis, proliferation and inflammation [19]. This usually occurs when the ligand thymic stromal lymphopoietin (Tslp) binds to the Crlf2/IL-7Rα receptor (Fig. 1.1) [15,20,21].

In both *IGH-CRLF2* and *P2RY8-CRLF2* rearrangements, the entire coding sequence of *CRLF2* remains intact and the *P2RY8-CRLF2* breakpoint is identical in most patients [22]. The *IGH-CRLF2* rearrangement is likely a primary lesion due to its manifestation in haematopoietic precursor cells [23] and is more commonly observed in older ALL patients [25]. *P2RY8-CRLF2* fusions are likely secondary lesions and are the result of illegitimate V(D)J-mediated recombinations during B-cell ontogeny. Patients with *P2RY8-CRLF2* often also harbour primary genomic lesions such as intrachromasomal amplification of chromosome 21 (iAMP21) [23]. DS patients with *CRLF2r* are often

young with a mean of 5.5 years of age [11,24] and almost exclusively harbour *P2RY8-CRLF2* indicating that a PAR1 deletion is a common feature in these patients. The *P2RY8-CRLF2* fusion is found in a higher proportion of fusions identified in DS-ALL children (60%) compared to non-DS children (5–16%) [15,23,24,56]. However, when considering only patients with *CRLF2r*, the frequency of *P2RY8-CRLF2* is similar.

CRLF2 rearrangements are an obligate scaffold for *JAK2* mutations which occur in 50% of the subtype. These alterations often cluster in the pseudokinase domain at residue R683, however, have also been reported in the ATP and kinase domains [24,27,28]. Knockdown of *CRLF2* has demonstrated that Tslp signalling is cytokine independent when additional *JAK2* mutations are present [28]. A point mutation in *CRLF2* at 695 T > G causes constitutive activation of B-cell proliferation pathways and cooperates with Jak2 to provide significant growth advantage [24,29]. Mutations in *IL-7Rα* have been reported in the absence of *CRLF2* mutations [30,31]. These mutations in critical signalling genes are more significant in leukaemic transformation than the *P2RY8-CRLF2* fusion which may be lost at relapse [23] and instead *RAS* or *IKZF1* mutations often predominate. In 25% of *CRLF2r* DS-ALL cases a loss of the ubiquitin specific peptidase 9, X linked (*USP9X*) gene is observed [32]. Usp9x normally functions to stabilise phosphorylated Jak2 to confer active signalling, however, it is possible that activating *JAK* mutations are compensating for the loss of *USP9X* in these cases [32].

Non-DS-ALL frequently harbour polysomy 21 indicating that the gene dosage of chromosome 21 may be associated with the development of ALL [15,21,24,33]. A subset of patients with a gene signature similar to that of *BCR-ABL1* have been termed Philadelphia like (Ph-like). To date, no studies have identified concomitant DS-ALL with Ph-like ALL (15–20% of patients in non-DS-ALL) [34,35]. Studies comparing the genomic features of DS-ALL patients to other ALL patients have found an increase in deletions or mutations in the *PAX5*, *IKZF1*, and histone genes [18]. Histone gene mutation analysis and methylome sequencing have detailed numerous genes enriched for high or low methylation in DS-ALL patients compared to non-DS-ALL patients [14].

Despite the characteristic lesions of ALL observed in both DS and non-DS-ALL patients, there are specific DS-associated genes that are not dysregulated in non-DS-ALL and are being investigated as potential therapeutic targets for DS-ALL. Lane et al. [17] have produced a mouse model (Ts1Rhr) containing critical DS-genes that are linked to ALL and encode epigenetic regulators, signalling proteins (particularly regulators of the Pi3k pathway), transporter proteins and many with oncogenic effects (Table 1). However, these genes are yet to be investigated to fully elucidate their role in DS-ALL. Many more genes on chromosome 21 have also been linked to haematopoiesis and proliferative pathways in ALL but are also yet to be studied in the context of DS-ALL (Table 1).

Table 1
DS-critical genes located on chromosome 21 that may be associated with ALL due to the function of the resultant proteins [3,17,36].

Gene	Function of protein
ERG	haematopoietic oncoprotein
DYRK1A	regulates oncogenes and tumour suppressors (kinase)
ETS2	transcription factor and oncoprotein
IFNAR1	activates Jak/Stat signalling (membrane protein)
DSCR1	regulates expression of inflammatory markers
RUNX1	development of haematopoiesis
ETV6	regulates cell growth and differentiation (transcription factor)
TIAM	induces T-cell lymphoma and metastasis
GATA1	regulates haematopoietic development (transcription factor)
GABPA	regulates haematopoietic stem cells maintenance and differentiation (transcription factor)
SLC7A1	transports arginine
U2AF1	splicing factor
SLK1	governs morphogenesis and cell growth
PAXBP3	links PAX transcription factors to methylation machinery (adaptor protein)
NRIP1	transcriptional coregulator
USP25	ubiquitin specific protease
MCM3AP	initiates DNA replication
TTC3	degrades Akt
PIGP	anchors Pip in Pi3k pathway
BRWD1	governs epigenetic regulation and transcriptional activation
CHAF1B	chromatin regulator of histones
HMGN1	histone demethylase
MORC3	remodels chromatin
HLCS	binds biotin to histones
DNMT3L	DNA methyltransferase
PSMG1	proteasome chaperone
DSCR3	transports protein (suggested)

4. Therapeutic targeting of genomic lesions

Ruxolitinib was developed as an inhibitor for Jak1 and Jak2 in myeloproliferative neoplasms [37] and is being investigated in clinical trials to target ALL fusions involving *JAK*, *EPOR* and *CRLF2* with concomitant *JAK* mutations. *In vitro* studies have demonstrated ruxolitinib decreases the proliferation of ALL cell lines and patient samples with *CRLF2r* and *JAK* mutations [7,31,38–41]. Nevertheless, ALL fusions with cooperative lesions such as *JAK* mutations can survive by generating resistance to small molecule therapy targeting Jak, including ruxolitinib [42]. Kesarwani et al. [43] demonstrated a variety of Jak2 clones with different amino acid substitutions in both the kinase and pseudokinase domains that are resistant to ruxolitinib. A potential source of this survival is through the Pi3k pathway, as Jak phosphorylation can activate protein kinase B (Akt), promoting the transcription of cyclin D1 and inhibiting cyclin dependent kinase (CDK) inhibitors, progressing the cell cycle forward to the S phase. Further limitations of Jak TKI therapy include the short half-life of the drug which is approximately half a day, depending on the inhibitor [39]. Exposure to Jak inhibitors allows the accumulation of phosphorylated Jak2, however, once the inhibitor concentration reduces, Jak is already phosphorylated and downstream signalling can recommence [39].

Targeting Jak2 in myeloproliferative neoplasms has been successful with the competitive Jak2 inhibitor ruxolitinib, approved by the FDA after positive results from the COMFORT-I and II trials (NCT00952289 and NCT00934544). It was later approved for treatment of polycythaemia vera after the RESPONSE trial (NCT01243944) and is now currently in a phase II COG trial for the treatment of ALL for use alongside chemotherapy (NCT02723994), however, trisomy 21 patients are excluded from this study. Similarly, ruxolitinib has been included in the St. Jude phase II Total Therapy XVII trial for B and T-ALL patients (NCT03117751). A phase II trial for ruxolitinib with dasatinib is underway at MD Anderson (NCT02420717), while other small molecule inhibitors such as venetoclax for Bcl2 is in a phase I trial with chemotherapy at the Dana-Farber Cancer Institute (NCT03319901).

Due to a high incidence of *JAK2* mutations in both ALL and DS-ALL, combinatorial TKI targeting of Jak2 and the Pi3k pathway has demonstrated promise *in vitro* due to the cooperating signalling constituents [44]. Similarly, dual targeting of Jak and Pi3k has been successful against myeloproliferative neoplasms [26]. Combination therapies of the mechanistic target of rapamycin (mTOR) and Akt have also decreased proliferation of ALL cell lines [45] indicating that inhibition of multiple targets may be required for ALL therapy and similarly, DS-ALL therapy [46]. Histone deacetylase (HDAC) inhibitors have been found to overcome resistance to Jak TKI's and reduce treatment related toxicities in conjunction with chemotherapeutics for DS-ALL patients [47].

5. The role of trisomy 21 in ALL pathogenesis

The trisomy of chromosome 21 is the presence of a third, unmatched chromosome 21. The most common phenotype is Down Syndrome, however, somatic trisomy 21 can also be observed in ALL

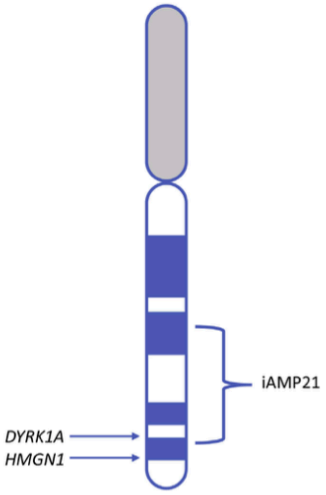

Fig. 2. Chromosome 21 depicting the intrachromosomal amplification of chromosome 21 (iAMP21) region and location of novel upregulated genes associated with ALL on the q arm. The iAMP21 region contains the DS critical genes that may have important functions for ALL (Table 1).

patients who do not have Down Syndrome. The link between trisomy 21 and disease has been well documented, yet not fully investigated in the context of leukaemia [36]. The presence of trisomy 21 may result in altered chromatin interactions, disrupting gene expression. However, a more likely scenario is that the increased dosage of chromosome 21 genes play a role in tumorigenesis or alter haematopoiesis (Fig. 2) [3]. There are at least 16 genes on chromosome 21 that are directly involved in haematological malignancies or abnormal haematopoiesis, and many more that are involved in epigenetic regulation which recent studies demonstrate may be a contributing factor to DS-ALL (Table 1) [3,17]. A region on chromosome 21 spanning 5.1–24 MB, that includes the *RUNX1* gene, is known as the intrachromosomal amplification of chromosome of 21 (iAMP21). While this region also encompasses the same DS-critical genes attributing to leukaemogenesis, it is not associated with DS-ALL and is instead a transforming lesion in non-DS-ALL [20,48].

Overexpression of dual specificity tyrosine-phosphorylated and regulated kinase 1A (*DYRK1A*) due to gene dosage (as a result of trisomy 21) has also been found to play a role in DS-ALL pathogenesis [49]. Dyrk1a controls the expression of cyclin D1 and regulates the cell cycle to cause entry or exit into quiescence or persistent arrest [50]. This is dependent on a balance between cyclin D1 and p21, however, with an increased dosage of *DYRK1A* in DS-ALL, the cell enters an extended G1 phase [51]. Dyrk1a dysregulation promotes ALL via negative regulation of the transcription factors Nfatc2, Nfatc3 and Nfatc4, which have tumour suppressive properties [52]. Conversely, Dyrk1a is a positive regulator of Nfatc1 which stabilises its structure, and has been demonstrated to promote oncogenic activity [50,53]. Dyrk1a also phosphorylates Stat3 and prolongs Erk activation, stimulating key signalling pathways in ALL as well as being associated with pre-B cell formation [51]. The multifaceted functions of Dyrk1a promote cell cycle perturbation and differentiation at critical stages of B-cell development that are susceptible to leukaemic transformation [51,54].

There is still much to learn about Dyrk1a's role in DS-ALL, however, therapeutic targeting of this protein has begun in other diseases. Small molecule inhibitors of Dyrk1a such as B-carboline alkaloid harmine and epigallocatechin-3-gallate (EGCG) have been identified as a potential therapeutic for Alzheimer's disease [55,56], however, their effects have not yet been investigated in DS-ALL.

6. Epigenetic modifications play a role in DS-ALL

Haematological malignancies harbour a variety of different epigenetic modifications causing chromatin dysregulation. Epigenetic modifications in ALL have not been as well characterised as activating mutations in the genes of key signalling pathway. Histone acetylase genes *CREBBP* and *EP300*, cytosine modifier *DNMT3A* and methylation associated genes *MLL1* and *EZH2* are commonly involved in gene fusions or mutated in ALL [25,34]. However, the signalling pathways that are altered due to epigenetic alterations are the main feature of dysregulation. DNA methylation profiles of B-ALL patients have demonstrated that important signalling molecules in the B-cell receptor (BCR) pathway including *CD79A* and *B*, *CD22*, *KRAS* and *NFKB1* are hypomethylated, while *SHP1*, *RAC2*, *AKT1*, *GSK3* and *MEK1* are hypermethylated [57]. The regulation of these integral molecules must be precise, however, the upstream epigenetic aberration may have a bigger contribution to leukaemic transformation [58] and epigenetic therapies are an avenue only recently being investigated [17,59,60]. Methyltransferase inhibitors targeting DOT1 Like Histone Lysine Methyltransferase (DOT1L) have completed phase I trials for *MLL* rearranged leukaemia (NCT02141828 & NCT01684150) [61] and inhibitors of the methyltransferase component of the polycomb repressor 2 (PRC2) complex, EZH2, are in phase II clinical trials for B-cell lymphoma (NCT01897571).

Few studies have considered epigenetic modifications in DS-ALL, besides well characterised genes such as *CREBBP*. Histone gene deletions occur more frequently in DS-ALL than non-DS-ALL, particularly at the 6p22 cluster and result in differential cytokine-cytokine receptor interactions [14,25]. One significant finding was that *CRLF2r* DS-ALL patients had more similarities to the DS-ALL genomic profile rather than the *CRLF2* profile in the Molecular Signatures Database [14,24,29]. This suggests that *CRLF2r* ALL and *CRLF2r* DS-ALL have significantly different downstream effects and require different therapies, highlighting the importance of precision medicine.

In DS-ALL, a transcriptional profile was defined based on analysis of B-lymphocytes [17]. The analyses revealed highly enriched clustering in pathways related to PRC2 targets and sites of trimethylated Lysine 27 of histone 3 (H3K27me3). H3K27me3 is the repressive epigenetic mark added by PRC2. DS-ALL demonstrates global reduction in H3K27me3, which in turn leads to an increased gene expression pattern that drives B-cell development. A nucleosome remodelling protein encoded on chromosome 21, Hmgn1, has been found to be responsible and implicated in H3 modification of critical genes in the B-cell developmental pathway in DS model Ts1Rhr mice [17]. Hmg proteins compete with the linker histone H1 for nucleosome binding in order to reduce chromatin compaction for transcriptional activation. This is achieved by decreasing phosphorylation of histone H3 at Ser10 and H2a at Ser1, while increasing the acetylation of H3 at Lys14 [62,63].

In the study of *HMGN1* overexpression in Ph+ B-ALL cells [17], the PRC2 targets of H3K27me3 were de-repressed by Hmgn1. This included the binding sites of transcription factor 3 (E2a) and lymphoid enhancer-binding factor 1 (Lef1) which are key transcription factors in lymphopoiesis and may contribute to the leukaemic phenotype. This study concluded that persistent expression of *HMGN1* was required for cell proliferation. Upon the administration of demethylase inhibitor GSK-J4, targeting Hmgn1, the methylation of critical lymphopoiesis transcription factors *E2a* and *LEF1*, was restored, decreasing proliferation (Fig. 3). Furthermore, when Hmgn1 was overexpressed, a more aggressive form of *BCR-ABL1*+ ALL was induced [17]. Targeting Hmgn1 in this setting, could therefore, provide a novel therapeutic focus. Inhibitors of demethylases, such as Hmgn1, are currently being investigated as potential therapeutics in DS-ALL [17,36].

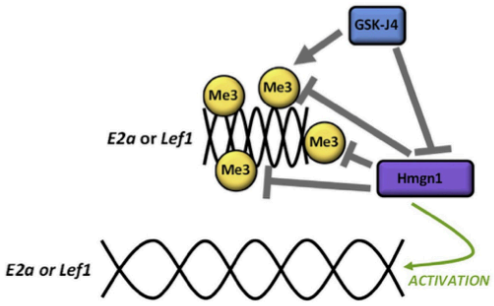

Fig. 3. Hmgn1 reverses the methylation of transcription factors Lef1 and E2a resulting in the relaxing of the chromatin to allow transcription of the gene. The H3K27 methylase inhibitor GSK-J4 inhibits Hmgn1, allowing methylation and silencing of E2a and Lef1.

7. Conclusion and future directions

Novel therapies for DS-ALL are being investigated to reduce the risk of relapse and improve the survival rates of DS-ALL patients. Small molecule inhibitors targeting Jak2, Bcl2, HDAC and methyltransferases are being considered in addition to chemotherapy. These therapeutics have the potential to be included in DS-ALL patients treatment regimens in the future, so that cytotoxic chemotherapeutics can be de-escalated. Currently, clinical trials are investigating Jak inhibitors for patients with *CRLF2r*, as well as reducing the dose of MTX for DS-ALL patients, and administering leucovorin earlier after high dose MTX. Genomic profiling of DS-ALL patients will improve knowledge of the cytogenetics these patients harbour, and will significantly aid in the investigation of new therapeutic targets. The predisposition of DS-ALL patients to acquire the *P2RY8-CRLF2* fusion is unknown, however, novel genes including *HMGN1* and *DYRK1A* have been identified as genes of interest, yet their specific roles in disease pathogenesis have not been elucidated [17,54]. Epigenetic modifications occur more frequently in DS-ALL than non-DS-ALL and may provide a novel therapeutic avenue targeting proteins such as Hmgn1. A personalised medicine approach is likely to improve the long term survival of DS-ALL patients with high-risk fusions by using targeted therapies and reducing the dosage of toxic elements of chemotherapy.

Conflicts of interest

DLW – Research support from Novartis and BMS, Honoraria from BMS.

Acknowledgements

The authors thank Laura Eadie and Tamara Leclercq (South Australian Health and Medical Research Institute) for their assistance with writing and editing of the manuscript.

References

[1] D. Tomizawa, A. Endo, M. Kajiwara, H. Sakaguchi, K. Matsumoto, M. Kaneda, T. Taga, Acute lymphoblastic leukemia in patients with Down syndrome with a previous history of acute myeloid leukemia, Pediatr. Blood Canc. 64 (2017).
[2] F. Meyr, G. Escherich, G. Mann, T. Klingebiel, A. Kulozik, C. Rossig, M. Schrappe, G. Henze, A. von Stackelberg, J. Hitzler, Outcomes of treatment for relapsed acute lymphoblastic leukaemia in children with Down syndrome, Br. J. Haematol. 162 (2013) 98–106.
[3] I. Roberts, S. Izraeli, Haematopoietic development and leukaemia in Down syndrome, Br. J. Haematol. 167 (2014) 587–599.
[4] S. Izraeli, A. Vora, C.M. Zwaan, J. Whitlock, How I treat ALL in Down's syndrome: pathobiology and management, Blood 123 (2014) 35–40.
[5] T.D. Buitenkamp, S. Izraeli, M. Zimmermann, E. Forestier, N.A. Heerema, M.M. van den Heuvel-Eibrink, R. Pieters, C.M. Korbijn, L.B. Silverman, K. Schmiegelow, D.C. Liang, K. Horibe, M. Arico, A. Biondi, G. Basso, K.R. Rabin, M. Schrappe, G. Cario, G. Mann, M. Morak, R. Panzer-Grümayer, V. Mondelaers, T. Lammens, H. Cavé, B. Stark, I. Ganmore, A.V. Moorman, A. Vora, S.P. Hunger, C.H. Pui, C.G. Mullighan, A. Manabe, G. Escherich, J.R. Kowalczyk, J.A. Whitlock, C.M. Zwaan, Acute lymphoblastic leukemia in children with Down syndrome: a retrospective analysis from the Ponte di Legno study group, Blood 123 (2014) 70–77.
[6] E. Forestier, S. Izraeli, B. Beverloo, O. Haas, A. Pession, K. Michalová, B. Stark, C.J. Harrison, A. Teigler-Schlegel, B. Johansson, Cytogenetic features of acute lymphoblastic and myeloid leukemias in pediatric patients with Down syndrome: an iBFM-SG study, Blood 111 (2008) 1575–1583.
[7] S.L. Maude, S.K. Tasian, T. Vincent, J.W. Hall, C. Sheen, K.G. Roberts, A.E. Seif, D.M. Barrett, I.M. Chen, J.R. Collins, C.G. Mullighan, S.P. Hunger, R.C. Harvey, C.L. Willman, J.S. Fridman, M.L. Loh, S.A. Grupp, D.T. Teachey, Targeting JAK1/2 and mTOR in murine xenograft models of Ph-like acute lymphoblastic leukemia, Blood 120 (2012) 3510–3518.
[8] J.A. Whitlock, Down syndrome and acute lymphoblastic leukaemia, Br. J. Haematol. 135 (2006) 595–602.
[9] M. Arico, O. Ziino, M.G. Valsecchi, G. Cazzaniga, C. Baronci, C. Messina, A. Pession, N. Santoro, G. Basso, V. Conter, I.A.o.P.H.a.O. (AIEOP), Acute lymphoblastic leukemia and Down syndrome: presenting features and treatment outcome in the experience of the Italian Association of Pediatric Hematology and Oncology (AIEOP), Cancer 113 (2008) 515–521.
[10] T.D. Buitenkamp, R.A. Mathôt, V. de Haas, R. Pieters, C.M. Zwaan, Methotrexate-induced side effects are not due to differences in pharmacokinetics in children with Down syndrome and acute lymphoblastic leukemia, Haematologica 95 (2010) 1106–1113.
[11] C. O'Rafferty, J. Kelly, L. Storey, C. Ryan, A. O'Marcaigh, O. Smith, Child and adolescent Down syndrome-associated leukaemia: the Irish experience, Ir. J. Med. Sci. 184 (2015) 877–882.
[12] A.C. Xavier, Y. Ge, J. Taub, Unique clinical and biological features of leukemia in Down syndrome children, Expet Rev. Hematol. 3 (2010) 175–186.
[13] N. Shah, A. Al-Ahmari, A. Al-Yamani, L. Dupuis, D. Stephens, J. Hitzler, Outcome and toxicity of chemotherapy for acute lymphoblastic leukemia in children with Down syndrome, Pediatr. Blood Canc. 52 (2009) 14–19.
[14] M.G. Loudin, J. Wang, H.C. Leung, S. Gurusiddappa, J. Meyer, G. Condos, D. Morrison, A. Tsimelzon, M. Devidas, N.A. Heerema, A.J. Carroll, S.E. Plon, S.P. Hunger, G. Basso, A. Pession, D. Bhojwani, W.L. Carroll, K.R. Rabin, Genomic profiling in Down syndrome acute lymphoblastic leukemia identifies histone gene deletions associated with altered methylation profiles, Leukemia 25 (2011) 1555–1563.
[15] C.G. Mullighan, J.R. Collins-Underwood, L.A. Phillips, M.G. Loudin, W. Liu, J. Zhang, J. Ma, E. Coustan-Smith, R.C. Harvey, C.L. Willman, F.M. Mikhail, J. Meyer, A.J. Carroll, R.T. Williams, J. Cheng, N.A. Heerema, G. Basso, A. Pession, C.H. Pui, S.C. Raimondi, S.P. Hunger, J.R. Downing, W.L. Carroll, K.R. Rabin, Rearrangement of CRLF2 in B-progenitor- and Down syndrome-associated acute lymphoblastic leukemia, Nat. Genet. 41 (2009) 1243–1246.
[16] S.I. Nikolaev, M. Garieri, F. Santoni, E. Falconnet, P. Ribaux, M. Guipponi, A. Murray, J. Groet, E. Giarin, G. Basso, D. Nizetic, S.E. Antonarakis, Frequent cases of RAS-mutated Down syndrome acute lymphoblastic leukaemia lack JAK2 mutations, Nat. Commun. 5 (2014) 4654.
[17] A.A. Lane, B. Chapuy, C.Y. Lin, T. Tivey, H. Li, E.C. Townsend, D. van Bodegom, T.A. Day, S.C. Wu, H. Liu, A. Yoda, G. Alexe, A.C. Schinzel, T.J. Sullivan, S. Malinge, J.E. Taylor, K. Stegmaier, J.D. Jaffe, M. Bustin, G. te Kronnie, S. Izraeli, M.H. Harris, K.E. Stevenson, D. Neuberg, L.B. Silverman, S.E. Sallan, J.E. Bradner, W.C. Hahn, J.D. Crispino, D. Pellman, D.M. Weinstock, Triplication of a 21q22 region contributes to B cell transformation through HMGN1 overexpression and loss of histone H3 Lys27 trimethylation, Nat. Genet. 46 (2014) 618–623.
[18] P. Lee, R. Bhansali, S. Izraeli, N. Hijiya, J.D. Crispino, The biology, pathogenesis and clinical aspects of acute lymphoblastic leukemia in children with Down syndrome, Leukemia 30 (2016) 1816–1823.
[19] J. Eswaran, P. Sinclair, O. Heidenreich, J. Irving, L.J. Russell, A. Hall, D.P. Calado, C.J. Harrison, J. Vormoor, The pre-B-cell receptor checkpoint in acute lymphoblastic leukaemia, Leukemia 29 (2015) 1623–1631.
[20] L.J. Russell, L. Jones, A. Enshaei, S. Tonin, S.L. Ryan, J. Eswaran, S. Nakjang, E. Papaemmanuil, J.M. Tubio, A.K. Fielding, A. Vora, P.J. Campbell, A.V. Moorman, C.J. Harrison, Characterisation of the genomic landscape of CRLF2-rearranged acute lymphoblastic leukemia, Genes Chromosomes Cancer 56 (2017) 363–372.
[21] T. Sadras, S.L. Heatley, C.H. Kok, P. Dang, K.M. Galbraith, B.J. McClure, W. Muskovic, N.C. Venn, S. Moore, M. Osborn, T. Revesz, A.S. Moore, T.P. Hughes, D. Yeung, R. Sutton, D.L. White, Differential expression of MUC4, GPR110 and IL2RA defines two groups of CRLF2-rearranged acute lymphoblastic leukemia patients with distinct secondary lesions, Canc. Lett. 408 (2017) 92–101.
[22] J.S. Woo, M.O. Alberti, C.A. Tirado, Childhood B-acute lymphoblastic leukemia: a genetic update, Exp. Hematol. Oncol. 3 (2014) 16.
[23] C. Vesely, C. Frech, C. Eckert, G. Cario, A. Mecklenbrauker, U. Zur Stadt, K. Nebral, F. Kraler, S. Fischer, A. Attarbaschi, M. Schuster, C. Bock, H. Cave, A. von Stackelberg, M. Schrappe, M.A. Horstmann, G. Mann, O.A. Haas, R. Panzer-Grumayer, Genomic and transcriptional landscape of P2RY8-CRLF2-positive childhood acute lymphoblastic leukemia, Leukemia 31 (7) (2017) 1491–1501.
[24] L. Hertzberg, E. Vendramini, I. Ganmore, G. Cazzaniga, M. Schmitz, J. Chalker, R. Shiloh, I. Iacobucci, C. Shochat, S. Zeligson, G. Cario, M. Stanulla, S. Strehl, L.J. Russell, C.J. Harrison, B. Bornhauser, A. Yoda, G. Rechavi, D. Bercovich, A. Borkhardt, H. Kempski, G. te Kronnie, J.P. Bourquin, E. Domany, S. Izraeli, Down

syndrome acute lymphoblastic leukemia, a highly heterogeneous disease in which aberrant expression of CRLF2 is associated with mutated JAK2: a report from the International BFM Study Group, Blood 115 (2010) 1006–1017.
[25] S.P. Hunger, C.G. Mullighan, Redefining ALL classification: toward detecting high-risk ALL and implementing precision medicine, Blood 125 (2015) 3977–3987.
[26] S. Bibi, M.D. Arslanhan, F. Langenfeld, S. Jeanningros, S. Cerny-Reiterer, E. Hadzijusufovic, L. Tchertanov, R. Moriggl, P. Valent, M. Arock, Co-operating STAT5 and AKT signaling pathways in chronic myeloid leukemia and mastocytosis: possible new targets of therapy, Haematologica 99 (2014) 417–429.
[27] N. Jain, K.G. Roberts, E. Jabbour, K. Patel, A.K. Eterovic, K. Chen, P. Zweidler-McKay, X. Lu, G. Fawcett, S.A. Wang, S. Konoplev, R.C. Harvey, I.M. Chen, D. Payne-Turner, M. Valentine, D. Thomas, G. Garcia-Manero, F. Ravandi, J. Cortes, S. Kornblau, S. O'Brien, S. Pierce, J. Jorgensen, K.R. Shaw, C.L. Willman, C.G. Mullighan, H. Kantarjian, M. Konopleva, Ph-like acute lymphoblastic leukemia: a high-risk subtype in adults, Blood 129 (2017) 572–581.
[28] L.J. Russell, M. Capasso, I. Vater, T. Akasaka, O.A. Bernard, M.J. Calasanz, T. Chandrasekaran, E. Chapiro, S. Gesk, M. Griffiths, D.S. Guttery, C. Haferlach, L. Harder, O. Heidenreich, J. Irving, L. Kearney, F. Nguyen-Khac, L. Machado, L. Minto, A. Majid, A.V. Moorman, H. Morrison, V. Rand, J.C. Strefford, C. Schwab, H. Tonnies, M.J. Dyer, R. Siebert, C.J. Harrison, Deregulated expression of cytokine receptor gene, CRLF2, is involved in lymphoid transformation in B-cell precursor acute lymphoblastic leukemia, Blood 114 (2009) 2688–2698.
[29] A. Yoda, Y. Yoda, S. Chiaretti, M. Bar-Natan, K. Mani, S.J. Rodig, N. West, Y. Xiao, J.R. Brown, C. Mitsiades, M. Sattler, J.L. Kutok, D.J. DeAngelo, M. Wadleigh, A. Piciocchi, P. Dal Cin, J.E. Bradner, J.D. Griffin, K.C. Anderson, R.M. Stone, J. Ritz, R. Foà, J.C. Aster, D.A. Frank, D.M. Weinstock, Functional screening identifies CRLF2 in precursor B-cell acute lymphoblastic leukemia, Proc. Natl. Acad. Sci. U. S. A. 107 (2010) 252–257.
[30] C.G. Mullighan, J. Zhang, R.C. Harvey, J.R. Collins-Underwood, B.A. Schulman, L.A. Phillips, S.K. Tasian, M.L. Loh, X. Su, W. Liu, M. Devidas, S.R. Atlas, I.M. Chen, R.J. Clifford, D.S. Gerhard, W.L. Carroll, G.H. Reaman, M. Smith, J.R. Downing, S.P. Hunger, C.L. Willman, JAK mutations in high-risk childhood acute lymphoblastic leukemia, Proc. Natl. Acad. Sci. U. S. A. 106 (2009) 9414–9418.
[31] K.G. Roberts, R.D. Morin, J. Zhang, M. Hirst, Y. Zhao, X. Su, S.C. Chen, D. Payne-Turner, M.L. Churchman, R.C. Harvey, X. Chen, C. Kasap, C. Yan, J. Becksfort, R.P. Finney, D.T. Teachey, S.L. Maude, K. Tse, R. Moore, S. Jones, K. Mungall, I. Birol, M.N. Edmonson, Y. Hu, K.E. Buetow, I.M. Chen, W.L. Carroll, L. Wei, J. Ma, M. Kleppe, R.L. Levine, G. Garcia-Manero, E. Larsen, N.P. Shah, M. Devidas, G. Reaman, M. Smith, S.W. Paugh, W.E. Evans, S.A. Grupp, S. Jeha, C.H. Pui, D.S. Gerhard, J.R. Downing, C.L. Willman, M. Loh, S.P. Hunger, M.A. Marra, C.G. Mullighan, Genetic alterations activating kinase and cytokine receptor signaling in high-risk acute lymphoblastic leukemia, Canc. Cell 22 (2012) 153–166.
[32] O. Schwartzman, A.M. Savino, M. Gombert, C. Palmi, G. Cario, M. Schrappe, C. Eckert, A. von Stackelberg, J.Y. Huang, M. Hameiri-Grossman, S. Avigad, G. Te Kronnie, I. Geron, Y. Birger, A. Rein, G. Zarfati, U. Fischer, Z. Mukamel, M. Stanulla, A. Biondi, G. Cazzaniga, A. Vetere, B.K. Wagner, Z. Chen, S.J. Chen, A. Tanay, A. Borkhardt, S. Izraeli, Suppressors and activators of JAK-STAT signaling at diagnosis and relapse of acute lymphoblastic leukemia in Down syndrome, Proc. Natl. Acad. Sci. U. S. A. 114 (2017) E4030–E4039.
[33] N.A. Heerema, S.C. Raimondi, J.R. Anderson, J. Biegel, B.M. Camitta, L.D. Cooley, P.S. Gaynon, B. Hirsch, R.E. Magenis, L. McGavran, S. Patil, M.J. Pettenati, J. Pullen, K. Rao, D. Roulston, N.R. Schneider, J.J. Shuster, W. Sanger, M.J. Sutcliffe, P. van Tuinen, M.S. Watson, A.J. Carroll, Specific extra chromosomes occur in a modal number dependent pattern in pediatric acute lymphoblastic leukemia, Genes Chromosomes Cancer 46 (2007) 684–693.
[34] K.G. Roberts, C.G. Mullighan, Genomics in acute lymphoblastic leukaemia: insights and treatment implications, Nat. Rev. Clin. Oncol. 12 (2015) 344–357.
[35] S.K. Tasian, M.L. Loh, S.P. Hunger, Childhood acute lymphoblastic leukemia: integrating genomics into therapy, Cancer 121 (2015) 3577–3590.
[36] S.E. Antonarakis, Down syndrome and the complexity of genome dosage imbalance, Nat. Rev. Genet. 18 (2017) 147–163.
[37] P. Bose, S. Verstovsek, JAK2 inhibitors for myeloproliferative neoplasms: what is next? Blood 130 (2017) 115–125.
[38] E. Leroy, S.N. Constantinescu, Rethinking JAK2 inhibition: towards novel strategies of more specific and versatile janus kinase inhibition, Leukemia 31 (2017) 1023–1038.
[39] E.M.P. Steeghs, I.S. Jerchel, W. de Goffau-Nobel, A.Q. Hoogkamer, J.M. Boer, A. Boeree, C. van de Ven, M.J. Koudijs, N.J.M. Besselink, H.A. de Groot-Kruseman, C.M. Zwaan, M.A. Horstmann, R. Pieters, M.L. den Boer, Aberrations in childhood B-cell precursor acute lymphoblastic leukemia, Oncotarget 8 (2017) 89923–89938.
[40] S.K. Tasian, D.T. Teachey, Y. Li, F. Shen, R.C. Harvey, I.M. Chen, T. Ryan, T.L. Vincent, C.L. Willman, A.E. Perl, S.P. Hunger, M.L. Loh, M. Carroll, S.A. Grupp, Potent efficacy of combined PI3K/mTOR and JAK or ABL inhibition in murine xenograft models of Ph-like acute lymphoblastic leukemia, Blood 129 (2017) 177–187.
[41] S.L. Maude, S. Dolai, C. Delgado-Martin, T. Vincent, A. Robbins, A. Selvanathan, T. Ryan, J. Hall, A.C. Wood, S.K. Tasian, S.P. Hunger, M.L. Loh, C.G. Mullighan, B.L. Wood, M.L. Hermiston, S.A. Grupp, R.B. Lock, D.T. Teachey, Efficacy of JAK/STAT pathway inhibition in murine xenograft models of early T-cell precursor (ETP) acute lymphoblastic leukemia, Blood 125 (2015) 1759–1767.
[42] J.R. Mayfield, D.R. Czuchlewski, J.M. Gale, K. Matlawska-Wasowska, M.A. Vasef, C. Nickl, G. Pickett, S.A. Ness, S.S. Winter, Integration of ruxolitinib into dose-intensified therapy targeted against a novel JAK2 F694L mutation in B-precursor acute lymphoblastic leukemia, Pediatr. Blood Canc. 64 (2017).
[43] M. Kesarwani, E. Huber, Z. Kincaid, C.R. Evelyn, J. Biesiada, M. Rance, M.B. Thapa, N.P. Shah, J. Meller, Y. Zheng, M. Azam, Targeting substrate-site in Jak2 kinase prevents emergence of genetic resistance, Sci. Rep. 5 (2015) 14538.
[44] S.K. Tasian, M.Y. Doral, M.J. Borowitz, B.L. Wood, I.M. Chen, R.C. Harvey, J.M. Gastier-Foster, C.L. Willman, S.P. Hunger, C.G. Mullighan, M.L. Loh, Aberrant STAT5 and PI3K/mTOR pathway signaling occurs in human CRLF2-rearranged B-precursor acute lymphoblastic leukemia, Blood 120 (2012) 833–842.
[45] L.M. Neri, A. Cani, A.M. Martelli, C. Simioni, C. Junghanss, G. Tabellini, F. Ricci, P.L. Tazzari, P. Pagliaro, J.A. McCubrey, S. Capitani, Targeting the PI3K/Akt/mTOR signaling pathway in B-precursor acute lymphoblastic leukemia and its therapeutic potential, Leukemia 28 (2014) 739–748.
[46] S. Izraeli, C. Shochat, N. Tal, I. Geron, Towards precision medicine in childhood leukemia–insights from mutationally activated cytokine receptor pathways in acute lymphoblastic leukemia, Canc. Lett. 352 (2014) 15–20.
[47] A.M. Savino, J. Sarno, L. Trentin, M. Vieri, G. Fazio, M. Bardini, C. Bugarin, G. Fossati, K.L. Davis, G. Gaipa, S. Izraeli, L.H. Meyer, G.P. Nolan, A. Biondi, G. Te Kronnie, C. Palmi, G. Cazzaniga, The histone deacetylase inhibitor givinostat (ITF2357) exhibits potent anti-tumor activity against CRLF2-rearranged BCP-ALL, Leukemia 31 (11) (2017) 2365–2375.
[48] S.K. Tasian, S.P. Hunger, Genomic characterization of paediatric acute lymphoblastic leukaemia: an opportunity for precision medicine therapeutics, Br. J. Haematol. 176 (2017) 867–882.
[49] S. Malinge, M. Bliss-Moreau, G. Kirsammer, L. Diebold, T. Chlon, S. Gurbuxani, J.D. Crispino, Increased dosage of the chromosome 21 ortholog Dyrk1a promotes megakaryoblastic leukemia in a murine model of Down syndrome, J. Clin. Invest. 122 (2012) 948–962.
[50] H. Liu, K. Wang, S. Chen, Q. Sun, Y. Zhang, L. Chen, X. Sun, NFATc1 phosphorylation by DYRK1A increases its protein stability, PLoS One 12 (2017) e0172985.
[51] B.J. Thompson, R. Bhansali, L. Diebold, D.E. Cook, L. Stolzenburg, A.S. Casagrande, T. Besson, B. Leblond, L. Desire, S. Malinge, J.D. Crispino, DYRK1A controls the transition from proliferation to quiescence during lymphoid development by destabilizing Cyclin D3, J. Exp. Med. 212 (2015) 953–970.
[52] J.R. Arron, M.M. Winslow, A. Polleri, C.P. Chang, H. Wu, X. Gao, J.R. Neilson, L. Chen, J.J. Heit, S.K. Kim, N. Yamasaki, T. Miyakawa, U. Francke, I.A. Graef, G.R. Crabtree, NFAT dysregulation by increased dosage of DSCR1 and DYRK1A on chromosome 21, Nature 441 (2006) 595–600.
[53] F. Macian, NFAT proteins: key regulators of T-cell development and function, Nat. Rev. Immunol. 5 (2005) 472–484.
[54] S. Izraeli, The acute lymphoblastic leukemia of Down Syndrome - genetics and pathogenesis, Eur. J. Med. Genet. 59 (2016) 158–161.
[55] T. Koyama, N. Yamaotsu, I. Nakagome, S.I. Ozawa, T. Yoshida, D. Hayakawa, S. Hirono, Multi-step virtual screening to develop selective DYRK1A inhibitors, J. Mol. Graph. Model. 72 (2017) 229–239.
[56] T.D. Buitenkamp, R. Pieters, N.E. Gallimore, A. van der Veer, J.P. Meijerink, H.B. Beverloo, M. Zimmermann, V. de Haas, S.M. Richards, A.J. Vora, C.D. Mitchell, L.J. Russell, C. Schwab, C.J. Harrison, A.V. Moorman, M.M. van den Heuvel-Eibrink, M.L. den Boer, C.M. Zwaan, Outcome in children with Down's syndrome and acute lymphoblastic leukemia: role of IKZF1 deletions and CRLF2 aberrations, Leukemia 26 (2012) 2204–2211.
[57] M.E. Figueroa, S.C. Chen, A.K. Andersson, L.A. Phillips, Y. Li, J. Sotzen, M. Kundu, J.R. Downing, A. Melnick, C.G. Mullighan, Integrated genetic and epigenetic analysis of childhood acute lymphoblastic leukemia, J. Clin. Invest. 123 (2013) 3099–3111.
[58] Y.R. Chung, E. Schatoff, O. Abdel-Wahab, Epigenetic alterations in hematopoietic malignancies, Int. J. Hematol. 96 (2012) 413–427.
[59] J.A. Faria, N.C. Corrêa, C. de Andrade, A.C. de Angelis Campos, R. Dos Santos Samuel de Almeida, T.S. Rodrigues, A.M. de Goes, D.A. Gomes, F.P. Silva, SET domain-containing protein 4 (SETD4) is a newly identified cytosolic and nuclear lysine methyltransferase involved in breast cancer cell proliferation, J. Canc. Sci. Ther. 5 (2013) 58–65.
[60] Z. Chatterton, L. Morenos, F. Mechinaud, D.M. Ashley, J.M. Craig, A. Sexton-Oates, M.S. Halemba, M. Parkinson-Bates, J. Ng, D. Morrison, W.L. Carroll, R. Saffery, N.C. Wong, Epigenetic deregulation in pediatric acute lymphoblastic leukemia, Epigenetics 9 (2014) 459–467.
[61] L. Morera, M. Lübbert, M. Jung, Targeting histone methyltransferases and demethylases in clinical trials for cancer therapy, Clin. Epigenet. 8 (2016) 57.
[62] J.H. Lim, F. Catez, Y. Birger, K.L. West, M. Prymakowska-Bosak, Y.V. Postnikov, M. Bustin, Chromosomal protein HMGN1 modulates histone H3 phosphorylation, Mol. Cell 15 (2004) 573–584.
[63] J.H. Lim, K.L. West, Y. Rubinstein, M. Bergel, Y.V. Postnikov, M. Bustin, Chromosomal protein HMGN1 enhances the acetylation of lysine 14 in histone H3, EMBO J. 24 (2005) 3038–3048.

Statement of Authorship

Title of Paper	Understanding the Role of Chromosome 21 for Precision Treatment in Down Syndrome Acute Lymphoblastic Leukaemia
Publication Status	☐ Published ☒ Accepted for Publication ☐ Submitted for Publication ☐ Unpublished and Unsubmitted work written in manuscript style
Publication Details	Page E, White D (2021) Understanding the Role of Chromosome 21 for Precision Treatment in Down Syndrome Acute Lymphoblastic Leukaemia. J Alzheimers Dis Parkinsonism 11: 508.

Principal Author

Name of Principal Author (Candidate)	Elyse Page		
Contribution to the Paper	Conducted literature review and wrote the manuscript		
Overall percentage (%)	95%		
Certification:	This paper reports on original research I conducted during the period of my Higher Degree by Research candidature and is not subject to any obligations or contractual agreements with a third party that would constrain its inclusion in this thesis. I am the primary author of this paper.		
Signature		Date	23/2/21

Co-Author Contributions

By signing the Statement of Authorship, each author certifies that:

i. the candidate's stated contribution to the publication is accurate (as detailed above);

ii. permission is granted for the candidate in include the publication in the thesis; and

iii. the sum of all co-author contributions is equal to 100% less the candidate's stated contribution.

Name of Co-Author	Deborah White		
Contribution to the Paper	Supervised, and edited the manuscript		
Signature		Date	25/2/21

Journal of
Alzheimer's Disease & Parkinsonism

Page and White, J Alzheimers Dis Parkinsonism 2020, 11:1

Commentary Open Access

Understanding the Role of Chromosome 21 for Precision Treatment in Down Syndrome Acute Lymphoblastic Leukaemia

Elyse Page[1,2] and Deborah White[1,2,3,4,5,6]*

[1]Cancer Program, Precision Medicine Theme, South Australian Health & Medical Research Institute, Australia
[2]School of Biological Sciences, University of Adelaide, Australia
[3]Discipline of Medicine, University of Adelaide, Australia
[4]Australian and New Zealand Children's Haematology/Oncology Group (ANZCHOG)
[5]Australian Genomic Health Alliance (AGHA), Australia
[6]Discipline of Paediatrics, University of Adelaide, Australia

Abstract

Children with Down Syndrome (DS) are predisposed to developing Acute Lymphoblastic Leukaemia (ALL) and experience lower overall survival (75%) compared to children without Down syndrome (85-90%). The mortality rate for paediatric DS-ALL patients is four times higher than non-DS-ALL patients in the first two years after their diagnosis. Increased chemotherapy-related toxicity is experienced by DS-ALL patients, however, new immunotherapies including bi-specific T-cell engagers and chimeric antigen receptor T-cell therapies are being pursued in clinical trials. Fundamental research has identified 31 genes in the Down syndrome critical region of chromosome 21 which play a role in leukaemogenesis. Understanding these genes will be critical to identify the predisposition DS patients have for developing ALL, as well as discovering new targeted therapeutic approaches. The aim is to identify the role(s) of chromosome 21 genes to establish less toxic treatment options for DS-ALL patients.

Keywords: Down syndrome; Leukaemia; Chromosome 21

Commentary

Trisomy of chromosome 21 occurs via nondisjunction at meiosis and results in Down Syndrome (DS) in 1 in 700 births. Chromosome 21 is the smallest human chromosome encoding ~225 genes. Trisomy of chromosome 21 is associated with neurodevelopmental disorders and early onset Alzheimer's disease. Increased expression of β-amyloid precursor protein (*APP*) encoded on chromosome 21 is implicated in Alzheimer's disease providing a mechanism of Alzheimer's development in DS patients [1]. Children with DS are predisposed to developing haematological malignancies and have a 150-fold and 20-fold increased risk of developing Acute Myeloid leukaemia (AML) and Acute Lymphoblastic Leukaemia (ALL), respectively [2]. Acute megakaryoblastic leukaemia (AMKL) is frequently observed in DS patients as trisomy 21 is required for AMKL development. DS-ALL patients have poor survival outcomes and experience significant treatment related-toxicity from contemporary chemotherapeutic regimes. Higher relapse rates and risk of infections are observed in DS-ALL patients compared to non-DS-ALL patients [3]. Therefore, improved treatment strategies are urgently needed to reduce adverse effects and improve survival outcomes.

DS-ALL patients experience toxicity from treatment due to the presence of trisomy 21. The roles of chromosome 21 genes, particularly in the Down syndrome critical region (DSCR) must be investigated to identify new targets for precision therapy (Figure 1). The DSCR encodes many genes involved in cancer associated pathways including cell signalling, proliferation and epigenetic pathways (Table 1) [4]. A number of genes have been identified to play roles in DS-AML, however, these genes do not necessarily have leukaemogenic roles in ALL. For example, *GATA1* mutations are prevalent in 30% of DS children, resulting in a pre-leukaemic haematological disorder called Transient Abnormal myelopoiesis (TAM). DS patients with TAM often undergo transformation to AML at a frequency of 20% [2,5,6]. However, *GATA1* mutations are not observed in DS-ALL patients. ETS-related gene (*ERG*) dysregulation on chromosome 21 has been demonstrated to promote TAM transformation to AML and recently, *DYRK1A* (the dual specificity tyrosine-phosphorylation-regulated kinase 1A) on chromosome 21 was demonstrated to promote AMKL growth [7,8]. These genes have not yet been fully investigated in the context of ALL. The high mobility group nucleosome binding protein 1 (*HMGN1*) has been demonstrated to activate transcription in B-cells and promote B-cell proliferation *in vivo* and may be involved in DS-ALL transformation [4,9].

DS-ALL patients harbour gene fusions involving cytokine receptor like factor 2 (*CRLF2*) at a frequency of 60%, compared to non-DS-ALL patients at 5-16%. *CRLF2* gene fusions are associated with activating mutations in Janus Kinase 2 (*JAK2*), constitutively activating JAK/STAT signalling [3]. JAK2 mutations are observed in 50% of *CRLF2* rearranged ALL patients, however, *RAS* activating mutations are prevalent when *JAK2* mutations are not present [10]. Interestingly, patients with intrachromosomal amplification of chromosome 21 (iAMP21) also have a high incidence of *CRLF2* rearrangements, suggesting a link between genes on chromosome 21 and *CRLF2*. Treatment for other cancers utilise many FDA approved small molecule inhibitors targeting JAK/STAT and RAS signalling that could be re-purposed for use in for a precision treatment approach in DS-ALL. Methotrexate that forms part of many chemotherapeutic regimens inhibits dihydrofolate reductase and interferes with thymidine synthesis to halt DNA replication. This can cause adverse effects for DS patients who have increased expression of genes involved in purine synthesis on chromosome 21 [2].

***Corresponding author:** Deborah White, Cancer Program, Precision Medicine Theme, South Australian Health & Medical Research Institute, Australia, Tel: +610401138305; E-mail: Deborah.White@sahmri.com

Received December 17, 2020; **Accepted** January 09, 2021; **Published** January 16, 2021

Citation: Page E, White D (2021) Understanding the Role of Chromosome 21 for Precision Treatment in Down Syndrome Acute Lymphoblastic Leukaemia. J Alzheimers Dis Parkinsonism 11: 508.

Citation: Page E, White D (2021) Understanding the Role of Chromosome 21 for Precision Treatment in Down Syndrome Acute Lymphoblastic Leukaemia. J Alzheimers Dis Parkinsonism 11: 508.

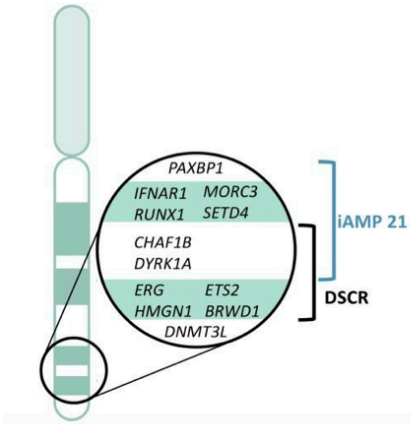

Figure 1: Chromosome 21 schematic depicting critical leukaemic genes located in the Down syndrome critical region and intrachromosomal amplification of chromosome 21 region observed in ALL patients.

Gene	Function
PAXBP1	Binds to PAX3 and PAX7 to regulate transcription
IFNAR1	Activates JAK/STAT signaling
RUNX1	Transcription factor that regulates development of hematopoiesis
MORC3	Chromatin remodeler
SETD4	Methyltransferase
CHAF1B	Chromatin regulator
DYRK1A	Kinase that regulates oncogenes and tumor suppressors
ERG	Hematopoietic oncoprotein
HMGN1	Histone demethylase
ETS2	Transcription factor and oncoprotein
BRWD1	Involved in chromatin regulation and transcriptional activation
DNMT3L	DNA methyltransferase

Table 1: Chromosome 21 genes with functions potentially implicated in leukaemic development or persistence.

Folinic acid (leucovorin) is administered to DS patients (NCT00103285 and NCT00075725) to combat the block in dihydrofolate reductase, as well as risk adapted chemotherapy (NCT01190930 and NCT03286634) which were previously the only precision approaches available for DS patients. Due to the risk of toxicity, DS patients have been excluded from trials of small molecule inhibitors (NCT02723994). However, recent advances have been made in immunotherapies including monoclonal antibodies (mAb), bi-specific T-cell engagers (BiTEs) and chimeric antigen receptor (CAR) T -cell therapies potentiating a new avenue of therapy for DS patients.

Blinatumomab is a single chain antibody construct with bi-specificity, binding to both cytotoxic T-cells through CD3 receptors and B-cells through CD19 receptors (Figure 2). The BiTE engages the immune system to eradicate both B-ALL and normal B-cells which received FDA approval in 2014 [11]. Multiple clinical trials of blinatumomab (NCT03914625, NCT04546399, NCT03117751 and NCT04307576) are currently being established for ALL and DS-ALL patients. Immunotherapies are considered to have less side effects due to their engagement with the patients' immune cells, compared to targeted small molecule inhibitors which are associated with off target effects.

Blinatumomab has been associated with toxicities including Cytokine Release Syndrome (CRS) and neurotoxicity in trials for lymphoma [12]. CRS symptoms can range from headache and fatigue, to multi system organ failure and therefore, must be monitored closely [13]. Despite high response rates, a higher relapse rate has also been observed with the use of blinatumomab. Therefore, blinatumomab is being considered as a bridging treatment prior to haematopoietic stem cell transplant (HSCT), although DS patients have poorer outcomes to HSCT compared to non-DS patients [14].

Trials for the anti-CD19 CAR T-cell, CTL019 (NCT02435849 and NCT02228096), have demonstrated promising results for the treatment of DS-ALL patients with high survival outcomes. Similar rates of toxicities including CRS, neutropenia and neurological effects were observed between DS and non-DS patients. However, a larger patient cohort is needed to determine the safety and efficacy of CTL019 in DS-ALL.

While trials for immunotherapies commence for DS-ALL patients, it is critical to continue investigating chromosome 21 genes and their roles in ALL development or persistence. Previous studies identified the genes responsible for the toxicity DS-ALL patients experience to chemotherapy, and different genes could also affect the

Citation: Page E, White D (2021) Understanding the Role of Chromosome 21 for Precision Treatment in Down Syndrome Acute Lymphoblastic Leukaemia. J Alzheimers Dis Parkinsonism 11: 508.

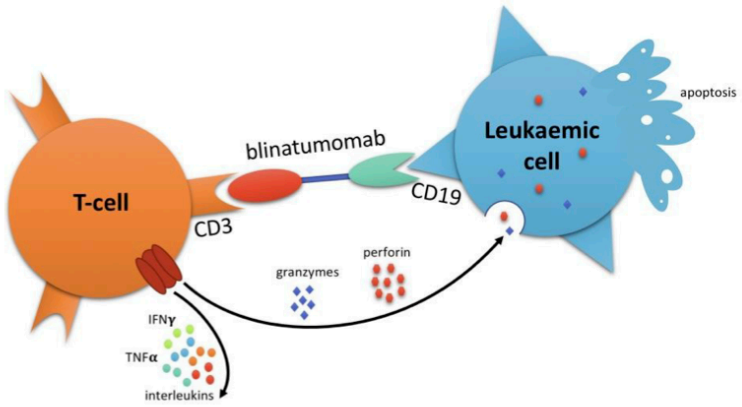

Figure 2: Blinatumomab binds to CD3 and CD19 to link cytotoxic T-cells to leukaemic cells and stimulate the release of interleukins, IFNγ and TNFα, as well as perforin and granzymes to initiate leukaemic cell apoptosis.

efficacy of immunotherapies or targeted approaches. Lessons learnt from the treatment of chronic myeloid leukaemia demonstrate a targeted molecule can revolutionise the treatment of haematological malignancies, transforming poor survival outcomes to a disease now on the brink of achieving treatment free remission [15]. Therefore, the roles of the 31 genes in the DSCR of chromosome 21 need to be fully elucidated to determine their targeting potential and discover the fundamental predisposition DS patients have to developing ALL. Transcriptional activation resulting from increased *HMGN1* expression activates B-cell receptor pathways including SRC kinases in pre-B cells, and JAK/STAT signalling in pro-B cells [9]. Therefore, the investigation of *HMGN1* has led to the identification of potential therapeutic targets including JAK/STAT signalling or protein kinase B (AKT) and BCL6 pathways in DS-ALL.

Interestingly, the gain of chromosome 21 (+21) is the most common cytogenetic abnormality observed in B-ALL patients, suggesting a link between genes located in the DSCR of chromosome 21 and ALL [16]. Investigating the roles these genes play in leukaemogenesis will be of the utmost importance to DS- ALL patient treatment, but also many other subsets of B-ALL patients harbouring +21 or iAMP21. The investigation of targeted therapies is necessary for the treatment of DS-ALL patients who currently experience toxicity to chemotherapy and have poor survival outcomes. While the introduction of immunotherapies is a great advancement for DS-ALL treatment, the fundamental research of DS-ALL aetiology will open new opportunities for safer and more effective treatment.

References

1. Kim S, Sato Y, Mohan PS, Peterhoff C, Pensalfini A, et al. (2016) Evidence that the rab5 effector APPL1 mediates APP-βCTF- induced dysfunction of endosomes in Down syndrome and Alzheimer's disease. Mol Psychiatry. 21: 707-716.
2. Maloney KW, Taub JW, Ravindranath Y, Roberts I, Vyas P (2015) Down syndrome preleukemia and leukemia. Pediatr Clin North Am. 62: 121-137.
3. Buitenkamp TD, Izraeli S, Zimmermann M, Forestier E, Heerema NA, et al. (2014) Acute lymphoblastic leukemia in children with Down syndrome: A retrospective analysis from the Ponte di Legno study group. Blood. 123(1): 70-77.
4. Lane AA, Chapuy B, Lin CY, Tivey T, Li H, et al. (2014) Triplication of a 21q22 region contributes to B cell transformation through HMGN1 overexpression and loss of histone H3 Lys27 trimethylation. Nat Genet. 46(6): 618-623.
5. Bhatnagar N, Nizery L, Tunstall O, Vyas P, Roberts I (2016) Transient abnormal myelopoiesis and AML in Down syndrome: An Update. Curr Hematol Malig Rep. 11(5): 333-341.
6. Hitzler JK, Cheung J, Li Y, Scherer SW, Zipursky A (2003) GATA1 mutations in transient leukemia and acute megakaryoblastic leukemia of Down syndrome. Blood. 101(11): 4301-4304.
7. Birger Y, Goldberg L, Chlon TM, Goldenson B, Muler I, et al. (2013) Perturbation of fetal hematopoiesis in a mouse model of Down syndrome's transient myeloproliferative disorder. Blood. 122(6): 988-998.
8. Malinge S, Bliss-Moreau M, Kirsammer G, Diebold L, Chlon T, et al. (2012) Increased dosage of the chromosome 21 ortholog Dyrk1a promotes megakaryoblastic leukemia in a murine model of Down syndrome. J Clin Invest. 122(3): 948-962.
9. Mowery CT, Reyes JM, Cabal-Hierro L, Higby KJ, Karlin KL, et al. (2018) Trisomy of a Down syndrome critical region globally amplifies transcription via HMGN1 overexpression. Cell Rep. 25(7): 1898-1911.e5.
10. Nikolaev SI, Garieri M, Santoni F, Falconnet E, Ribaux P, et al. (2014) Frequent cases of RAS-mutated Down syndrome acute lymphoblastic leukaemia lack JAK2 mutations. Nat Commun. 5: 4654.
11. Przepiorka D, Ko CW, Deisseroth A, Yancey CL, Candau-Chacon R, et al. (2015) FDA approval: Blinatumomab. Clin Cancer Res. 21(18): 4035-4039.
12. Bargou R, Leo E, Zugmaier G, Klinger M, Goebeler M, et al. (2008) Tumor regression in cancer patients by very low doses of a T cell-engaging antibody. Science. 321: 974-977.
13. Shimabukuro-Vornhagen A, Godel P, Subklewe M, Stemmler HJ, Schlober HA, et al. (2018) Cytokine release syndrome. J Immunother Cancer 6: 56.
14. Aldoss I, Song J, Stiller T, Nguyen T, Palmer J, et al. (2017) Correlates of resistance and relapse during blinatumomab therapy for relapsed/refractory acute lymphoblastic leukemia. Am J Hematol. 92(9): 858-865.
15. Goldman JM (2007) How I treat chronic myeloid leukemia in the imatinib era. Blood. 110: 2828-2837.
16. Heerema NA, Raimondi SC, Anderson JR, Biegel J, Camitta BM, et al. (2007) Specific extra chromosomes occur in a modal number dependent pattern in pediatric acute lymphoblastic leukemia. Genes Chromosomes Cancer. 46: 684-693.

Project Rationale

CRLF2 rearrangements (*CRLF2r*) represent the largest subgroup of high-risk ALL patients with poor survival outcomes. Down Syndrome (DS) patients are predisposed to developing *CRLF2r* and experience extreme treatment related toxicity. Genes located in the Down Syndrome critical region of chromosome 21 are potentially involved in *CRLF2r* leukaemogenesis. Recent reports have implicated *HMGN1* in gene activation of leukaemic cells, however, its role in ALL and particularly, *CRLF2r* ALL remains unknown.

I hypothesise that *HMGN1* increases the leukaemogenicity of *CRLF2r* ALL cells, which can be targeted with small molecule inhibitors. Therefore, this project investigates *HMGN1* using a CRISPR/Cas9 knockout to determine whether it plays key roles in leukaemic cell survival. An overexpression model using Ba/F3 cells was also used to characterise the function of *HMGN1*. This study is critical for our understanding of the predisposition of DS-ALL patients to developing *P2RY8-CRLF2.* Furthermore, validating HMGN1 as a therapeutic target for rational combination treatment approaches, has the potential to reduce the toxicity DS *CRLF2r* ALL patients currently experience with contemporary chemotherapeutic regimens.

The specific aims for this project are:

Aim 1: Identify the role of *HMGN1* in the proliferation and survival of trisomy 21 *CRLF2*+ cells using an *in vivo* xenograft knockout model (Chapter 2).

Aim 2: Explore the cooperation between *P2RY8-CRLF2* and *HMGN1* in a Ba/F3 model and compare active signalling pathways (Chapter 2).

Aim 3: Determine targetability of *P2RY8-CRLF2*, *CRLF2* p.F232C and/or *HMGN1* expressing cells with small molecule inhibitors (Chapters 2 and 4).

Aim 4: Create an endogenously expressed *P2RY8-CRLF2* model using CRISPR/Cas9 to use as a research tool for identification of cooperating oncogenes (Chapter 3).

These aims will be addressed via the processes outlined in figure 1.

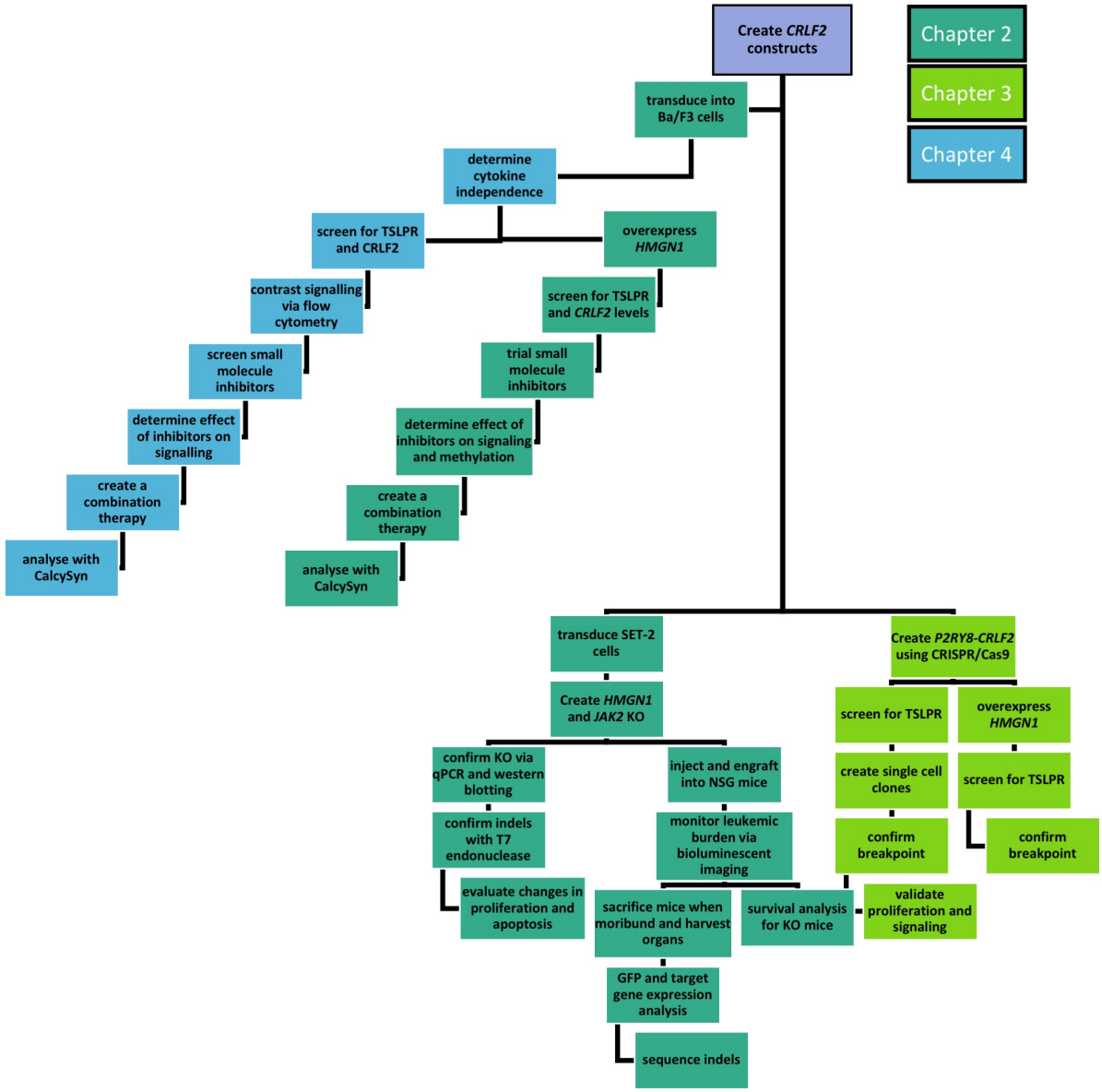

Figure 1: Flow chart outlining the methodology used to address the thesis aims and subsequent thesis result chapters

.

Chapter 2:

HMGN1 is necessary for leukemic cell transformation and proliferation in *CRLF2* related Down Syndrome leukemia

Statement of Authorship

Title of Paper	*HMGN1* is necessary for Down Syndrome leukemic cell proliferation and cooperates with the *P2RY8-CRLF2* fusion to result in leukemic transformation.
Publication Status	☐ Published ☐ Accepted for Publication ☒ Submitted for Publication ☐ Unpublished and Unsubmitted work written in manuscript style
Publication Details	Page, E. C., Heatley, S. L., Eadie, L. J., McClure, B. J., Yeung, D. T., Hughes, T. P., Thomas, P. Q., & White, D. L. (2020). *HMGN1* is necessary for Down Syndrome leukemic cell proliferation and cooperates with the *P2RY8-CRLF2* fusion to result in leukemic transformation. Submitted to *Blood Cancer Journal*

Principal Author

Name of Principal Author (Candidate)	Elyse Page		
Contribution to the Paper	Conceived, designed and performed experiments, analysed results and wrote manuscript		
Overall percentage (%)	95%		
Certification:	This paper reports on original research I conducted during the period of my Higher Degree by Research candidature and is not subject to any obligations or contractual agreements with a third party that would constrain its inclusion in this thesis. I am the primary author of this paper.		
Signature		Date	23/2/21

Co-Author Contributions

By signing the Statement of Authorship, each author certifies that:

i. the candidate's stated contribution to the publication is accurate (as detailed above);

ii. permission is granted for the candidate in include the publication in the thesis; and

iii. the sum of all co-author contributions is equal to 100% less the candidate's stated contribution.

Name of Co-Author	Susan Heatley		
Contribution to the Paper	Supervised, and edited the manuscript		
Signature		Date	23.2.21

Name of Co-Author	Laura Eadie		
Contribution to the Paper	Edited the manuscript		
Signature		Date	23/02/21

Name of Co-Author	Barbara McClure
Contribution to the Paper	Edited the manuscript 25/02/2021

Name of Co-Author	David Yeung		
Contribution to the Paper	Edited the manuscript		
Signature		Date	24 FEB 2021

Name of Co-Author	Timothy Hughes		
Contribution to the Paper	Edited the manuscript		
Signature		Date	23/2/2021

Name of Co-Author	Paul Thomas		
Contribution to the Paper	Supervised, and edited the manuscript		
Signature		Date	24/2/2021

Name of Co-Author	Deborah White		
Contribution to the Paper	Supervised, and edited the manuscript		
Signature		Date	24-2/2021

***HMGN1* is necessary for leukemic cell proliferation and cooperates with the *P2RY8-CRLF2* fusion to result in leukemic transformation**

***HMGN1* is necessary for *CRLF2*+ DS leukemia**

Keywords: acute lymphoblastic leukemia, *P2RY8-CRLF2*, *HMGN1*, Down Syndrome, cell signaling, precision medicine, combination therapy

Elyse C Page[1, 2], Susan L Heatley[1, 3, 4], Laura N Eadie[1, 3], Barbara J McClure[1, 3], David T Yeung[1, 3, 7, 8, 9, 10], Timothy P Hughes[1, 3, 8, 9], Paul Q Thomas[3, 5], and *Deborah L White[1, 2, 3, 4, 6, 7]

1. Cancer Program, Precision Medicine Theme, South Australian Health & Medical Research Institute. Adelaide, SA, Australia

2. School of Biological Sciences, University of Adelaide, Adelaide, SA, Australia

3. Discipline of Medicine, University of Adelaide, Adelaide, SA, Australia

4. Australian and New Zealand Children's Haematology/Oncology Group (ANZCHOG)

5. Gene Editing Program, Precision Medicine Theme, South Australian Health & Medical Research Institute. Adelaide, SA, Australia

6. Australian Genomic Health Alliance (AGHA)

7. Discipline of Paediatrics, University of Adelaide, Adelaide, SA, Australia

8. Australasian Leukaemia and Lymphoma Group, Melbourne, VIC.

9. Department of Haematology, Royal Adelaide Hospital and SA Pathology, Adelaide, SA.

10. School of Pharmacy and Medical Science, University of South Australia, Adelaide, SA.

Visual Abstract

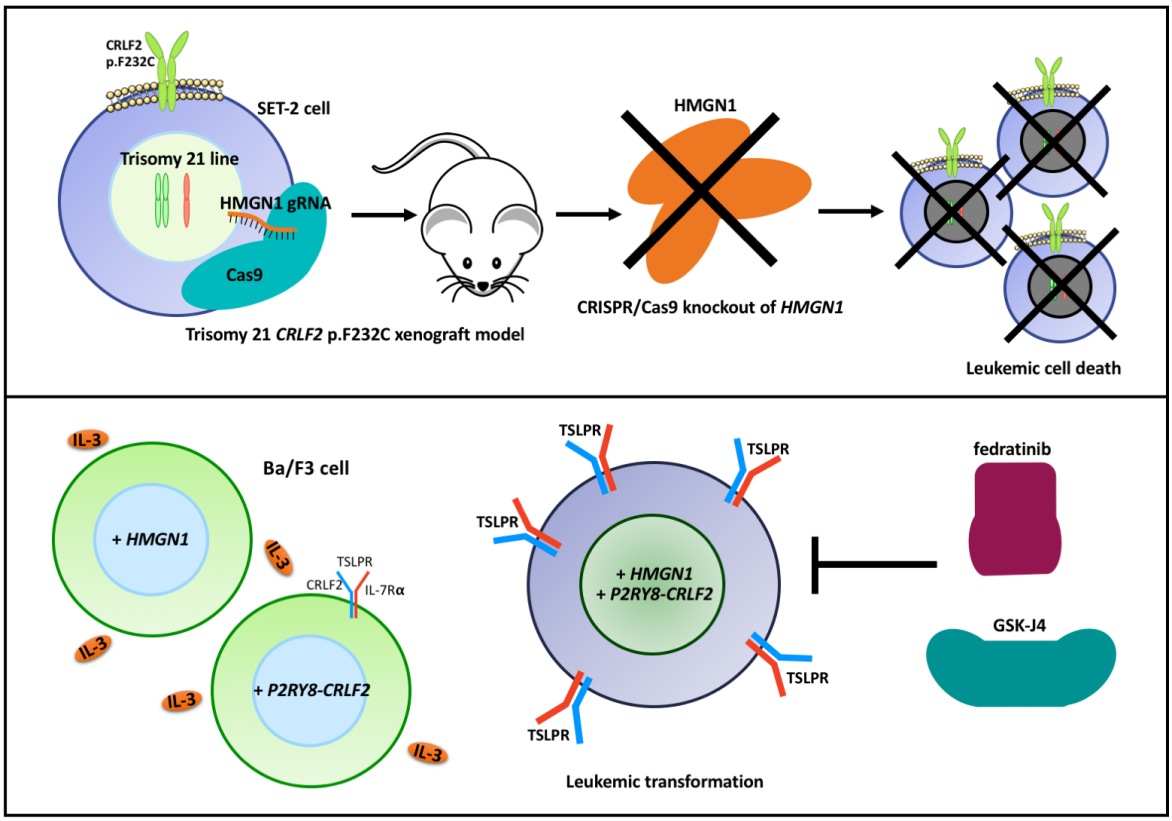

Abstract

The genetic basis for the predisposition for Down Syndrome (DS) patients to develop cytokine receptor like factor 2 rearranged (*CRLF2r*) acute lymphoblastic leukemia (ALL) is currently unknown. As DS is characterised by trisomy 21, genes located on this chromosome and expressed in hematopoietic cells are likely candidates for investigation in *CRLF2r* DS-ALL pathogenesis. Here, we explored the chromosome 21 gene, *HMGN1* (high mobility group nucleosome binding protein 1), in an inducible CRISPR/Cas9 knockout *in vivo* xenograft model to assess the effect of *HMGN1* loss of function on leukemic burden. We also present an *in vitro* model with *HMGN1* overexpression in combination with either *CRLF2r* or the *CRLF2* p.F232C activating mutation, to confirm its role in proliferation and survival. This identified a novel role for *HMGN1* in the upregulation of thymic stromal lymphopoietin receptor (TSLPR). Finally, *in vitro* screening determined targetability of *CRLF2r* and *HMGN1* co-expressing cells using a combination of fedratinib (JAK2 inhibitor), and GSK-J4 (demethylase inhibitor). Increased expression of *HMGN1* due to trisomy 21 provides a proliferative and survival advantage to *CRLF2r* or *CRLF2* p.F232C DS-ALL cells and identified here is a synergistic combination of small molecule inhibitors to target these cells. Together, these data provide critical insight into the development and persistence of *CRLF2r* DS-ALL and identify a potential target for a precision treatment approach to reduce the toxicity DS-ALL patients experience from current treatment regimes.

Introduction

Down Syndrome (DS) is characterised by the triplication of chromosome 21, commonly arising from nondisjunction during meiosis. DS patients display an elevated risk of neurodevelopmental disorders, congenital heart defects and hematological malignancies including acute lymphoblastic leukemia (ALL)[1] Trisomy 21 is implicated in many cancer associated pathways[3-5] as 16 genes overexpressed on chromosome 21 are directly involved in hematopoiesis, tumorigenesis and epigenetic regulation[1,2]. Children diagnosed with ALL have an overall survival (OS) of 85-90% however, DS-ALL patients have a lower OS of 75%, and a mortality rate four times greater than non-DS patients within the first two years of diagnosis[6]. Higher relapse rates and treatment related toxicities are observed in DS-ALL cohorts compared to non-DS ALL[7,8].

Approximately 60% of DS-ALL patients, compared to 5-16% of non-DS-ALL patients, harbor rearrangement of cytokine receptor like factor 2 (*CRLF2r*), associated with poor survival outcomes[9-12]. An interstitial deletion of the intervening genes between *CRLF2* and the purinergic receptor (*P2RY8*) on the X/Y chromosome result in the *P2RY8-CRLF2* fusion gene; the most common alteration seen in children with DS-ALL[13]. Of these, ~9% acquire the aggressive *CRLF2* p.F232C activating mutation[10]. *CRLF2r* are often associated with point mutations in Janus Kinase 2 (*JAK2*) which is essential for leukemic transformation in *CRLF2r* cells[14], resulting in an increase in thymic stromal lymphopoietin receptor (TSLPR) and JAK/STAT signaling. There is currently no effective targeted treatment against *CRLF2r* ALL, despite it being one of the most frequently observed high risk subtypes of ALL in children[15-17]. However, ruxolitinib (a JAK1/2 inhibitor) is currently being assessed in a Phase 2 trial, in combination with

chemotherapy, for children with *CRLF2r* and/or JAK mutations (NCT02723994). Interestingly, DS is an exclusion criterion for this study. Due to the toxicities DS patients experience from chemotherapy[15] the development of personalised treatment approaches are of particular significance for the treatment of DS-ALL.

Increased gene dosage as a result of trisomy 21 have been implicated in the development of DS-ALL[1, 18]. Recent reports have demonstrated a role for the high mobility group nucleosome binding protein 1 (*HMGN1*) in global activation of transcription in DS-ALL patients[4,19]. HMGN1 is a chromatin modulator that competes with histone H1 for binding to the nucleosome to modulate histone post-translational modifications[20,21] and changes the expression pattern of 1,200 genes[22]. There are no current pharmacological inhibitors of HMGN1, however, previous studies have demonstrated efficacy using the demethylase inhibitor GSK-J4 to reduce global demethylation and counteract HMGN1[4,23].

We hypothesised targeting *HMGN1* could decrease the leukemic burden of DS-ALL patients harboring the *P2RY8-CRLF2* fusion. We report *in vitro* and *in vivo* findings of the involvement of *HMGN1* in leukemic proliferation and transformation of previously non-transformed *P2RY8-CRLF2* B-cells via the upregulation of TSLPR and JAK/STAT, ERK and S6 signaling pathways. This study interrogates the biology and function of increased gene dosage of *HMGN1* by modelling with *CRLF2r* ALL and the findings presented here have the potential to positively impact treatment for 60% of DS-ALL patients who harbor the *P2RY8-CRLF2* fusion.

Results

Generation of a *HMGN1*-null *CRLF2* Down Syndrome leukemic cell pool in SET-2 cells

The trisomy 21 acute megakaryoblastic leukemia (AMKL) cell line, SET-2, the only trisomy 21 leukemic cell line currently available, was transduced to express the *CRLF2* p.F232C *(CRLF2^{F232C})* activating mutation. An 11-fold upregulation of surface TSLPR was demonstrated by flow cytometry (Fig S1A) compared to isotype control. Using this model, a CRISPR/Cas9 KO of *HMGN1* was created via transduction of Cas9 and a single inducible guide RNA (gRNA) system[25] (Fig S1B) to create a frameshift mutation in an early coding exon of the gene. SET-2 cells endogenously express the *JAK2* p.V617F mutation that is responsible for driving cell proliferation[26]. To contrast the effects of the *HMGN1* KO, a KO of *JAK2* was also generated. As a control, *HMGN1* and *JAK2* KOs were replicated in the non-trisomy 21, non-*CRLF2* expressing Jurkat cell line (Fig S1C).

The targeted exon of each gene was amplified, and Sanger sequencing confirmed the presence of an indel (Δ) (Δ*HMGN1* exon 5 or Δ*JAK2* exon 5) and subsequent frameshift mutation in the pool of CRISPR/Cas9 edited cells (Fig 1A & C). CRISPR/Cas9 ICE gene-editing analysis indicated a KO score of 53 in *JAK2* (r^2=0.94) with 55% of alleles containing indels and a KO score of 56 in *HMGN1* (r^2=0.93) with 66% of the alleles containing indels (Fig 1B & D). The SET-2 *CRLF2^{F232C}* and Jurkat *JAK2* and *HMGN1* KO lines each had a two-fold depletion in mRNA expression of the KO gene compared to the Cas9 control lines (Fig 1E, *JAK2* p=0.01; Fig 1F, *HMGN1* p=0.048).

To examine specificity of the CRISPR/Cas9 *HMGN1* gRNA, the expression level of *HMGN2* was confirmed to remain the same regardless of *HMGN1* KO (Fig S2A). Western blotting confirmed a 98% reduction of HMGN1 (p=0.009) and an 80% reduction in JAK2 (p=0.017) protein expression in SET-2 $CRLF2^{F232C}$ KO lines (Fig 1G-H & S3) and a 60% reduction of HMGN1 and 40% reduction of JAK2 protein expression in Jurkat KO cells compared to their respective Cas9 control lines.

HMGN1 is necessary for Down Syndrome leukemic cell proliferation and survival

To elucidate the effect of *HMGN1* on proliferation rates, a CellTiter-Glo 2.0® proliferation assay was used to determine the effect of HMGN1 loss of function in SET-2 $CRLF2^{F232C}$ and Jurkat cells. gRNA expression was induced at day 0 and luminescence was measured daily for five days. While the SET-2 $CRLF2^{F232C}$ Cas9 line proliferated over the five-day period, the *JAK2* and *HMGN1* KO cells halted proliferation post day three [*JAK2*: p<0.001; *HMGN1*: p=0.005 compared to Cas9 control line (Fig 2A)]. This finding was specific to the SET-2 $CRLF2^{F232C}$ cells as *JAK2* and *HMGN1* KOs in Jurkat cells proliferated throughout the five-day period (Fig 2B). These results were replicated with an alternate set of gRNAs to confirm on target effects (Fig S4).

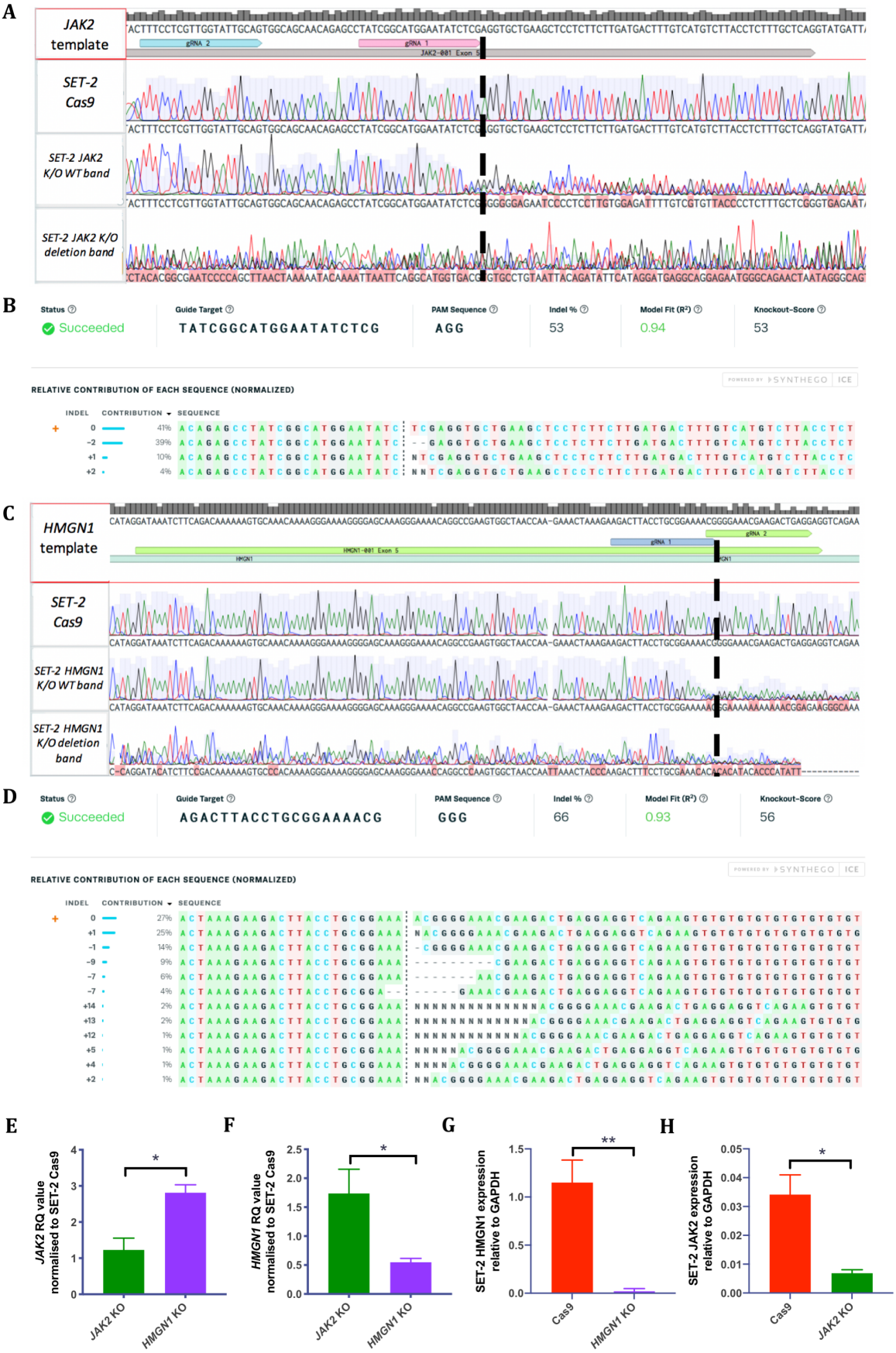
A
JAK2 template
SET-2 Cas9
SET-2 JAK2 K/O WT band
SET-2 JAK2 K/O deletion band
B
Status
Succeeded
Guide Target
TATCGGCATGGAATATCTCG
PAM Sequence
AGG
Indel %
53
Model Fit (R²)
0.94
Knockout-Score
53
RELATIVE CONTRIBUTION OF EACH SEQUENCE (NORMALIZED)
INDEL
CONTRIBUTION
SEQUENCE
C
HMGN1 template
SET-2 Cas9
SET-2 HMGN1 K/O WT band
SET-2 HMGN1 K/O deletion band
D
Status
Succeeded
Guide Target
AGACTTACCTGCGGAAAACG
PAM Sequence
GGG
Indel %
66
Model Fit (R²)
0.93
Knockout-Score
56
RELATIVE CONTRIBUTION OF EACH SEQUENCE (NORMALIZED)
E
JAK2 RQ value normalised to SET-2 Cas9
JAK2 KO
HMGN1 KO
F
HMGN1 RQ value normalised to SET-2 Cas9
JAK2 KO
HMGN1 KO
G
SET-2 HMGN1 expression relative to GAPDH
Cas9
HMGN1 KO
H
SET-2 JAK2 expression relative to GAPDH
Cas9
JAK2 KO

Figure 1: Knockouts of *JAK2* and *HMGN1* were generated in SET-2 *CRLF2* p.F232C and Jurkat cell lines by CRISPR/Cas9. JAK2 and *HMGN1* KO was confirmed by Sanger sequencing and electropherograms show mixed trace downstream of the gRNA cut site (indicated by the dotted line) in *JAK2* **(A)** and *HMGN1* **(C)** compared to the Cas9 control cell line. Synthego ICE analysis demonstrating sequencing variations and KO score in *JAK2* **(B)** and *HMGN1* **(D)** KO line DNA. Fold change of mRNA production in *JAK2* **(E)** and *HMGN1* **(F)** KOs in SET-2 *CRLF2* p.F232C cells normalised to Cas9 control line and housekeeper **β**-actin gene. Quantification of western blotting using a LiCor Odyssey® and ImageStudio™ for HMGN1 **(G)** and JAK2 **(H)** KOs in SET-2 cells relative to GAPDH housekeeper protein. All graphs show mean of n=3 with SEM error bars, *$p<0.05$, **$p<0.01$, ***$p<0.001$ using *t*-test comparing the gRNA lines to the Cas9 control line.

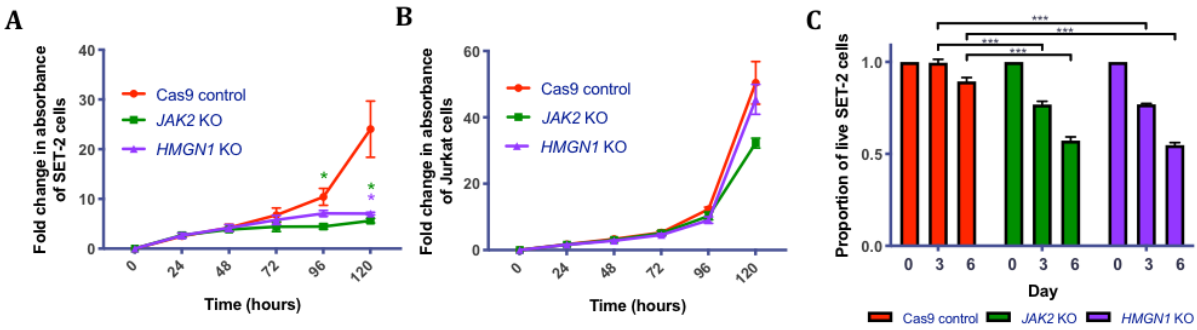

Figure 2: Knockouts of *JAK2* or *HMGN1* result in decreased proliferation and survival of SET-2 cells expressing *CRLF2* p.F232C. The fold change in proliferation of **A)** SET-2 and **B)** control Jurkat cells when either *JAK2* or *HMGN1* gRNA was induced with doxycycline at day 0 was measured by CellTiter Glo 2.0® and assessed over 5 days. Absorbance reading measured using a Perkin Elmer Victor X5 luminometer. **C)** Viable cells from Aqua LIVE/DEAD™ cell death assay when gRNA was induced at day 0 to day 3 and 6 in SET-2 cells. All graphs represent the mean of biological replicate n=3 with SEM error bars, *p<0.05, **p<0.01, ***p<0.001 using t-test comparing the gRNA lines to the Cas9 control line.

To ascertain whether the *HMGN1* KO also induced cell-death, gRNAs were induced in both cell lines at day 0 and were stained with Aqua LIVE/DEAD™ on day 3 and 6. The SET-2 $CRLF2^{F232C}$ KO lines demonstrated a 50% reduction in viability by day 6 ($p<0.001$ compared to Cas9 control, Fig 2C), while the equivalent Jurkat KO cells did not induce cell death (Fig S2B).

Knockout of *HMGN1* in *CRLF2* Down Syndrome cells reduces leukemic burden *in vivo*

SET-2 $CRLF2^{F232C}$ cells harboring Cas9 only, or the *HMGN1* or *JAK2* gRNA, and a luciferase construct were injected into 6-week old sub-lethally irradiated NSG mice (Fig 3A). The mice were monitored via bioluminescent imaging for precise quantification of leukemic burden and response to the KO of *JAK2* or *HMGN1*. BM leukemic engraftment was observed on day 10 with a radiance signal of $\sim 1x10^4$ $p/s/cm^2/sr$ (Fig 3B). Following gRNA induction (day 11), a significant reduction in tumor burden (Cas9: $8.4x10^5 \pm 1.7x10^5$; *JAK2*: $2.7x10^4 \pm 8.9x10^3$; *HMGN1*: $1.5x10^5 \pm 1.7x10^4 p/s/cm^2/sr$) was observed in both prone and supine views of the *JAK2* and *HMGN1* KO mice by day 20 [*JAK2* and *HMGN1* KO compared to Cas9: prone: $p<0.001$; supine: $p=0.005$ (Fig 3C & S5C) consistent with previous pilot study (Fig S5)].

Cas9 control mice (n=6) were culled at day 35 due to advancing leukemia and subsequent health deterioration as per experimental protocol. To directly compare the leukemic burden of the KO and control mice, 3 each of the *JAK2* and *HMGN1* KO mice were also culled at day 35. Blood counts from the Cas9, *JAK2* and *HMGN1* KO mice indicated similar white blood cell (WBC) counts ($p>0.05$, Fig 4A), however, the *HMGN1*

KO mice had significantly increased platelet counts and hematocrit (HCT) and *JAK2* KO mice demonstrated the same trend (Fig 4B-C, *HMGN1* KO platelets: 1503±83 K/μL, $p<0.001$; HCT: 38±3.4%, $p=0.004$; *JAK2* KO platelets: 3046±775 K/μL; HCT: 47±6.8%) compared to Cas9 mice (platelets: 705±43 K/μL, HCT: 22.5±2%). KO mice also had reduced spleen weight [(Fig 4D) *HMGN1*: 51±6 mg, $p=0.046$; *JAK2*: 46±2 mg, $p=0.019$ compared to Cas9: 81±7 mg] and liver weight (Fig 4E). Megakaryoblastic infiltration was noted in the spleen, liver and BM of Cas9 mice but not in KO mice; these were large cells with irregular nuclei and high nuclear-cytoplasmic ratio (Fig 4G & S6A). This correlated with decreased *HMGN1* or *JAK2* expression in respective organs of KO mice compared to Cas9 mice as demonstrated by RQ-PCR (Fig 4H-I). Importantly, *JAK2* and *HMGN1* KO mice survived 62 and 56 days respectively, as compared to Cas9 control mice that had to be culled at 35 days. [$p=0.0009$ (Fig 4F)].

To determine gene editing efficacy in the persisting cells (post day 35), gDNA was extracted from the GFP+ BM cells of *JAK2* and *HMGN1* KO mice. Predominantly WT *JAK2* or *HMGN1* was detected, along with a non-lethal isoform Δ*JAK2* or Δ*HMGN1* exon 5 present in KO mice demonstrating evidence of gene editing that resulted in outgrowth of cells harboring functional genes rather than a KO (Fig S6C-E). CRISPR ICE editing analysis performed on the non-lethal, 69 bp Δ*HMGN1* exon 5, identified only 23% indels in the population with a KO score of 10 ($r^2=0.23$) in the forward sequence and 7% indels in the reverse with a KO score of 2 [$r^2=0.07$ (Fig S6F-G)].

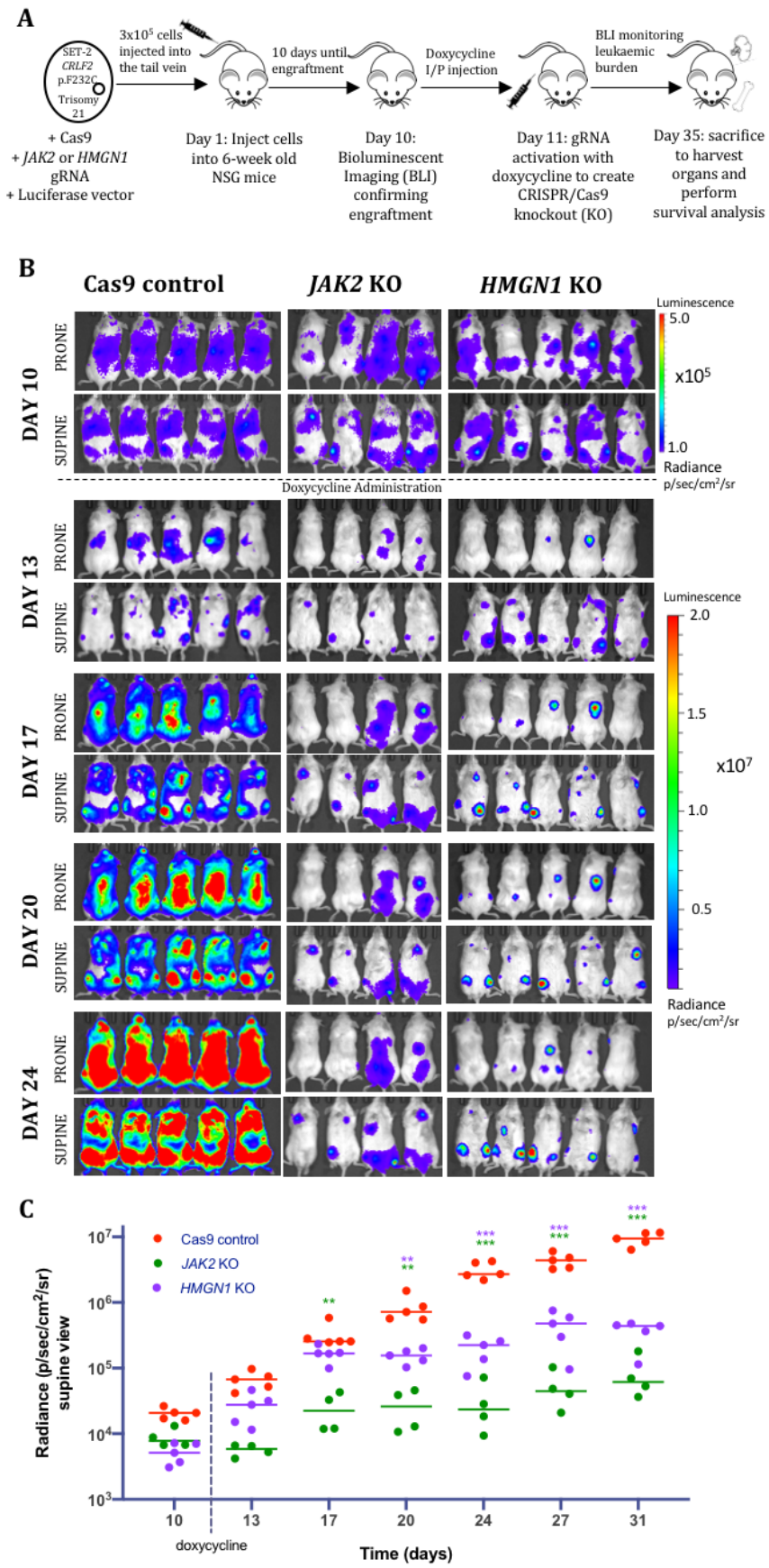
A
SET-2
CRLF2
p.F232C
Trisomy 21
+ Cas9
+ JAK2 or HMGN1 gRNA
+ Luciferase vector
3x10^5 cells injected into the tail vein
Day 1: Inject cells into 6-week old NSG mice
10 days until engraftment
Day 10: Bioluminescent Imaging (BLI) confirming engraftment
Doxycycline I/P injection
Day 11: gRNA activation with doxycycline to create CRISPR/Cas9 knockout (KO)
BLI monitoring leukaemic burden
Day 35: sacrifice to harvest organs and perform survival analysis
B
Cas9 control
JAK2 KO
HMGN1 KO
DAY 10
DAY 13
DAY 17
DAY 20
DAY 24
PRONE
SUPINE
Doxycycline Administration
Luminescence
5.0
x10^5
1.0
Radiance p/sec/cm²/sr
2.0
1.5
x10^7
1.0
0.5
C
Cas9 control
JAK2 KO
HMGN1 KO
Radiance (p/sec/cm²/sr) supine view
10
13
17
20
24
27
31
doxycycline
Time (days)

Figure 3: Knockout of *HMGN1* reduces *CRLF2* p.F232C leukemic burden *in vivo*. A) Inducible CRISPR/Cas9 xenograft model schematic. **B)** Bioluminescent imaging of NSG mice engrafted with SET-2 *CRLF2* p.F232C cells with Cas9 vector only, or with a gRNA targeting *JAK2* or *HMGN1*. Doxycycline was administered on day 11 (dashed line) to induce KO. Images taken using a Perkin Elmer IVIS Imager and analysed using Living Image® Software. **C)** Luminescent data of each mouse as a region of interest (ROI) shown in radiance, normalised to the background signal ROI and luminescence signal of cell lines injected. Graph represents median, *p<0.05, **p<0.01, ***p<0.001 using *t*-test comparing the KO mice to the Cas9 control mice.

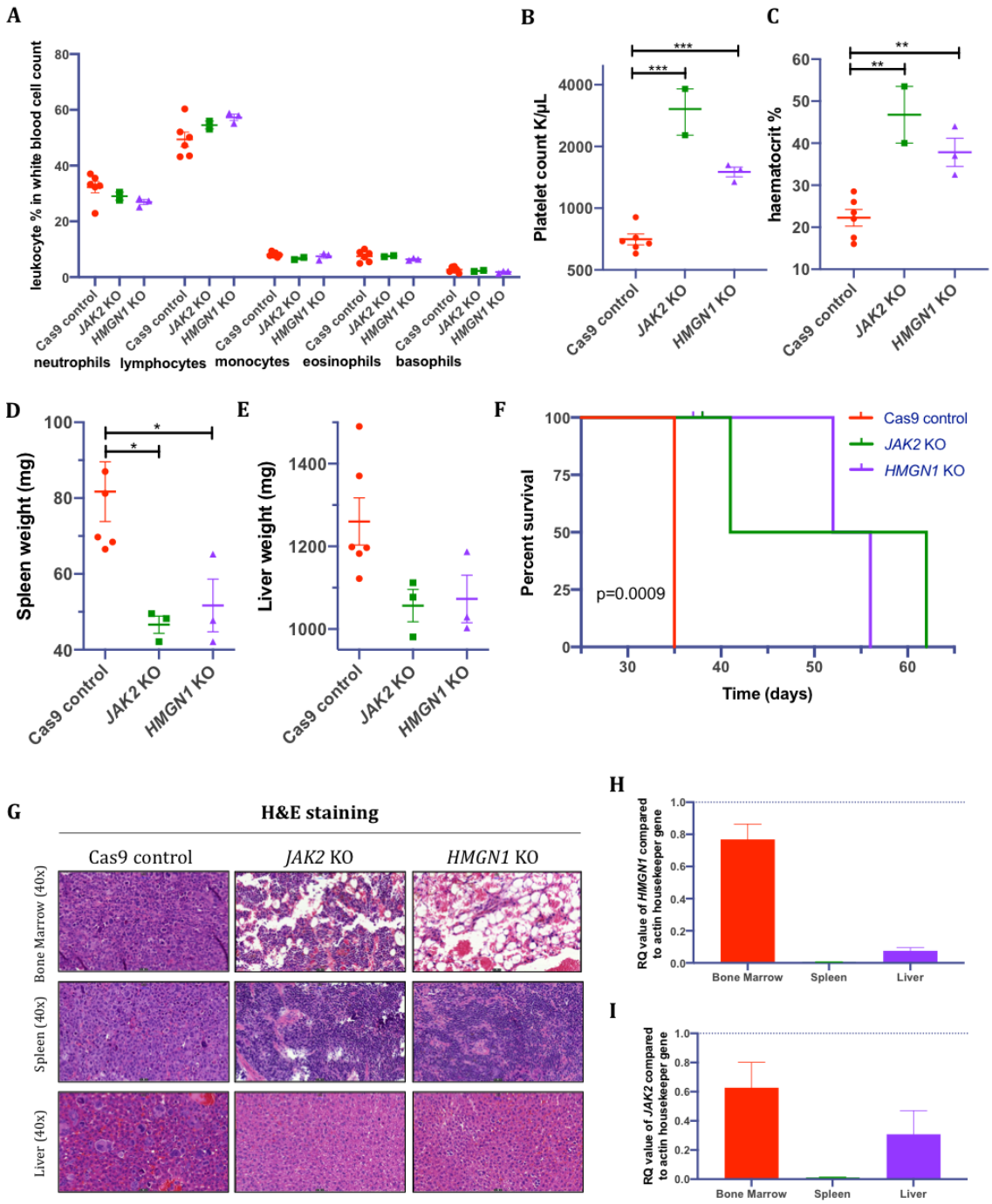

Figure 4. Knockout of *HMGN1* does not alter leukocyte counts, increases platelets, rescues leukemic phenotype and increases survival outcomes. Complete blood counts performed on Cas9 control (n=6) and *JAK2* (n=2) or *HMGN1* (n=3) KO mouse cohorts at Day 35, leukocyte count **(A)**, platelet count **(B)** and hematocrit **(C)**. Spleen **(D)** and liver **(E)** weights from Cas9, *JAK2* KO and *HMGN1* KO

mice at day 35. Values represent mean ± SEM. Student's *t*-test was used to determine significance *$p<0.05$, **$p<0.01$, ***$p<0.001$. Note: *JAK2* KO mice n=2 due to insufficient sample. **F)** Kaplan-Meier survival curve of NSG mice with a *JAK2* or *HMGN1* KO in SET-2 *CRLF2* p.F232C cells. Cas9 n=6, *JAK2* KO n=3, *HMGN1* KO n=3. Significance determined using a log-rank test. Censored mice culled at days 37 and 38 are indicated. **G)** Representative H&E staining of BM, spleen and liver sections from Cas9, *JAK2* KO and *HMGN1* KO mice. Images analyzed at 40x magnification using CaseViewer Software. RQ-PCR demonstrating decreased expression of *HMGN1* **(H)** or *JAK2* **(I)** in *HMGN1* or *JAK2* KO mice organs compared to Cas9 control mice.

P2RY8-CRLF2 and _HMGN1_ contribute to leukemic transformation in DS-ALL

To characterise the leukemic potential of *HMGN1* in a *CRLF2* altered ALL model, overexpression constructs of *HMGN1* alone, *P2RY8-CRLF2 (CRLF2r),* WT *CRLF2 (CRLF2^{WT})* or *CRLF2^{F232C}* ±*HMGN1* were expressed in Ba/F3 cells. *CRLF2* and *HMGN1* overexpression was confirmed by RQ-PCR (Fig S7B) and surface TSLPR expression by flow cytometry (Fig S7A). Cells were cultured without IL-3 allowing the driver potential of each lesion to be assessed. Under these conditions parental Ba/F3 cells, *CRLF2r*, *CRLF2^{WT}* and *HMGN1* individually expressing lines were unable to proliferate (Fig 5A). Importantly, the co-expression of *HMGN1* in *CRLF2r* and *CRLF2^{WT}* lines was associated with cytokine independent growth and a 1000-fold increase in proliferation (p<0.001) indicating the addition of *HMGN1* is sufficient for leukemic transformation when *CRLF2* is present. Ba/F3 *CRLF2^{F232C}* cells were also cytokine independent as previously reported[10,27], however, the proliferation rate did not change with the co-expression of *HMGN1*.

Overexpression of _HMGN1_ results in upregulation of _P2RY8-CRLF2_ and cell signaling pathways

To explore the relationship between *CRLF2r*, *CRLF2^{F232C}* and *HMGN1*, Ba/F3 cells expressing *CRLF2* with or without *HMGN1* were used. Significantly, *CRLF2r*+*HMGN1* cells resulted in a 7-fold increase in TSLPR [mean fluorescence intensity (MFI) 141 to 7680, p=0.008] compared to cells expressing *CRLF2r* alone (Fig 5B-C). The co-expression of *HMGN1* with *CRLF2^{WT}* or *CRLF2^{F232C}* cells also resulted in an increasing trend in TSLPR expression (normalised MFI from 83 to 128 and 200 to 266 respectively, both p>0.05).

Similarly, RQ-PCR for *CRLF2* demonstrated a significant, 5.8-fold increase in *CRLF2* mRNA expression in *CRLF2r*+*HMGN1* cells (p=0.034). Interestingly, *CRLF2*^{F232C}+*HMGN1* cells had lower expression of *CRLF2* mRNA than *CRLF2r*+*HMGN1* cells (Fig 5D, p=0.028) despite having equivalent TSLPR surface expression (Fig 5B), indicating *HMGN1* may be influencing post translational modifications in addition to influencing mRNA expression. These results suggest a direct link exists between *HMGN1* and *CRLF2r* specifically.

In *CRLF2r* or *CRLF2*^{WT} cells, overexpression of *HMGN1* resulted in increased levels of phosphorylated (p)STAT5 (*CRLF2r*: p<0.001, *CRLF2*^{WT}: p=0.013), pERK (*CRLF2*^{WT} & *CRLF2r*: p<0.001) and pS6 kinase (*CRLF2*^{WT} & *CRLF2r*: p<0.001, Fig 5E-G & S8). A decrease in H3K9me2 (*CRLF2*^{WT}: p<0.001) and H3K27me3 (both p<0.01) and increase in H3K9ac [both p=0.04 (Fig 5H-J)] was also observed. The impact of the addition of *HMGN1* was markedly different in the *CRLF2*^{F232C} cells. While an increase in H3K9ac (p=0.028) was also noted in *CRLF2*^{F232C}+*HMGN1* cells, there was no increase in pSTAT5, or pERK, nor was there significant reductions in H3K9me2 or H3K27me3. A significant decrease in pS6 (p<0.001) was noted in *CRLF2*^{F232C}+*HMGN1* cells, suggesting that the addition of *HMGN1* to Ba/F3 *CRLF2*^{F232C} cells impacts different pathways.

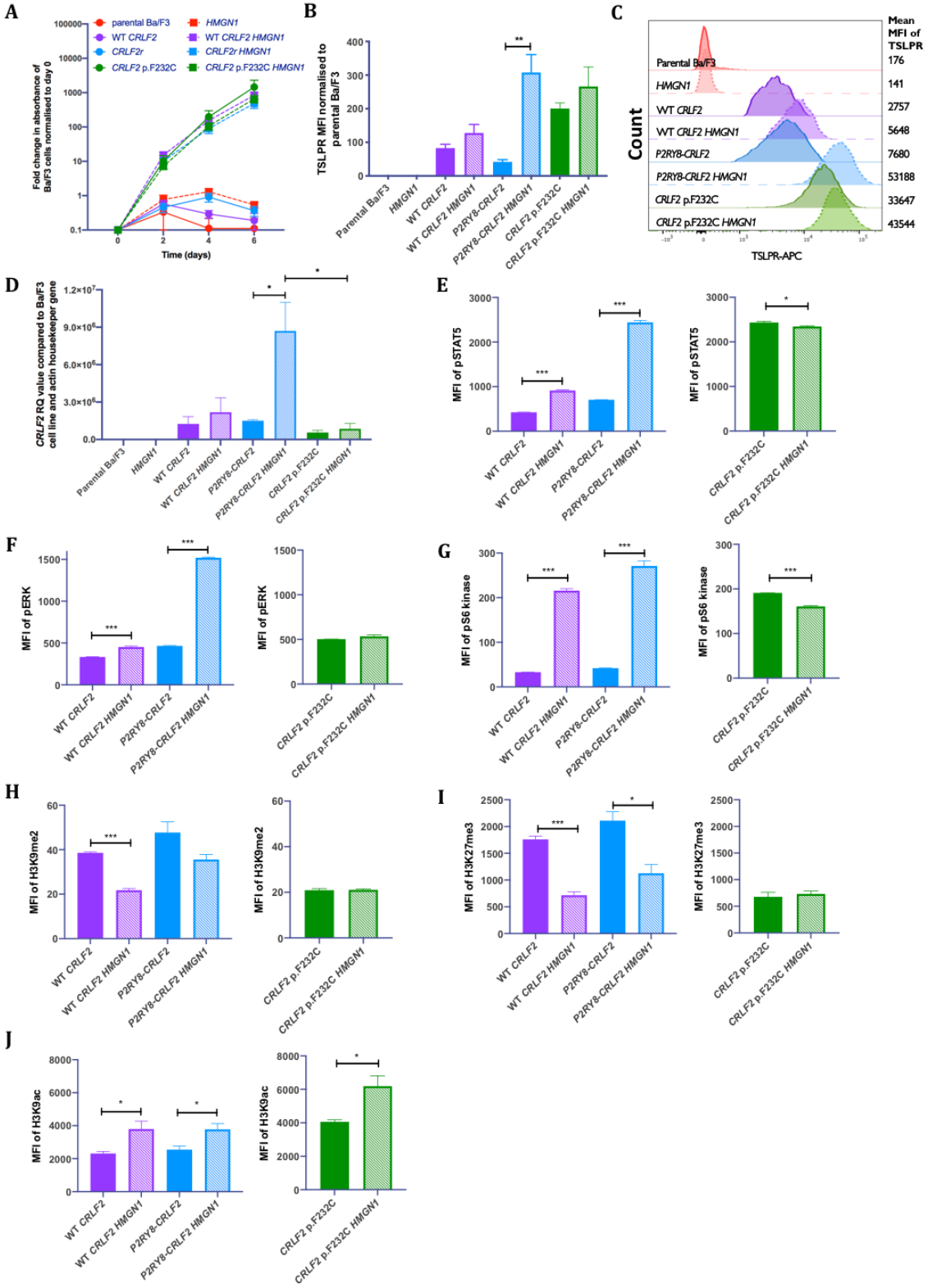

Figure 5: Characterising the signaling profile when *HMGN1* is overexpressed in *CRLF2*+ Ba/F3 cells. A) Factor independent growth was assessed by CellTiter Glo 2.0® proliferation assay over 6 days, culturing Ba/F3 cells in media in the absence of IL-3.

Absorbance reading measured using a Perkin Elmer Victor X5 luminometer. **B)** Quantifying the surface expression of TSLPR-APC in Ba/F3 *HMGN1* and *CRLF2* cell lines starved of IL-3 for 6 hours via flow cytometry. **C)** Representative histogram depicting data displayed in panel B. **D)** Using RQ-PCR to measure *CRLF2* mRNA expression in Ba/F3 *HMGN1* and *CRLF2* cell lines starved of IL-3 for 6 hours. RQ values were determined using housekeeper actin expression and normalised to the parental Ba/F3 control cell line. Phosphorylation levels of STAT5-PE **(E)**, ERK-PE **(F)**, S6 kinase-APC **(G)**, and methylation of H3K9me2 **(H)**, H3K27me3 **(I)** and acetylation of H3K9-AF647 **(J)** of Ba/F3 cell lines expressing *CRLF2r* and/or *HMGN1* measured by intracellular flow cytometry after being starved of IL-3 for 6 hours. All graphs represent the mean of biological replicate of n=3 with SEM error bars and a Student's *t*-test was used between each Ba/F3 cell line and its corresponding +*HMGN1* expressing line to determine significance, *$p<0.05$, **$p<0.01$, ***$p<0.001$.

Drug targeting of cells co-expressing *P2RY8-CRLF2* and *HMGN1* using a combination of fedratinib and GSK-J4

Although a targeted inhibitor specific to *HMGN1* does not currently exist, decreased global methylation as a result of *HMGN1* can be corrected by GSK-J4 (J4), a demethylase inhibitor, as demonstrated in a Ba/F3 model[4,19]. We confirmed a dose dependent decrease in viability of Ba/F3 cells co-expressing *CRLF2*+*HMGN1* when treated with J4 (Fig 6A). *CRLF2r*+*HMGN1* were the most sensitive ($LD50^{J4}$ 3.6 μM±0.04, $CRLF2^{WT}$+*HMGN1* (LD_{50}^{J4} 3.7 μM±0.05) and $CRLF2^{F232C}$+*HMGN1* were the least sensitive (LD_{50}^{J4} 4.4 μM±0.04). Inhibition of de-methylation influenced signaling, as demonstrated by a decrease in pSTAT5 and pS6 kinase (p<0.05) and a significant increase in pERK (p<0.05) when cells were treated with J4 for 2 hours compared to the vehicle control in all *CRLF2*±*HMGN1* lines (Fig 6B-D & S9). Interestingly, an increase in H3K9me2 (p<0.05) was observed in all J4 treated cells (Fig 6E), despite *HMGN1* having no impact on $CRLF2^{F232C}$ methylation (Fig 5H-I). No change was observed in H3K27me3 when comparing to the vehicle control in *CRLF2*±*HMGN1* lines, except for a decrease in $CRLF2^{F232C}$+*HMGN1* [p=0.004 (Fig 6F)].

We demonstrated that JAK2 inhibition could influence survival of *HMGN1* expressing cells by using the specific JAK2 inhibitor, fedratinib, in a cell death assay. The $LD_{50}^{fedratinib}$ in *CRLF2r*+*HMGN1* cells was 0.58±0.02 μM (Fig 6G) and $CRLF2^{WT}$+*HMGN1* lines was 0.8±0.1 μM. $CRLF2^{F232C}$+*HMGN1* cells were less sensitive [LD_{50} of 1.6±0.07 μM (Fig 6G)], but still within the clinically achievable range of 1-3 μM[28]. When J4 and fedratinib were combined, a significant synergistic effect [Combination Index CI (CI<1)] was observed for all Ba/F3+*HMGN1* expressing lines (Fig 6H & Table SIV);

CRLF2r+HMGN1 (0.3 μM fedratinib+1 μM J4), *CRLF2*^{WT}*+HMGN1* (0.6 μM fedratinib+2.1μM J4) and *CRLF2*^{F232C}*+HMGN1* (0.84 μM fedratinib+2.1 μM J4).

CRLF2^{F232C}*+HMGN1* cells exhibited altered phosphorylation of pSTAT5, pERK and pS6 kinase, compared to WT or *CRLF2r+HMGN1* cells, but still increased gene activation marks H3K9ac (Fig 5E-G & J). To determine the effect of *HMGN1* on *CRLF2*^{F232C} cells, RQ-PCR was performed on genes downstream of STAT5. *CDKN1*, *MYC*, *MCL1* and *BCL2* were significantly increased (3-5-fold) compared to *CRLF2*^{F232C} cells, whereas this upregulation was not observed in *CRLF2*^{WT} or *CRLF2r+HMGN1* lines (Fig 6I).

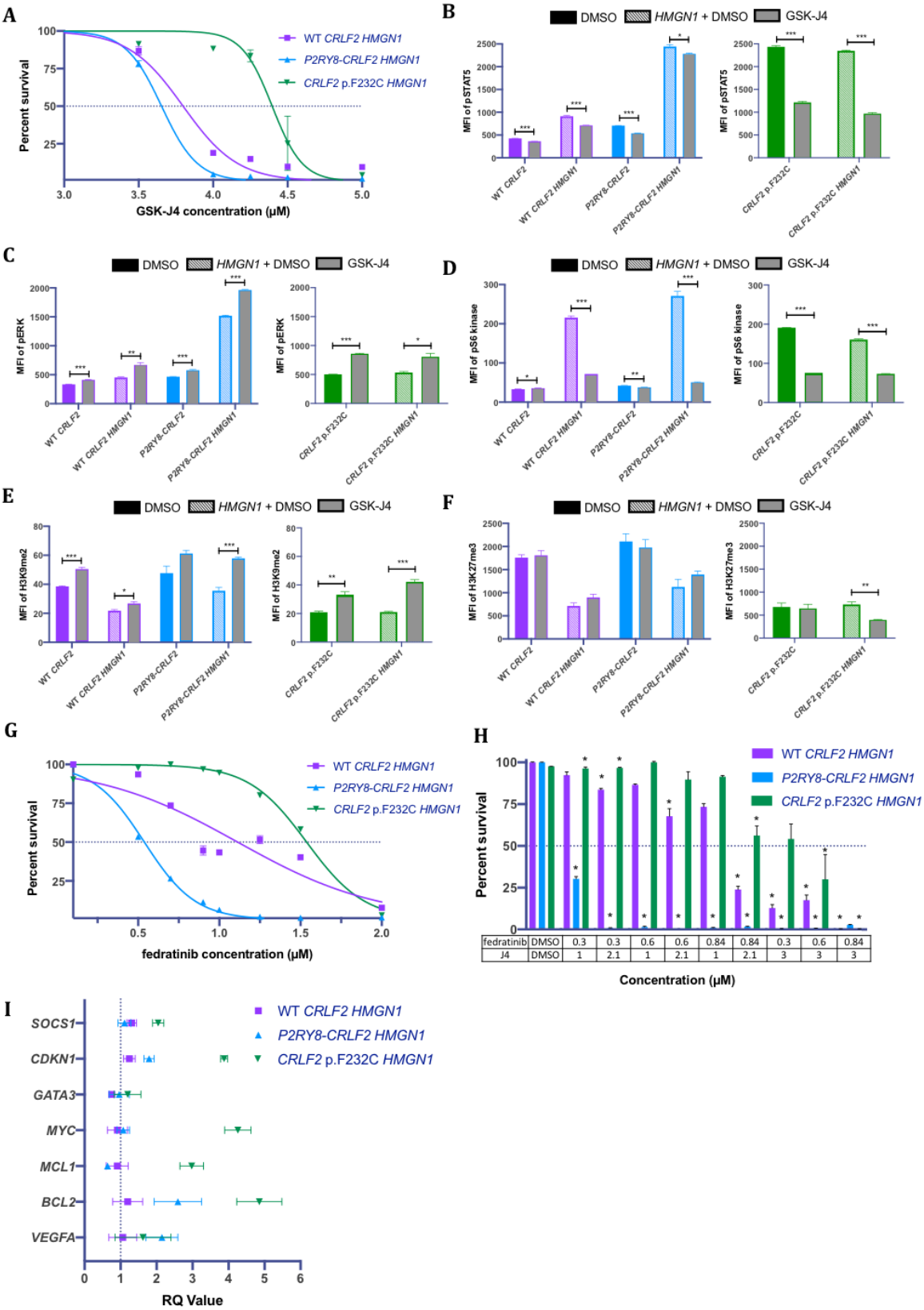
A
Percent survival
GSK-J4 concentration (μM)
WT CRLF2 HMGN1
P2RY8-CRLF2 HMGN1
CRLF2 p.F232C HMGN1
B
DMSO
HMGN1 + DMSO
GSK-J4
MFI of pSTAT5
C
MFI of pERK
D
MFI of pS6 kinase
E
MFI of H3K9me2
F
MFI of H3K27me3
G
fedratinib concentration (μM)
H
Concentration (μM)
fedratinib DMSO 0.3 0.3 0.6 0.6 0.84 0.84 0.3 0.6 0.84
J4 DMSO 1 2.1 1 2.1 1 2.1 3 3 3
I
SOCS1
CDKN1
GATA3
MYC
MCL1
BCL2
VEGFA
RQ Value

Figure 6: Effective targeting of Ba/F3 cell lines expressing *CRLF2* and *HMGN1* with fedratinib and GSK-J4 combination therapy. The H3K27 demethylase inhibitor GSK-J4 was assessed for its ability to induce cell death as assessed by AnnexinV/7-AAD over three days**(A)**. LD_{50} determined using non-linear regression model. Levels of pSTAT5-PE **(B)**, pERK-PE **(C)**, pS6 kinase-APC **(D)**, H3K9me2-AF647 **(E)** or H3K27me3-AF647 **(F)** measured by intracellular flow cytometry in Ba/F3 cells harboring *CRLF2* and/or *HMGN1* after being starved of IL-3 for 6 hours and exposed to 3 μM GSK-J4 for 2 hours. All graphs represent the mean of biological replicate of n=3 with SEM error bars and a Student's *t*-test was used between each Ba/F3 cell line and its corresponding +*HMGN1* expressing line to determine significance, *p<0.05, **p<0.01, ***p<0.001. The effect of the JAK2 inhibitor, fedratinib **(G)**, or synergistic combinations of fedratinib and GSK-J4 **(H)** on cell death was assessed by AnnexinV/7-AAD over three days. LD_{50} determined using non-linear regression model. CalcuSyn used to determine synergistic combinations where *=CI<1. **I)** RQ-PCR of STAT5 downstream genes: *SOCS1*, *CDKN1*, *GATA3*, *MYC*, *MCL1*, *BCL2* and *VEGFA* to determine differential mRNA expression between *CRLF2* expressing Ba/F3 cells with the addition of *HMGN1*. RQ values determined using housekeeper actin expression and each +*HMGN1* line normalised to the corresponding -*HMGN1* control line. Filled bar represent vehicle control, hashed bars *HMGN1* + vehicle and grey bars with GSK-J4.

Discussion

Genes located in the Down Syndrome critical region of chromosome 21 have been implicated in the development of ALL in DS patients[1,18]. Here, a CRISPR/Cas9 KO of *HMGN1* in a trisomy 21 leukemic cell line (SET-2) and xenograft have been generated to develop a deeper understanding of the role of *HMGN1* in DS-ALL development and progression. To exclude the limitations of CRISPR/Cas9 such as off-target effects[29,30], two sets of gRNAs targeting each gene have been used and characterised in parallel. An inducible CRISPR/Cas9 system[25] allows for the identification of possible driver genes that may be lethal to the cell if knocked-out.

HMGN1 plays a central role in cell-cycle and transcriptional events[31] and here, using an *in vitro HMGN1* KO and control *JAK2* KO, the important role of HMGN1 in both proliferation and survival pathways of trisomy 21 SET-2 *CRLF2*^{F232C} cells were confirmed. While the SET-2 cell line is not an ALL line, it is the only trisomy 21 leukemic cell line available to model *CRLF2* altered DS-ALL. Previous reports have implicated aberrant *HMGN1* expression in the transcriptional dysregulation of over 1000 genes[19,22] and increased global transcription, which is hypothesised to enhance oncogenesis. We hypothesised pre-leukemic, trisomy 21 cells rely on the enhanced transcription profile provided by the increased dosage of *HMGN1* expressed from chromosome 21, to prime the cell for leukemic transformation. *JAK2* p.V617F is the core driving mutation in SET-2 cells, and hence KO of *JAK2* is expected to arrest cellular proliferation. Remarkably, the *HMGN1* KO in SET-2 *CRLF2*^{F232C} cells resulted in the same reduction in proliferation and cell survival *in vitro* as the *JAK2* KO cells. This is

the first demonstration that *HMGN1* can play a driving role in a hematological malignancy.

In our DS-ALL xenograft model, the Cas9 control mice at day 35 demonstrated hepatosplenomegaly, thrombocytopenia and anemia, consistent with a phenotype of DS AMKL and ALL[32]. *JAK2* and *HMGN1* KO mice demonstrated a rescued AMKL phenotype with no hepatosplenomegaly, cytopenia or BM megakaryoblastic infiltration. SET-2 *CRLF2*^{F232C} leukemic cells were significantly reduced in the spleen and BM of *JAK2* or *HMGN1* KO mice by day 10 post leukemic engraftment, while the leukemic burden of Cas9 control mice increased until they became moribund at day 35. Cells that did not incur a KO of *JAK2* or *HMGN1 in vivo* expanded in the BM, as evident by the late outgrowth, indicating either *JAK2* or *HMGN1* expression provides a survival advantage in this system. Importantly, consistent with our *in vitro* data, *HMGN1* KO resulted in the same proliferative arrest in our xenograft model as the *JAK2* KO. Together, this body of data is the first evidence of *HMGN1* driving leukemic cell growth, suggesting the need for further investigation into its contribution to leukemogenesis and its potential as a therapeutic target.

Cytokine dependent Pro-B Ba/F3 cells allowed for assessment of *HMGN1* gene dosage effects, as occurs in trisomy 21, in combination with either *CRLF2*^{WT}, the *P2RY8-CRLF2* gene fusion or *CRLF2*^{F232C}. The *P2RY8-CRLF2* gene fusion is not leukemogenic, but requires additional lesions, such as *JAK* mutations[13,33]. While overexpression of *HMGN1* alone in Ba/F3 cells is also non-transforming, co-expression with the *P2RY8-CRLF2* gene fusion or *CRLF2*^{WT} leads to cytokine independence and altered methylation and

signaling profiles. Previous studies have established the important role of HMGN1 in transcriptomic activation[4,19,22,34] and we confirm that HMGN1 decreases gene silencing marks H3K9me2 and H3K27me3and increases activation mark H3K9ac when co-expressed with *CRLF2r* and *CRLF2*^{WT}. This increase in gene activation facilitated by HMGN1 appears to overcome the need for an additional co-occurring lesion usually required for *P2RY8-CRLF2* to cause leukemic transformation in DS-ALL patients.

Interestingly, previous reports have identified a similar pattern in activation of constitutive pSTAT5, AKT and pS6 kinase[39] signaling when the *P2RY8-CRLF2* fusion is coupled with mutations in *JAK2*[13,35-38]. However, these activated signaling pathways were not observed in *CRLF2*^{F232C}+*HMGN1* cells. *CRLF2*^{F232C} alone is a highly aggressive lesion in ALL and is found in approximately 9% of *CRLF2*+ DS-ALL patients[10,18]. It is possible that additional leukemic events are unnecessary for cells with this lesion as there is no evolutionary pressure to develop a secondary lesion in this genomic subtype, or that HMGN1 is modulating other mechanisms[19], such as directly upregulating mRNA expression. An increase in expression of *CDKN1*, *MYC*, *MCL1* and *BCL2* was identified in *CRLF2*^{F232C}+*HMGN1* cells, indicating possible targetability with a BET and BCL2 inhibitor which is being trialled in double hit lymphoma[40].

A significant upregulation of *CRLF2* mRNA and TSLPR was unique to *P2RY8-CRLF2+HMGN1* cells, demonstrating the important relationship between *HMGN1* and *P2RY8-CRLF2*. Further studies are warranted to determine whether HMGN1 is having a direct nucleosome remodelling effect on the *P2RY8* promotor. A previous report has demonstrated HMGN1 binding to specific gene regulatory elements in promoter

regions to modulate gene regulation and also interact with transcription factors[41] which we hypothesise to be the case for HMGN1 binding to the *P2RY8* promoter. This could indicate a role for HMGN1 in leukemic development rather than progression. Recent studies[19] have shown that increased *HMGN1* expression shifts B-cells towards a progenitor phenotype, which is required for ALL development.

The involvement of *HMGN1* in DS-ALL progression and survival revealed here makes it an attractive candidate for targeted therapy. We demonstrated the efficacy of the inhibitor J4 against cells overexpressing *HMGN1*[4]. J4 is a specific inhibitor of JMJD3 and UTX[23], both potent demethylases responsible for removing repressive methylation marks from DNA. *HMGN1*s role of unravelling silenced chromatin has a similar effect[31] and consequently, cells overexpressing *HMGN1* are more sensitive to J4[4] and result in a significant reduction pSTAT5 and pS6 signaling which has not previously been reported.

Furthermore, we observed a synergistic effect between J4 and the JAK2 inhibitor, fedratinib, in *CRLF2+HMGN1* cells, particularly cells harboring *P2RY8-CRLF2*. Recently, fedratinib was the first new drug approved for the treatment of myelofibrosis in almost 10 years[42] which could be another promising agent for *CRLF2r* ALL patients. Trials for JAK2 inhibitors to treat *CRLF2r* patients have been conducted (NCT02723994 and NCT02420717). By combining fedratinib and J4, a significant synergistic decrease in leukemic cell viability was observed at much lower concentrations than when either drug was used alone and needs to be explored further *in vivo*. Such approaches would

be invaluable in DS-ALL, where patients are disproportionately affected by toxicities from chemotherapy[7,15].

This study reveals the critical role of *HMGN1* in the proliferation and survival of trisomy 21 *CRLF2* expressing cells and provides a novel target for improved therapeutic outcomes for DS-ALL patients. Specifically, our results indicate the KO of *HMGN1* in a *CRLF2* DS leukemia has the ability to terminate leukemic cell proliferation and provide a survival advantage in our xenograft model. The involvement of *HMGN1* in transforming the transcriptomic profile to upregulate *CRLF2* and TSLPR is a significant finding for DS-ALL patients as trisomy 21 predisposes 60% of patients to develop *P2RY8-CRLF2* ALL. Interestingly, the combination of fedratinib and J4 was able to synergistically instigate cell death in cells expressing *CRLF2*+*HMGN1*; comprising a prospective therapeutic approach for DS-ALL patients. Patients with DS-ALL have extremely poor outcomes and elevated toxicity to chemotherapy, therefore a precision or genomic subset specific approach is required. As demonstrated by this study, it would be extremely valuable to develop a targeted small molecule inhibitor to HMGN1 in order to improve survival for this group of high-risk patients.

Methods

Cell lines and maintenance

HEK293T (ATCC, Manassas, VA) cells were maintained in DMEM supplemented with 10% Fetal Calf Serum (FCS). Jurkat and Ba/F3 cells (DSMZ, Braunschweig, Germany) were maintained in RPMI supplemented with 10% FCS and Ba/F3 cells supplemented 5% WEHI-3B conditioned media as a source of murine IL-343. The trisomy 21 acute

megakaryoblastic leukemia (AMKL) cell line with *JAK2* p.V617F, SET-2 (DSMZ), was maintained in RPMI supplemented with 20% FCS. All cell line media contained 200 mM L-Glutamine (SAFC Biosciences), 5000 U/mL penicillin and 5000 µg/mL streptomycin sulphate.

Constructing the FgH1tUTG gRNA vector

The Benchling gRNA design tool (Biology Software, 2019, https://benchling.com) was used to design two sets of 20 bp gRNAs targeting exon 5 of *HMGN1* or *JAK2* (Table SII) with 5' *Esp*3I restriction sites. The FUCas9Cherry and FgH1tUTG plasmids were a gift from Marco Herold (Addgene, Watertown, MA) (*29*). FgH1tUTG vector was digested with *Esp*3I and rSAP (New England Biolabs (NEB), Notting Hill, VIC) for 1 hour at 37°C. The complementary gRNAs were phosphorylated at a final concentration of 10 µM using T4 PNK (NEB), then diluted 1:125 with nuclease free water. Five ng/µL of FgH1tUTG vector was digested with 0.8 pmol of diluted gRNA and ligated with T4 ligase overnight (NEB) at 4°C.

Site directed mutagenesis

The NEBaseChanger® tool was used to design mutagenesis primers (Table SII) to create *CRLF2* p.F232C. The pRufIRES-WT-*CRLF2*-mCherry vector was used as template for the mutagenesis reaction, and the Q5 Site Directed Mutagenesis Kit (NEB) was used according to the manufacturer's instructions.

Viral Transduction

Retrovirus or lentivirus was produced by transfecting 1 x 10^6 HEK293T cells in 5 mL recipient cell media in a T25 culture flask with 4 µg of the pRUF-IRES-*CRLF2* p.F232C vector, 4 µg of the pEQ-Eco packaging vector and 20 µL lipofectamine (Invitrogen, Carlsbad, CA) or 5.5 µg of the FuCas9mCherry vector and FgH1tUTG gRNA vector, with packaging constructs pMD2.G (2.25 µg), pMDL-PRRE (3.375 µg) and pRSV-REV (1.575 µg) with 30 µL lipofectamine respectively. Viral supernatant was harvested 48 hours post transfection, spun and passed through a 0.45 µm filter. Jurkat or SET-2 cells at a concentration of 5 x 10^5/mL or Ba/F3 cells at a concentration of 3 x 10^5/mL were centrifuged at 1800rpm for 1 hour with 30 µg/mL polybrene in 4 mL of viral supernatant in a 6-well plate at room temperature. Cells were washed 24 hours later and sub-cultured in original media. SET-2 *CRLF2* p.F232C and Jurkat cells were sorted at a concentration of 1 x 10^7/mL in RPMI and 2% FCS on a BD FACSAria™ for GFP and mCherry double positive cells and Ba/F3 cells were sorted for GFP and TSLPR at >95% purity.

Animal Model

Experiments with mice were conducted according to the guidelines of the South Australian Health and Medical Research Institute animal ethics committee. The pCDH-EF1a-eFFly-eGFP vector was a gift from Irmela Jeremias (Addgene)[24]. NOD.Cg-Prkdc^{scid}Il2rg^{tm1Wjl}/SzJ (NSG) mice (The Jackson Laboratory) were treated with 0.1 mg Baytril in 0.9% sodium chloride per 10 g bodyweight prior to sub-lethal gamma-irradiation at 200 cGy. SET-2 *CRLF2* p.F232C CRISPR/Cas9 cells transduced with pCDH-EF1a-eFFly-eGFP to express firefly luciferase (3x10^5 cells) were injected into the tail vein of NSG mice (Cas9 n=6, *HMGN1* KO n=5, *JAK2* KO n=4). Mice were injected

intraperitoneally with 0.2 mL of 30 mg/mL D-Luciferin (BioSynth, Staad, SG) in 1xPBS prior to 5% isoflurane administration at 2 L/min. Mice were subsequently imaged for bioluminescence using a Perkin Elmer IVIS imager and analysed using Living-Image® software by measuring radiance (photons/second/cm2/steradian) quantified over the whole animal normalised to the background signal. Tumor engraftment was confirmed on day 10 when bioluminescent imaging had reached a radiance of ~$1x10^4$ photons/second/cm^2/steradian and tumor burden was visible in the bone marrow (BM). On day 11, 100 µg doxycycline in 0.9% sodium chloride was administered intraperitoneally to activate the gRNAs for knockout (KO) induction. Leukemic burden was monitored with ongoing bioluminescent imaging twice weekly. Mice were maintained on 0.3 mg/mL Baytril supplemented water for the duration of the experiment. Animals were monitored daily and were euthanized when moribund. A cardiac bleed and complete blood count were performed and spleen, liver and BM harvested. Formalin fixed organ sections were stained with hematoxylin and eosin (H&E).

Genome targeting efficiency assay

SET-2 *CRLF2* p.F232C and Jurkat cells containing Cas9 and gRNA vectors for *JAK2* or *HMGN1* (Table SI) were exposed to aqueous 1 µg/mL doxycycline hyclate (dox) (Sigma-Aldrich, St. Louis, MO) for 72 hrs to induce a frameshift mutation. Genomic DNA was isolated from dox treated cells by phenol chloroform extraction and the targeted exon of *JAK2* or *HMGN1* was amplified via PCR using Phusion kit (NEB) using primer sequences outlined in Table SII. Heteroduplexes were formed by denaturing and re-annealing the exon amplification PCR product which was digested with T7

endonuclease (NEB). The resulting products were gel purified using a QIAquick gel extraction kit (Qiagen, Venlo, NL) and Sanger sequenced. Synthego Performance ICE Analysis (V2.0. Synthego; 2019) was used to determine the percentage of the population containing insertion/deletions (indels) with a knockout score above 50 indicating a successful gene knockout.

Western blotting

Total protein lysates from cell lines were prepared in NP40 lysis buffer containing protease and phosphatase inhibitors (Table SI). Lysates were quantified using the DC Assay (BioRad, Hercules, CA) and measured on the Perkin Elmer Victor X5 luminometer. Total protein lysates were separated via 4–15% Criterion™ TGX Stain-Free™ Protein Gel (BioRad) and transferred to PVDF membrane via BioRad TransBlot-Turbo. Membranes were blocked in Odyssey® Blocking Buffer (Millenium Science, Mulgrave, VIC) and probed with antibodies purchased from (Cell Signalling Technologies (CST), Table SIII) compared to Chameleon Duo Marker (Millenium Science). Membranes were imaged on a Li-Cor Odyssey® CLx Infrared scanner and quantified using ImageStudio™ software.

Real Time PCR Analysis

RNA was isolated from transduced Ba/F3 cells using TRIzol® (Invitrogen) and cDNA was synthesised using Quantitect reverse transcriptase (Qiagen). SYBR green reagents (Qiagen) were used with 10 μM qPCR primers outlined in Table SII.

Proliferation assay

Jurkat cells were seeded at 390 cells/mL in a 24-well plate and SET-2 cells were seeded at 12,500 cells/mL in 1 ml in duplicate. On days 0, 2, 4 and 6, 20 µL of CellTiter-Glo 2.0® reagent (Promega, Madison, WI) was added to 20 µL of cell suspension. Following 30 min incubation in the dark, luminescence was measured on a Perkin Elmer Victor X5 luminometer set to luminescence at 0.1 seconds.

Flow cytometric analysis of Annexin V / 7AAD staining, intracellular staining analysis

Cell death was assessed by seeding Jurkat cells at $8x10^4$ cells/mL and SET-2 cells at $6x10^5$ cells/mL in a 96-well plate with doxycycline and incubated for 6-days. Cells were then stained with 0.1 µL Aqua LIVE/DEAD™ diluted 1:10 in water (ThermoFisher, Waltham, MA) and analysed on a FASCanto™ analyser. Ba/F3 cell death was assessed by seeding at $3.5x10^4$ cells/mL in a 96-well plate with a dose-response of drug (in the presence of 0.5% IL-3 conditioned supernatant if required) for a 3-day cell death assay. At 72 hours cells were stained with 0.4 µL AnnexinV-PE (BD, Franklin Lakes, NJ) and 0.04 µL 7-AAD (ThermoFisher) in 20 µL HANKS with 1% HEPES and 5% $CaCl_2$. Drug synergy was calculated using CalcuSyn where the combination index (CI) <1 indicated synergy. Following a 6-hour starvation of Ba/F3 cells were fixed with a final concentration of 1.6% paraformaldehyde for 10 mins, washed in 1xPBS and then permeabilised with 80% methanol overnight at -80°C. Cells were then washed in 1xPBS, and subsequently in 1xPBS/1% bovine serum albumin (BSA). Cells were stained with antibodies outlined in Table SIII and all intracellular staining was carried out in the dark, on ice, for 60 mins at room temperature in 1xPBS/1% BSA. Cells were washed in 1xPBS before reading on a BD FACSCanto™ analyser.

Quantification and Statistical Analysis

GraphPad Prism software Version 8.4.0© (GraphPad Software Inc.) and FlowJo software version 10.6.1 (FlowJo LLC) were used for analyses. All assays were carried out in triplicate and graphs represent the median value or mean with stand error of the mean (SEM) error bars as indicated in the figure legends. Unpaired *t*-test was used to determine the difference between experimental groups. Kaplan-Meier survival curve was analysed using log-rank test. Differences were considered statistically significant when the *p*-value was <0.05. **p*<0.05, ***p*<0.01, ****p*<0.001.

Materials and Correspondence

Additional data and requests for resources should be directed to the lead contact, Deborah White (deborah.white@sahmri.com). Materials can be obtained via material transfer agreement from authors' institutions upon reasonable request to corresponding authors.

Acknowledgements

Funding of this study was provided by NHMRC, Beat Cancer and LFA. ECP was supported by an RTP University of Adelaide scholarship.

Flow cytometry analysis and cell sorting was performed at the South Australian Health Medical Research Institute (SAHMRI) in the ACRF Cellular Imaging and Cytometry Core Facility. The Facility is generously supported by the Detmold Hoopman Group, Australian Cancer Research Foundation and Australian Government through the Zero Childhood Cancer Program.

Animal models were performed in the Bioresources Core Facility at SAHMRI and we would like to acknowledge the technical support provided.

The authors acknowledge the facilities and scientific and technical assistance of the National Imaging Facility, a National Collaborative Research Infrastructure Strategy (NCRIS) capability, at the Preclinical Imaging and Research Laboratories / Bioresources, South Australian Health and Medical Research Institute.

This study has been performed as partial fulfilment of the requirement for a PhD degree from the University of Adelaide Faculty of Sciences for ECP.

Authorship contributions

ECP, SLH and DLW conceived of and designed the experiments. BJM, PQT and DLW provided all study materials. ECP collected, assembled and analysed the data and wrote the manuscript. DLW, SLH, PQT, LNE, BJM, DTY and TPH critically appraised the manuscript. All authors gave final approval of the manuscript.

Conflict of Interest

D.L.W receives research support from BMS, and Honoraria from BMS and AMGEN. D.T.Y receives research support from BMS & Novartis, and Honoraria from BMS, Novartis, Pfizer and AMGEN. T.P.H receives research support from BMS & Novartis, and Honoraria from BMS, Novartis, and Fusion Pharma. None of these agencies have had a role in the preparation of this manuscript. All other authors declare no conflicts of interest.

References

1. Antonarakis SE. Down syndrome and the complexity of genome dosage imbalance. *Nat Rev Genet*. Mar 2017;18(3):147-163. doi:10.1038/nrg.2016.154

2. Ghosh S, Feingold E, Dey SK. Etiology of Down syndrome: Evidence for consistent association among altered meiotic recombination, nondisjunction, and maternal age across populations. *Am J Med Genet A*. Jul 2009;149A(7):1415-20. doi:10.1002/ajmg.a.32932

3. Figueroa ME, Chen SC, Andersson AK, et al. Integrated genetic and epigenetic analysis of childhood acute lymphoblastic leukemia. *J Clin Invest*. Jul 2013;123(7):3099-111. doi:10.1172/JCI66203

4. Lane AA, Chapuy B, Lin CY, et al. Triplication of a 21q22 region contributes to B cell transformation through HMGN1 overexpression and loss of histone H3 Lys27 trimethylation. *Nat Genet*. Jun 2014;46(6):618-23. doi:10.1038/ng.2949

5. Roberts I, Izraeli S. Haematopoietic development and leukaemia in Down syndrome. *Br J Haematol*. Dec 2014;167(5):587-99. doi:10.1111/bjh.13096

6. Buitenkamp TD, Izraeli S, Zimmermann M, et al. Acute lymphoblastic leukemia in children with Down syndrome: a retrospective analysis from the Ponte di Legno study group. *Blood*. Jan 2014;123(1):70-7. doi:10.1182/blood-2013-06-509463

7. Izraeli S, Vora A, Zwaan CM, Whitlock J. How I treat ALL in Down's syndrome: pathobiology and management. *Blood*. Jan 2014;123(1):35-40. doi:10.1182/blood-2013-07-453480

8. Whitlock JA. Down syndrome and acute lymphoblastic leukaemia. *Br J Haematol*. Dec 2006;135(5):595-602. doi:10.1111/j.1365-2141.2006.06337.x

9. Buitenkamp TD, Pieters R, Gallimore NE, et al. Outcome in children with Down's syndrome and acute lymphoblastic leukemia: role of IKZF1 deletions and CRLF2 aberrations. *Leukemia*. Oct 2012;26(10):2204-11. doi:10.1038/leu.2012.84

10. Hertzberg L, Vendramini E, Ganmore I, et al. Down syndrome acute lymphoblastic leukemia, a highly heterogeneous disease in which aberrant expression of CRLF2 is associated with mutated JAK2: a report from the International BFM Study Group. *Blood*. Feb 2010;115(5):1006-17. doi:10.1182/blood-2009-08-235408

11. Den Boer ML, van Slegtenhorst M, De Menezes RX, et al. A subtype of childhood acute lymphoblastic leukaemia with poor treatment outcome: a genome-wide classification study. *The Lancet Oncology*. Feb 2009;10(2):125-34. doi:S1470-2045(08)70339-5 [pii]
10.1016/S1470-2045(08)70339-5 [doi]

12. Vesely C, Frech C, Eckert C, et al. Genomic and transcriptional landscape of P2RY8-CRLF2-positive childhood acute lymphoblastic leukemia. *Leukemia*. Jan 06 2017;doi:10.1038/leu.2016.365

13. Mullighan CG, Collins-Underwood JR, Phillips LA, et al. Rearrangement of CRLF2 in B-progenitor- and Down syndrome-associated acute lymphoblastic leukemia. *Nat Genet*. Nov 2009;41(11):1243-6. doi:10.1038/ng.469

14. Mullighan CG, Zhang J, Harvey RC, et al. JAK mutations in high-risk childhood acute lymphoblastic leukemia. *Proc Natl Acad Sci U S A*. Jun 2009;106(23):9414-8. doi:10.1073/pnas.0811761106

15. Meyr F, Escherich G, Mann G, et al. Outcomes of treatment for relapsed acute lymphoblastic leukaemia in children with Down syndrome. *Br J Haematol*. Jul 2013;162(1):98-106. doi:10.1111/bjh.12348

16. Russell LJ, Capasso M, Vater I, et al. Deregulated expression of cytokine receptor gene, CRLF2, is involved in lymphoid transformation in B-cell precursor acute

lymphoblastic leukemia. *Blood*. Sep 24 2009;114(13):2688-98. doi:10.1182/blood-2009-03-208397

17. Page EC, Heatley SL, Yeung DT, Thomas PQ, White DL. Precision medicine approaches may be the future for CRLF2 rearranged Down Syndrome Acute Lymphoblastic Leukaemia patients. *Cancer letters*. Sep 28 2018;432:69-74. doi:10.1016/j.canlet.2018.05.045

18. Lee P, Bhansali R, Izraeli S, Hijiya N, Crispino JD. The biology, pathogenesis and clinical aspects of acute lymphoblastic leukemia in children with Down syndrome. *Leukemia*. Sep 2016;30(9):1816-23. doi:10.1038/leu.2016.164

19. Mowery CT, Reyes JM, Cabal-Hierro L, et al. Trisomy of a Down Syndrome Critical Region Globally Amplifies Transcription via HMGN1 Overexpression. *Cell Rep*. Nov 2018;25(7):1898-1911.e5. doi:10.1016/j.celrep.2018.10.061

20. Lim JH, Catez F, Birger Y, et al. Chromosomal protein HMGN1 modulates histone H3 phosphorylation. *Mol Cell*. Aug 2004;15(4):573-84. doi:10.1016/j.molcel.2004.08.006

21. Catez F, Brown DT, Misteli T, Bustin M. Competition between histone H1 and HMGN proteins for chromatin binding sites. *EMBO Rep*. Aug 2002;3(8):760-6. doi:10.1093/embo-reports/kvf156

22. Rochman M, Taher L, Kurahashi T, et al. Effects of HMGN variants on the cellular transcription profile. *Nucleic Acids Res*. May 2011;39(10):4076-87. doi:10.1093/nar/gkq1343

23. Li Y, Zhang M, Sheng M, et al. Therapeutic potential of GSK-J4, a histone demethylase KDM6B/JMJD3 inhibitor, for acute myeloid leukemia. *J Cancer Res Clin Oncol*. Jun 2018;144(6):1065-1077. doi:10.1007/s00432-018-2631-7

24. Sandhöfer N, Metzeler KH, Rothenberg M, et al. Dual PI3K/mTOR inhibition shows antileukemic activity in MLL-rearranged acute myeloid leukemia. *Leukemia*. Apr 2015;29(4):828-38. doi:10.1038/leu.2014.305

25. Aubrey BJ, Kelly GL, Kueh AJ, et al. An inducible lentiviral guide RNA platform enables the identification of tumor-essential genes and tumor-promoting mutations in vivo. *Cell Rep*. Mar 2015;10(8):1422-32. doi:10.1016/j.celrep.2015.02.002

26. Gozgit JM, Bebernitz G, Patil P, et al. Effects of the JAK2 inhibitor, AZ960, on Pim/BAD/BCL-xL survival signaling in the human JAK2 V617F cell line SET-2. *J Biol Chem*. Nov 2008;283(47):32334-43. doi:10.1074/jbc.M803813200

27. Yoda A, Yoda Y, Chiaretti S, et al. Functional screening identifies CRLF2 in precursor B-cell acute lymphoblastic leukemia. *Proc Natl Acad Sci U S A*. Jan 2010;107(1):252-7. doi:10.1073/pnas.0911726107

28. Mullally A, Hood J, Harrison C, Mesa R. Fedratinib in myelofibrosis. *Blood Adv*. Apr 2020;4(8):1792-1800. doi:10.1182/bloodadvances.2019000954

29. Cho SW, Kim S, Kim Y, et al. Analysis of off-target effects of CRISPR/Cas-derived RNA-guided endonucleases and nickases. *Genome Res*. Jan 2014;24(1):132-41. doi:10.1101/gr.162339.113

30. Adikusuma F, Piltz S, Corbett MA, et al. Large deletions induced by Cas9 cleavage. *Nature*. 08 2018;560(7717):E8-E9. doi:10.1038/s41586-018-0380-z

31. Bustin M. Chromatin unfolding and activation by HMGN(*) chromosomal proteins. *Trends Biochem Sci*. Jul 2001;26(7):431-7.

32. Hama A, Yagasaki H, Takahashi Y, et al. Acute megakaryoblastic leukaemia (AMKL) in children: a comparison of AMKL with and without Down syndrome. *Br J Haematol*. Mar 2008;140(5):552-61. doi:10.1111/j.1365-2141.2007.06971.x

33. Tasian SK, Loh ML. Understanding the biology of CRLF2-overexpressing acute lymphoblastic leukemia. *Crit Rev Oncog*. 2011;16(1-2):13-24.

34. Li Q, Chen J, Li X, et al. Increased expression of high-mobility group nucleosomal-binding domain 2 protein in various tumor cell lines. *Oncol Lett*. Apr 2018;15(4):4517-4522. doi:10.3892/ol.2018.7898

35. Maude SL, Dolai S, Delgado-Martin C, et al. Efficacy of JAK/STAT pathway inhibition in murine xenograft models of early T-cell precursor (ETP) acute lymphoblastic leukemia. *Blood*. Mar 2015;125(11):1759-67. doi:10.1182/blood-2014-06-580480

36. Roberts KG, Li Y, Payne-Turner D, et al. Targetable kinase-activating lesions in Ph-like acute lymphoblastic leukemia. *The New England journal of medicine*. Sep 11 2014;371(11):1005-15. doi:10.1056/NEJMoa1403088

37. Tasian SK, Doral MY, Borowitz MJ, et al. Aberrant STAT5 and PI3K/mTOR pathway signaling occurs in human CRLF2-rearranged B-precursor acute lymphoblastic leukemia. *Blood*. Jul 2012;120(4):833-42. doi:10.1182/blood-2011-12-389932

38. Tasian SK, Teachey DT, Li Y, et al. Potent efficacy of combined PI3K/mTOR and JAK or ABL inhibition in murine xenograft models of Ph-like acute lymphoblastic leukemia. *Blood*. Jan 2017;129(2):177-187. doi:10.1182/blood-2016-05-707653

39. Hurtz C, Wertheim GB, Loftus JP, et al. Oncogene-independent BCR-like signaling adaptation confers drug resistance in Ph-like ALL. *J Clin Invest*. Jul 2020;130(7):3637-3653. doi:10.1172/JCI134424

40. Li W, Gupta SK, Han W, et al. Targeting MYC activity in double-hit lymphoma with MYC and BCL2 and/or BCL6 rearrangements with epigenetic bromodomain inhibitors. *J Hematol Oncol*. 07 2019;12(1):73. doi:10.1186/s13045-019-0761-2

41. Zhu N, Hansen U. HMGN1 modulates estrogen-mediated transcriptional activation through interactions with specific DNA-binding transcription factors. *Mol Cell Biol*. Dec 2007;27(24):8859-73. doi:10.1128/MCB.01724-07

42. Fedratinib Becomes New Option in Myelofibrosis. *Cancer Discov*. Oct 2019;9(10):1332. doi:10.1158/2159-8290.CD-NB2019-102

43. Palacios R, Steinmetz M. Il-3-dependent mouse clones that express B-220 surface antigen, contain Ig genes in germ-line configuration, and generate B lymphocytes in vivo. *Cell*. Jul 1985;41(3):727-34. doi:10.1016/s0092-8674(85)80053-2

Supplementary Materials

HMGN1 is necessary for leukemic cell transformation and proliferation in *CRLF2* related Down Syndrome leukemia

Elyse C Page[1, 2], Susan L Heatley[1, 3, 4], Laura N Eadie[1, 3], Barbara J McClure[1, 3], David T Yeung[1, 3, 7, 8, 9, 10], Timothy P Hughes[1, 3, 8, 9], Paul Q Thomas[3, 5], and *Deborah L White[1, 2, 3, 4, 6, 7]

Supplementary Methods

Cell lines and maintenance

HEK293T (ATCC, Manassas, VA) cells were maintained in DMEM supplemented with 10% Fetal Calf Serum (FCS). Jurkat and Ba/F3 cells (ATCC) were maintained in RPMI supplemented with 10% FCS and Ba/F3 cells supplemented 5% WEHI-3B conditioned media as a source of murine IL-3[43]. The trisomy 21 acute megakaryoblastic leukemia (AMKL) cell line with *JAK2* p.V617F, SET-2 (ATCC), was maintained in RPMI supplemented with 20% FCS. All cell line media contained 200 mM L-Glutamine (SAFC Biosciences), 5000 U/mL penicillin and 5000 µg/mL streptomycin sulphate. All cell lines were mycoplasma negative according to MycoAlert™ Mycoplasma Detection Kit (Lonza, Basel, Switzerland).

Constructing the FgH1tUTG gRNA vector

The Benchling gRNA design tool (Biology Software, 2019, https://benchling.com) was used to design two sets of 20 bp gRNAs targeting exon 5 of *HMGN1* or *JAK2* (Table SII) with 5' *Esp*3I restriction sites. The FUCas9Cherry and FgH1tUTG plasmids were a gift from Marco Herold (Addgene) (*29*). FgH1tUTG vector was digested with *Esp*3I and rSAP (New England Biolabs (NEB), Notting Hill, VIC) for 1 hour at 37°C. The complementary gRNAs were phosphorylated at a final concentration of 10 µM using T4 PNK (NEB), then diluted 1:125 with nuclease free water. Five ng/µL of FgH1tUTG vector was digested with 0.8 pmol of diluted gRNA and ligated with T4 ligase overnight (NEB) at 4°C.

Site directed mutagenesis

The NEBaseChanger® tool was used to design mutagenesis primers (Table SII) to create *CRLF2* p.F232C. The pRufIRES-WT-*CRLF2*-mCherry vector was used as template for the mutagenesis reaction, and the Q5 Site Directed Mutagenesis Kit (NEB) was used according to the manufacturer's instructions.

Viral Transduction

Retrovirus or lentivirus was produced by transfecting 1 x 10^6 HEK293T cells in 5 mL recipient cell media in a T25 culture flask with 4 µg of the pRUF-IRES-*CRLF2* p.F232C vector, 4 µg of the pEQ-Eco packaging vector and 20 µL lipofectamine (Invitrogen, Carlsbad, CA) or 5.5 µg of the FuCas9mCherry vector and FgH1tUTG gRNA vector, with packaging constructs pMD2.G (2.25 µg), pMDL-PRRE (3.375 µg) and pRSV-REV (1.575 µg) with 30 µL lipofectamine respectively. Viral supernatant was harvested 48 hours post transfection, spun and passed through a 0.45 µm filter. Jurkat or SET-2 cells at a concentration of 5 x 10^5/mL or Ba/F3 cells at a concentration of 3 x 10^5/mL were centrifuged at 1800rpm for 1 hour with 30 µg/mL polybrene in 4 mL of viral supernatant in a 6-well plate at room temperature. Cells were washed 24 hours later and sub-cultured in original media. SET-2 *CRLF2* p.F232C and Jurkat cells were sorted at a concentration of 1 x 10^7/mL in RPMI and 2% FCS on a BD FACSAria™ for GFP and mCherry double positive cells and Ba/F3 cells were sorted for GFP and TSLPR at >95% purity.

Genome targeting efficiency assay

SET-2 *CRLF2* p.F232C and Jurkat cells containing Cas9 and gRNA vectors for *JAK2* or *HMGN1* (Table SI) were exposed to aqueous 1 µg/mL doxycycline hyclate (dox) (Sigma-

Aldrich, St. Louis, MO) for 72 hrs to induce a frameshift mutation. Genomic DNA was isolated from dox treated cells by phenol chloroform extraction and the targeted exon of *JAK2* or *HMGN1* was amplified via PCR using Phusion kit (NEB) using primer sequences outlined in Table SII. Heteroduplexes were formed by denaturing and re-annealing the exon amplification PCR product which was digested with T7 endonuclease (NEB). The resulting products were gel purified using a QIAquick gel extraction kit (Qiagen, Venlo, NL) and Sanger sequenced. Synthego Performance ICE Analysis (V2.0. Synthego; 2019) was used to determine the percentage of the population containing insertion/deletions (indels) with a knockout score above 50 indicating a successful gene knockout.

Western blotting

Total protein lysates from cell lines were prepared in NP40 lysis buffer containing protease and phosphatase inhibitors (Table SI). Lysates were quantified using the DC Assay (BioRad, Hercules, CA) and measured on the Perkin Elmer Victor X5 luminometer. Total protein lysates were separated via 4–15% Criterion™ TGX Stain-Free™ Protein Gel (BioRad) and transferred to PVDF membrane via BioRad TransBlot-Turbo. Membranes were blocked in Odyssey® Blocking Buffer (Millenium Science, Mulgrave, VIC) and probed with antibodies purchased from (Cell Signalling Technologies (CST), Table SIII) compared to Chameleon Duo Marker (Millenium Science). Membranes were imaged on a Li-Cor Odyssey® CLx Infrared scanner and quantified using ImageStudio™ software.

Real Time PCR Analysis

RNA was isolated from transduced Ba/F3 cells using TRIzol® (Invitrogen) and cDNA was synthesised using Quantitect reverse transcriptase (Qiagen). SYBR green reagents (Qiagen) were used with 10 μM qPCR primers in Table SII.

Proliferation assay

Jurkat cells were seeded at 390 cells/mL in a 24-well plate and SET-2 cells were seeded at 12,500 cells/mL in 1 ml in duplicate. On days 0, 2, 4 and 6, 20 μL of CellTiter-Glo 2.0® reagent (Promega, Madison, WI) was added to 20 μL of cell suspension. Following 30 min incubation in the dark, luminescence was measured on a Perkin Elmer Victor X5 luminometer set to luminescence at 0.1 seconds.

Statistical Analysis

GraphPad Prism software Version 8.4.0© (GraphPad Software Inc.) and FlowJo software version 10.6.1 (FlowJo LLC) were used for analyses. All assays were carried out in triplicate and graphs represent the median value or mean with stand error of the mean (SEM) error bars as indicated in the figure legends. Unpaired *t*-test was used to determine the difference between experimental groups. Kaplan-Meier survival curve was analysed using log-rank test. Differences were considered statistically significant when the *p*-value was <0.05. *$p<0.05$, **$p<0.01$, ***$p<0.001$.

Table SI: Materials	
Western Blotting Lysis Buffer Reagents	
Reagent	**Concentration**
Tris-HCL pH 7.4	10 mM
NaCl	137 mM
Glycerol	10%
NP-40 (Igepal™)	1%
β-glycerol phosphate	10 mM
Sodium Vanadate	2 mM
Sodium Fluoride	2 mM
PMSF	2 mM
Sodium Pyrophosphate	10 mM
Leupeptin	1 µg/mL
Aprotinin	5 µg/mL
Complete, mini EDTA-free protease inhibitors Cocktail tablet (Roche)	1 per 10 mL
Vectors	
FUCas9Cherry	Addgene plasmid Cat no: 70182
FgH1tUTG	Addgene plasmid Cat no: 70183
pCDH-EF1a-eFFly-eGFP	Addgene plasmid Cat no: 104834
pLenti6.2/V5-DEST-HMGN1	DNASU Cat no: 330173
MSCV-*P2RY8*-*CRLF2*-GFP	This paper
pRufIRES-*CRLF2*-F232C-mCherry	This paper
pRufIRES-WT-*CRLF2*-mCherry	This paper
Other Reagents	
Doxycycline Hyclate	Sigma-Aldrich Cat no: D9891
PCR Phusion Kit	NEB Cat no: E0553L
Q5 Site Directed Mutagenesis Kit	NEB Cat no: E0554
TRIzol	Invitrogen Cat no: 15596026
Quantitect reverse transcriptase	Qiagen # Cat no: 205313
SYBR Green	Qiagen # Cat no: 330503
CellTiter-Glo 2.0®	Promega # Cat No: G9243
T7 endonuclease	NEB Cat no: M0263L
QIAquick gel extraction kit	Qiagen Cat no: 28704
D-Luciferin	BioSynth Cat No: L-8220
Esp3I	NEB Cat no: R0734L
rSAP	NEB Cat no: M0371L
T4 PNK	NEB Cat no: M0201L
T4 Ligase	NEB Cat no: M0204L
Lipofectamine 2000	Invitrogen Cat no: 11668-019
BioRad DC Assay	BioRad Cat no: 5000111
Odyssey blocking buffer	Millenium Science Cat no: 927-40000

Table SII: Primer Sequences	
Sigma-Aldrich	
JAK2 gRNA	5′ -TTTCCTCGTTGGTATTGCAG- 3′
HMGN1 gRNA	5′ -CGGGGAAACGAAGACTGAGG- 3′
JAK2 gRNA 2	5′ -TATCGGCATGGAATATCTCG- 3′
HMGN1 gRNA 2	5′ -AGACTTACCTGCGGAAAACG- 3′
CRLF2 F232C F	5′ -CTGTCCAAAT**G**TATTTTAATTTCCAGCC- 3′
CRLF2 F232C R	5′ -CTTTGGTTTGGGAGGCGT- 3′
JAK2 exon 5 F	5′ -TGTATTTGAACTATTTGGAAGC- 3′
JAK2 exon 5 R	5′ -AACTGCAATTTTCCCATATG- 3′
HMGN1 exon 5 F	5′ -GCACATTACTTGTCTGACATG- 3′
HMGN1 exon 5 R	5′ -TCACTTTGGGATACCGTACA- 3′
CRLF2 qPCR F	5′ -TGGATCACAGACACCCAGAA- 3′
CRLF2 qPCR R	5′ -TCTTGGCCAACTGGACTACC- 3′
HMGN1 qPCR F	5′ -TGCAAACAAAAGGGAAAAGG- 3′
HMGN1 qPCR R	5′ -CATCAGAGGCTGGACTCTCC- 3′
*mVEGFA*_qPCR_F	5′ -AGCACAGCAGATGTGAATGC- 3′
*mVEGFA*_qPCR_R	5′ -TTTCTTGCGCTTTCGTTTTT- 3′
*mBCL2*_qPCR_F	5′ -AAGCTGTCACAGAGGGGCTA- 3′
*mBCL2*_qPCR_R	5′ -CAGGCTGGAAGGAGAAGATG- 3′
*mMCL1*_qPCR_F	5′ -GCTCCGGAAACTGGACATTA- 3′
*mMCL1*_qPCR_R	5′ -CCCAGTTTGTTACGCCATCT- 3′
*mMYC*_qPCR_F	5′ -CCAGATCCCTGAATTGGAAA- 3′
*mMYC*_qPCR_R	5′ -TCGTCTGCTTGAATGGACAG- 3′
*mGATA3*_qPCR_F	5′ -CTTATCAAGCCCAAGCGAAG- 3′
*mGATA3*_qPCR_R	5′ -CATTAGCGTTCCTCCTCCAG- 3′
*mCDKN1A*_qPCR_F	5′ -CGGTGGAACTTTGACTTCGT- 3′
*mCDKN1A*_qPCR_R	5′ -CAGGGCAGAGGAAGTACTGG- 3′
*mSOCS1*_qPCR_F	5′ -CCTCCTCGTCCTCGTCTTC- 3′
*mSOCS1*_qPCR_R	5′ -AAGGTGCGGAAGTGAGTGTC- 3′

Table SIII: Antibodies List		
Protein	**Conjugate**	**Manufacturer**
pSTAT5		Millipore # 05-495
STAT5		CST # 94205s
HMGN1		CST # 5692
JAK2		CST # 3230s
GAPDH		CST # 14C10
pERK		CST # 9106
ERK		CST # 9102
donkey-anti-rabbit-IRDye	680LT	Li-Cor # 926-68023
donkey-anti-mouse-IRDye	800CW	Li-Cor # 926-32212
TSLPR	APC	Invitrogen # 17-5499-41
IgG2a	APC	Invitrogen # 17-4724-81
IgG2a	PE	BD # 556653
IgG1	APC	BD # 551019
IgG XP	AF647	CST # 2985
pSTAT5	PE	BD # 612567
pERK	PE	BD # 612566
pS6 kinase	APC	CST # 665426
pJAK2	AF647	Abcam # ab200340
Total H3	AF647	CST # 12230
H3K9ac	AF647	CST # 4484
H3K27me3	AF647	CST # 12158
H3K9me2	AF647	CST # 66070
Annexin V	PE	BD # 556421
7-AAD		ThermoFisher # A1310
Aqua LIVE/DEAD™		ThermoFisher # L34957

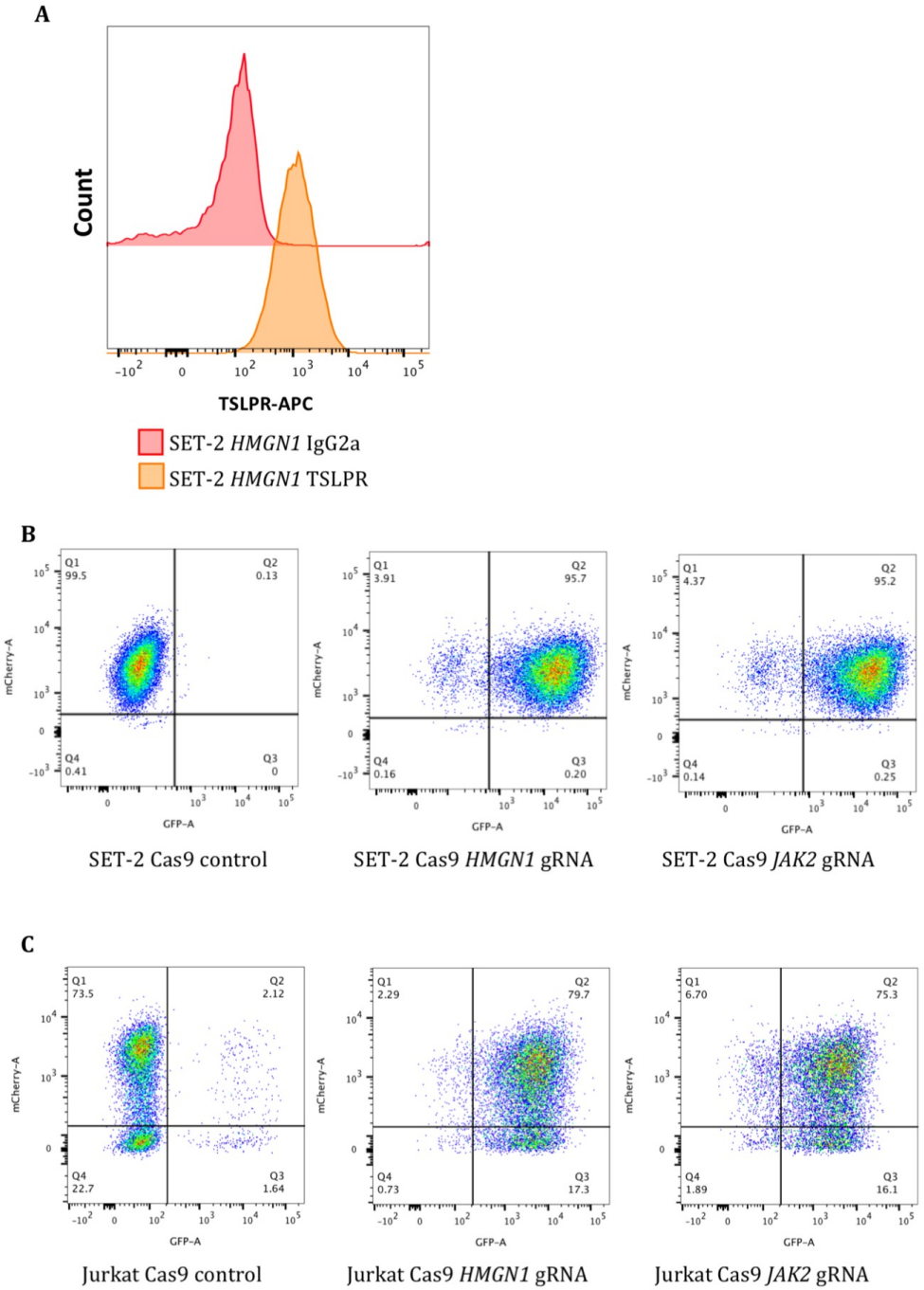

Supplementary Figure 1: Generation of a SET-2 *CRLF2* p.F232C CRISPR/Cas9 cell line model. A) surface Expression of TSLPR in SET-2 cells and SET-2 cells transduced with the *CRLF2* p.F232C mutation measured by flow cytometry. **B)** SET-2 *CRLF2* p.F232C or Jurkat **(C)** cells were transduced with the FuCas9mCherry vector and FgH1tUTG gRNA encoding GFP and gRNAs targeting *JAK2* or *HMGN1*. Cells were sorted using the FACSAria™ cells expressing both mCherry and GFP.

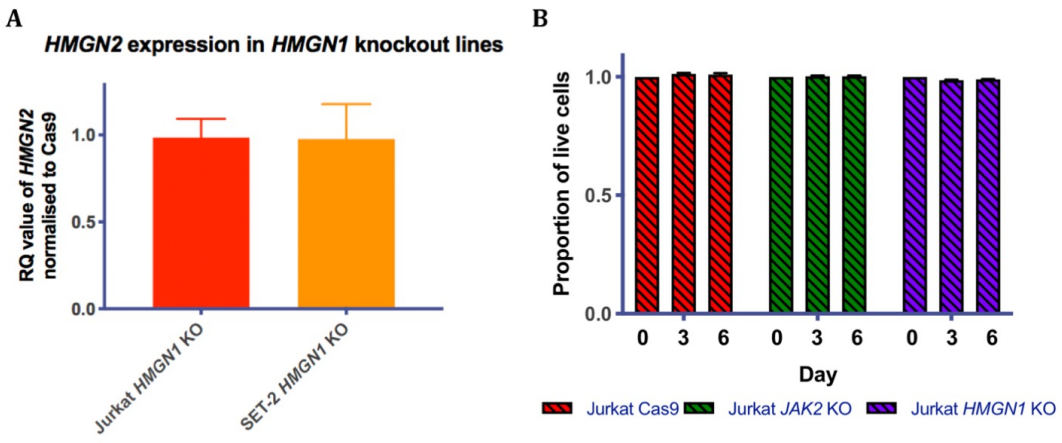

Supplementary Figure 2: Confirming on target effects of *HMGN1* gRNA in SET-2 and Jurkat knockout cells by screening *HMGN2* expression. A) RQ-PCR used to measure *HMGN2* expression in SET-2 *CRLF2* p.F232C *HMGN1* KO and Jurkat *HMGN1* KO cells compared to their respective Cas9 control cells. RQ values determined using housekeeper actin expression and normalised to the Cas9 control cell lines. **B)** Viable cells from Aqua LIVE/DEAD™ cell death assay when gRNA was induced at day 0 to day 3 and 6 in Jurkat cells. All graphs represent the mean of biological replicate n=3 with SEM error bars, *p<0.05, **p<0.01, ***p<0.001 using t-test comparing the gRNA lines to the Cas9 control line.

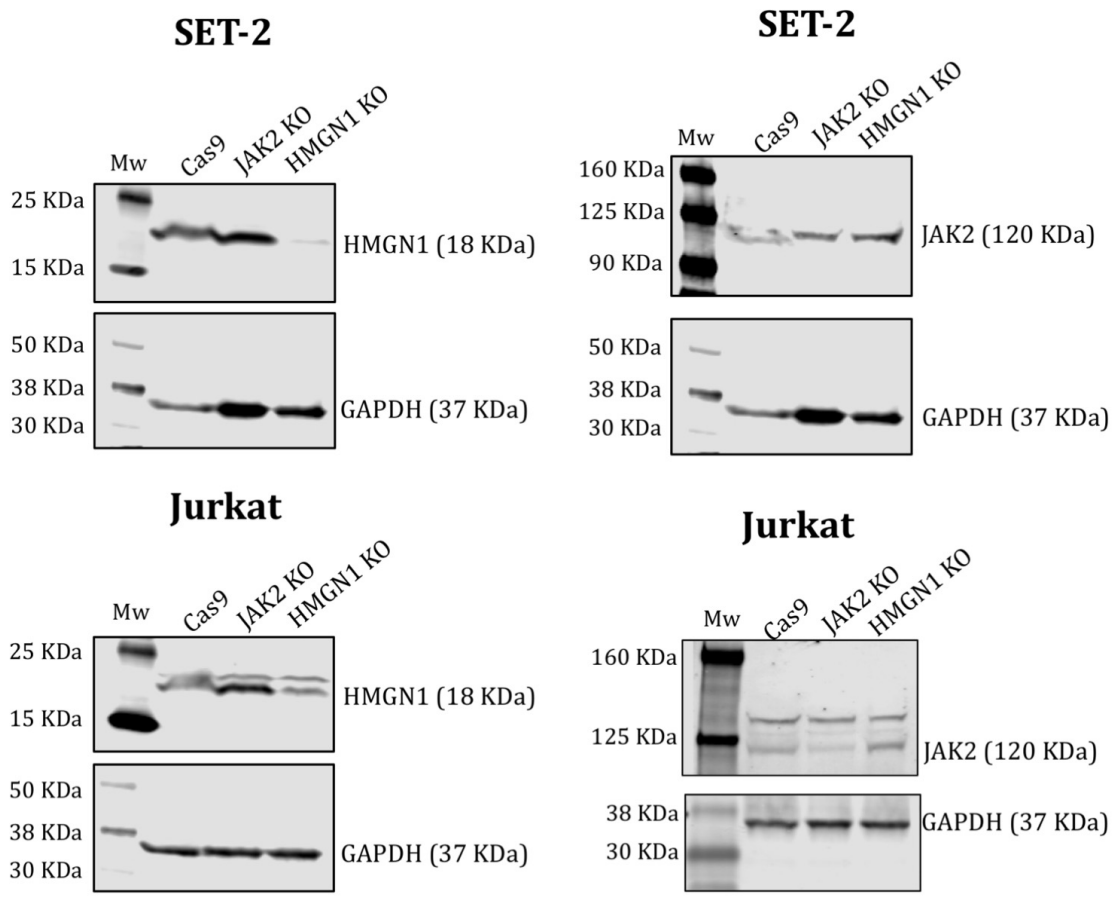

Supplementary Figure 3: Immunoblotting confirms reduced protein expression of JAK2 or HMGN1 following either *JAK2* and *HMGN1* knockout in SET-2 *CRLF2* p.F232C and Jurkat cell lines. Western blotting for total JAK2 and HMGN1 KOs in SET-2 *CRLF2* p.F232C and Jurkat cells compared to GAPDH housekeeper protein. Western blots imaged on a LiCor Odyssey® are representative of biological replicate n=3.

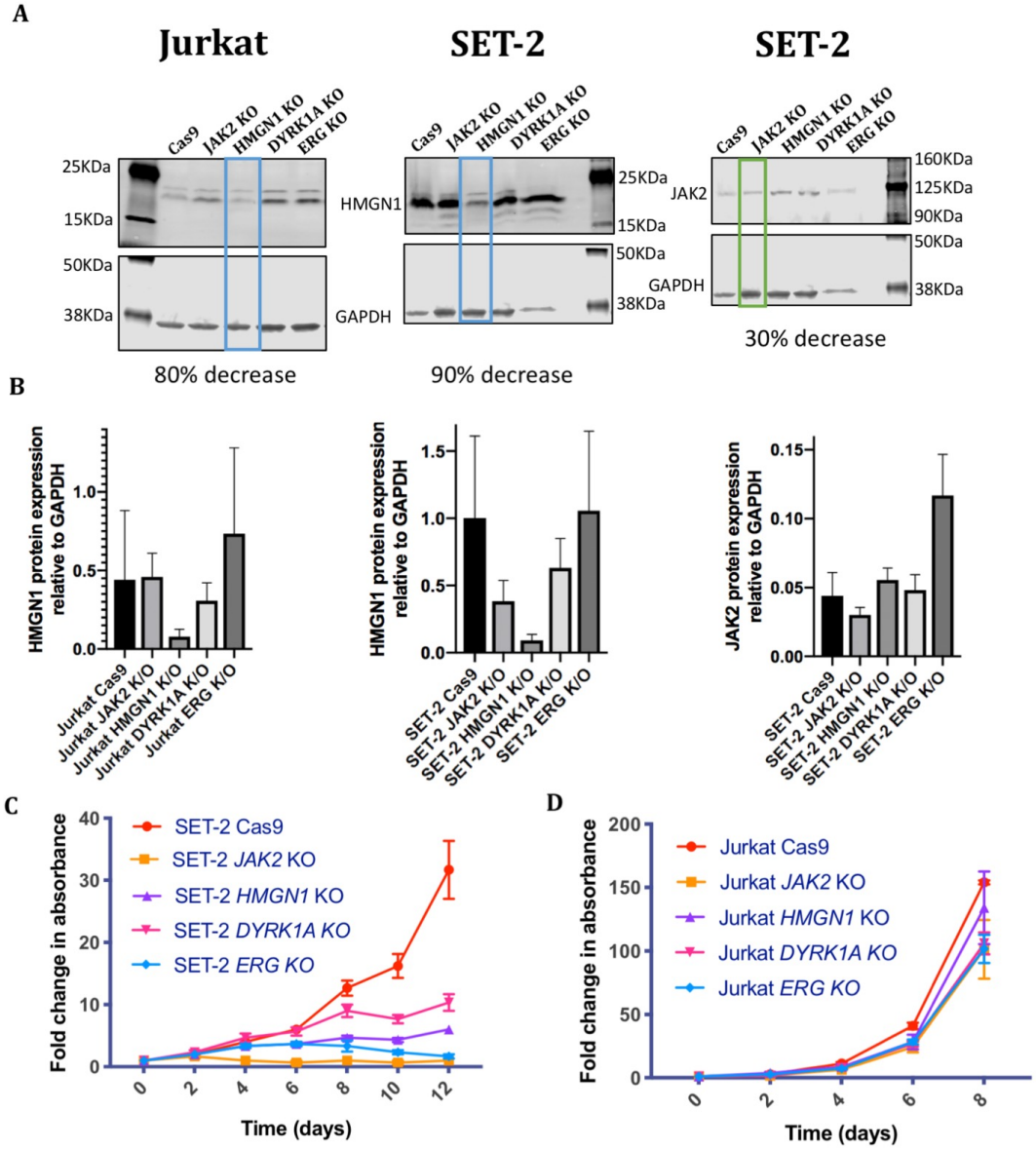

Supplementary Figure 4: Assessing protein expression and proliferation of *JAK2* and *HMGN1* knockouts in SET-2 *CRLF2* p.F232C and Jurkat cell lines using a second gRNA to confirm specificity, efficacy and targeted effects of gRNA. A) Western blotting using a LiCor Odyssey® and ImageStudio™ software for total JAK2 and HMGN1 KOs in SET-2 and Jurkat cells compared to GAPDH housekeeper protein and relative to another two gene knockout lines, *DYRK1A* and *ERG*. Western blots are representative of biological replicate n=3. Highlighted box indicates relevant KO line for each protein probed for. **B)** Quantification of western blotting using ImageStudio™

for JAK2 and HMGN1 KOs in SET-2 cells relative to GAPDH housekeeper protein. All graphs show mean of n=3 with SEM error bars. The fold change in proliferation of SET-2 **(C)** and control Jurkat cells **(D)** when a second *JAK2* or *HMGN1* gRNA was induced with doxycycline over 120 hours. Absorbance reading measured using a Perkin Elmer Victor X5 luminometer.

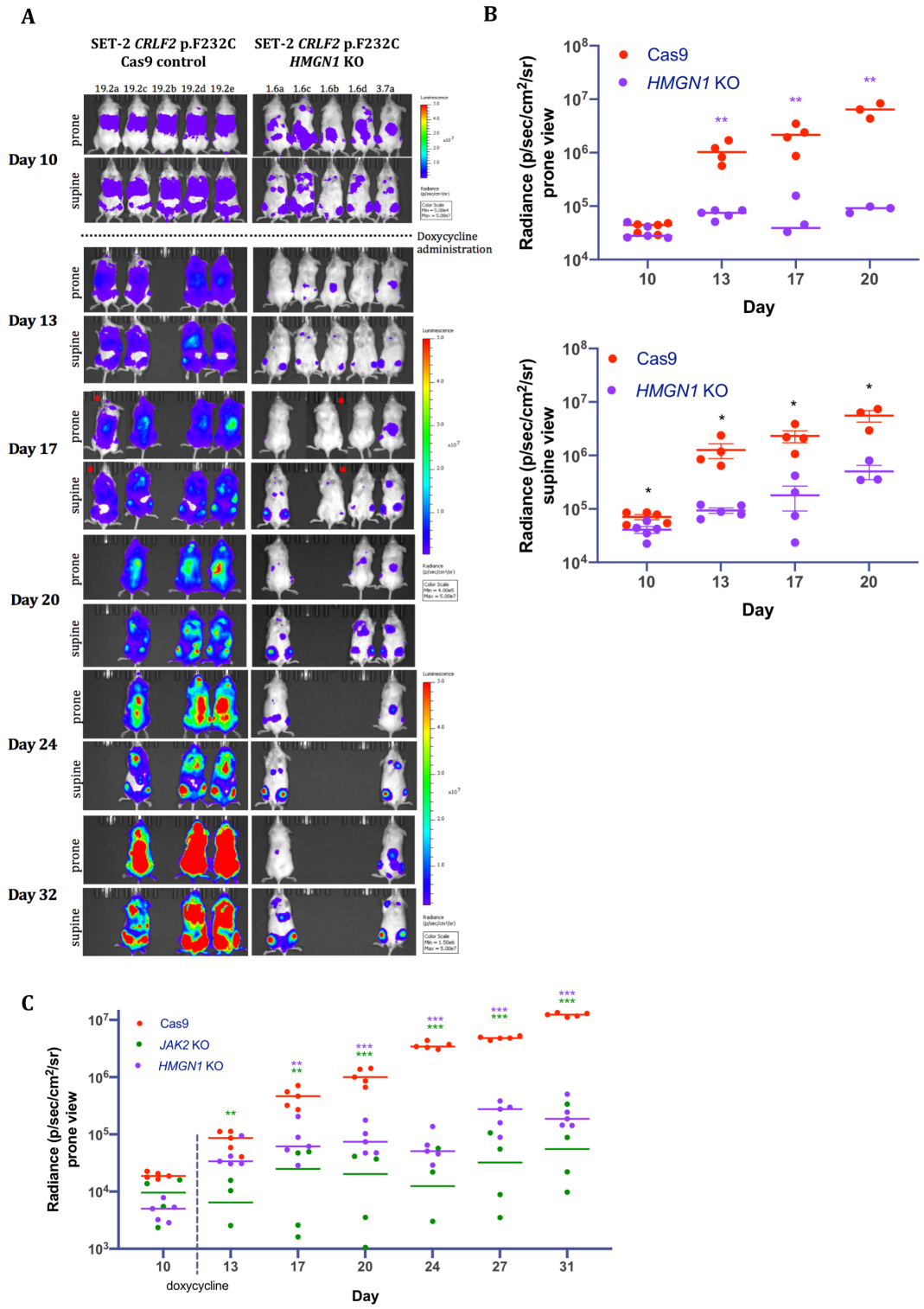

Supplementary Figure 5: Pilot Study to assess *in vivo HMGN1* knockout in SET-2 *CRLF2* p.F232C cells. A) Bioluminescent Imaging of NSG mice engrafted with SET-2 *CRLF2* p.F232C cells with Cas9 only, or with a HMGN1 gRNA. Doxycycline administered on day 11 to induce KO. Images captured using a Perkin Elmer IVIS Imager and Living

Image® software. * indicates images taken on day 16. **B)** Luminescent data normalised to the background signal. t-test used to calculate significance. Day 13 prone: p=0.001, supine: p=0.011, day 17: prone and supine: p=0.009, day 20 prone: p=0.005, supine: p=0.02. *JAK2* KO data not plotted due to non-significant number of mice remaining after day 12. **C)** Prone view BLI quantification of experimental study normalised to background signal and luminescence signal of cell lines injected. Graph represents median, *p<0.05, **p<0.01, ***p<0.001 using t-test comparing the KO mice to the Cas9 control mice.

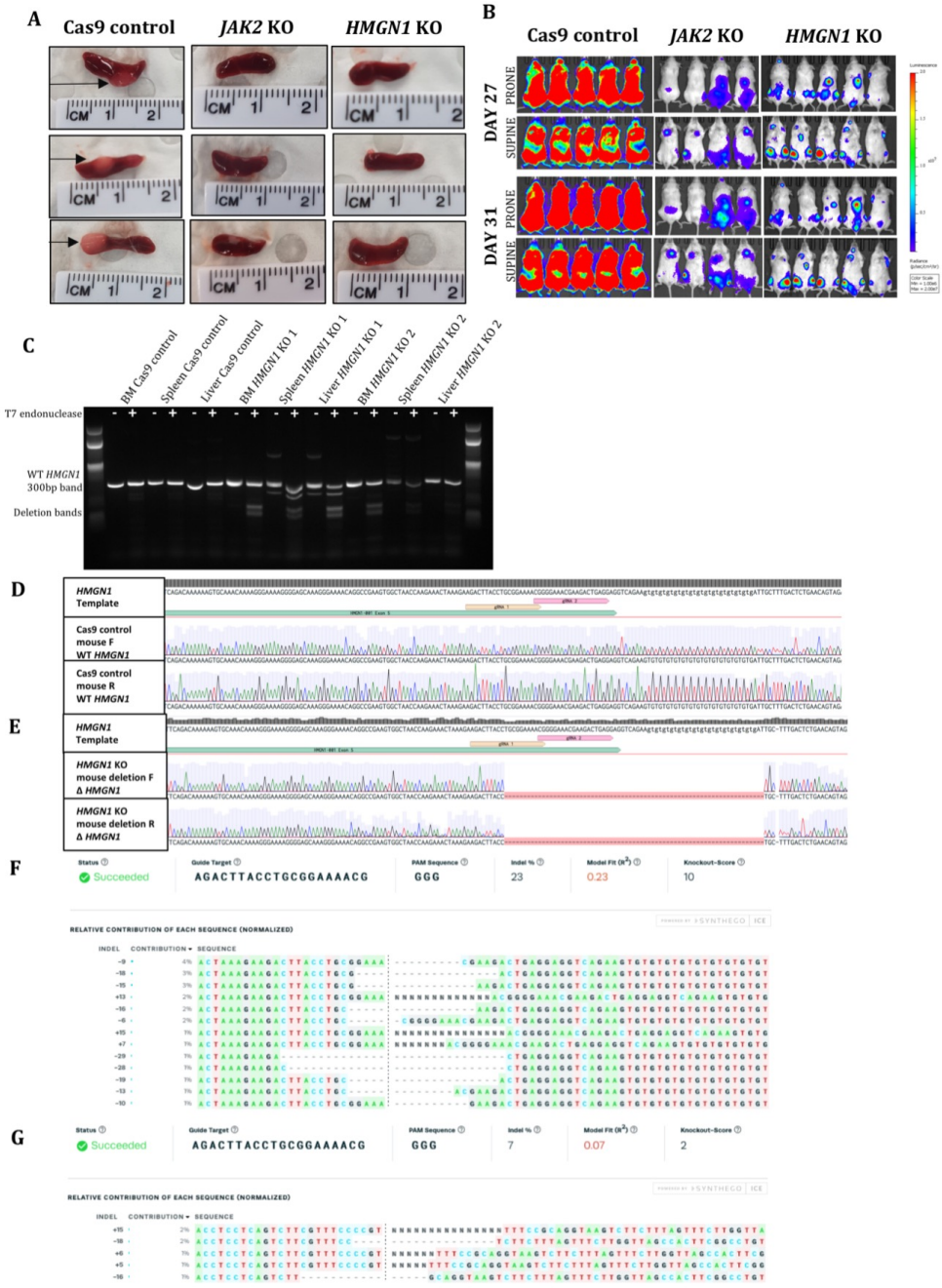

Supplementary Figure 6: Analysis of *HMGN1* CRISPR/Cas9 gene editing from *HMGN1* KO mouse organs. A) Spleens harvested from Cas9 control mice demonstrate white megakaryoblast growths, whereas *JAK2* or *HMGN1* KO mice spleens have a small appearance at day 35. **B)** Bioluminescent Imaging indicates a non-lethal knockout isoform of HMGN1 results in outgrowth of leukemic cells in BM of *HMGN1* knockout

mice at 27 days post engraftment. **C)** *HMGN1* was amplified from gDNA extracted from mouse organ harvested cells harvested at day 52 and 56 via PCR and electrophorized on an agarose gel. The product was denatured and reannealed and mismatched DNA was digested with T7 endonuclease to reveal indels. Sanger sequencing of WT *HMGN1* 300 bp band **(D)** and *HMGN1* with 69 bp deletion **(E)**. Synthego ICE analysis used to determine the KO score and percentage of indels in the forwards **(F)** and reverse **(G)** sequence of *HMGN1* Δ 69 bp.

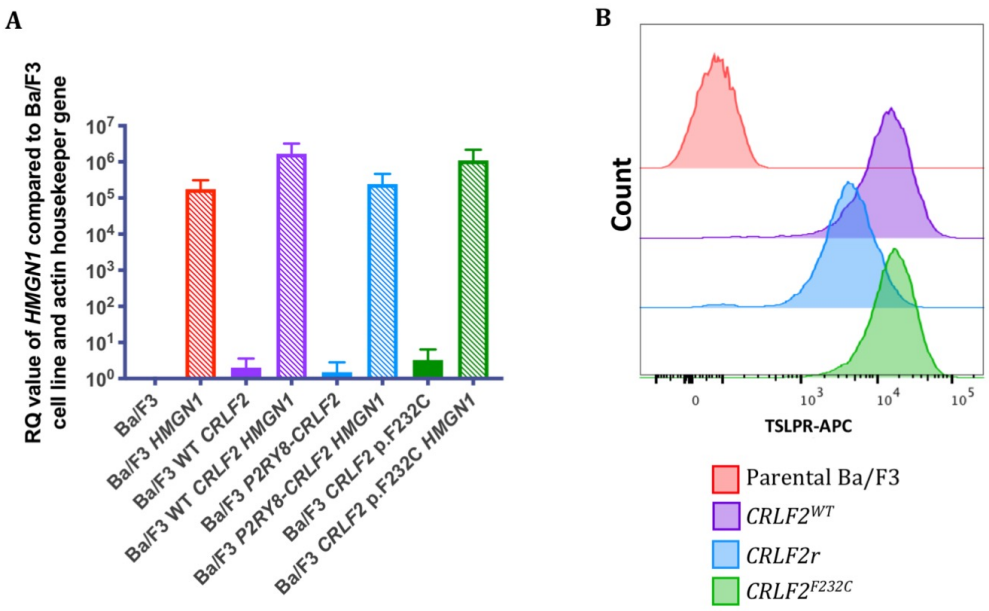

Supplementary Figure 7: Confirming overexpression of *HMGN1* in transduced Ba/F3 cells. A) *HMGN1* overexpression in Ba/F3 cells increase *HMGN1* mRNA expression. RQ values determined using housekeeper actin expression and normalised to the parental Ba/F3 control cell line. Graph represents the mean of biological replicate of n=3 with SEM error bars. *p<0.05, **p<0.01, ***p<0.001 using t-test comparing the -*HMGN1* line to the +*HMGN1* line. **B)** Measuring the surface expression of TSLPR in transduced Ba/F3 cell lines via flow cytometry. Histogram represents biological replicate of n=3.

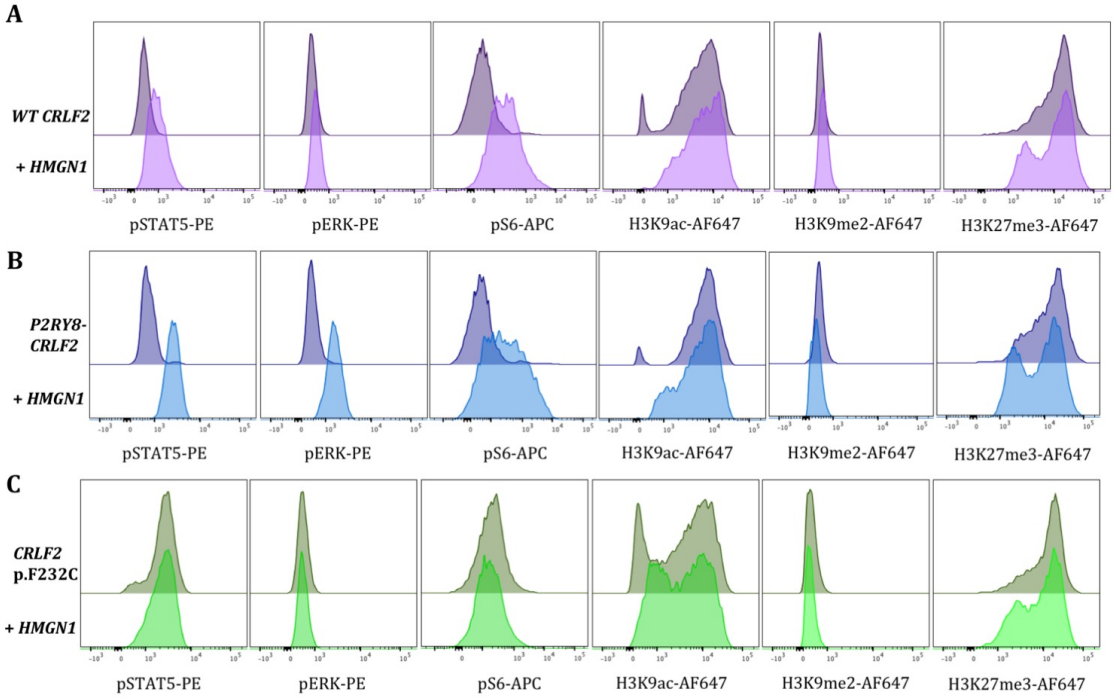

Supplementary Figure 8: Characterising signaling profiles of Ba/F3 cells with *CRLF2* ± *HMGN1*. Ba/F3 cells were starved of IL-3 for six hours to determine effect of *HMGN1* expression on signaling pathways. pSTAT5, pERK, pS6 kinase, H3K9ac, H3K9me2 and H3K27me3 were measured by intracellular flow cytometry. WT *CRLF2* **(A)**, *CRLF2r* **(B)** and *CRLF2*^{F232C} **(C)**. Representative histograms from biological replicate of n=3.

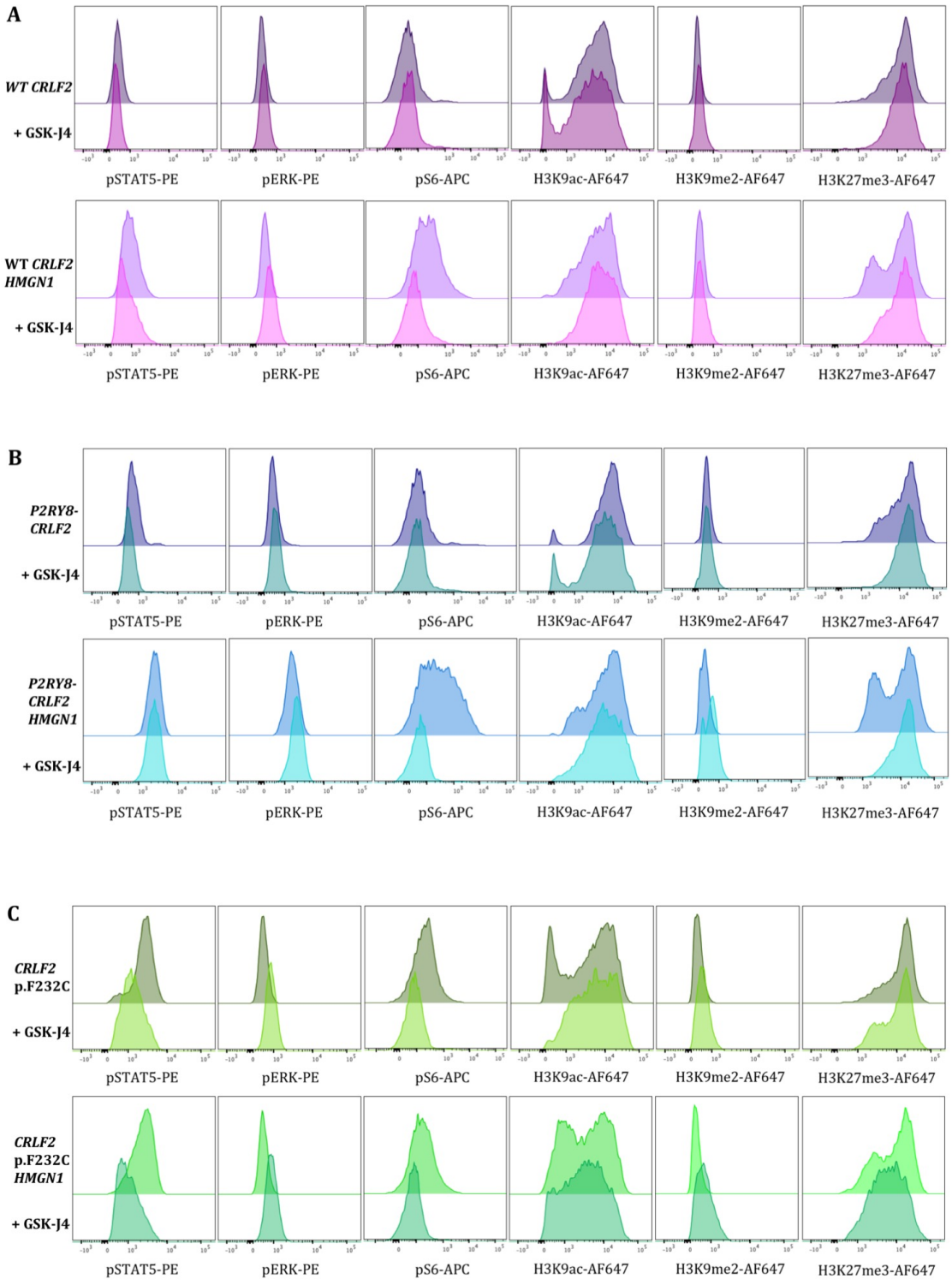

Supplementary Figure 9: Profiling signaling changes in Ba/F3 cells with *CRLF2* ± *HMGN1*, with or without GSK-J4 treatment. Ba/F3 cells were starved of IL-3 for six hours to determine effect of *HMGN1* expression and/or 2-hour GSK-J4 treatment.

pSTAT5, pERK, pS6 kinase, H3K9ac, H3K9me2 and H3K27me3 were measured by intracellular flow cytometry. WT *CRLF2* **(A)**, *CRLF2r* **(B)** and *CRLF2*^{F232C} **(C)**. Representative histograms from biological replicate of n=3.

Table SIV: Synergistic combinations of fedratinib and GSK-J4

fedratinib	0.3	0.3	0.6	0.6	0.84	0.84	0.3	0.6	0.84
J4	1	2.1	1	2.1	1	2.1	3	3	3
HMGN1	**0.839**	**0.749**	1.081	**0.936**	1.089	**0.530**	**0.634**	**0.660**	**0.619**
WT *CRLF2* *HMGN1*	1.016	**0.845**	**1.224**	**0.977**	1.237	**0.678**	**0.742**	**0.918**	**0.409**
P2RY8-CRLF2 *HMGN1*	**0.782**	**0.378**	**0.578**	**0.487**	**0.653**	**0.782**	**0.625**	**0.837**	1.258
CRLF2 p.F232C *HMGN1*	**0.789**	**0.882**	1.208	1.113	1.316	**0.963**	1.021	**0.952**	**0.273**

Supplementary Table IV: Synergistic combinations of fedratinib and GSK-J4 on Ba/F3 *HMGN1* and *CRLF2* cell lines were identified using CalcuSyn where CI<1. Synergistic concentrations are highlighted in bold text; red text indicates synergistic concentration at LD_{50}.

This page has been intentionally left blank

Chapter 3:

Unique modelling of *P2RY8-CRLF2* using CRISPR/Cas9 reveals *HMGN1* as a predisposing factor in Down Syndrome Acute Lymphoblastic Leukemia

Statement of Authorship

Title of Paper	Unique modelling of the high-risk acute lymphoblastic leukemia *P2RY8-CRLF2* gene fusion using CRISPR/Cas9 reveals *HMGN1* as a predisposing factor in Down Syndrome ALL.
Publication Status	☐ Published ☐ Accepted for Publication ☒ Submitted for Publication ☐ Unpublished and Unsubmitted work written in manuscript style
Publication Details	Page, E. C., Heatley, S. L., Thomas, P. Q., & White, D. L. (2021). Unique modelling of the high-risk acute lymphoblastic leukemia *P2RY8-CRLF2* gene fusion using CRISPR/Cas9 reveals *HMGN1* as a predisposing factor in Down Syndrome ALL.

Principal Author

Name of Principal Author (Candidate)	Elyse Page		
Contribution to the Paper	Conceived, designed and performed experiments, analysed results and wrote manuscript		
Overall percentage (%)	95%		
Certification:	This paper reports on original research I conducted during the period of my Higher Degree by Research candidature and is not subject to any obligations or contractual agreements with a third party that would constrain its inclusion in this thesis. I am the primary author of this paper.		
Signature		Date	23/2/21

Co-Author Contributions

By signing the Statement of Authorship, each author certifies that:

i. the candidate's stated contribution to the publication is accurate (as detailed above);

ii. permission is granted for the candidate in include the publication in the thesis; and

iii. the sum of all co-author contributions is equal to 100% less the candidate's stated contribution.

Name of Co-Author	Susan Heatley		
Contribution to the Paper	Supervised, and edited the manuscript		
Signature		Date	23.2.21

Name of Co-Author	Paul Thomas		
Contribution to the Paper	Supervised, and edited the manuscript		
Signature		Date	24/2/2021

Name of Co-Author	Deborah White		
Contribution to the Paper	Supervised, and edited the manuscript		
Signature		Date	25/2/2021

Unique modelling of *P2RY8-CRLF2* using CRISPR/Cas9 reveals *HMGN1* as a predisposing factor in Down Syndrome Acute Lymphoblastic Leukemia

Elyse C Page[1, 2], Susan L Heatley[1, 3, 4], Paul Q Thomas[3, 5], and *Deborah L White[1, 2, 3, 4, 6, 7]

1. Cancer Program, Precision Medicine Theme, South Australian Health & Medical Research Institute, Adelaide, SA, Australia

2. School of Biological Sciences, University of Adelaide, Adelaide, SA, Australia

3. Discipline of Medicine, University of Adelaide, Adelaide, SA, Australia

4. Australian and New Zealand Children's Haematology/Oncology Group (ANZCHOG)

5. Gene Editing Program, Precision Medicine Theme, South Australian Health & Medical Research Institute, Adelaide, SA, Australia

6. Australian Genomic Health Alliance (AGHA)

7. Discipline of Paediatrics, University of Adelaide, Adelaide, SA, Australia

Visual Abstract

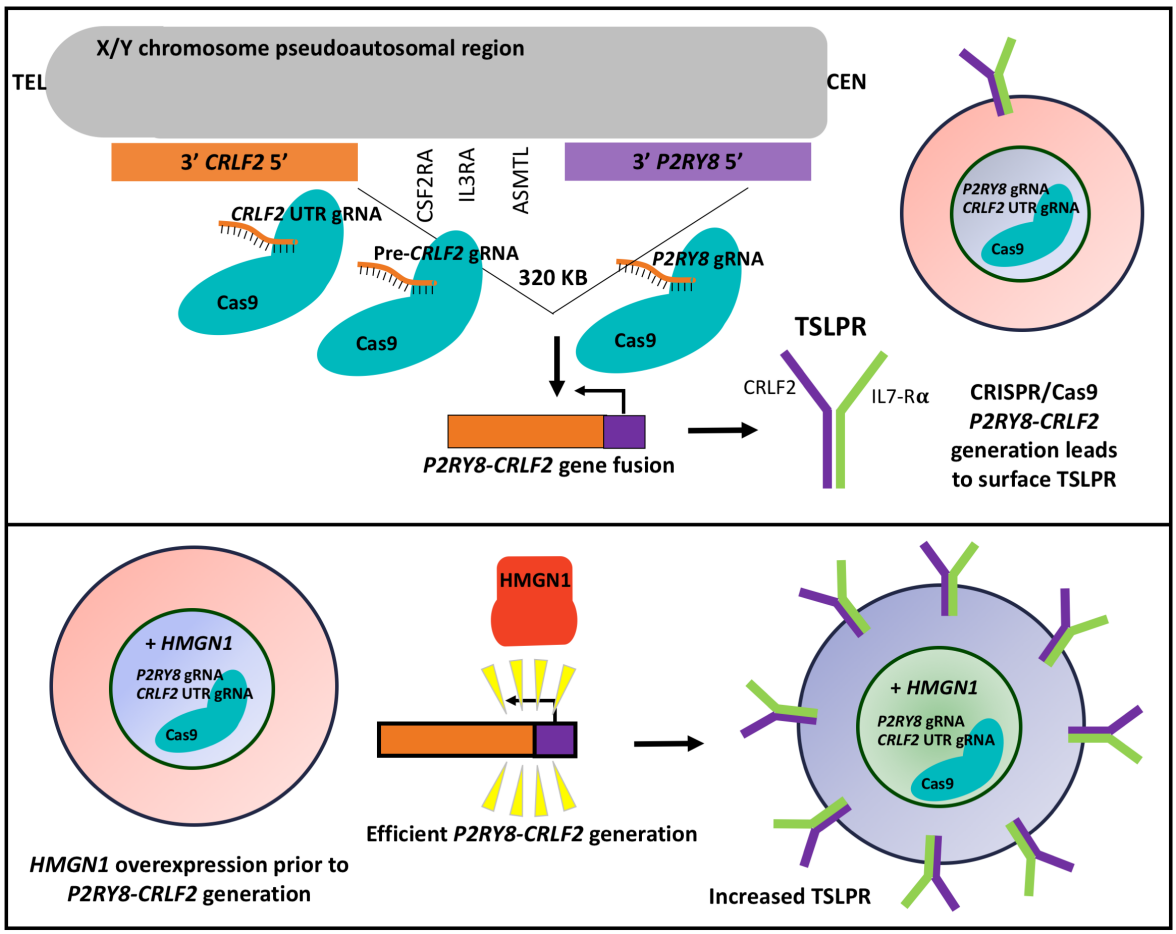

Abstract

Gene fusions are an integral part of acute lymphoblastic leukemia (ALL) pathogenesis and have allowed for risk-stratified subtypes to be identified. CRISPR/Cas9 presents the opportunity to model ALL gene fusions endogenously rather than overexpressing them in a cell-line. We efficiently generate a 320 KB deletion in the pseudoautosomal region of the X/Y chromosome in leukemic cells resulting in the purinergic receptor and cytokine receptor-like factor-2 (*P2RY8-CRLF2)* gene fusion found in 60% of Down Syndrome (DS) ALL patients. CRISPR/Cas9 generated *P2RY8-CRLF2* cells exhibit increased proliferation, thymic stromal lymphopoietin receptor expression and JAK/STAT signaling consistent with patient *P2RY8-CRLF2* cells. We use this model to investigate potential oncogenes cooperating with *P2RY8-CRLF2* in DS-ALL such as the high mobility group nucleosome binding-protein 1 (*HMGN1*) and validate *HMGN1* as a potential predisposing factor to *P2RY8-CRLF2* development. Using CRISPR/Cas9 to model gene fusions provides valuable insight into their functions and a clinically relevant tool for further studies.

Introduction

The genome engineering system CRISPR/Cas9[1, 2] has delivered the potential to create permanent, precise changes in a living cell, with reduced off target effects compared to RNA interference (RNAi)[3]. CRISPR/Cas9 has the potential to revolutionise personalised medicine with the ability to model individual patient mutations or gene rearrangements *in vitro* or *in vivo.* This application can result in physiological level of fusion gene expression for precise study and drug testing. Currently, acute lymphoblastic leukemia (ALL) modelling relies on the use of viral expression vectors which risks insertional mutagenesis, and also elicits a host immune response in the cell line, which can unintentionally change the expression patterns of other genes in the cell[4]. Modelling loss of function tumor suppressors or gain of function oncogenes is fundamental to studying cancer, and CRISPR/Cas9 has streamlined this process with higher efficacy than technologies including zinc finger nucleases and transcription-activator-like effector nucleases[3, 5]. Although many groups[6-8] have used CRISPR/Cas9 to create or reverse interchromosomal translocations, or CRISPR directed mutagenesis[9, 10] to model gene variants, including the chronic myeloid leukemia gene fusion, *BCR-ABL1*[11], or to induce the p.T315I mutation[12], this technology has only recently been applied to acute myeloid leukemia (AML) gene fusions and translocations, but not acute lymphoblastic leukemia (ALL). A lentiviral CRISPR/Cas9 approach was used to induce the ALL *MLL-AF9* fusion gene to demonstrate its role in tumorigenesis[13] which was previously modelled using TALENs[14], establishing the benefit of modelling leukemic fusion genes to inform disease outcome.

ALL is frequently characterised by gene fusions resulting in upregulated cell signaling[15]. A particular gene fusion found in 5-16% of ALL patients[16-18] occurs when a 320 KB deletion in the pseudoautosomal region (PAR1) of the X or Y chromosome arises, resulting in the coding sequence of cytokine receptor like factor 2 (*CRLF2*) being placed downstream of the first non-coding exon of the purinergic receptor (*P2RY8*)[19]. This generates the *P2RY8-CRLF2* gene fusion which allows CRLF2 to heterodimerise with IL-7Rα and results in the thymic stromal lymphopoietin receptor (TSLPR) and upregulated cell signaling[15]. The *P2RY8-CRLF2* fusion is not alone sufficient for leukemic transformation and frequently co-occurs with mutations in Janus kinase 2 (*JAK2*)[16]. *P2RY8-CRLF2* is abundant among Down Syndrome (DS) ALL patients with a frequency of ~60%[18, 20, 21]. Patients with *CRLF2* alterations are high risk and there are no effective targeted therapies for this cohort[22]. Currently, there are no cell lines endogenously expressing the *P2RY8-CRLF2* fusion to investigate the subtype and use for pre-clinical drug testing. Creating the *P2RY8-CRLF2* fusion endogenously allows for the exploration of the genomic landscape to determine predisposing factors or cooperating genes involved in leukemogenesis.

Recently, we identified the high mobility group nucleosome binding domain containing 1 (HMGN1) protein to cooperate with the *P2RY8-CRLF2* gene fusion to cause leukemic transformation in Ba/F3 cells. HMGN1 is a nucleosome remodelling protein expressed in haematopoietic cells, encoded on chromosome 21, and therefore, overexpressed in Down Syndrome patients[23]. The use of CRISPR/Cas9 to create the *P2RY8-CRLF2* gene fusion will allow for further investigation into HMGN1 to determine whether it could be predisposing DS patients to develop *P2RY8-CRLF2* ALL.

We hypothesise a physiological expression level of the *P2RY8-CRLF2* fusion can be generated using CRISPR/Cas9 which will create a novel platform to investigate new aspects of *CRLF2* rearranged ALL compared to viral overexpression. We report efficient generation and screening of the *P2RY8-CRLF2* fusion using CRISPR/Cas9 in an ALL cell line and the use of this platform to identify *HMGN1* as a predisposing factor to increase the probability of *P2RY8-CRLF2* generation.

Results

A 320 KB CRISPR/Cas9 deletion generates cells expressing the *P2RY8-CRLF2* fusion

The *P2RY8-CRLF2* fusion frequently occurs with a consistent breakpoint in ALL patients, with an increased prevalence in DS-ALL patients[16]. In all cases, the first non-coding exon of *P2RY8* is juxtaposed to the first exon of *CRLF2*, leaving the entire coding sequence of *CRLF2* intact[24]. Currently, there is no human ALL cell line model harboring *P2RY8-CRLF2*. Two sets of gRNAs were designed targeting the first intron of *P2RY8* and either upstream of *CRLF2* exon 1 (pre-*CRLF2*) or the 5'UTR (*CRLF2* UTR) with reported[16] cryptic splice site intact upstream of the *CRLF2* start codon (Fig 1). Cas9-mCherry and gRNA-GFP constructs were transduced into the ALL Jurkat cell line with high efficiency (Fig 2A) and sorted for two pure populations for cells harboring either *P2RY8* and pre-*CRLF2* gRNAs or *P2RY8* and *CRLF2* UTR gRNAs. Jurkat cells are a human T-ALL cell line with a fast doubling time of 25 hrs suitable for viral transduction and developing clonal lines from a single cell. Jurkat cells from both pre-*CRLF2* and *CRLF2*

UTR populations were activated with doxycycline for 72 hrs to induce the *P2RY8-CRLF2* fusion resulting in increased CRLF2 expression and cells were single cell sorted for the CRLF2/IL-7Rα heterodimer (TSLPR) as outlined in figure 2B.

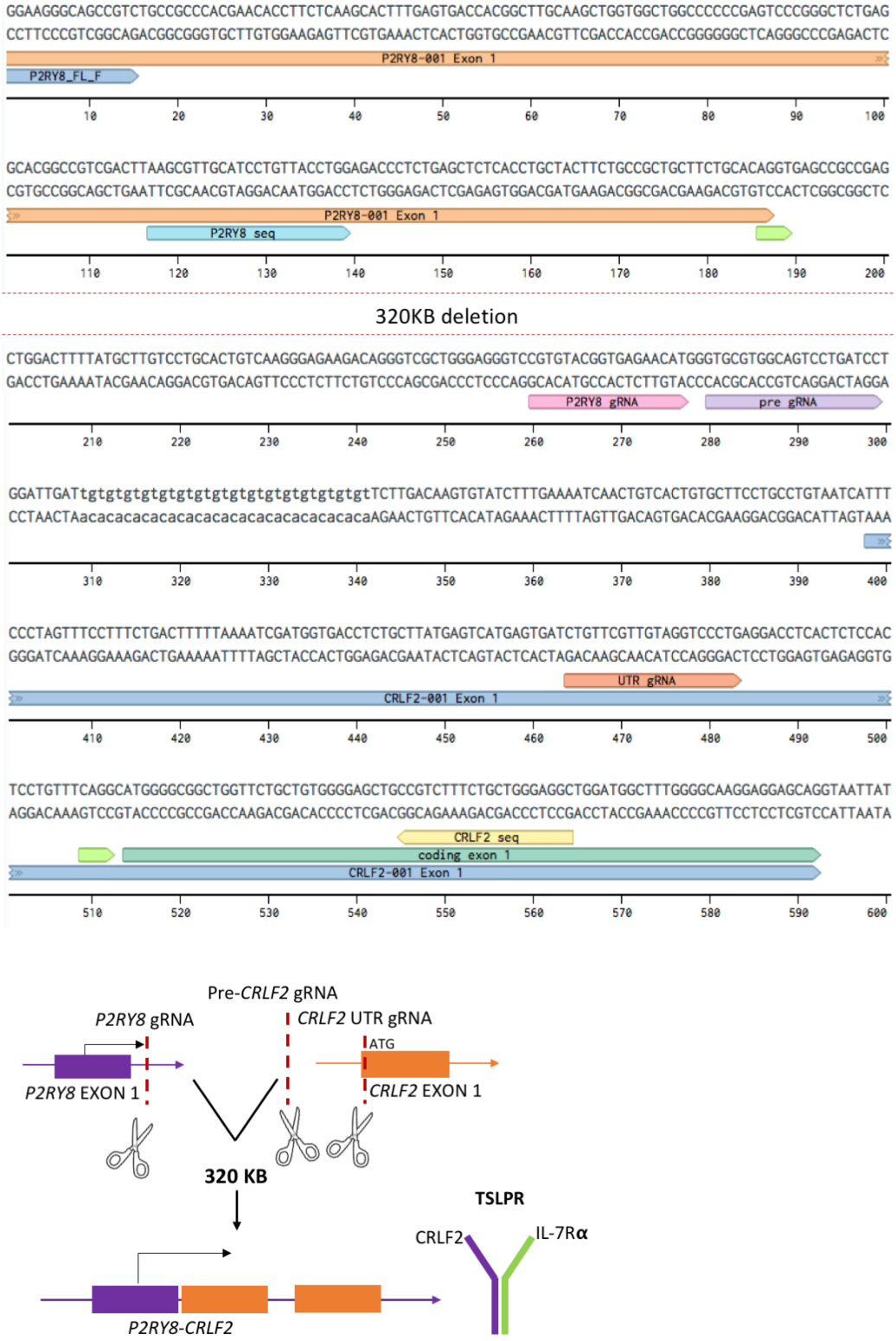

Figure 1: CRISPR/Cas9 gRNA design to create *P2RY8-CRLF2*. gRNAs designed using Benchling targeting the intron after the first non-coding exon of *P2RY8* and either the

DNA region upstream of *CRLF2* or the *CRLF2* 5' UTR to create the *P2RY8-CRLF2* breakpoint found in patients. Primers and gRNAs are shown, and reported splice sites are depicted in lime green.

Breakpoint PCR from genomic DNA (gDNA) confirmed the presence of the *P2RY8-CRLF2* fusion in a polyclonal pool and single cell clones of CRISPR/Cas9 edited TSLPR+ cells with distinct isoforms present in the pre-*CRLF2* cells compared to the *CRLF2* UTR cells (Fig 3A). The *CRLF2* UTR isoform was comparable in size to Ba/F3 cells overexpressing the *P2RY8-CRLF2* fusion originating from patient cDNA(Fig S1A), while the pre-*CRLF2* isoform was ~200 bp larger, consistent with the gRNA target sites. Both isoforms observed have been identified in patient samples (Table SI), however, the *CRLF2* UTR isoform is most prevalent. Negative control cell line gDNA without *CRLF2* rearrangements (Jurkat Cas9, Ba/F3 and SET-2) and a cell line with an *IGH-CRLF2* rearrangement (MUTZ5) were also used (Fig S1A).

To characterize the difference in breakpoint between the two different isoforms detected, gDNA and cDNA breakpoint PCRs were sequenced. The *CRLF2* UTR pool of cells and clonal lines resulted in the same sized PCR product regardless of DNA template used as the first exon of *P2RY8* was juxtaposed to the first exon of *CRLF2* and therefore, no intron sequence was included in the gene fusion (Fig 3C-D). Sequencing identified only 4 bp present between the first *P2RY8* exon and the beginning of the *CRLF2* coding sequence in the UTR pool and clones, the same canonical breakpoint identified in patients[16] (Fig 3B-D). The pre-*CRLF2* cDNA PCR product resulted in two isoforms of which sequencing identified 6 different breakpoints (Fig S2), predominantly with either intron retention either side of the gRNAs, or a 55 bp insertion at the cut site of the *P2RY8* gRNA resulting in a larger product (Fig 3E). The smaller pre-*CRLF2* cDNA product resulted in a band the same size as the *CRLF2* UTR isoform which contained a partial 5'UTR sequence of *CRLF2* (Fig 3F). Importantly,

mutations in the splice site and within the first 20 bp from the *CRLF2* start site frequently occurred in the pre-*CRLF2* population (Fig S2), however, the sequence was conserved in the *CRLF2* UTR population.

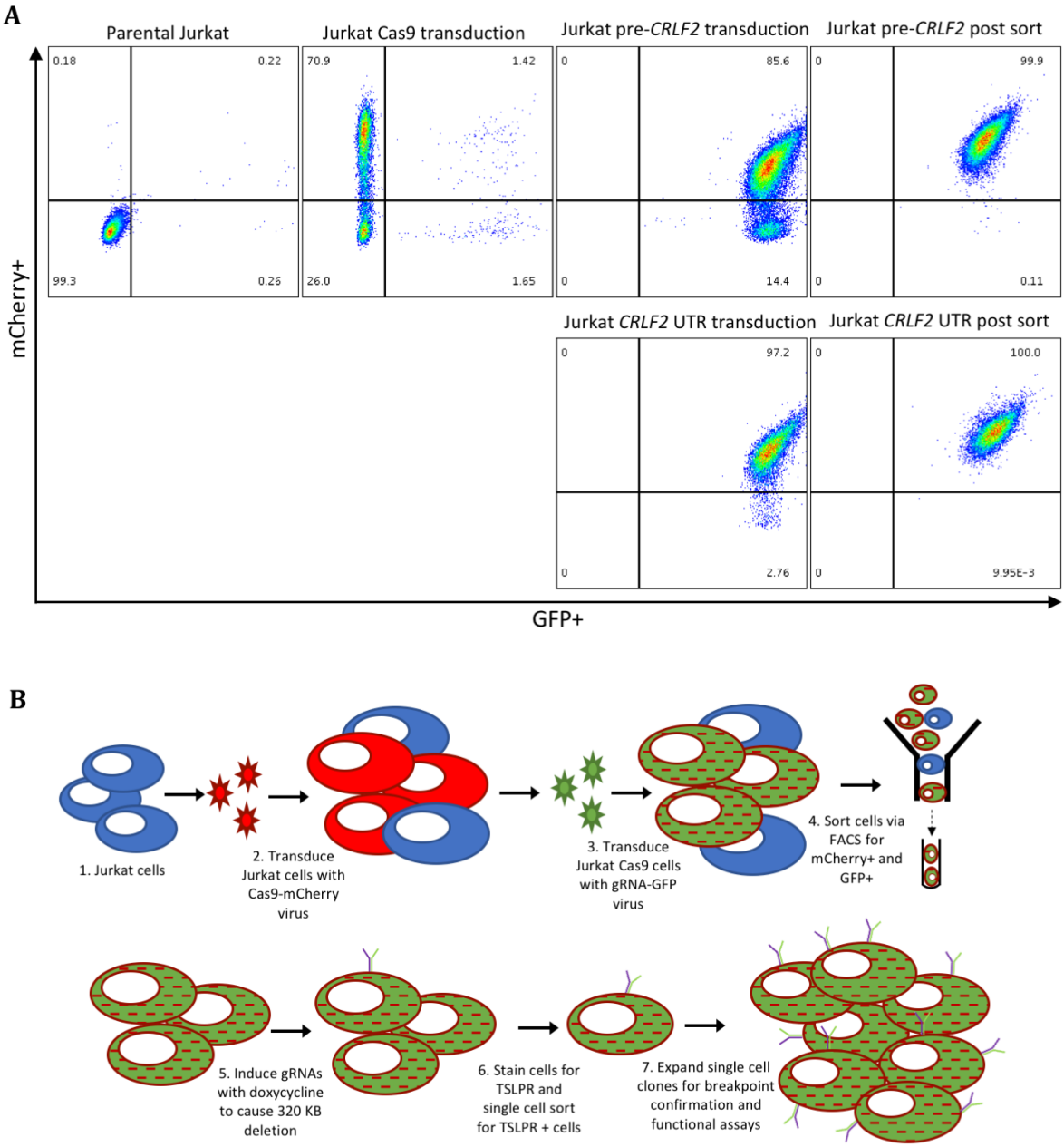

Figure 2: Experimental strategy to create the *P2RY8-CRLF2* fusion using CRISPR/Cas9. A) Transduction of the Cas9-mCherry and gRNA-GFP constructs into Jurkat cells sorted for dual mCherry/GFP + populations of either *P2RY8* +pre-*CRLF2* gRNA or *P2RY8* + *CRLF2* UTR gRNA. **B)** Schematic for creating *P2RY8-CRLF2* by sorting CRISPR/Cas9 edited cells to select for TSLPR+ cells harboring *P2RY8-CRLF2*.

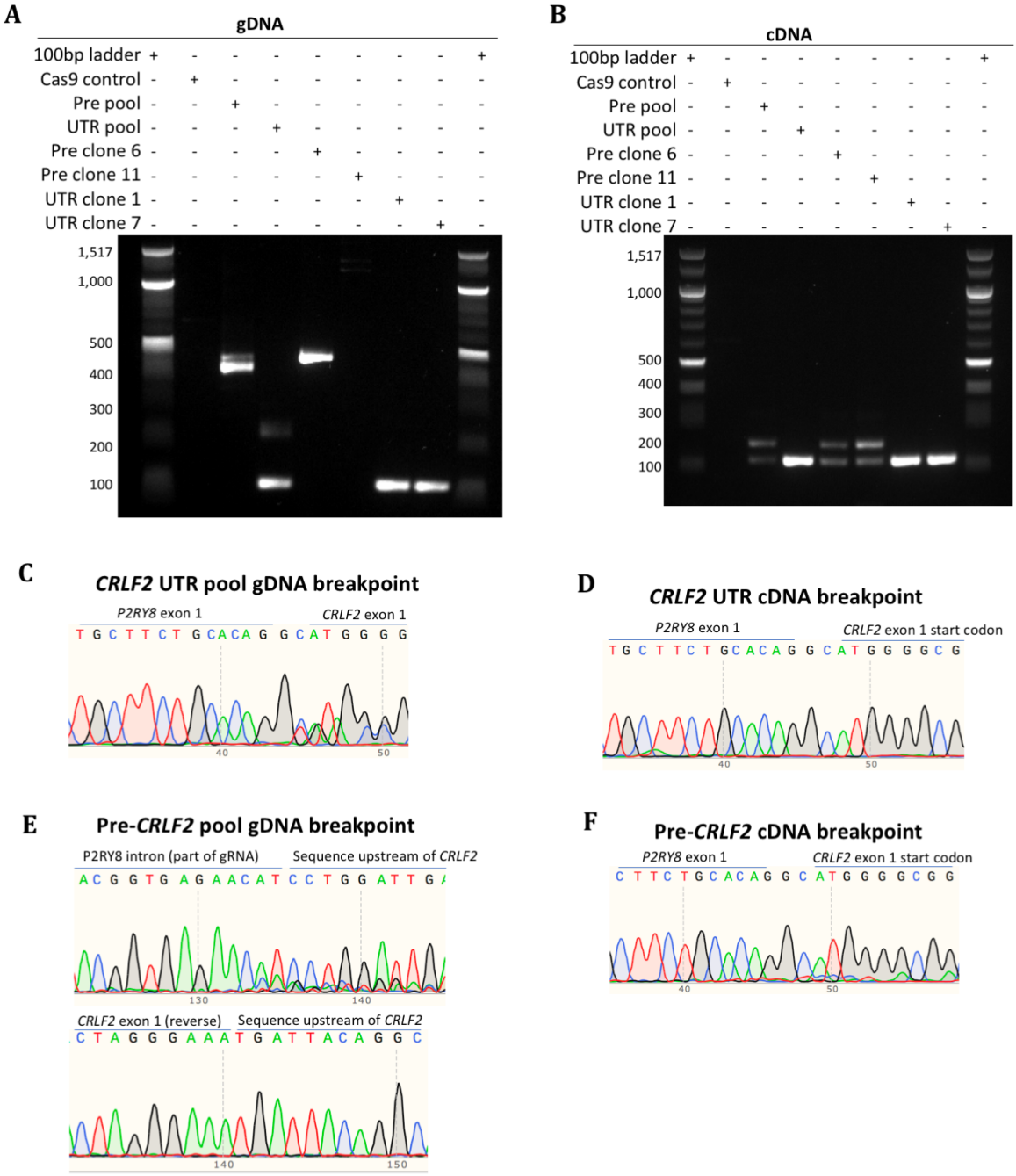

Figure 3: Generating *P2RY8-CRLF2* expressing cells. PCR amplification from gDNA **(A)** and cDNA **(B)** of the *P2RY8-CRLF2* breakpoint in a pool and single cell clones of Jurkat CRISPR/Cas9 edited *P2RY8-CRLF2* cells. Sanger sequencing of pooled populations of Jurkat CRISPR/Cas9 edited *CRLF2* UTR cells **(C-D)** or pre-*CRLF2* cells **(E-F)**.

CRISPR/Cas9 edited *P2RY8-CRLF2* clones increase TSLPR, proliferation and JAK/STAT signaling

Successful generation of the *P2RY8-CRLF2* in a pool of CRISPR/Cas9 edited cells allowed TSLPR+ cells to be seeded as single cells to generate clonal populations for further investigation (Fig 2B). Twelve clones from each of the pre-*CRLF2* and *CRLF2* UTR populations were screened for surface levels of TSLPR (Fig 4A-C). Pre-*CRLF2* clones expressed TSLPR at low levels (MFI: 510 ± 94), while *CRLF2* UTR clones had significantly higher TSLPR expression (MFI: 35,902 ± 2,638) ($p<0.001$). gDNA *P2RY8-CRLF2* breakpoint PCR from clonal populations revealed 33% of TSLPR+ pre-*CRLF2* clones harbored the *P2RY8-CRLF2* fusion compared to 100% of TSLPR+ *CRLF2* UTR clones (Fig S1B), indicating the *CRLF2* UTR gRNA was more efficient and resulted in a product more functionally similar to *CRLF2* ALL patient cells.

To confirm all fusions were functional and resulted in increased *CRLF2* expression, qRT-PCR was used to assess mRNA expression. Similar to the surface expression of TSLPR in each population, the *CRLF2* UTR populations had significantly higher expression of *CRLF2* compared to the pre-*CRLF2* populations (pre-*CRLF2* RQ: 47 ± 10; *CRLF2* UTR RQ: $4.8 \times 10^7 \pm 1.3 \times 10^7$ $p<0.001$) (Fig 4D), demonstrating this fusion isoform is more active than the fusion produced from pre-*CRLF2* cells, possibly due to the retention of *CRLF2* enhancer elements rather than relying on the *P2RY8* promoter in pre-*CRLF2* cells.

The downstream effects from the *P2RY8-CRLF2* fusion were then assessed to determine if the CRISPR/Cas9 generated fusion exhibited the same signaling and proliferation changes as normally observed in ALL patients. A CellTiter-Glo 2.0® Assay was used to measure the proliferation rate of Jurkat cells with *P2RY8-CRLF2* compared to Cas9 control cells over a period of 6 days. The pre-*CRLF2* pool of cells proliferated at the same rate as the Cas9 control cells, however, the *CRLF2* UTR pool of cells grew at a significantly more rapid rate, 7-fold higher than Cas9 control cells (Fig 4E) ($p<0.001$ comparing to Cas9 control cells at day 4). This result was the same for the clonal populations, with the *CRLF2* UTR clones proliferating at a 7-fold higher rate than the pre-*CRLF2* clones (*CRLF2* UTR #1: $p=0.005$; *CRLF2* UTR #7: $p=0.015$ compared to Cas9 control cells at day 4) (Fig 4F).

The activation of JAK/STAT, PI3K and Ras signaling pathways were investigated to determine if the CRISPR/Cas9 generated *P2RY8-CRLF2* cells were able to activate JAK/STAT signaling as observed in patients with *CRLF2* rearranged ALL. The *CRLF2* UTR clones exhibited significantly increased phosphorylation (p) of STAT5 with an MFI of 2500 compared to Cas9 control cells MFI of 250 (Fig 4G; $p<0.001$). This increase in pSTAT5 is consistent with Ba/F3 cells expressing *P2RY8-CRLF2* from an expression vector encoding a patient fusion transcript (Fig S3). An upregulation of pERK from a MFI of 690 in Cas9 control cells to 2300 (Fig 4H) and downregulation of pS6 kinase from an MFI of 9500 in Cas9 control cells to 450 ($p<0.001$, Fig 4I) were also observed in both *CRLF2* UTR clones, once again consistent with Ba/F3 *P2RY8-CRLF2* cells. These results suggest cells harboring the CRISPR/Cas9 *P2RY8-CRLF2* gene fusion have proliferation and signaling characteristics that are equivalent to those seen in patients.

The pre-*CRLF2* clones, however, displayed different signaling patterns to one another and the *CRLF2* UTR clones. Pre-*CRLF2* #6 displayed similar signaling patterns to the *CRLF2* UTR clones and sequencing of this clone demonstrated a normal ATG start codon. The pre-*CRLF2* #11 displayed a much lower level of activation of pSTAT5 with an MFI of 390 ($p<0.001$). It was also the only clone to demonstrate an increase in pS6 kinase with an MFI of 23,500 ($p<0.001$) and no change in pERK (Fig S4). Sequencing of this clone indicated a 1 bp deletion 8 bp upstream of the *CRLF2* start codon, therefore these signaling changes may be due to a non-functional or shorter *P2RY8-CRLF2* transcript.

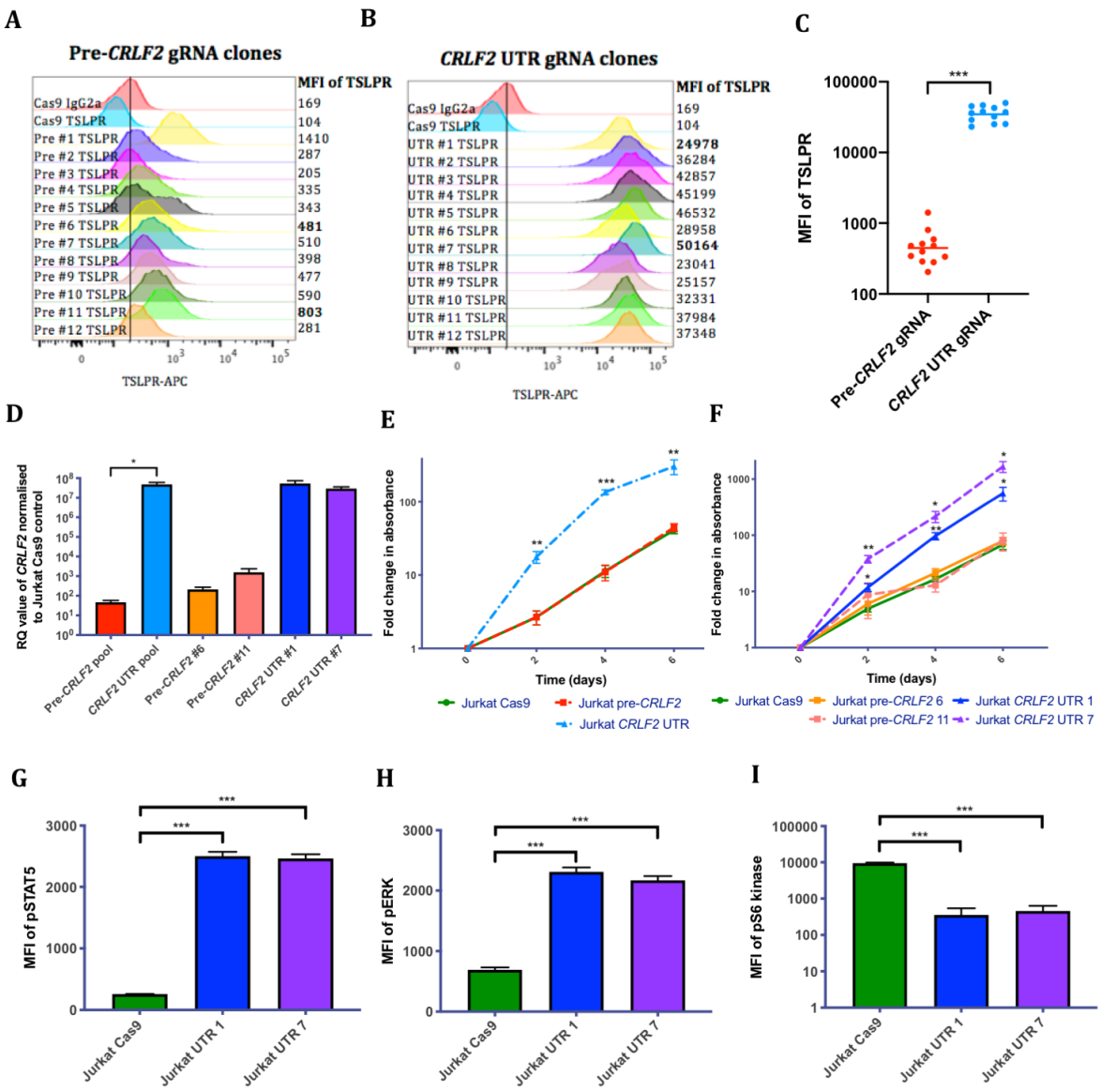

Figure 4: Evaluation of functional changes in CRISPR/Cas9 edited *P2RY8-CRLF2* cells. A-C) TSLPR expression of single cell clones of Jurkat CRISPR/Cas9 edited *P2RY8-CRLF2* cells measured by flow cytometry. **D)** Using qRT-PCR to measure *CRLF2* mRNA expression in Jurkat CRISPR/Cas9 edited *P2RY8-CRLF2* cell lines. RQ values determined using housekeeper actin expression and normalised to the parental Jurkat Cas9 control cells. The fold change in proliferation of Jurkat CRISPR/Cas9 edited *P2RY8-CRLF2* cells **(E)** or single cell clones **(F)** measured over a period of 6 days. Phosphorylation levels of STAT5 **(G)**, ERK **(H)**, S6 kinase **(I)** of Jurkat CRISPR/Cas9

edited *P2RY8-CRLF2* cells measured by flow cytometry. All graphs represent the mean of biological replicate of n=3 with SEM error bars and a student's *t*-test was used between each *P2RY8-CRLF2* cell line comparing to control Jurkat Cas9 cells to determine significance, *$p<0.05$, **$p<0.01$, ***$p<0.001$.

High expression of *HMGN1* increases efficacy of *P2RY8-CRLF2* fusion generation

As an example of how this system can be used to validate candidate predisposing factors for the development of *P2RY8-CRLF2*, the nucleosome remodelling protein HMGN1 encoded on chromosome 21 has been investigated. *HMGN1* was virally expressed at a low level to recapitulate a trisomy expression level in Jurkat cells harboring Cas9 and gRNAs targeting *P2RY8* and *CRLF2* as previously described. After 72 hours of *HMGN1* expression, cells expressed *HMGN1* 1.8-fold higher than Cas9 control cells confirmed by qRT-PCR (Fig S5A), similar to a trisomy expression level. The gRNAs were subsequently activated in Jurkat cells. Another 72 hours post gRNA induction, the cells were stained for TSLPR. Cell populations with increased *HMGN1* expression upregulated TSLPR on the cells surface in both the pre-*CRLF2* cells from 0.45 to 0.71 with *HMGN1* expression (p=0.003) and *CRLF2* UTR cells from 0.3 to 0.5 with *HMGN1* expression (p=0.034, Fig 5A). This indicates the effect of HMGN1 could be assisting in the repair of the Cas9 mediated double stranded DNA breaks to result in a productive *P2RY8-CRLF2* gene fusion.

TSLPR+ cells were sorted to create a pure population of high TSLPR expressing cells. Co-expressing *HMGN1* and pre-*CRLF2* cells resulted in a 50% increase in TSLPR+ cells sorted compared to pre-*CRLF2* cells without *HMGN1* expression. Co-expressing *HMGN1* and *CRLF2* UTR cells resulted in a 130% increase in TSLPR+ cells sorted compared to *CRLF2* UTR cells without *HMGN1* expression (Fig S5B), therefore *HMGN1* expression promotes *P2RY8-CRLF2* formation. An increase in *CRLF2* mRNA expression was identified in *P2RY8-CRLF2* cells expressing *HMGN1* (Fig 5B, p=0.019). Interestingly, no

difference in proliferation was observed between *P2RY8-CRLF2* cells with or without *HMGN1* expression, despite the increase in *CRLF2* and TSLPR (Fig 5C).

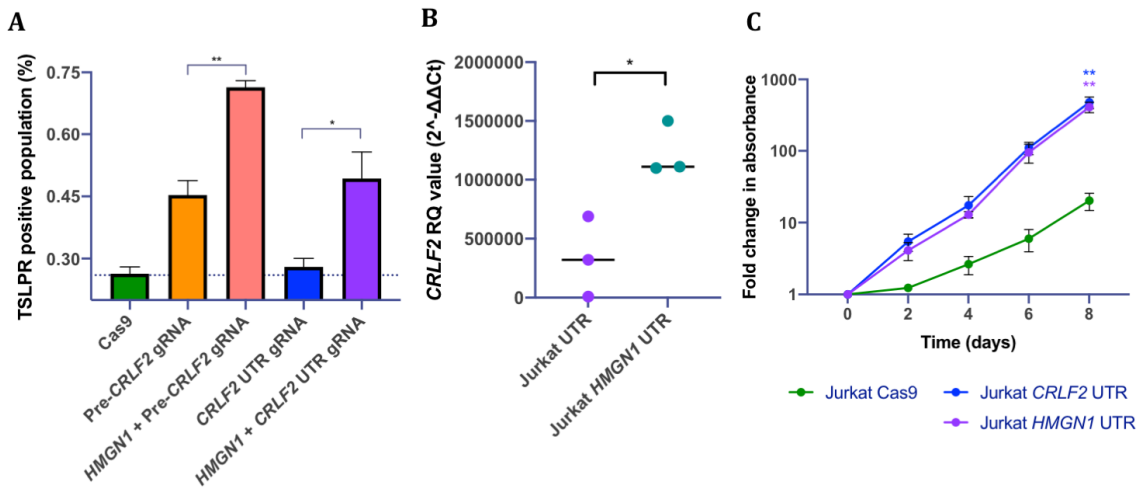

Figure 5: *HMGN1* expression facilitates repair and creation of *P2RY8-CRLF2.* A) Jurkat cells with or without HMGN1 expression were stained with TSLPR for flow cytometry after three days of gRNA induction to assess the efficiency of *P2RY8-CRLF2* generation. **B)** Using qRT-PCR to measure *CRLF2* mRNA expression in Jurkat CRISPR/Cas9 edited *P2RY8-CRLF2* cell lines. RQ values determined using housekeeper actin expression and normalised to the parental Jurkat Cas9 control cells. The fold change in proliferation of Jurkat CRISPR/Cas9 edited *P2RY8-CRLF2* cells. **C)** The fold change in proliferation of Jurkat CRISPR/Cas9 edited *P2RY8-CRLF2* cells measured over a period of 6 days. Graphs represents the mean of biological replicate of n=3 with SEM error bars and a student's *t*-test was used between each *P2RY8-CRLF2* cell line comparing to control Jurkat Cas9 cells to determine significance, *$p<0.05$, **$p<0.01$.

The *HMGN1* expressing cells *P2RY8-CRLF2* breakpoints were sequenced from the pure TSLPR+ populations. gDNA breakpoint PCR identified the same sized band from pre-*CRLF2* cells and *HMGN1* pre-*CRLF2* cells. However, when comparing cells overexpressing *HMGN1* in the *CRLF2* UTR population, a different isoform of 280 bp was revealed compared to the *CRLF2* UTR only 100 bp isoform (Fig 6A). Sanger sequencing revealed a new breakpoint in the 280 bp *HMGN1 CRLF2* UTR product with *P2RY8* intron retention upstream of the *P2RY8* gRNA, which has been identified in patients, compared to only 4 bp of intron present in the *CRLF2* UTR only cells, however both populations resulted in the same *P2RY8-CRLF2* transcript produced once splicing occurred (Fig 6C-D).

Cas9 gene editing activity was quantified with or without *HMGN1* expression using a T7 endonuclease assay to reveal heteroduplexes present in the purified PCR product. The pre-*CRLF2* or *CRLF2* UTR only lines resulted in only one isoform after T7 endonuclease digestion, whereas the co-expressing *HMGN1* lines resulted in increased gene editing with three bands present in each population (Fig 6B). This demonstrates *HMGN1* expression could influence the development of *P2RY8-CRLF2* via increased gene editing and cellular repair activity. Increased isoforms due to outgrowth of clones has been excluded due to the same proliferation rates observed between the *P2RY8-CRLF2* and co-expressing *HMGN1* lines previously demonstrated.

To determine the effect of HMGN1 on cell signalling, phosphoflow was once again used to assess phosphorylation levels of STAT5, AKT and ERK. Interestingly, a stepwise increase in phosphorylation of all three proteins was observed from the Cas9 control

cells, to *CRLF2* UTR cells, to *CRLF2* UTR + *HMGN1* cells. (Fig 7A-C, all $p<0.001$). As HMGN1 is a demethylase protein, the acetylation of H3K9 and trimethylation of H3K27 were also assessed. No change in gene activation was identified (Fig 7D), however, once again, a stepwise decrease in H3K27me3 was identified from Cas9 control cells to *CRLF2* UTR cells (Fig 7E, $p<0.001$) and then a further reduction in *CRLF2* UTR + *HMGN1* cells ($p=0.003$). This reduction in H3K27me3 indicated genes that were previously silenced have become active in this line. To screen for gene activation downstream of the main signalling pathway, pSTAT5, qRT-PCR was used. Interestingly, a higher expression level of *BCL2*, *CDKN1* and particularly *MCL1* and *MYC* was identified in cells co-expressing *HMGN1* and *P2RY8-CRLF2* compared to Cas9 control cells (Fig 7F). A decrease in GATA3 expression was also observed, indicating a shift in T-cell differentiation.

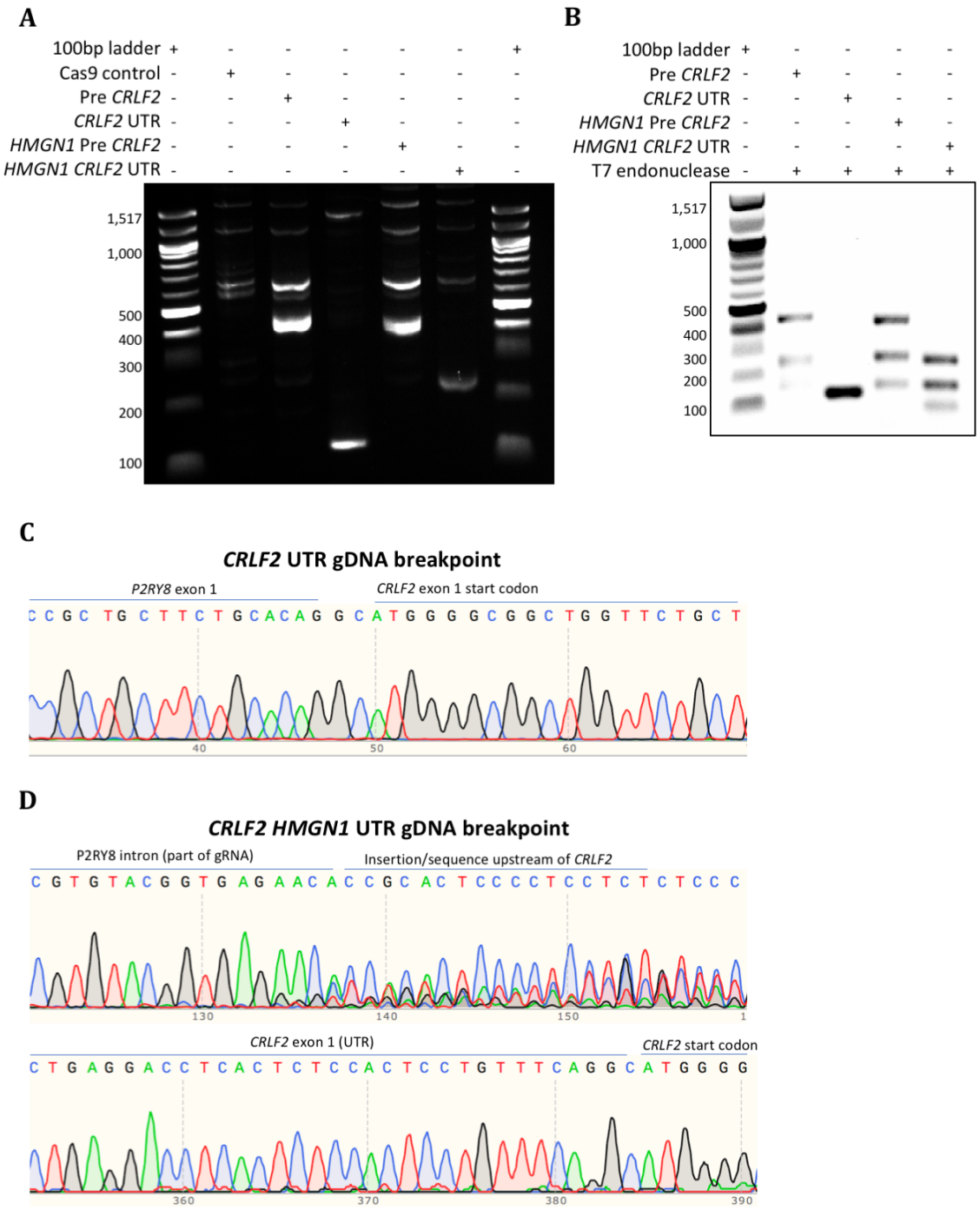

Figure 6: Characterising breakpoints of *HMGN1* expressing *P2RY8-CRLF2* cells. A) PCR amplification from gDNA of the *P2RY8-CRLF2* breakpoint in Jurkat CRISPR/Cas9 edited *P2RY8-CRLF2* cells with and without *HMGN1* overexpression. **B)** T7 endonuclease gene editing analysis identifies additional *P2RY8-CRLF2* breakpoint PCR

products present in *HMGN1* expressing cells. **C-D)** Sanger sequencing from gDNA of the *P2RY8-CRLF2* breakpoint in Jurkat CRISPR/Cas9 edited *CRLF2* UTR *P2RY8-CRLF2* cells with or without *HMGN1* overexpression.

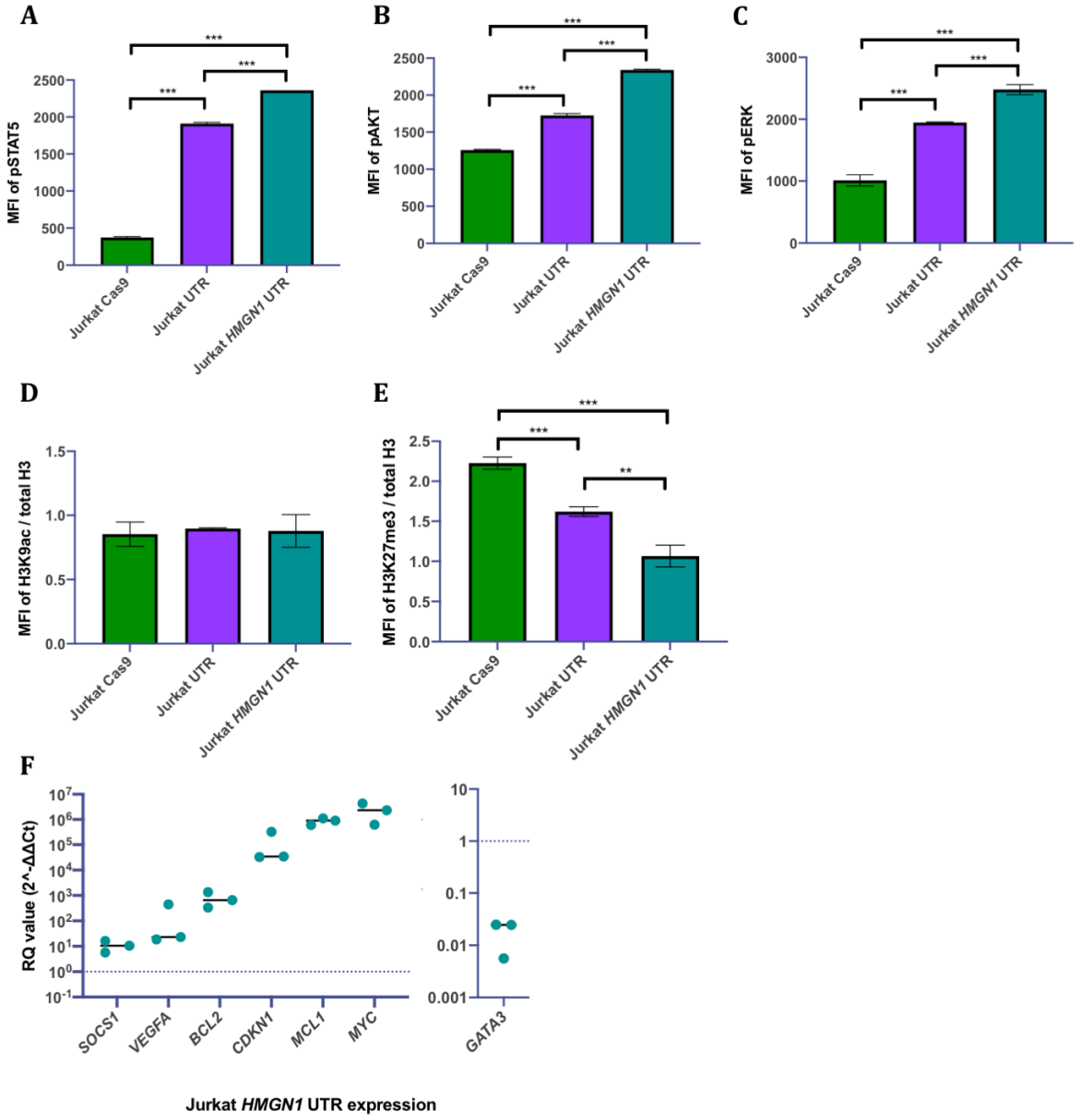

Figure 7: Assessing the functional effect of *HMGN1* expression on CRISPR/Cas9 edited *P2RY8-CRLF2* cells. Phosphorylation levels of STAT5 **(A)**, AKT **(B)**, ERK **(C)** or H3K9ac **(D)** and H3K27me3 **(E)** of Jurkat CRISPR/Cas9 edited *P2RY8-CRLF2* cells with or without *HMGN1* measured by flow cytometry. **F)** Measuring the expression of STAT5 downstream genes by qRT-PCR in Jurkat CRISPR/Cas9 edited *P2RY8-CRLF2* cell lines. RQ values determined using housekeeper actin expression and normalised to the

parental Jurkat Cas9 control cells. Graphs represents the mean of biological replicate of n=3 with SEM error bars and a student's *t*-test was used between each *P2RY8-CRLF2* cell line comparing to control Jurkat Cas9 cells to determine significance, *$p<0.05$, **$p<0.01$, ***$p<0.001$.

Discussion

Gene fusions are a hallmark of ALL; countless recurrent chromosomal alterations have been discovered and novel fusions are still being identified today[25]. To personalise treatment for ALL patients, these genomic alterations need to be modelled using *in vitro* and *in vivo* systems to understand the downstream pathways they activate and their driver potential. Subsequently, mechanistic assays and drug panels can be used to identify an approach to eliminate the leukemic cells. Current modelling of ALL chromosomal alterations involves cloning, which can be complex for fusion genes with repetitive sequences or very large transcripts. CRISPR/Cas9 presents a solution to overcome these difficulties and has been used to create chromosomal alterations found in other diseases [6-8, 11], but has not previously been attempted in ALL.

This study demonstrates the creation of a 320 KB deletion of PAR1 on the X or Y chromosome in leukemic Jurkat cells using two CRISPR/Cas9 gRNAs and employing cellular non homologous end joining (NHEJ) machinery. Previously, CRISPR/Cas9 has been used to create a 30 KB deletion in *Saccharomyces cerevisiae* [26] and a 105 KB deletion in a rabbit embryo[27] utilising NHEJ. This is the first report of a 320 KB deletion resulting in a clinically relevant fusion gene found in ALL. This deletion was significantly larger than previously attempted, and therefore a lower efficiency than the aforementioned studies was to be expected. The experimental system involved leukemic cell lines which relied on the use of a lentiviral CRISPR/Cas9 system[28] rather than a nucleofection[29] or microinjection[27] system previously described with high editing efficiencies. However, the *P2RY8-CRLF2* fusion occurring from the 320 KB deletion also results in the upregulation of *CRLF2* mRNA production and an increase in

TSLPR[15]. Therefore, it is possible to screen these cells for a productive fusion gene by measuring surface levels of TSLPR; which is not expressed basally in Jurkat cells and therefore streamlined this process with a very accurate selection marker.

The use of two different gRNAs targeting *CRLF2* resulted in two different isoforms of *P2RY8-CRLF2*. Both isoforms produced functional mRNA transcripts concordant to *P2RY8-CRLF2* patient transcripts. The *CRLF2* UTR cells increased proliferation, TSLPR expression and had the most clinically relevant trends in cell signaling compared to previous reports of patient *CRLF2* cell signaling[30] and was the prime candidate for further experiments. Therefore, the use of CRISPR/Cas9 to create endogenous gene fusions could be a useful tool for modelling clinically relevant gene fusions in ALL for further investigation. The endogenously expressed gene fusion will reproduce the characteristics of precious patient material to allow for xenograft studies or drug screening[31]. A frameshift mutation at *CRLF2* +15 bp of pre-*CRLF2* #11 may have resulted in a non-functional transcript as the fusion generated from this clone did not display the characteristics anticipated from *P2RY8-CRLF2* patient cells[18, 19], however pre-*CRLF2* #6 maintained signaling and proliferation increases comparable to the *CRLF2* UTR cells. Due to the discrepancy between clones in the pre-*CRLF2* group, these cells have been used as a gRNA control for fusion development rather than the experimental system.

Once the efficiency of the CRISPR/Cas9 *P2RY8-CRLF2* model was confirmed by screening TSLPR and exhibiting the same transcripts and signaling pathways expected in a patient cell, the system was able to be exploited to investigate the phenotypic

impact of the gene fusion. DS-ALL patients are predisposed to developing the *P2RY8-CRLF2* fusion as it is found in 60% of patients[16]. However, it has been difficult to assess predisposing factors without a useful model system. Many reports have implicated chromosome 21 genes from the Down Syndrome critical region in the leukemogenesis of DS-ALL but not yet demonstrated why *P2RY8-CRLF2* occurs so frequently [18, 20, 23, 32-34]. As an example of this application, this study investigated the potential of *HMGN1* promoting leukemogenesis in DS-ALL. By overexpressing *HMGN1* prior to the induction of the gene fusion, it allows for the exploration of the effects of one specific chromosome 21 gene on *P2RY8-CRLF2*. Previous reports have demonstrated increased *HMGN1* expression results in a B-cell progenitor phenotype[23]. Therefore, to test the hypothesis that *HMGN1* is a predisposing factor for *P2RY8-CRLF2* development, a cell line in a state prior to developing *P2RY8-CRLF2* was required. This model system was tailored to test this hypothesis and demonstrated *HMGN1* expression does increase the efficiency of *P2RY8-CRLF2* occurring. While many reports[15, 23, 32, 34-37] have shown roles for *HMGN1* in ALL, this is the first report to validate increased *HMGN1* expression as a pre-disposing factor for *P2RY8-CRLF2* generation. In addition, it will be of interest to confirm these findings in a DS-ALL patient cohort.

To confirm the role of *HMGN1* cooperating with *P2RY8-CRLF2*, increased JAK/STAT, PI3K and RAS signalling pathways were identified, along with a decrease in the gene silencing mark H3K27me3. As HMGN1 is a demethylase, a level of increased transcriptional activity is expected, as previously reported[23]. In addition to the increased cell signalling pathways, this study also identifies an increase in a variety of STAT5 downstream genes, including *MCL1* and *MYC*; proposing potential leukemic

survival mechanisms in DS patients who have increased expression of *HMGN1* and the *P2RY8-CRLF2* fusion. Similar rates in proliferation were observed between *CRLF2*-UTR populations with or without *HMGN1* expression, despite the increase in *CRLF2* expression, suggesting *HMGN1* plays epigenetic roles, rather than a direct role on cell proliferation.

This study provides valuable evidence of using CRISPR/Cas9 to create a large deletion and endogenous ALL fusion gene that exhibits a clinically relevant phenotype. This type of model will be of particular use to investigate the heterogenous landscape of ALL patients. Endogenous expression of fusion genes is a more accurate model than retroviral overexpression of fusion genes to create xenograft models or trial small molecule inhibitors to create a personalised approach for the treatment of ALL patients. Importantly, as described here, this model will be valuable to advance the field by investigating leukemic initiating events due to the inducible gRNAs allowing for a pre-leukemic state to be modelled. Here, *HMGN1* expression has been identified as a predisposing event for *P2RY8-CRLF2* generation in DS-ALL patients. Further evaluation has demonstrated *HMGN1* and *P2RY8-CRLF2* cooperating to increase cell signalling via increased TSLPR and increased *CRLF2* and STAT5 downstream gene expression. Modelling the cells of individual ALL patients to understand gene relationships, cell signalling and to create targeted therapeutic approaches will likely be the future of ALL research.

Acknowledgements

Flow cytometry analysis and cell sorting was performed at the South Australian Health Medical Research Institute (SAHMRI) in the ACRF Cellular Imaging and Cytometry Core Facility. The Facility is generously supported by the Detmold Hoopman Group, Australian Cancer Research Foundation and Australian Government through the Zero Childhood Cancer Program.

Funding of this study was provided by NHMRC, Beat Cancer and LFA.

This study has been performed as partial fulfilment of the requirement for a PhD degree from the University of Adelaide Faculty of Sciences for ECP.

Authorship and conflict-of-interest statements

Contribution: ECP, SLH, PQT and DLW conceived of, designed and wrote the manuscript. SLH, PQT and DLW provided all study materials. ECP collected, assembled and analysed the data. All authors gave final approval of the manuscript.

Conflict-of-interest disclosure: D.L.W receives research support from BMS, and Honoraria from BMS and AMGEN. None of these agencies have had a role in the preparation of this manuscript. All other authors declare no conflicts of interest.

Methods

Contact for reagent and resource sharing

Additional data and requests for resources should be directed to the lead contact, Deborah White (deborah.white@sahmri.com). Materials can be obtained via material transfer agreement from authors' institutions upon reasonable request to corresponding authors.

Experimental Model and Subject Details

Cell lines and maintenance

HEK293T cells (ATCC, Manassas, VA) were maintained in DMEM and Jurkat cells (ATCC, Manassas, VA) in RPMI, supplemented with 10% Fetal Calf Serum (FCS), 200 mM L-Glutamine (SAFC Biosciences), 5000 U/mL penicillin and 5000 µg/mL streptomycin sulphate.

Constructing the FgH1tUTG gRNA vector

The Benchling gRNA design tool (Biology Software, 2019, https://benchling.com) was used to design gRNAs targeting the intron following the first non-coding exon of *P2RY8* and preceding the first exon of *CRLF2* with 5' *Esp*3I restriction sites (Table SI). The FUCas9Cherry and FgH1tUTG plasmids were a gift from Marco Herold (Addgene # 70182 and # 70183)[21]. FgH1tUTG vector was digested with *Esp*3I (New England Biolabs (NEB) # R0734L) and rSAP (NEB # M0371L) for 1 hour at 37°C. The complementary gRNAs were phosphorylated at a final concentration of 10 µM using T4 PNK (NEB # M0201L), then diluted 1:125 with nuclease free water. Five ng/µL of

FgH1tUTG vector was digested with 0.8 pmol of diluted gRNA and ligated with T4 ligase overnight (NEB # M0204L) at 4°C.

Lentiviral Transduction

Lentivirus was produced by transfecting 5.5 µg of the FuCas9mCherry vector or FgH1tUTG gRNA vector, with packaging constructs pMD2.G (2.25 µg), pMDL-PRRE (3.375 µg) and pRSV-REV (1.575 µg) with 30 µL lipofectamine added into $1x10^6$ HEK293T cells in a T25 culture flask in 5mL media. Viral supernatant was harvested 48 hours later and passed through a 0.45 µm filter. Jurkat cells at a concentration of $5x10^5$ /mL were centrifuged at 1800 rpm for 1 hour with 30 µg/mL polybrene in 4 mL of viral supernatant in a 6-well plate at room temperature.

Flow cytometry cell sorting

Jurkat cells transduced with FuCas9mCherry and FgH1tUTG were resuspended in 1 mL of RPMI with 2% FCS at a concentration of $1x10^7$ cells. This suspension was sorted on a BD FACSAria™ for GFP and mCherry double positive cells. Pure populations were resuspended in 1 mL RPMI with 2% FCS and sorted into single cells in a 96-well round bottom plate with 100 µL RPMI with 20% FCS on a BD FACS Melody™. Clones were sub-cultured into 1 mL of media in a 24 well plate three weeks post sort.

Method Details

Genome targeting efficiency assay

Jurkat cells transduced with Cas9 and gRNA vectors (Key Resources Table) were exposed to 1 µg/mL doxycycline hyclate (Sigma-Aldrich, St. Louis, MO) in milli-Q water

for 72 hrs to induce the 320 KB deletion. gDNA was isolated from transduced cells by phenol chloroform extraction and the *P2RY8-CRLF2* fusion breakpoint was amplified via PCR using Phusion kit (New England Biolabs (NEB), Notting Hill, VIC). Primer sequences are outlined in the Key Resources Table. Heteroduplexes were formed by denaturing and re-annealing the breakpoint amplification PCR product which was digested with T7 endonuclease (NEB). The resulting products were gel purified (Qiagen, Venlo, NL) and Sanger sequenced.

Surface flow cytometry

Transduced Jurkat cells were stained with TSLPR-APC or isotype control IgG2a (Invitrogen, Carlsbad, CA) for 30 min in 100 µL RPMI with 10% FCS on ice. Approximately $5x10^6$ cells were washed with 1 mL RPMI with 10% FCS and resuspended in 200 µL 1x PBS and read on a BD FACS Fortessa™ analyser.

Phospho-flow cytometry

Jurkat cells were fixed with a final concentration of 1.6% paraformaldehyde for 10 mins, washed in 1 x PBS and then permeabilised with 80% methanol overnight at -80°C. Cells were then washed in 1x PBS, and subsequently in 1 x PBS containing 1% bovine serum albumin (BSA). All intracellular staining was carried out in the dark, on ice, for 60 mins at room temperature in 1 x PBS/ 1% BSA with antibodies outlined in the Key Resources Table. Cells were washed in 1x PBS before reading on a BD FACSCanto™ analyser.

Real Time PCR Analysis

RNA was isolated from transduced Jurkat cells using TRIzol® (Invitrogen) and cDNA was synthesised using Quantitect reverse transcriptase (Qiagen). SYBR green reagents (Qiagen) were used with 10μM *CRLF2* OR *HMGN1* primers outlined in the Key Resources Table.

Proliferation assay

Jurkat cells were seeded at 390 cells/mL in a 24-well plate in duplicate. On days 0, 2, 4 and 6 20 μL of CellTiter-Glo 2.0® reagent (Promega, Fitchburg, WI) was added to 20 μL of cell suspension. Following 30 min incubation in the dark, luminescence was measured on a Perkin Elmer Victor X5 luminometer set to luminescence at 0.1 seconds.

Quantification and Statistical Analysis

GraphPad Prism software Version 8.4.0© (GraphPad Software Inc.) and FlowJo software (FlowJo LLC) were used for analyses. Graphs represent the median value or mean with stand error of the mean (SEM) error bars as stated in the figure legends. Students *t*-test was used to determine the difference between experimental groups. Differences were considered statistically significant when the p-value was <0.05. Experiments were carried out a minimum of three times (n=3) unless otherwise stated.

References

1. Jinek M, Chylinski K, Fonfara I, Hauer M, Doudna JA, Charpentier E. A programmable dual-RNA-guided DNA endonuclease in adaptive bacterial immunity. *Science.* 2012;337(6096):816-821.
2. Deltcheva E, Chylinski K, Sharma CM, et al. CRISPR RNA maturation by trans-encoded small RNA and host factor RNase III. *Nature.* 2011;471(7340):602-607.
3. Sayin VI, Papagiannakopoulos T. Application of CRISPR-mediated genome engineering in cancer research. *Cancer Lett.* 2017;387:10-17.
4. Vargas JE, Chicaybam L, Stein RT, Tanuri A, Delgado-Cañedo A, Bonamino MH. Retroviral vectors and transposons for stable gene therapy: advances, current challenges and perspectives. *J Transl Med.* 2016;14(1):288.
5. Tzelepis K, Koike-Yusa H, De Braekeleer E, et al. A CRISPR Dropout Screen Identifies Genetic Vulnerabilities and Therapeutic Targets in Acute Myeloid Leukemia. *Cell Rep.* 2016;17(4):1193-1205.
6. Torres R, Martin MC, Garcia A, Cigudosa JC, Ramirez JC, Rodriguez-Perales S. Engineering human tumour-associated chromosomal translocations with the RNA-guided CRISPR-Cas9 system. *Nat Commun.* 2014;5:3964.
7. Vanoli F, Tomishima M, Feng W, et al. CRISPR-Cas9-guided oncogenic chromosomal translocations with conditional fusion protein expression in human mesenchymal cells. *Proc Natl Acad Sci U S A.* 2017;114(14):3696-3701.
8. Jiang J, Zhang L, Zhou X, et al. Induction of site-specific chromosomal translocations in embryonic stem cells by CRISPR/Cas9. *Sci Rep.* 2016;6:21918.
9. García-Tuñón I, Hernández-Sánchez M, Ordoñez JL, et al. The CRISPR/Cas9 system efficiently reverts the tumorigenic ability of BCR/ABL in vitro and in a

xenograft model of chronic myeloid leukemia. *Oncotarget.* 2017;8(16):26027-26040.

10. Tamai M, Inukai T, Kojika S, et al. T315I mutation of BCR-ABL1 into human Philadelphia chromosome-positive leukemia cell lines by homologous recombination using the CRISPR/Cas9 system. *Sci Rep.* 2018;8(1):9966.
11. Corral J, Lavenir I, Impey H, et al. An Mll-AF9 fusion gene made by homologous recombination causes acute leukemia in chimeric mice: a method to create fusion oncogenes. *Cell.* 1996;85(6):853-861.
12. Page EC, Heatley SL, Yeung DT, Thomas PQ, White DL. Precision medicine approaches may be the future for CRLF2 rearranged Down Syndrome Acute Lymphoblastic Leukaemia patients. *Cancer Lett.* 2018;432:69-74.
13. Mullighan CG, Collins-Underwood JR, Phillips LA, et al. Rearrangement of CRLF2 in B-progenitor- and Down syndrome-associated acute lymphoblastic leukemia. *Nat Genet.* 2009;41(11):1243-1246.
14. Vesely C, Frech C, Eckert C, et al. Genomic and transcriptional landscape of P2RY8-CRLF2-positive childhood acute lymphoblastic leukemia. *Leukemia.* 2017.
15. Hertzberg L, Vendramini E, Ganmore I, et al. Down syndrome acute lymphoblastic leukemia, a highly heterogeneous disease in which aberrant expression of CRLF2 is associated with mutated JAK2: a report from the International BFM Study Group. *Blood.* 2010;115(5):1006-1017.
16. Russell LJ, Capasso M, Vater I, et al. Deregulated expression of cytokine receptor gene, CRLF2, is involved in lymphoid transformation in B-cell precursor acute lymphoblastic leukemia. *Blood.* 2009;114(13):2688-2698.

17. Buitenkamp TD, Pieters R, Gallimore NE, et al. Outcome in children with Down's syndrome and acute lymphoblastic leukemia: role of IKZF1 deletions and CRLF2 aberrations. *Leukemia.* 2012;26(10):2204-2211.

18. Den Boer ML, van Slegtenhorst M, De Menezes RX, et al. A subtype of childhood acute lymphoblastic leukaemia with poor treatment outcome: a genome-wide classification study. *Lancet Oncol.* 2009;10(2):125-134.

19. Meyr F, Escherich G, Mann G, et al. Outcomes of treatment for relapsed acute lymphoblastic leukaemia in children with Down syndrome. *Br J Haematol.* 2013;162(1):98-106.

20. Mowery CT, Reyes JM, Cabal-Hierro L, et al. Trisomy of a Down Syndrome Critical Region Globally Amplifies Transcription via HMGN1 Overexpression. *Cell Rep.* 2018;25(7):1898-1911.e1895.

21. Aubrey BJ, Kelly GL, Kueh AJ, et al. An inducible lentiviral guide RNA platform enables the identification of tumor-essential genes and tumor-promoting mutations in vivo. *Cell Rep.* 2015;10(8):1422-1432.

22. Woo JS, Alberti MO, Tirado CA. Childhood B-acute lymphoblastic leukemia: a genetic update. *Exp Hematol Oncol.* 2014;3:16.

23. Iacobucci I, Mullighan CG. Genetic Basis of Acute Lymphoblastic Leukemia. *J Clin Oncol.* 2017;35(9):975-983.

24. Hao H, Wang X, Jia H, et al. Large fragment deletion using a CRISPR/Cas9 system in Saccharomyces cerevisiae. *Anal Biochem.* 2016;509:118-123.

25. Song Y, Yuan L, Wang Y, et al. Efficient dual sgRNA-directed large gene deletion in rabbit with CRISPR/Cas9 system. *Cell Mol Life Sci.* 2016;73(15):2959-2968.

26. Adikusuma F, Pfitzner C, Thomas PQ. Versatile single-step-assembly CRISPR/Cas9 vectors for dual gRNA expression. *PLoS One.* 2017;12(12):e0187236.

27. Tasian SK, Doral MY, Borowitz MJ, et al. Aberrant STAT5 and PI3K/mTOR pathway signaling occurs in human CRLF2-rearranged B-precursor acute lymphoblastic leukemia. *Blood.* 2012;120(4):833-842.

28. Roberts KG, Yang YL, Payne-Turner D, et al. Oncogenic role and therapeutic targeting of ABL-class and JAK-STAT activating kinase alterations in Ph-like ALL. *Blood Adv.* 2017;1(20):1657-1671.

29. Lane AA, Chapuy B, Lin CY, et al. Triplication of a 21q22 region contributes to B cell transformation through HMGN1 overexpression and loss of histone H3 Lys27 trimethylation. *Nat Genet.* 2014;46(6):618-623.

30. Malinge S, Izraeli S, Crispino JD. Insights into the manifestations, outcomes, and mechanisms of leukemogenesis in Down syndrome. *Blood.* 2009;113(12):2619-2628.

31. Izraeli S. The acute lymphoblastic leukemia of Down Syndrome - Genetics and pathogenesis. *Eur J Med Genet.* 2016;59(3):158-161.

32. Lee P, Bhansali R, Izraeli S, Hijiya N, Crispino JD. The biology, pathogenesis and clinical aspects of acute lymphoblastic leukemia in children with Down syndrome. *Leukemia.* 2016;30(9):1816-1823.

33. Rochman M, Taher L, Kurahashi T, et al. Effects of HMGN variants on the cellular transcription profile. *Nucleic Acids Res.* 2011;39(10):4076-4087.

34. Antonarakis SE. Down syndrome and the complexity of genome dosage imbalance. *Nat Rev Genet.* 2017;18(3):147-163.

Supplementary Materials

Unique modelling of *P2RY8-CRLF2* using CRISPR/Cas9 reveals *HMGN1* as a predisposing factor in Down Syndrome Acute Lymphoblastic Leukemia

Elyse C Page[1, 2], Susan L Heatley[1, 3, 4], Paul Q Thomas[3, 5], and *Deborah L White[1, 2, 3, 4, 6, 7]

Key Resources Table

REAGENT or RESOURCE	SOURCE	IDENTIFIER
Antibodies		
TSLPR-APC	Invitrogen	Cat#17-5499-41
IgG2a-APC	Invitrogen	Cat#17-4724-81
IgG2a-PE	BD	Cat#556653
IgG1-APC	BD	Cat#551019
pSTAT5-PE	BD	Cat#612567
pERK-PE	BD	Cat#665426
pS6 kinase	Cell Signaling Technologies	Cat#665426
pAKT	BD	Cat#560378
H3K9ac	Cell Signaling Technologies	Cat#4484
H3K27me3	Cell Signaling Technologies	Cat#12158
Bacterial and Virus Strains		
FuCas9mCherry	Addgene	Cat#70182
FgH1tUTG	Addgene	Cat#70183
pMD2.G	Addgene	Cat#12259
pMDL-PRRE	Addgene	Cat#12251
pRSV-REV	Addgene	Cat#12253
pMImCII HMGN1	This paper	
Chemicals, Peptides, and Recombinant Proteins		
Doxycycline Hyclate	Sigma-Aldrich	Cat#D9891
Esp3I	New England Biolabs	Cat#R0734L
rSAP	New England Biolabs	Cat#M0371L
T4 PNK	New England Biolabs	Cat#M0201L
T4 Ligase	New England Biolabs	Cat#M0204L
Lipofectamine 2000	Invitrogen	Cat#11668-019
Polybrene	Merck	Cat#TR-1003-G
TRIzol	Invitrogen	Cat#15596026
T7 endonuclease	New England Biolabs	Cat#M0263L
Critical Commercial Assays		
CellTiter Glo 2.0	Promega	Cat#G9243
SYBR Green	Qiagen	Cat#330503
PCR Phusion Kit	New England Biolabs	Cat#E0553L
Quantitect Reverse Transcriptase	Qiagen	Cat#205313
QIAquick Gel extraction kit	Qiagen	Cat#28706
Experimental Models: Cell Lines		
Jurkat cells	ATCC	(ATCC® TIB-152™)
HEK293T cells	ATCC	(ATCC® CRL-11268™)
Experimental Models: Organisms/Strains		
DH5α	New England Biolabs	Cat#12297016

Oligonucleotides		
P2RY8 intron gRNA 5' -CGTGTACGGTGAGAACATGG- 3'	This Paper	N/A
Pre-*CRLF2* gRNA 5' -GTGCGTGGCAGTCCTGATCC- 3'	This Paper	N/A
CRLF2 UTR gRNA 5' -CTGTTCGTTGTAGGTCCCTG- 3'	This Paper	N/A
CRLF2 qPCR F 5' -TGGATCACAGACACCCAGAA- 3'	This Paper	N/A
CRLF2 qPCR R 5' -TCTTGGCCAACTGGACTACC- 3'	This Paper	N/A
HMGN1 qPCR F 5' -TGCAAACAAAAGGGAAAAGG- 3'	This Paper	N/A
HMGN1 qPCR R 5' -CATCAGAGGCTGGACTCTCC- 3'	This Paper	N/A
P2RY8 seq 5' -AAGCGTTGCATCCTGTTACCTGG- 3'	This Paper	N/A
CRLF2 seq 5' -GCCTCCCAGCAGAAAGACGG- 3'	This Paper	N/A
*VEGFA*_qPCR_F 5' –AGCACAGCAGATGTGAATGC- 3'	This Paper	N/A
*VEGFA*_qPCR_R 5' –TTTCTTGCGCTTTCGTTTTT- 3'	This Paper	N/A
*BCL2*_qPCR_F 5' -AAGCTGTCACAGAGGGGCTA- 3'	This Paper	N/A
*BCL2*_qPCR_R 5' -CAGGCTGGAAGGAGAAGATG- 3'	This Paper	N/A
*MCL1*_qPCR_F 5' -GCTCCGGAAACTGGACATTA- 3'	This Paper	N/A
*MCL1*_qPCR_R 5' -CCCAGTTTGTTACGCCATCT- 3'	This Paper	N/A
*MYC*_qPCR_F 5' -CCAGATCCCTGAATTGGAAA- 3'	This Paper	N/A
*MYC*_qPCR_R 5' -TCGTCTGCTTGAATGGACAG- 3'	This Paper	N/A
*GATA3*_qPCR_F 5' -CTTATCAAGCCCAAGCGAAG- 3'	This Paper	N/A
*GATA3*_qPCR_R 5' -CATTAGCGTTCCTCCTCCAG- 3'	This Paper	N/A
*CDKN1A*_qPCR_F 5' -CGGTGGAACTTTGACTTCGT- 3'	This Paper	N/A
*CDKN1A*_qPCR_R 5' -CAGGGCAGAGGAAGTACTGG- 3'	This Paper	N/A
*SOCS1*_qPCR_F 5' -CCTCCTCGTCCTCGTCTTC- 3'	This Paper	N/A
*SOCS1*_qPCR_R 5' -AAGGTGCGGAAGTGAGTGTC- 3'	This Paper	N/A
Software and Algorithms		
Prism version 8.4.0	GraphPad	https://www.graphpad.com
FlowJo	FlowJo, LLC	https://www.flowjo.com/solutions/
Benchling	Biology Software, 2019	https://benchling.com

Sample	target_length	Query	Type	Variant_name	Ratio	Expression	Min_coverage	Sequence
AYAII-0492-DIA1	longSeq	P2RY8_exon1_CRLF2_exon1	Insertion	77:/TCCCTGAGGACCTCACTCTCCACTCCTGTTTCAGG:77	0.16	22.7	0	ACTTAAGCGTTGCATCCTGTTACCTGGAGACCCTCTGAGCTCTCACCTGCTACTTCTGCCGCTGCTTCTGCACAGGTCCCTGAGGACCTCACTCTCCACTCCTGTTTCAGGCATGGGGCGGCTGGTTCTGCTGGGAGAGCTGCCGTCTTTCTGCTGGGAGGCTGGATGGCTTTGGGGCAAGGAG
CH-A1747-REL1	longSeq	P2RY8_exon1_CRLF2_exon1	Insertion	77:/TCCCTGAGGACCTCACTCTCCACTCCTGTTTCAGG:77	0.058	21	0	ACTTAAGCGTTGCATCCTGTTACCTGGAGACCCTCTGAGCTCTCACCTGCTACTTCTGCCGCTGCTTCTGCACAGGTCCCTGAGGACCTCACTCTCCACTCCTGTTTCAGGCATGGGGCGGCTGGTTCTGCTGGGAGAGCTGCCGTCTTTCTGCTGGGAGGCTGGATGGCTTTGGGGCAAGGAG
CH-A2273	longSeq	P2RY8_exon1_CRLF2_exon1	Insertion	77:/TCCCTGAGGACCTCACTCTCCACTCCTGTTTCAGG:77	0.154	43.7	0	ACTTAAGCGTTGCATCCTGTTACCTGGAGACCCTCTGAGCTCTCACCTGCTACTTCTGCCGCTGCTTCTGCACAGGTCCCTGAGGACCTCACTCTCCACTCCTGTTTCAGGCATGGGGCGGCTGGTTCTGCTGGGAGAGCTGCCGTCTTTCTGCTGGGAGGCTGGATGGCTTTGGGGCAAGGAG
CH-A2426	longSeq	P2RY8_exon1_CRLF2_exon1	Reference		1	35	35	ACTTAAGCGTTGCATCCTGTTACCTGGAGACCCTCTGAGCTCTCACCTGCTACTTCTGCCGCTGCTTCTGCACAGGCATGGGGCGGCTGGTTCTGCTGTGGGGAGCTGCCGTCTTTCTGCTGGGAGGCTGGATGGCTTTGGGGCAAGGAG
CH-A3100-DIA1	longSeq	P2RY8_exon1_CRLF2_exon1	Reference		1	5	102	ACTTAAGCGTTGCATCCTGTTACCTGGAGACCCTCTGAGCTCTCACCTGCTACTTCTGCCGCTGCTTCTGCACAGGCATGGGGCGGCTGGTTCTGCTGTGGGGAGCTGCCGTCTTTCTGCTGGGAGGCTGGATGGCTTTGGGGCAAGGAG
CH-A3100-DIA1	longSeq	P2RY8_exon1_CRLF2_exon1	Insertion	77:/TCCCTGAGGACCTCACTCTCCACTCCTGTTTCAGG:77	0.185	38.9	5	ACTTAAGCGTTGCATCCTGTTACCTGGAGACCCTCTGAGCTCTCACCTGCTACTTCTGCCGCTGCTTCTGCACAGGTCCCTGAGGACCTCACTCTCCACTCCTGTTTCAGGCATGGGGCGGCTGGTTCTGCTGGGAGAGCTGCCGTCTTTCTGCTGGGAGGCTGGATGGCTTTGGGGCAAGGAG
CH-A4680-REL1	longSeq	P2RY8_exon1_CRLF2_exon1	Reference		1	13	13	ACTTAAGCGTTGCATCCTGTTACCTGGAGACCCTCTGAGCTCTCACCTGCTACTTCTGCCGCTGCTTCTGCACAGGCATGGGGCGGCTGGTTCTGCTGTGGGGAGCTGCCGTCTTTCTGCTGGGAGGCTGGATGGCTTTGGGGCAAGGAG
CHI-0171	longSeq	P2RY8_exon1_CRLF2_exon1	Reference	NA	1	22	22	ACTTAAGCGTTGCATCCTGTTACCTGGAGACCCTCTGAGCTCTCACCTGCTACTTCTGCCGCTGCTTCTGCACAGGCATGGGGCGGCTGGTTCTGCTGTGGGGAGCTGCCGTCTTTCTGCTGGGAGGCTGGATGGCTTTGGGGCAAGGAG
CHI-0197-REL1	longSeq	P2RY8_exon1_CRLF2_exon1	Reference		1	17	238	ACTTAAGCGTTGCATCCTGTTACCTGGAGACCCTCTGAGCTCTCACCTGCTACTTCTGCCGCTGCTTCTGCACAGGCATGGGGCGGCTGGTTCTGCTGTGGGGAGCTGCCGTCTTTCTGCTGGGAGGCTGGATGGCTTTGGGGCAAGGAG
CHI-0197-REL1	longSeq	P2RY8_exon1_CRLF2_exon1	Insertion	77:/TCCCTGAGGACCTCACTCTCCACTCCTGTTTCAGG:77	0.151	60.1	17	ACTTAAGCGTTGCATCCTGTTACCTGGAGACCCTCTGAGCTCTCACCTGCTACTTCTGCCGCTGCTTCTGCACAGGTCCCTGAGGACCTCACTCTCCACTCCTGTTTCAGGCATGGGGCGGCTGGTTCTGCTGGGAGAGCTGCCGTCTTTCTGCTGGGAGGCTGGATGGCTTTGGGGCAAGGAG
CHI-0251-REL1	longSeq	P2RY8_exon1_CRLF2_exon1	Reference		1	6	34	ACTTAAGCGTTGCATCCTGTTACCTGGAGACCCTCTGAGCTCTCACCTGCTACTTCTGCCGCTGCTTCTGCACAGGCATGGGGCGGCTGGTTCTGCTGTGGGGAGCTGCCGTCTTTCTGCTGGGAGGCTGGATGGCTTTGGGGCAAGGAG
CHI-0354	longSeq	P2RY8_exon1_CRLF2_exon1	Reference		1	7	97	ACTTAAGCGTTGCATCCTGTTACCTGGAGACCCTCTGAGCTCTCACCTGCTACTTCTGCCGCTGCTTCTGCACAGGCATGGGGCGGCTGGTTCTGCTGTGGGGAGCTGCCGTCTTTCTGCTGGGAGGCTGGATGGCTTTGGGGCAAGGAG
CHI-0354	longSeq	P2RY8_exon1_CRLF2_exon1	Insertion	77:/TCCCTGAGGACCTCACTCTCCACTCCTGTTTCAGG:77	0.205	41.9	7	ACTTAAGCGTTGCATCCTGTTACCTGGAGACCCTCTGAGCTCTCACCTGCTACTTCTGCCGCTGCTTCTGCACAGGTCCCTGAGGACCTCACTCTCCACTCCTGTTTCAGGCATGGGGCGGCTGGTTCTGCTGGGAGAGCTGCCGTCTTTCTGCTGGGAGGCTGGATGGCTTTGGGGCAAGGAG
CHI-0399	longSeq	P2RY8_exon1_CRLF2_exon1	Insertion	77:/TCCCTGAGGACCTCACTCTCCACTCCTGTTTCAGG:77	0.179	31	0	ACTTAAGCGTTGCATCCTGTTACCTGGAGACCCTCTGAGCTCTCACCTGCTACTTCTGCCGCTGCTTCTGCACAGGTCCCTGAGGACCTCACTCTCCACTCCTGTTTCAGGCATGGGGCGGCTGGTTCTGCTGGGAGAGCTGCCGTCTTTCTGCTGGGAGGCTGGATGGCTTTGGGGCAAGGAG
CHI-0429-DIA1-PB	longSeq	P2RY8_exon1_CRLF2_exon1	Reference		1	5	92	ACTTAAGCGTTGCATCCTGTTACCTGGAGACCCTCTGAGCTCTCACCTGCTACTTCTGCCGCTGCTTCTGCACAGGCATGGGGCGGCTGGTTCTGCTGTGGGGAGCTGCCGTCTTTCTGCTGGGAGGCTGGATGGCTTTGGGGCAAGGAG
CHI-0429-DIA1-PB	longSeq	P2RY8_exon1_CRLF2_exon1	Insertion	77:/TCCCTGAGGACCTCACTCTCCACTCCTGTTTCAGG:77	0.202	53.2	5	ACTTAAGCGTTGCATCCTGTTACCTGGAGACCCTCTGAGCTCTCACCTGCTACTTCTGCCGCTGCTTCTGCACAGGTCCCTGAGGACCTCACTCTCCACTCCTGTTTCAGGCATGGGGCGGCTGGTTCTGCTGGGAGAGCTGCCGTCTTTCTGCTGGGAGGCTGGATGGCTTTGGGGCAAGGAG
QCTB-0894	longSeq	P2RY8_exon1_CRLF2_exon1	Reference		1	26	26	ACTTAAGCGTTGCATCCTGTTACCTGGAGACCCTCTGAGCTCTCACCTGCTACTTCTGCCGCTGCTTCTGCACAGGCATGGGGCGGCTGGTTCTGCTGTGGGGAGCTGCCGTCTTTCTGCTGGGAGGCTGGATGGCTTTGGGGCAAGGAG
QCTB-1629901	longSeq	P2RY8_exon1_CRLF2_exon1	Reference		1	44	44	ACTTAAGCGTTGCATCCTGTTACCTGGAGACCCTCTGAGCTCTCACCTGCTACTTCTGCCGCTGCTTCTGCACAGGCATGGGGCGGCTGGTTCTGCTGTGGGGAGCTGCCGTCTTTCTGCTGGGAGGCTGGATGGCTTTGGGGCAAGGAG
AYAII-0492-DIA1	medSeq	P2RY8_exon1_CRLF2_exon1	Insertion	52:/TCCCTGAGGACCTCACTCTCCACTCCTGTTTCAGG:52	0.134	15.8	0	GGAGACCCTCTGAGCTCTCACCTGCTACTTCTGCCGCTGCTTCTGCACAGGTCCCTGAGGACCTCACTCTCCACTCCTGTTTCAGGCATGGGGCGGCTGGTTCTGCTGTGGGGAGCTGCCGTCTTTCTGCTGGGA
CH-A1747-REL1	medSeq	P2RY8_exon1_CRLF2_exon1	Insertion	52:/TCCCTGAGGACCTCACTCTCCACTCCTGTTTCAGG:52	0.041	13.7	0	GGAGACCCTCTGAGCTCTCACCTGCTACTTCTGCCGCTGCTTCTGCACAGGTCCCTGAGGACCTCACTCTCCACTCCTGTTTCAGGCATGGGGCGGCTGGTTCTGCTGTGGGGAGCTGCCGTCTTTCTGCTGGGA
CH-A2273	medSeq	P2RY8_exon1_CRLF2_exon1	Insertion	52:/TCCCTGAGGACCTCACTCTCCACTCCTGTTTCAGG:52	0.126	29.8	0	GGAGACCCTCTGAGCTCTCACCTGCTACTTCTGCCGCTGCTTCTGCACAGGTCCCTGAGGACCTCACTCTCCACTCCTGTTTCAGGCATGGGGCGGCTGGTTCTGCTGTGGGGAGCTGCCGTCTTTCTGCTGGGA
CH-A2426	medSeq	P2RY8_exon1_CRLF2_exon1	Reference		1	35	35	GGAGACCCTCTGAGCTCTCACCTGCTACTTCTGCCGCTGCTTCTGCACAGGCATGGGGCGGCTGGTTCTGCTGTGGGGAGCTGCCGTCTTTCTGCTGGGA
CH-A3100-DIA1	medSeq	P2RY8_exon1_CRLF2_exon1	Reference		1	5	102	GGAGACCCTCTGAGCTCTCACCTGCTACTTCTGCCGCTGCTTCTGCACAGGCATGGGGCGGCTGGTTCTGCTGTGGGGAGCTGCCGTCTTTCTGCTGGGA
CH-A3100-DIA1	medSeq	P2RY8_exon1_CRLF2_exon1	Insertion	52:/TCCCTGAGGACCTCACTCTCCACTCCTGTTTCAGG:52	0.174	33.4	5	GGAGACCCTCTGAGCTCTCACCTGCTACTTCTGCCGCTGCTTCTGCACAGGTCCCTGAGGACCTCACTCTCCACTCCTGTTTCAGGCATGGGGCGGCTGGTTCTGCTGTGGGGAGCTGCCGTCTTTCTGCTGGGA
CH-A4680-REL1	medSeq	P2RY8_exon1_CRLF2_exon1	Reference		1	16	16	GGAGACCCTCTGAGCTCTCACCTGCTACTTCTGCCGCTGCTTCTGCACAGGCATGGGGCGGCTGGTTCTGCTGTGGGGAGCTGCCGTCTTTCTGCTGGGA
CHI-0171	medSeq	P2RY8_exon1_CRLF2_exon1	Reference	NA	1	22	22	GGAGACCCTCTGAGCTCTCACCTGCTACTTCTGCCGCTGCTTCTGCACAGGCATGGGGCGGCTGGTTCTGCTGTGGGGAGCTGCCGTCTTTCTGCTGGGA
CHI-0197-REL1	medSeq	P2RY8_exon1_CRLF2_exon1	Reference		1	17	238	GGAGACCCTCTGAGCTCTCACCTGCTACTTCTGCCGCTGCTTCTGCACAGGCATGGGGCGGCTGGTTCTGCTGTGGGGAGCTGCCGTCTTTCTGCTGGGA
CHI-0197-REL1	medSeq	P2RY8_exon1_CRLF2_exon1	Insertion	52:/TCCCTGAGGACCTCACTCTCCACTCCTGTTTCAGG:52	0.127	43.5	17	GGAGACCCTCTGAGCTCTCACCTGCTACTTCTGCCGCTGCTTCTGCACAGGTCCCTGAGGACCTCACTCTCCACTCCTGTTTCAGGCATGGGGCGGCTGGTTCTGCTGTGGGGAGCTGCCGTCTTTCTGCTGGGA
CHI-0251-REL1	medSeq	P2RY8_exon1_CRLF2_exon1	Reference		1	34	34	GGAGACCCTCTGAGCTCTCACCTGCTACTTCTGCCGCTGCTTCTGCACAGGCATGGGGCGGCTGGTTCTGCTGTGGGGAGCTGCCGTCTTTCTGCTGGGA
CHI-0354	medSeq	P2RY8_exon1_CRLF2_exon1	Reference		1	7	97	GGAGACCCTCTGAGCTCTCACCTGCTACTTCTGCCGCTGCTTCTGCACAGGCATGGGGCGGCTGGTTCTGCTGTGGGGAGCTGCCGTCTTTCTGCTGGGA
CHI-0354	medSeq	P2RY8_exon1_CRLF2_exon1	Insertion	52:/TCCCTGAGGACCTCACTCTCCACTCCTGTTTCAGG:52	0.19	33.5	7	GGAGACCCTCTGAGCTCTCACCTGCTACTTCTGCCGCTGCTTCTGCACAGGTCCCTGAGGACCTCACTCTCCACTCCTGTTTCAGGCATGGGGCGGCTGGTTCTGCTGTGGGGAGCTGCCGTCTTTCTGCTGGGA
CHI-0399	medSeq	P2RY8_exon1_CRLF2_exon1	Insertion	52:/TCCCTGAGGACCTCACTCTCCACTCCTGTTTCAGG:52	0.157	23.1	0	GGAGACCCTCTGAGCTCTCACCTGCTACTTCTGCCGCTGCTTCTGCACAGGTCCCTGAGGACCTCACTCTCCACTCCTGTTTCAGGCATGGGGCGGCTGGTTCTGCTGTGGGGAGCTGCCGTCTTTCTGCTGGGA
CHI-0429-DIA1-PB	medSeq	P2RY8_exon1_CRLF2_exon1	Reference		1	5	92	GGAGACCCTCTGAGCTCTCACCTGCTACTTCTGCCGCTGCTTCTGCACAGGCATGGGGCGGCTGGTTCTGCTGTGGGGAGCTGCCGTCTTTCTGCTGGGA
CHI-0429-DIA1-PB	medSeq	P2RY8_exon1_CRLF2_exon1	Insertion	52:/TCCCTGAGGACCTCACTCTCCACTCCTGTTTCAGG:52	0.175	35.6	5	GGAGACCCTCTGAGCTCTCACCTGCTACTTCTGCCGCTGCTTCTGCACAGGTCCCTGAGGACCTCACTCTCCACTCCTGTTTCAGGCATGGGGCGGCTGGTTCTGCTGTGGGGAGCTGCCGTCTTTCTGCTGGGA
QCTB-0894	medSeq	P2RY8_exon1_CRLF2_exon1	Reference	NA	1	26	26	GGAGACCCTCTGAGCTCTCACCTGCTACTTCTGCCGCTGCTTCTGCACAGGCATGGGGCGGCTGGTTCTGCTGTGGGGAGCTGCCGTCTTTCTGCTGGGA
QCTB-1629901	medSeq	P2RY8_exon1_CRLF2_exon1	Reference		1	44	44	GGAGACCCTCTGAGCTCTCACCTGCTACTTCTGCCGCTGCTTCTGCACAGGCATGGGGCGGCTGGTTCTGCTGTGGGGAGCTGCCGTCTTTCTGCTGGGA
AYAII-0492-DIA1	shortSeq	P2RY8_exon1_CRLF2_exon1	Insertion	33:/TCCCTGAGGACCTCACTCTCCACTCCTGTTTCAGG:33	0.111	11.6	5	ACCTGCTACTTCTGCCGCTGCTTCTGCACAGGTCCCTGAGGACCTCACTCTCCACTCCTGTTTCAGGCATGGGGCGGCTGGTTCTGCTGTGGGGAGC
AYAII-0492-DIA1	shortSeq	P2RY8_exon1_CRLF2_exon1	Reference		1	5	66	ACCTGCTACTTCTGCCGCTGCTTCTGCACAGGCATGGGGCGGCTGGTTCTGCTGTGGGGAGC
CH-A1747-REL1	shortSeq	P2RY8_exon1_CRLF2_exon1	Insertion	33:/TCCCTGAGGACCTCACTCTCCACTCCTGTTTCAGG:33	0.065	24.3	10	ACCTGCTACTTCTGCCGCTGCTTCTGCACAGGTCCCTGAGGACCTCACTCTCCACTCCTGTTTCAGGCATGGGGCGGCTGGTTCTGCTGTGGGGAGC
CH-A1747-REL1	shortSeq	P2RY8_exon1_CRLF2_exon1	Reference		1	10	271	ACCTGCTACTTCTGCCGCTGCTTCTGCACAGGCATGGGGCGGCTGGTTCTGCTGTGGGGAGC
CH-A2273	shortSeq	P2RY8_exon1_CRLF2_exon1	Insertion	33:/TCCCTGAGGACCTCACTCTCCACTCCTGTTTCAGG:33	0.096	19.3	9	ACCTGCTACTTCTGCCGCTGCTTCTGCACAGGTCCCTGAGGACCTCACTCTCCACTCCTGTTTCAGGCATGGGGCGGCTGGTTCTGCTGTGGGGAGC
CH-A2273	shortSeq	P2RY8_exon1_CRLF2_exon1	Reference		1	9	160	ACCTGCTACTTCTGCCGCTGCTTCTGCACAGGCATGGGGCGGCTGGTTCTGCTGTGGGGAGC
CH-A2426	shortSeq	P2RY8_exon1_CRLF2_exon1	Reference		1	35	35	ACCTGCTACTTCTGCCGCTGCTTCTGCACAGGCATGGGGCGGCTGGTTCTGCTGTGGGGAGC
CH-A3100-DIA1	shortSeq	P2RY8_exon1_CRLF2_exon1	Insertion	33:/TCCCTGAGGACCTCACTCTCCACTCCTGTTTCAGG:33	0.126	17.6	5	ACCTGCTACTTCTGCCGCTGCTTCTGCACAGGTCCCTGAGGACCTCACTCTCCACTCCTGTTTCAGGCATGGGGCGGCTGGTTCTGCTGTGGGGAGC
CH-A3100-DIA1	shortSeq	P2RY8_exon1_CRLF2_exon1	Reference		1	5	102	ACCTGCTACTTCTGCCGCTGCTTCTGCACAGGCATGGGGCGGCTGGTTCTGCTGTGGGGAGC
CH-A4680-REL1	shortSeq	P2RY8_exon1_CRLF2_exon1	Reference	NA	1	16	16	ACCTGCTACTTCTGCCGCTGCTTCTGCACAGGCATGGGGCGGCTGGTTCTGCTGTGGGGAGC
CHI-0171	shortSeq	P2RY8_exon1_CRLF2_exon1	Reference	NA	1	22	22	ACCTGCTACTTCTGCCGCTGCTTCTGCACAGGCATGGGGCGGCTGGTTCTGCTGTGGGGAGC
CHI-0197-REL1	shortSeq	P2RY8_exon1_CRLF2_exon1	Insertion	33:/TCCCTGAGGACCTCACTCTCCACTCCTGTTTCAGG:33	0.099	29.3	17	ACCTGCTACTTCTGCCGCTGCTTCTGCACAGGTCCCTGAGGACCTCACTCTCCACTCCTGTTTCAGGCATGGGGCGGCTGGTTCTGCTGTGGGGAGC
CHI-0197-REL1	shortSeq	P2RY8_exon1_CRLF2_exon1	Reference		1	17	244	ACCTGCTACTTCTGCCGCTGCTTCTGCACAGGCATGGGGCGGCTGGTTCTGCTGTGGGGAGC
CHI-0251-REL1	shortSeq	P2RY8_exon1_CRLF2_exon1	Reference	NA	1	34	34	ACCTGCTACTTCTGCCGCTGCTTCTGCACAGGCATGGGGCGGCTGGTTCTGCTGTGGGGAGC
CHI-0354	shortSeq	P2RY8_exon1_CRLF2_exon1	Insertion	33:/TCCCTGAGGACCTCACTCTCCACTCCTGTTTCAGG:33	0.155	20.7	7	ACCTGCTACTTCTGCCGCTGCTTCTGCACAGGTCCCTGAGGACCTCACTCTCCACTCCTGTTTCAGGCATGGGGCGGCTGGTTCTGCTGTGGGGAGC
CHI-0354	shortSeq	P2RY8_exon1_CRLF2_exon1	Reference		1	7	97	ACCTGCTACTTCTGCCGCTGCTTCTGCACAGGCATGGGGCGGCTGGTTCTGCTGTGGGGAGC
CHI-0399	shortSeq	P2RY8_exon1_CRLF2_exon1	Insertion	33:/TCCCTGAGGACCTCACTCTCCACTCCTGTTTCAGG:33	0.149	20.6	13	ACCTGCTACTTCTGCCGCTGCTTCTGCACAGGTCCCTGAGGACCTCACTCTCCACTCCTGTTTCAGGCATGGGGCGGCTGGTTCTGCTGTGGGGAGC
CHI-0399	shortSeq	P2RY8_exon1_CRLF2_exon1	Reference		1	13	91	ACCTGCTACTTCTGCCGCTGCTTCTGCACAGGCATGGGGCGGCTGGTTCTGCTGTGGGGAGC
CHI-0429-DIA1-PB	shortSeq	P2RY8_exon1_CRLF2_exon1	Insertion	33:/TCCCTGAGGACCTCACTCTCCACTCCTGTTTCAGG:33	0.101	12.9	5	ACCTGCTACTTCTGCCGCTGCTTCTGCACAGGTCCCTGAGGACCTCACTCTCCACTCCTGTTTCAGGCATGGGGCGGCTGGTTCTGCTGTGGGGAGC
CHI-0429-DIA1-PB	shortSeq	P2RY8_exon1_CRLF2_exon1	Reference		1	5	92	ACCTGCTACTTCTGCCGCTGCTTCTGCACAGGCATGGGGCGGCTGGTTCTGCTGTGGGGAGC
QCTB-0894	shortSeq	P2RY8_exon1_CRLF2_exon1	Reference	NA	1	26	26	ACCTGCTACTTCTGCCGCTGCTTCTGCACAGGCATGGGGCGGCTGGTTCTGCTGTGGGGAGC
QCTB-1629901	shortSeq	P2RY8_exon1_CRLF2_exon1	Reference	NA	1	44	44	ACCTGCTACTTCTGCCGCTGCTTCTGCACAGGCATGGGGCGGCTGGTTCTGCTGTGGGGAGC

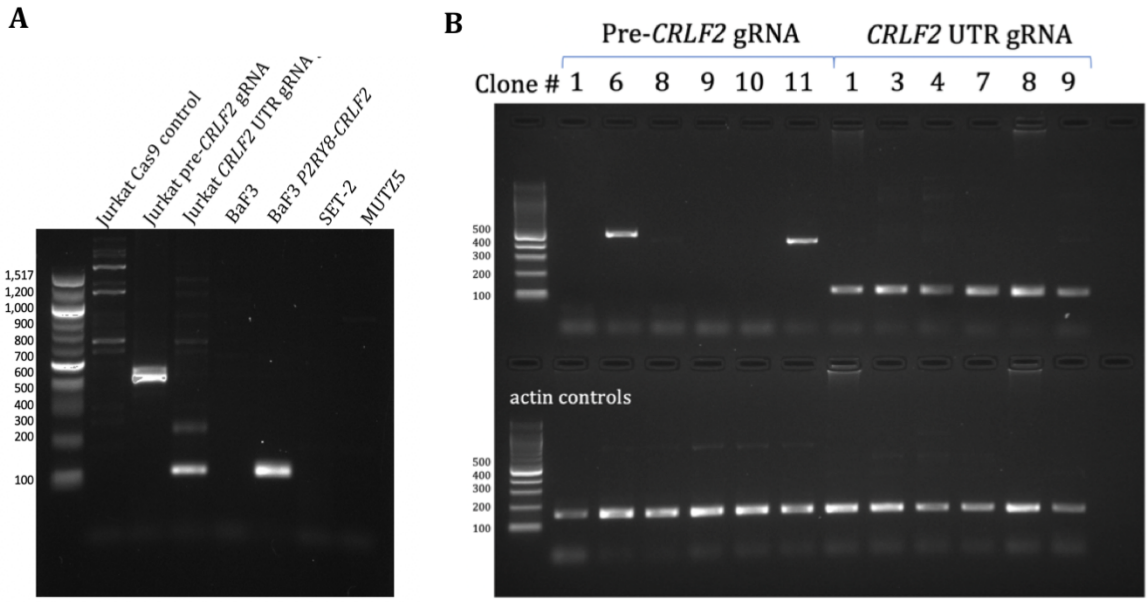

Supplementary Figure 1: Confirmation of the *P2RY8-CRLF2* breakpoint in Jurkat CRISPR/Cas9 cells. A) Two isoforms of the *P2RY8-CRLF2* breakpoint detected by breakpoint PCR in Jurkat CRISPR/Cas9 edited cells with the pre-*CRLF2* gRNA and the *CRLF2* UTR gRNA. **B)** PCR amplification of the *P2RY8-CRLF2* breakpoint in single cell clones of Jurkat CRISPR/Cas9 edited *P2RY8-CRLF2* cells.

***P2RY8-CRLF2* alignment with *CRLF2* UTR sequences**

***P2RY8-CRLF2* alignment with pre-*CRLF2* sequences**

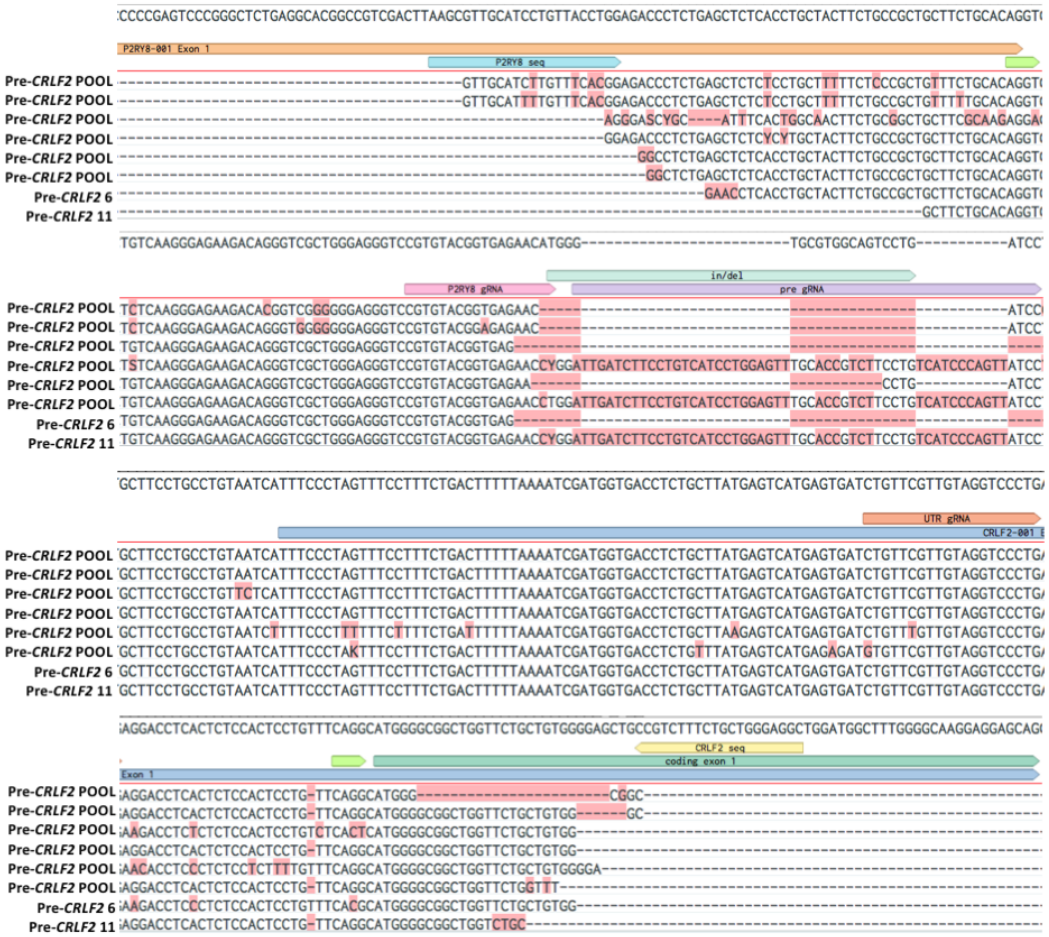

Supplementary Figure 2: Characterising the breakpoints of Jurkat *P2RY8-CRLF2* cells. Sequencing alignments identifying multiple *P2RY8-CRLF2* breakpoints in *CRLF2* UTR and pre-*CRLF2* cells.

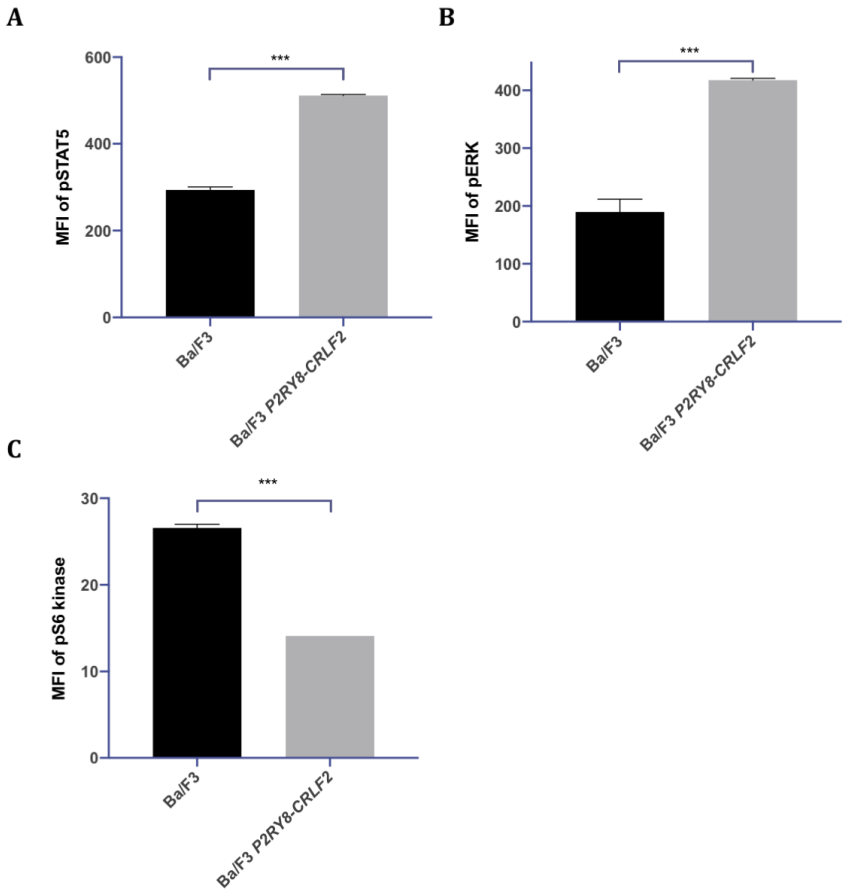

Supplementary Figure 3: Characterising the signaling profile of Ba/F3 cells expressing *P2RY8-CRLF2* from patient cDNA. Ba/F3 cells overexpressing *P2RY8-CRLF2* have increased phosphorylation of STAT5 and ERK, and decreased phosphorylation of S6 kinase compared to Ba/F3 control cells. Protein phosphorylation measured by flow cytometry. All graphs represent the mean of biological replicate of n=3 with SEM error bars and a student's *t*-test was used between the Ba/F3 cell line and the Ba/F3 *P2RY8-CRLF2* expressing line to determine significance, ***$p<0.001$.

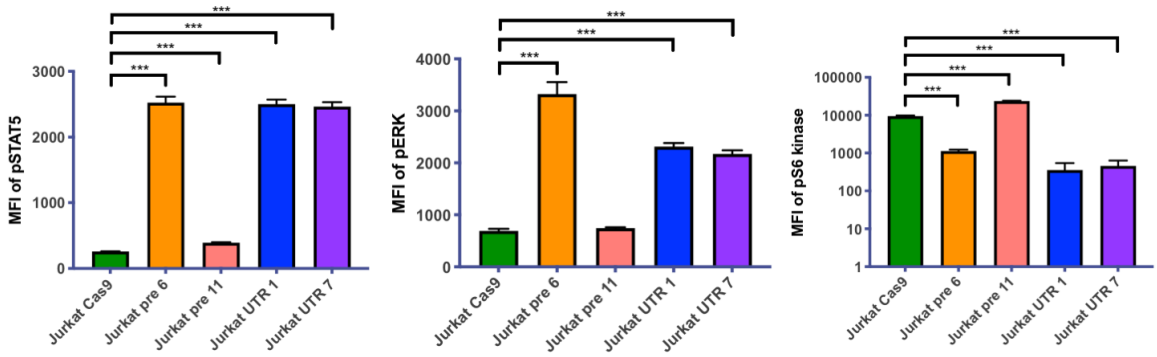

Supplementary Figure 4: Signalling profile pf pre-*CRLF2* cells compared to *CRLF2* UTR and Cas9 control cells.

Phosphorylation levels of STAT5, ERK and S6 kinase of Jurkat CRISPR/Cas9 edited *P2RY8-CRLF2* cells measured by flow cytometry.All graphs represent the mean of biological replicate of n=3 with SEM error bars and a student's *t*-test was used between the Jurkat Cas9 cell line and each *P2RY8-CRLF2* expressing line to determine significance, ***$p<0.001$.

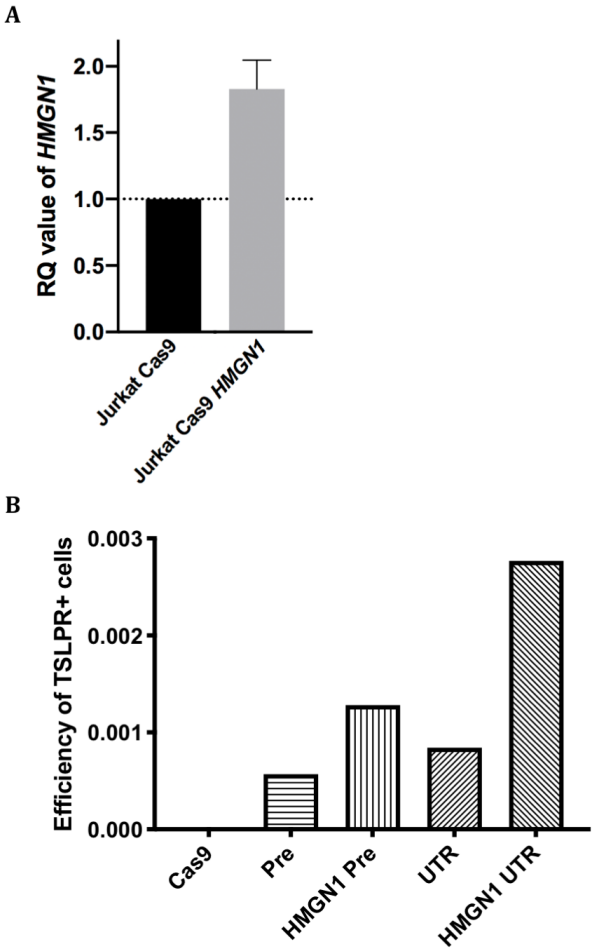

Cell line name	Total number of events	Number of TSLPR+ cells
Jurkat Pre-*CRLF2* gRNA	3,304,950	1,898
Jurkat *CRLF2* UTR gRNA	3,217,190	2,706
Jurkat *HMGN1* Pre-*CRLF2* gRNA	3,152,885	4,043
Jurkat *HMGN1 CRLF2* UTR gRNA	3,307,666	9,170

Supplementary Figure 5: Efficacy of sorting high expressing TSLPR+ Jurkat CRISPR/Cas9 edited cells with and without *HMGN1* expression. A) Using qRT-PCR to measure *HMGN1* mRNA expression in Jurkat CRISPR/Cas9 cell lines prior to transduction of gRNAs. RQ values determined using housekeeper actin expression and normalised to the parental Jurkat Cas9 control cells. **B)** Number of TSLPR + cells sorted from CRISPR/Cas9 *P2RY8-CRLF2* cells with or without *HMGN1* overexpression.

Chapter 4:

Dual targeting of JAK and MEK is effective against *CRLF2*+ Acute Lymphoblastic Leukaemia

Statement of Authorship

Title of Paper	Dual targeting of JAK and MEK is effective against *CRLF2*+ Acute Lymphoblastic Leukaemia
Publication Status	☐ Published ☐ Accepted for Publication ☐ Submitted for Publication ☒ Unpublished and Unsubmitted work written in manuscript style
Publication Details	Page EC, Heatley SL, Thomas PQ, White DL (2021) Dual targeting of JAK and MEK is effective against *CRLF2*+ Acute Lymphoblastic Leukaemia

Principal Author

Name of Principal Author (Candidate)	Elyse Page		
Contribution to the Paper	Conceived, designed and performed experiments, analysed results and wrote manuscript		
Overall percentage (%)	95%		
Certification:	This paper reports on original research I conducted during the period of my Higher Degree by Research candidature and is not subject to any obligations or contractual agreements with a third party that would constrain its inclusion in this thesis. I am the primary author of this paper.		
Signature		Date	23/2/21

Co-Author Contributions

By signing the Statement of Authorship, each author certifies that:

i. the candidate's stated contribution to the publication is accurate (as detailed above);

ii. permission is granted for the candidate in include the publication in the thesis; and

iii. the sum of all co-author contributions is equal to 100% less the candidate's stated contribution.

Name of Co-Author	Susan Heatley		
Contribution to the Paper	Supervised, and edited the manuscript		
Signature		Date	23.2.21

Name of Co-Author	Paul Thomas		
Contribution to the Paper	Supervised, and edited the manuscript		
Signature		Date	24/2/2021

Name of Co-Author	Deborah White		
Contribution to the Paper	Supervised, and edited the manuscript		
Signature		Date	25/2/2021

Dual targeting of JAK and MEK is effective against *CRLF2*+ Acute Lymphoblastic Leukaemia

Elyse C Page[1, 2], Susan L Heatley[1, 3, 4], Paul Q Thomas[3, 5], and Deborah L White[1, 2, 3, 4, 6, 7]

1. Cancer Program, Precision Medicine Theme, South Australian Health & Medical Research Institute, Adelaide, SA, Australia

2. School of Biological Sciences, University of Adelaide, Adelaide, SA, Australia

3. Discipline of Medicine, University of Adelaide, Adelaide, SA, Australia

4. Australian and New Zealand Children's Haematology/Oncology Group (ANZCHOG)

5. Gene Editing Program, Precision Medicine Theme, South Australian Health & Medical Research Institute, Adelaide, SA, Australia

6. Australian Genomic Health Alliance (AGHA)

7. Discipline of Paediatrics, University of Adelaide, Adelaide, SA, Australia

Abstract

Gene fusions converging on cytokine receptors and activating kinase signalling pathways in acute lymphoblastic leukaemia (ALL) are targetable with specific small molecule inhibitors to arrest cell proliferation. Activating mutations in the JAK/STAT and RAS signalling pathways are frequently observed in cytokine receptor like factor 2 (*CRLF2*) rearranged ALL patients. *CRLF2* gene fusions and activating mutations make up approximately 50% of high-risk ALL patients. We explore cell signalling using the Pro-B Ba/F3 cell line model harbouring *P2RY8-CRLF2* or the *CRLF2* p.F232C mutation to identify the need for different treatment approaches dependent on the individual upregulated signalling pathways. Twelve clinically available small molecule inhibitors that target the JAK/STAT, RAS, PI3K and epigenetic pathways have been screened to determine their efficacy. A synergistic combination of fedratinib and selumetinib was identified to reduce viability of human B-ALL cells harbouring *IGH-CRLF2* with *JAK2* p.R683G or the aggressive *CRLF2* p.F232C mutation in Ba/F3 cells. We demonstrate the ability of fedratinib/selumetinib to terminate pSTAT5 and pERK signalling, resulting in leukaemic cell death as well as decreasing the expression level of *c-MYC*. Targeting these signalling pathways with a precision medicine approach, in addition to chemotherapy, could improve survival outcomes for high-risk ALL patients.

Introduction

Targeted small molecule inhibitors (SMI) have been introduced into the therapeutic regime for acute lymphoblastic leukaemia (ALL) patients with Philadelphia positive (Ph+) ALL[1]. These patients harbour a reciprocal translocation between chromosomes 9 and 22 known as the Philadelphia chromosome[2], resulting in the *BCR-ABL1* gene fusion. Ph+ ALL occurs in less than 5% of children with ALL[3, 4], and there are currently no clinically available targeted SMI for the remaining 95% of paediatric ALL patients at diagnosis, therefore, conventional chemotherapy is the only treatment approach. Approximately 20% of childhood ALL patients harbour kinase activating gene fusions with a gene signature similar to the *BCR-ABL1* fusion[4]. Paediatric ALL patients with these kinase activating fusions are high risk and approximately 50% of these patients harbour a rearrangement of cytokine receptor like factor 2 (*CRLF2r*)[5, 6].

CRLF2 is commonly rearranged in two ways; a 320 KB deletion in the X or Y chromosome, placing the entire coding sequence of *CRLF2* directly downstream of the first non-coding exon of the purinergic receptor (*P2RY8*) creating *P2RY8-CRLF2*[7]. The second *CRLF2* rearrangement is via a translocation to the chromosome 14 immunoglobulin heavy chain (*IGH*) enhancer elements, resulting in the *IGH-CRLF2* fusion[8,9]. Both *CRLF2* gene fusions result in the upregulation of the thymic stromal lymphopoietin receptor (TSLPR) and increased cell signalling, however, these fusions are not sufficient to cause leukaemic transformation alone and additional lesions are required[10]. A point mutation in the transmembrane domain of CRLF2 at position p.F232C induces constitutive JAK/STAT signalling[8, 9]. Patients harbouring *CRLF2* p.F232C do not require additional lesions for leukaemic transformation[11]. Approximately 50% of *CRLF2r* ALL cases harbour point mutations in Janus Kinase 2

(*JAK2*)[1]. Therefore, targeting JAK/STAT signalling with SMI is a viable treatment option for *CRLF2r* patients[2, 5, 12, 13], and the JAK1/2 inhibitor, ruxolitinib, is currently in phase 2 clinical trials (NCT02723994 and NCT03117751).

Ruxolitinib was originally approved in 2011 by the US Federal Drug Administration (FDA) for the treatment of myelofibrosis[14]. Ten years later, the highly selective JAK2 ATP competitive inhibitor, fedratinib, also gained approval for myelofibrosis treatment [15-17]. JAK2 inhibitors have become important in the treatment of hematological malignancies[18], and will be central to developing a precision medicine approach for high-risk ALL patients[12, 19]. Point mutations in *JAK2* are acquired in many subtypes of ALL[20], particularly in the pseudokinase domain, resulting in constitutive activation of JAK/STAT signalling. *JAK2* can also be rearranged with 14 known partner genes[21], therefore it is an attractive candidate for targeted therapy in ALL.

Many ALL gene fusions or point mutations including *CRLF2r* activate JAK/STAT, PI3K or RAS signalling pathways[1] which have the potential to be targeted with different SMI that are already clinically available[5,22]. Currently, clinical trials of targeted SMI for ALL patients incorporate not only ruxolitinib, but also the PI3K inhibitor idealisib, β-raf inhibitor, sorafenib, and the multiple receptor tyrosine kinase (RTK) inhibitor, sunitinib (NCT02779283). In this trial, the targeted inhibitor used is determined via precision medicine functional laboratory testing. Similarly, trial NCT02551718 uses personal gene expression data and drug sensitivity assays to guide treatment using a variety of SMI and other drugs in combination with chemotherapy.

RAS pathways mutations are also commonly observed in ALL [23], particularly in patients with *CRLF2r* lacking *JAK* mutations[21, 23]. Inhibitors for RAS pathway constituents β-Raf and MEK are being considered for use in ALL[24, 25]. The highly selective allosteric MEK1/2 inhibitor selumetinib[25] has been trialled in solid tumours[26] and more recently in acute myeloid leukaemia (AML)[27]. Selumetinib has been demonstrated to act synergistically in combination therapies including chemotherapy[28, 29] and with the JAK inhibitor AZD1480 in ALL[30] and is a potential candidate for targeting multiple subsets of ALL including *CRLF2r*, hypodiploidy and early thymic precursor (ETP) ALL[13].

We hypothesised cells harbouring *CRLF2* rearrangements or the *CRLF2* p.F232C point mutation would activate different signalling pathways, and therefore, be targetable with different small molecule inhibitors. We have screened 12 SMI for efficacy and identified a synergistic combination of fedratinib and selumetinib against *CRLF2r* and the *CRLF2* p.F232C activating mutation. Using a combination of SMI in ALL treatment could lead to improved survival outcomes for high-risk ALL patients.

Materials and Methods

Cell lines and maintenance

HEK293T (ATCC, Manassas, VA) cells were maintained in DMEM supplemented with 10% Fetal Calf Serum (FCS). Jurkat and Ba/F3 cells (ATCC) were maintained in RPMI supplemented with 10% FCS and Ba/F3 cells supplemented 5% WEHI-3B conditioned media as a source of murine IL-3[31]. The human B-ALL cell line with *IGH-CRLF2* and *JAK2* p.R683G, MUTZ5 (ATCC), and NALM-19 (ATCC) were maintained in RPMI supplemented with 20% FCS. All cell line media contained 200 mM L-Glutamine (SAFC Biosciences), 5000 U/mL penicillin and 5000 μg/mL streptomycin sulphate.

Site directed mutagenesis

The NEBaseChanger® tool was used to design mutagenesis primers (Table SI) to create *CRLF2* p.F232C. The pRufIRES-WT-*CRLF2*-mCherry vector was used as template for the mutagenesis reaction, and the Q5 Site Directed Mutagenesis Kit (New England Biolabs (NEB), Notting Hill, VIC) was used according to the manufacturer's instructions.

Viral Transduction

Retrovirus was produced by transfecting 1 x 10^6 HEK293T cells in 5 mL recipient cell media in a T25 culture flask with 4 µg of the pRuf-IRES-*CRLF2* p.F232C vector, or the MSCV *P2RY8-CRLF2* vector, 4 µg of the pEQ-ECO packaging vector and 20 µL lipofectamine (Invitrogen, Carlsbad, CA). Viral supernatant was harvested 48 hours post transfection, spun and passed through a 0.45 µm filter. Ba/F3 cells at a concentration of 3 x 10^5/mL were centrifuged at 1800rpm for 1 hour with 30 µg/mL polybrene in 4 mL of viral supernatant in a 6-well plate at room temperature. Cells were washed 24 hours later and sub-cultured in original media before sorting at a concentration of 1 x 10^7/mL in RPMI and 2% FCS on a BD FACSAria™ for GFP and TSLPR expression at >95% purity.

Proliferation assay

Ba/F3 cells were seeded at 390 cells/mL in media starved of IL-3 in a 24-well plate in duplicate. On days 0, 2, 4 and 6, 20 µL of CellTiter-Glo 2.0® reagent (Promega, Madison, WI) was added to 20 µL of cell suspension. Following 30 min incubation in the dark, luminescence was measured on a Perkin Elmer Victor X5 luminometer set to luminescence at 0.1 seconds.

Flow cytometric analysis

Transduced Ba/F3 cells were stained with TSLPR-APC (Invitrogen) on ice for 30 mins and were analysed on a BD FACSCanto™ analyser. Ba/F3 cell death was assessed by seeding at $3.5x10^4$ cells/mL in a 96-well plate with a dose-response of drug (in the presence of 0.5% IL-3 conditioned supernatant if required) for a 3-day cell death assay. At 72 hours cells were stained with 0.4 µL AnnexinV-PE (BD, Franklin Lakes, NJ) and 0.04 µL 7-AAD (ThermoFisher, Waltham, MA) in 20 µL HANKS with 1% HEPES and 5% $CaCl_2$. Drug synergy was calculated using CalcuSyn where the combination index (CI) <1 indicated synergy. Following a 6-hour starvation from IL-3, Ba/F3 cells were fixed with a final concentration of 1.6% paraformaldehyde for 10 mins, washed in 1xPBS and then permeabilised with 80% methanol overnight at -80°C. Cells were then washed in 1xPBS, and subsequently in 1xPBS/1% bovine serum albumin (BSA). Cells were stained with antibodies outlined in Table SI and all intracellular staining was carried out in the dark, on ice, for 60 mins at room temperature in 1xPBS/1% BSA. Cells were washed in 1xPBS before reading on a BD FACSCanto™ analyser.

Real Time PCR Analysis

RNA was isolated from transduced Ba/F3 cells using TRIzol® (Invitrogen) and cDNA was synthesised using Quantitect reverse transcriptase (Qiagen, Venlo, NL). SYBR green reagents (Qiagen) were used with 10µM primers outlined in Table SI.

Statistical Analysis

GraphPad Prism software Version 8.4.0© (GraphPad Software Inc.) and FlowJo software version 10.6.1 (FlowJo LLC) were used for analyses. All assays were carried

out in triplicate and graphs represent the median value or mean with stand error of the mean (SEM) error bars as indicated in the figure legends. Unpaired *t*-test was used to determine the difference between experimental groups. Benjamini-Hochberg false discovery rate adjustment was used for multiple comparisons. LD_{50} was determined from cell death assays by applying a nonlinear regression model and using the 95% confidence interval. Differences were considered statistically significant when the *p*-value was <0.05. **p*<0.05, ***p*<0.01, ****p*<0.001.

Results

CRLF2 p.F232C confers cytokine independence in Ba/F3 cells through activation of JAK/STAT signalling

Ba/F3 cells transduced with *P2RY8-CRLF2* or *CRLF2* p.F232C (*CRLF2*^{F232C}) were starved of IL-3 over 6 days in a cytokine independent assay. Non-transduced Ba/F3 cells or *P2RY8-CRLF2* cells were unable to proliferate past day 2 and 4, respectively, while *CRLF2*^{F232C} cells underwent cellular transformation (Fig 1A, *p*<0.001 compared to parental Ba/F3 cells). The amount of *CRLF2* mRNA expressed by the transduced Ba/F3 cells was quantified using RQ-PCR. *P2RY8-CRLF2* produced significantly more *CRLF2* mRNA with an RQ value of $1.5x10^6 \pm 8x10^4$, compared to *CRLF2*^{F232C} cells RQ of $5.6x10^5 \pm 1.7x10^5$ (Fig 1B, *p*=0.008). Conversely, a higher level of TSLPR was detected on the surface of *CRLF2*^{F232C} cells (MFI: 13,344) compared to *P2RY8-CRLF2* cells (MFI: 4,162, *p*<0.001, Fig 1C).

The phosphorylation levels of *P2RY8-CRLF2* and *CRLF2*^{F232C} Ba/F3 cells indicated different signalling profiles. *CRLF2*^{F232C} cells significantly upregulated pSTAT5

compared to parental Ba/F3 cells after a 5-hour starvation from IL-3 (Fig 1D, MFI: 182 ± 26, compared to Ba/F3 cells MFI: 49 ± 10, p=0.043). *P2RY8-CRLF2* cells resulted in a significant increase in pAKT (Fig 1E, MFI: 85 ± 8, compared to Ba/F3 cells MFI: 12 ± 1, p=0.013) and pERK (Fig 1F, MFI: 99 ± 9, compared to Ba/F3 cells MFI: 28 ± 5, p=0.019). A 15 min TSLP stimulation did not have an effect on *CRLF2*^{F232C} cells (Fig 1G-I), however an increase in pSTAT5 was observed in TSLP stimulated *P2RY8-CRLF2* cells (Fig 1G, MFI: 57 ± 16 compared to DMSO control MFI: 49 ± 10, p=0.022).

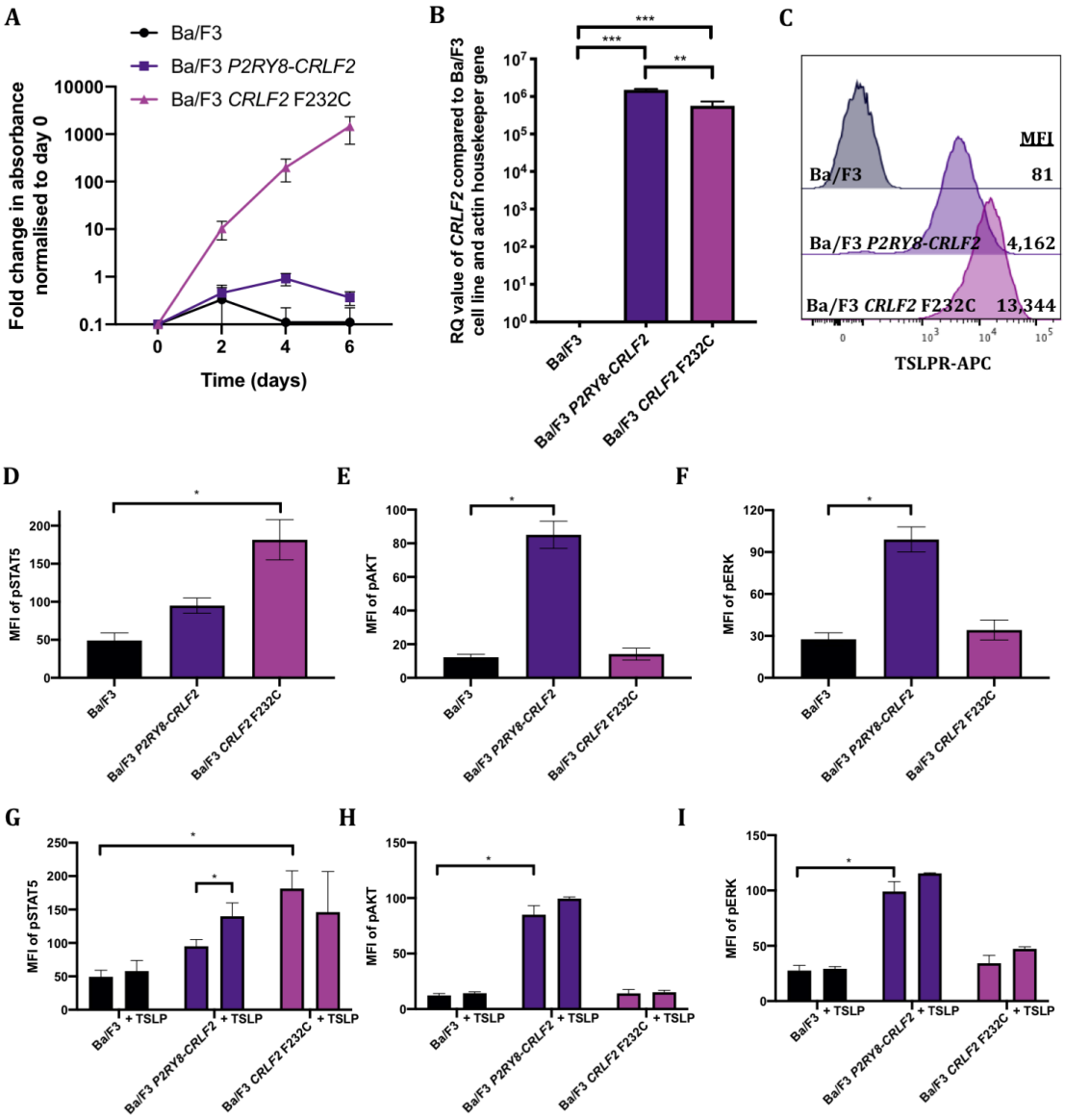

Figure 1: Characterising the signalling profile of *CRLF2r* Ba/F3 cells. A) Cytokine independence assessed by CellTiter Glo 2.0® proliferation assay over 6 days, culturing Ba/F3 cells in media with no IL-3. Absorbance reading measured using a Perkin Elmer Victor X5 luminometer. **B)** Using qRT-PCR to measure *CRLF2* mRNA expression in Ba/F3 *HMGN1* and *CRLF2* cell lines starved of IL-3 for 6 hours. RQ values determined using housekeeper actin expression and normalised to the parental Ba/F3 control cell line. **C)** Representative histogram depicting TSLPR-APC expression of Ba/F3 *CRLF2* cell lines starved of IL-3 for 6 hours. Phosphorylation levels of STAT5-PE **(D)**, AKT-PE **(E)** or ERK-PE **(F)** basally or with the addition of 15min TSLP stimulation before

staining **(G, H & I)** of Ba/F3 cell lines expressing *CRLF2r* measured by phospho-flow cytometry after being starved of IL-3 for 6 hours. All graphs represent the mean of biological replicate of n=3 with SEM error bars and a student's t-test was used between parental Ba/F3 cells and *CRLF2r* or *CRLF2*mut cells to determine significance, *p<0.05, **p<0.01, ***p<0.001.

Screening small molecule inhibitors against *P2RY8-CRLF2* and *CRLF2* p.F232C cells

Due to the increase in JAK/STAT, PI3K and RAS signalling pathways, small molecule inhibitors of each pathways were trialled against *P2RY8-CRLF2* and *CRLF2*^{F232C} cells. The JAK2 inhibitors fedratinib, AZ960, ruxolitinib and cerdulatinib reduced the viability of *P2RY8-CRLF2* cells at similar concentrations with LD_{50} ~350 nM (Fig 2A). The JAK inhibitors were less effective against *CRLF2*^{F232C} cells with LD_{50} ~750 nM for AZ960 and cerdulatinib and LD_{50} ~3-4 μM for both ruxolitinib and fedratinib (Fig 2B). All doses were within the clinically achievable range.

The PI3K inhibitors GSK-1059615 and MK-2206 had similar high LD_{50} between 5-7 μM for both *P2RY8-CRLF2* and *CRLF2*^{F232C} cells, while duvelisib did not impact cell viability in either line (Fig 2C-D). Therefore, the investigation of PI3K pathway inhibitors against these lines was discontinued. The RAS pathway inhibitors selumetinib and PD0325901 were more effective against *P2RY8-CRLF2* cells than *CRLF2*^{F232C} cells. *P2RY8-CRLF2* cells had LD_{50} values, $LD_{50}^{selumetinib}$ 10 μM and $LD_{50}^{PD0325901}$ 4.5 μM (Fig 2E), however, PD0325901 had no effect on *CRLF2*^{F232C} cells up to 10 μM and selumetinib had a higher LD_{50} of ~12 μM (Fig F). The histone deacetylase (HDAC) inhibitor givinostat had LD_{50} of 200 nM for *P2RY8-CRLF2* cells and 450 nM for *CRLF2*^{F232C} cells, and panobinostat had LD_{50} of 25 nM for *P2RY8-CRLF2* cells and 75 nM for *CRLF2*^{F232C} cells. The last inhibitor trialled was luminespib, inhibiting heat shock protein 90 (HSP90) which targeted *P2RY8-CRLF2* and *CRLF2*^{F232C} cells similarly, with an LD_{50} of 400 nM (Fig 2G-H).

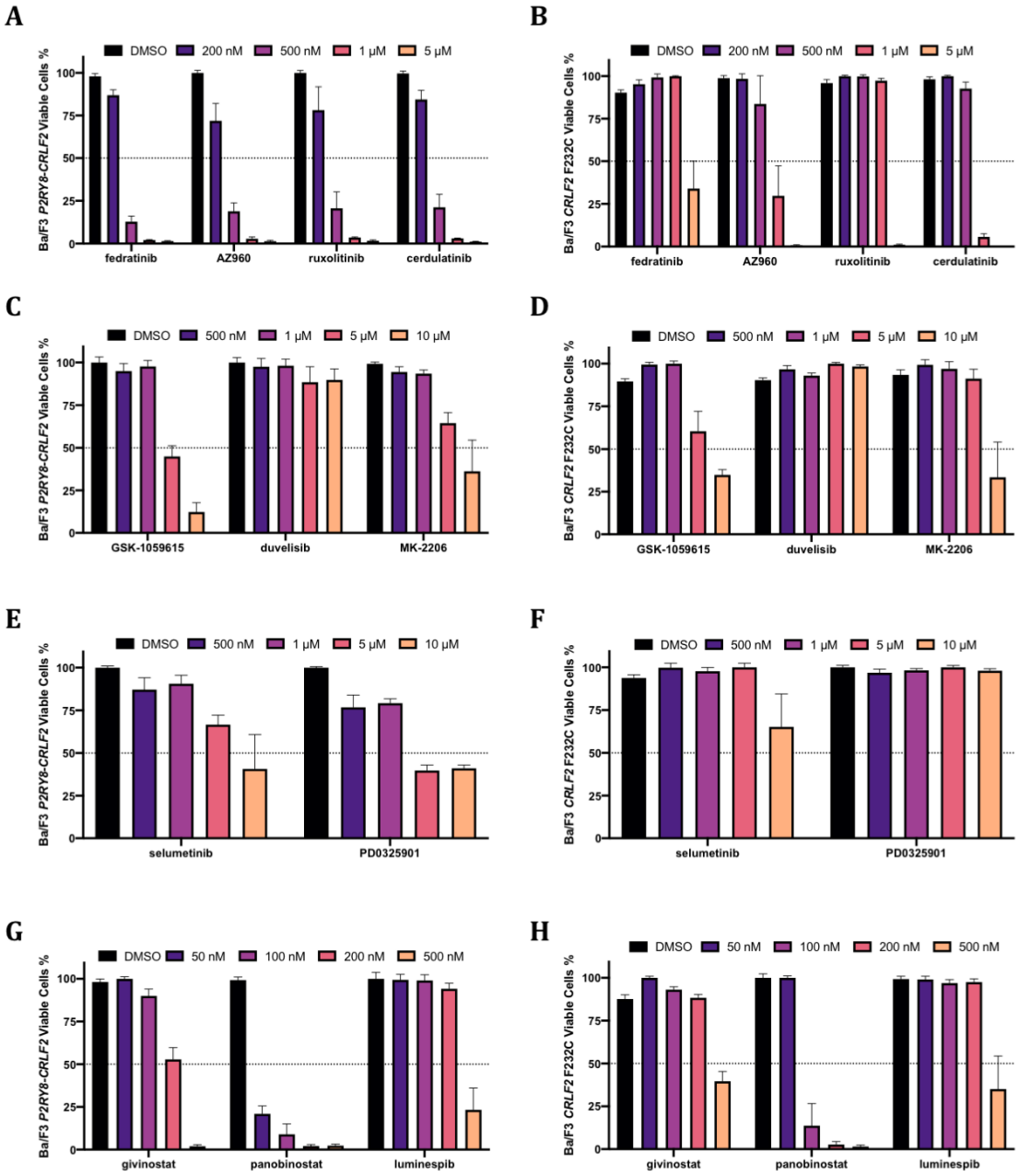

Figure 2: Screening small molecule inhibitors effective against *CRLF2r* Ba/F3 cells. **A & B)** JAK2 inhibitors, **C & D)** PI3K pathway inhibitors, **E & F)** RAS pathway inhibitors, or **G & H)** HDAC or HSP90 inhibitors were assessed via an AnnexinV/7-AAD cell death assay over three days against Ba/F3 *P2RY8-CRLF2* cells, supplemented with 2.5% IL-3 (left) or Ba/F3 *CRLF2*^{F232C} cells starved of IL-3 (right).

A combination of fedratinib and selumetinib is mildly synergistic against the *CRLF2* p.F232C activating mutation

The *CRLF2*^{F232C} mutation stimulates constitutively active signalling pathways through a CRLF2 homodimer receptor. A combination of the JAK2 inhibitor, fedratinib, and the MEK inhibitor, selumetinib, was trialled to target both JAK/STAT and RAS pathways. A significant decrease in cell viability was achieved with a combination of 1 μM fedratinib and 1 or 2 μM selumetinib (CI=0.9, Fig 3A). The human B-ALL cell line MUTZ5 harbouring *IGH-CRLF2* and *JAK2* p.R683G also achieved the same synergistic combinations as the Ba/F3 *CRLF2*^{F232C} line (CI=0.9), in addition to lower concentrations of 0.5 μM fedratinib and 1 or 2 μM selumetinib (CI=0.6) as well as 1 μM fedratinib and 0.5 μM selumetinib (Fig 3B, CI=0.9). The human B-ALL line, NALM-19 was used as a negative *CRLF2* control and the fedratinib and selumetinib combination was not synergistic for this line (Fig 3C, CI>1) indicating specificity for *CRLF2*+ lines.

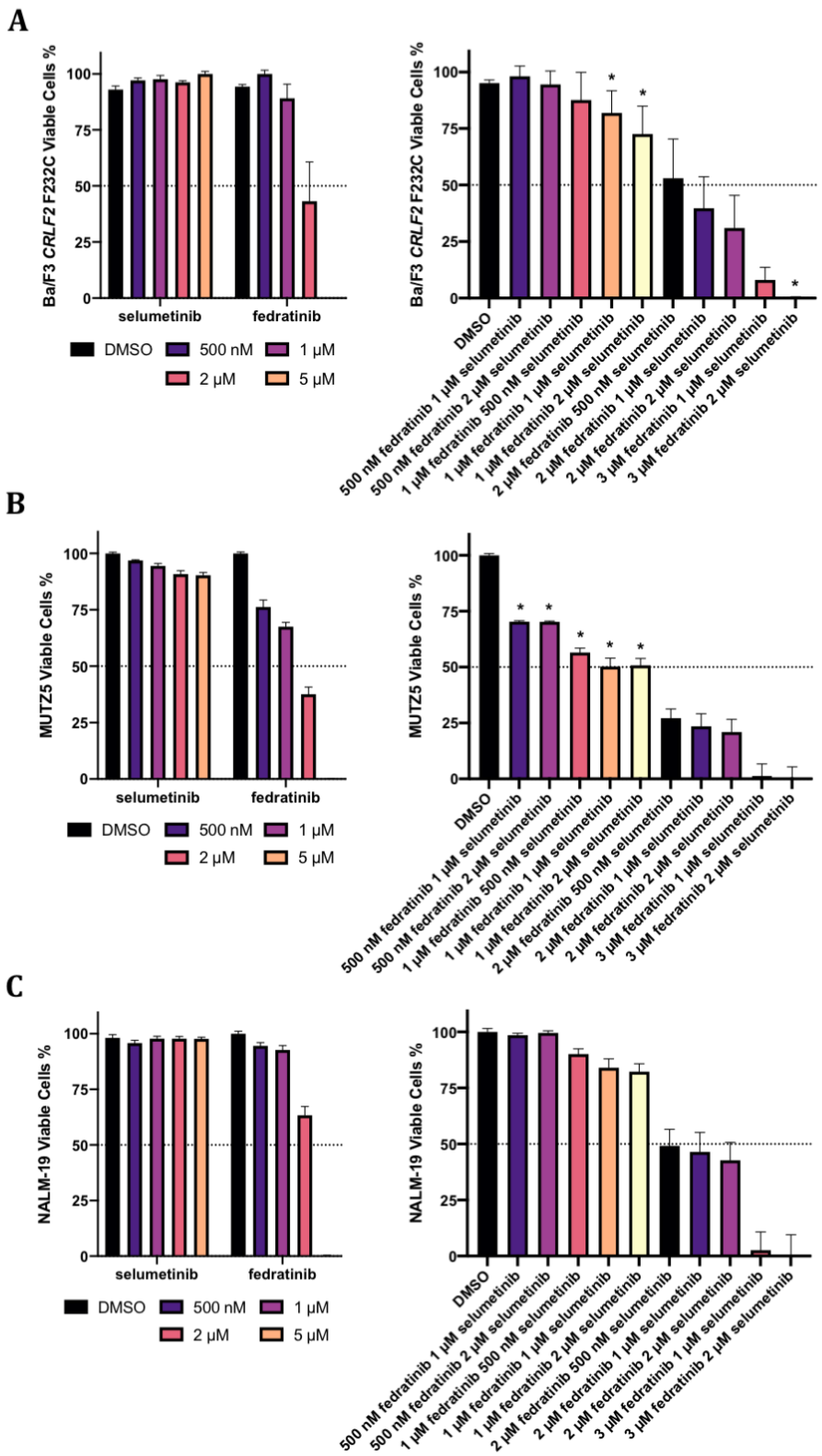

Figure 3: Effective targeting of Ba/F3 cell lines expressing *CRLF2* p.F232C or human *IGH-CRLF2* +*JAK2* p.R683G cells with fedratinib and selumetinib combination therapy. The inhibitors fedratinib, selumetinib, or a combination of the

two were assessed by an AnnexinV/7-AAD cell death assay over three days against Ba/F3 *CRLF2*^{F232C} cells **(A)**, MUTZ5 cells **(B)**, or control human NALM-19 cells **(C)**. All graphs represent the mean of biological replicate of n=3 with SEM error bars and *synergistic combinations were identified using CalcuSyn where CI<1.

To determine the functional effect of the combination$^{fed/sel}$, pSTAT5 and pERK were profiled using phosphoflow (Fig 4). Interestingly, neither fedratinib alone or the combination were sufficient to reduce pSTAT5 in the Ba/F3 *CRLF2*^{F232C} line (Fig 4C). However, a significant decrease in pERK was observed when *CRLF2*^{F232C} cells were treated with selumetinib alone (p=0.006) or the combination$^{fed/sel}$ (p=0.009, Fig 4D). The *CRLF2*^{F232C} line was compared to the parental Ba/F3 line starved of IL-3 for 6 hours which expressed low levels of pSTAT5 and pERK (Fig 4A-B). fedratinib alone (p=0.044) and the combination$^{fed/sel}$ (p=0.014) decreased pSTAT5 in Ba/F3 cells, and a non-significant decrease of pERK was observed with selumetinib or combination$^{fed/sel}$ treatment. Interestingly, fedratinib (p=0.015) and the combination$^{fed/sel}$ (p=0.013) treatment of MUTZ5 cells resulted in a significant decrease in pSTAT5 (Fig 4E), however, the selumetinib and combination$^{fed/sel}$ treatment did not result in a significant decrease in pERK (Fig 4F). The human NALM-19 line was used as a control with nominal pSTAT5 expression and minor pERK expression, of which none of the treatments had an effect (Fig 4G-H).

Using the Ba/F3 *CRLF2*+ cell lines, the expression of genes downstream of pSTAT5 were quantified using RQ-PCR after treatment with 1 μM fedratinib and 2 μM selumetinib (Fig 4I). Interestingly, the expression of *MYC* was decreased with combination$^{fed/sel}$ treatment in parental Ba/F3, *P2RY8-CRLF2* and *CRLF2*^{F232C} lines. *GATA3* expression was also reduced in parental Ba/F3 and *P2RY8-CRLF2* cells, however, *GATA3* expression in *CRFL2*^{F232C} cells was not sensitive to treatment. *CDKN1* and *SOCS1* expression were only decreased in parental Ba/F3 cells with combination$^{fed/sel}$ treatment, and their expression was not altered in drug treated *CRLF2*+ lines.

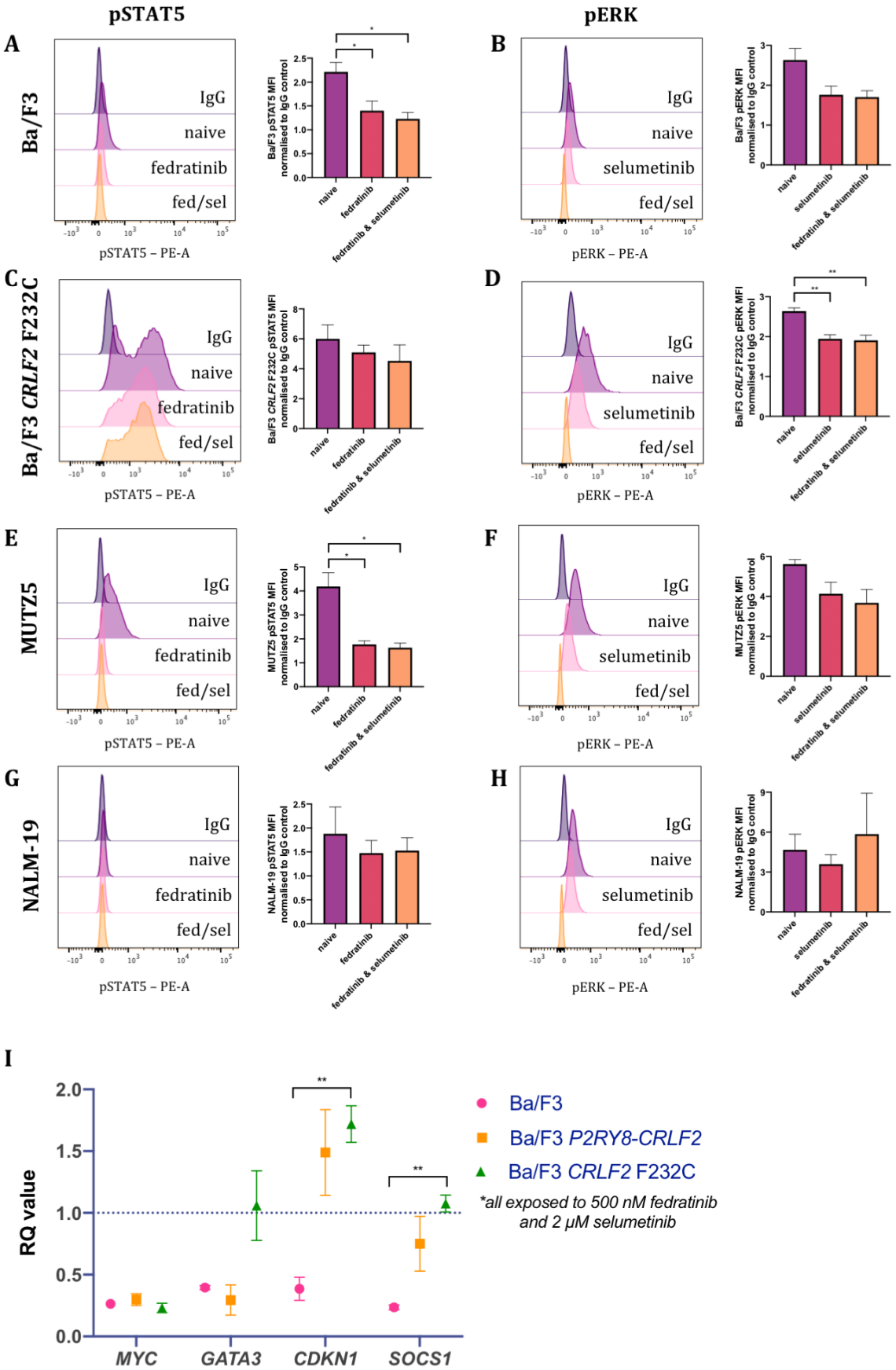
pSTAT5
pERK
A
B
C
D
E
F
G
H
I
Ba/F3
Ba/F3 CRLF2 F232C
MUTZ5
NALM-19
IgG
naive
fedratinib
fed/sel
selumetinib
pSTAT5 – PE-A
pERK – PE-A
Ba/F3 pSTAT5 MFI normalised to IgG control
Ba/F3 pERK MFI normalised to IgG control
Ba/F3 CRLF2 F232C pSTAT5 MFI normalised to IgG control
Ba/F3 CRLF2 F232C pERK MFI normalised to IgG control
MUTZ5 pSTAT5 MFI normalised to IgG control
MUTZ5 pERK MFI normalised to IgG control
NALM-19 pSTAT5 MFI normalised to IgG control
NALM-19 pERK MFI normalised to IgG control
fedratinib & selumetinib
RQ value
MYC
GATA3
CDKN1
SOCS1
Ba/F3
Ba/F3 P2RY8-CRLF2
Ba/F3 CRLF2 F232C
*all exposed to 500 nM fedratinib and 2 μM selumetinib

Figure 4: A combination of fedratinib and selumetinib decreases JAK/STAT and RAS signalling in *CRLF2* expressing cells. Levels of pSTAT5-PE **(A, C, E, G)** or pERK-PE **(B, D, F, H)** measured via flow cytometry in parental Ba/F3 cells or cells harbouring *CRLF2*^{F232C} after being starved of IL-3 for 6 hours and MUTZ5 or NALM-19 cells exposed to 1 μM fedratinib and 2 μM selumetinib for 2 hours. All histograms are representative of biological replicate of n=3. All graphs represent the mean of biological replicate of n=3 with SEM error bars and a student's *t*-test was used between each treatment and its corresponding vehicle control to determine significance, *p<0.05, **p<0.01, ***p<0.001. **I)** Using qRT-PCR to measure *MYC*, *GATA3*, *CDKN1*, and *SOCS1* mRNA expression in Ba/F3 *CRLF2* cell lines starved of IL-3 for 6 hours and exposed to 1 μM fedratinib and 2 μM selumetinib for 2 hours. RQ values determined using β-actin expression and normalised to the vehicle control of each cell line.

Discussion

The use of JAK inhibitors for *CRLF2* rearranged ALL is well established with ruxolitinib in Phase II trials[32]. Ruxolitinib was approved for the use in treating myelofibrosis[14], and recently, the JAK2 inhibitor fedratinib was also approved for myelofibrosis in 2019[15]. Fedratinib is likely to enter clinical trials for ALL, following in the footsteps of ruxolitinib. However, patients with the aggressive *CRLF2*^{F232C} mutation rarely harbour *JAK* mutations[8] and therefore, JAK inhibitors are not always sufficient to target *CRLF2*+ B-ALL cells. The MEK inhibitor, selumetinib has been demonstrated to target B-ALL in combination therapies[28, 29], in particular, combined with JAK inhibitors for *JAK*-mutated ALL[30]. Here, we have demonstrated efficacy of fedratinib and selumetinib in combination to target *CRLF2*^{F232C} cells and *JAK2* mutated cells harbouring *IGH-CRLF2*.

We have used the Pro-B Ba/F3 cell line to model the *P2RY8-CRLF2* gene fusion and *CRLF2*^{F232C} activating mutation. Consistent with previous reports[8,9], we demonstrated cytokine independent growth of *CRLF2*^{F232C} cells, but not *P2RY8-CRLF2* Ba/F3 cells. After 6 hours IL-3 starve of Ba/F3 cells, an increase in different signalling pathways in cells harbouring *P2RY8-CRLF2* compared to *CRLF2*^{F232C} was observed. *P2RY8-CRLF2* cells increased phosphorylation of pAKT and pERK, whereas *CRLF2*^{F232C} cells relied solely on STAT5 signalling. This could be due to the CRLF2/IL7Rα heterodimer that occurs in *P2RY8-CRLF2* cells, compared to homodimerization of CRLF2 in *CRLF2*^{F232C} cells[11]. To consolidate this model, an increase in pSTAT5 in *P2RY8-CRLF2* cells upon TSLP stimulation was demonstrated, as previously described[33].

To determine efficacy of SMI against *P2RY8-CRLF2* and *CRLF2*^{F232C} cells, 12 SMI were screened in a cell death assay. Overall, *P2RY8-CRLF2* cells were more sensitive to all

SMI compared to *CRLF2*^{F232C} cells as expected from the activating mutation. We demonstrate efficacy of type 1 JAK2 inhibitors fedratinib, AZ960, ruxolitinib and cerdulatinib in a dose dependent manner against *P2RY8-CRLF2* cells. Due to the lower sensitivity of type 1 JAK2 inhibitors in *CRLF2*^{F232C} cells, type 2 inhibitors including CHZ868 may be a better candidate as recently identified to target the mutated receptor[34].

PI3K pathway dysregulation is observed in *CRLF2r* patients[12, 33], therefore, inhibition of PI3K or AKT was hypothesised to be efficacious against *P2RY8-CRLF2* or *CRLF2*^{F232C}. The PI3K and AKT inhibitors trialled were effective against *P2RY8-CRLF2* cells as an increase in pAKT was also observed, however *CRLF2*^{F232C} cells were less sensitive as they did not activate pAKT. The inhibitor, duvelisib, which is FDA approved for the treatment of chronic lymphocytic leukaemia[35] was not successful in targeting either of the *CRLF2*+ lines.

The allosteric MEK inhibitors selumetinib and PD0325901 decreased the viability of *P2RY8-CRLF2* cells in a dose dependent manner, while *CRLF2*^{F232C} cells required a higher concentration of selumetinib to be affected, and no change in viability was observed with the use of PD0325901. Interestingly, the RAS signalling pathway is often upregulated in iamp21[36] and Down Syndrome ALL[23, 37], both of which frequently co-occur with *CRLF2r*[38] indicating MEK inhibitors may be viable candidates for the therapeutic targeting *CRLF2r* ALL.

Alterations in epigenetic regulator genes are also frequently associated with *CRLF2r* ALL[11]. The HDAC inhibitors givinostat and panobinostat both potently reduced *P2RY8-*

CRLF2 and *CRLF2*^{F232C} cell viability. Sensitivity to givinostat has been demonstrated in *CRLF2r* and JAK inhibitor resistant *CRLF2r* cells[39] and could be a potential candidate for treatment resistant or relapsed ALL patients. HSP90 inhibition is proposed to be effective against aggressive ALL subtypes. In particular, HSP90 inhibitors target *CRLF2r* cells that rely on JAK2, by promoting JAK2 degradation[40, 41]. In this study, the HSP90 inhibitor luminespib effectively targeted *P2RY8-CRLF2* and *CRLF2*^{F232C} cells, confirming efficacy of targeting this pathway. Similarly to the HDAC inhibitors, HSP90 inhibition has been demonstrated to overcome JAK inhibitor resistance in *CRLF2r* cells[41].

The emergence of resistance to either chemotherapy, or targeted inhibitors has led to trials of combination therapies[1]. We have endeavoured to dual target *CRLF2*+ cells with the JAK2 inhibitor, fedratinib and the MEK inhibitor, selumetinib. Synergistic therapies that result in a lower dose of either drug are associated with less toxicity and minimal resistance generation[42]. JAK2 inhibitors have previously been trialled in combination with other SMI[43]. Interestingly, selumetinib has shown efficacy when used in combination therapies in ALL[44] and AML[27]. We demonstrated efficacy of fedratinib and selumetinib in combination against both *CRLF2*^{F232C} and the *IGH-CRLF2* gene fusion with the *JAK2* p.R683G activating mutation. Individually, selumetinib was not effective unless used at high concentrations of 10 μM, whereas in combination with fedratinib, this concentration was reduced to 2 μM. *CRLF2r* cells rely on JAK/STAT signalling[11], therefore, ERK pathway activation may only occur when JAK/STAT signalling is terminated allowing selumetinib to be effective. This mild synergistic effect was specific to *CRLF2* expressing lines, as the control NALM-19 cell line did not exhibit synergy.

The combination of fedratinib and selumetinib ceased pSTAT5 and pERK signalling in MUTZ5 cells. However, pSTAT5 signalling remained active in *CRLF2*^{F232C} cells as the p.F232C results in homodimer formation and constitutive JAK2 recruitment[9]. A type 2 JAK inhibitor in combination with selumetinib may be more beneficial when targeting the aggressive *CRLF2*^{F232C} mutation[34]. The combination was, however, able to decrease expression of *MYC* in *CRLF2*^{F232C} cells, but not *GATA3*, *CDKN1* or *SOCS1*, confirming active STAT5 signalling. Combination JAK2 and c-MYC inhibition has been successful in targeting *CRLF2r* and *JAK* mutant B-ALLs, demonstrating the importance of MYC expression cessation[45]. RAS pathway and JAK mutations are two of the most frequently observed lesions in high-risk ALL[21], therefore, a synergistic combination of a JAK and MEK inhibitor such as fedratinib and selumetinib may be a therapeutic option for a range of ALL subtypes. However, this will need to be explored further in preliminary *in vivo* models.

High-risk ALL patients are associated with lower survival rates and higher relapse rates[21,39]. A precision medicine approach using targeted inhibitors could greatly increase their chances of survival. Currently, clinical trials are evaluating the use of gene expression data to inform treatment using targeted inhibitors. We have screened 12 SMI and discovered an effective combination therapy using fedratinib and selumetinib to arrest pSTAT5 and pERK signalling which could benefit not only *CRLF2r* patients, but many high-risk ALL patients with activating mutations in JAK or RAS signalling pathways.

References

1. Tasian SK, Loh ML, Hunger SP. Childhood acute lymphoblastic leukemia: Integrating genomics into therapy. *Cancer*. Oct 15 2015;121(20):3577-90. doi:10.1002/cncr.29573

2. Zhou Y, Kanagal-Shamanna R, Zuo Z, Tang G, Medeiros LJ, Bueso-Ramos CE. Advances in B-lymphoblastic leukemia: cytogenetic and genomic lesions. *Ann Diagn Pathol*. Aug 2016;23:43-50. doi:10.1016/j.anndiagpath.2016.02.002

3. Hunger SP, Mullighan CG. Acute Lymphoblastic Leukemia in Children. *N Engl J Med*. Oct 2015;373(16):1541-52. doi:10.1056/NEJMra1400972

4. Roberts KG, Mullighan CG. Genomics in acute lymphoblastic leukaemia: insights and treatment implications. *Nat Rev Clin Oncol*. Jun 2015;12(6):344-57. doi:10.1038/nrclinonc.2015.38

5. Roberts KG, Li Y, Payne-Turner D, et al. Targetable kinase-activating lesions in Ph-like acute lymphoblastic leukemia. *N Engl J Med*. Sep 11 2014;371(11):1005-15. doi:10.1056/NEJMoa1403088

6. Steeghs EMP, Jerchel IS, de Goffau-Nobel W, et al. aberrations in childhood B-cell precursor acute lymphoblastic leukemia. *Oncotarget*. Oct 2017;8(52):89923-89938. doi:10.18632/oncotarget.21027

7. Mullighan CG, Collins-Underwood JR, Phillips LA, et al. Rearrangement of CRLF2 in B-progenitor- and Down syndrome-associated acute lymphoblastic leukemia. *Nat Genet*. Nov 2009;41(11):1243-6. doi:10.1038/ng.469

8. Hertzberg L, Vendramini E, Ganmore I, et al. Down syndrome acute lymphoblastic leukemia, a highly heterogeneous disease in which aberrant expression of CRLF2 is associated with mutated JAK2: a report from the International BFM Study Group. *Blood*. Feb 2010;115(5):1006-17. doi:10.1182/blood-2009-08-235408

9. Yoda A, Yoda Y, Chiaretti S, et al. Functional screening identifies CRLF2 in precursor B-cell acute lymphoblastic leukemia. *Proc Natl Acad Sci U S A*. Jan 2010;107(1):252-7. doi:10.1073/pnas.0911726107

10. Russell LJ, Capasso M, Vater I, et al. Deregulated expression of cytokine receptor gene, CRLF2, is involved in lymphoid transformation in B-cell precursor acute lymphoblastic leukemia. *Blood*. Sep 24 2009;114(13):2688-98. doi:10.1182/blood-2009-03-208397

11. Vesely C, Frech C, Eckert C, et al. Genomic and transcriptional landscape of P2RY8-CRLF2-positive childhood acute lymphoblastic leukemia. *Leukemia*. Jan 06 2017;doi:10.1038/leu.2016.365

12. Maude SL, Tasian SK, Vincent T, et al. Targeting JAK1/2 and mTOR in murine xenograft models of Ph-like acute lymphoblastic leukemia. *Blood*. Oct 2012;120(17):3510-8. doi:10.1182/blood-2012-03-415448

13. Tasian SK, Hunger SP. Genomic characterization of paediatric acute lymphoblastic leukaemia: an opportunity for precision medicine therapeutics. *Br J Haematol*. Mar 2017;176(6):867-882. doi:10.1111/bjh.14474

14. Mascarenhas J, Hoffman R. Ruxolitinib: the first FDA approved therapy for the treatment of myelofibrosis. *Clin Cancer Res*. Jun 2012;18(11):3008-14. doi:10.1158/1078-0432.CCR-11-3145

15. Fedratinib Becomes New Option in Myelofibrosis. *Cancer Discov*. Oct 2019;9(10):1332. doi:10.1158/2159-8290.CD-NB2019-102

16. Bewersdorf JP, Jaszczur SM, Afifi S, Zhao JC, Zeidan AM. Beyond Ruxolitinib: Fedratinib and Other Emergent Treatment Options for Myelofibrosis. *Cancer Manag Res*. 2019;11:10777-10790. doi:10.2147/CMAR.S212559

17. Talpaz M, Kiladjian JJ. Fedratinib, a newly approved treatment for patients with myeloproliferative neoplasm-associated myelofibrosis. *Leukemia*. Jul 2020;doi:10.1038/s41375-020-0954-2

18. Drennan AC, Rui L. HiJAKing the epigenome in leukemia and lymphoma. *Leuk Lymphoma*. 11 2017;58(11):2540-2547. doi:10.1080/10428194.2017.1312370

19. Roberts KG, Morin RD, Zhang J, et al. Genetic alterations activating kinase and cytokine receptor signaling in high-risk acute lymphoblastic leukemia. *Cancer Cell*. Aug 2012;22(2):153-66. doi:10.1016/j.ccr.2012.06.005

20. Mullighan CG, Zhang J, Harvey RC, et al. JAK mutations in high-risk childhood acute lymphoblastic leukemia. *Proc Natl Acad Sci U S A*. Jun 2009;106(23):9414-8. doi:10.1073/pnas.0811761106

21. Hunger SP, Mullighan CG. Redefining ALL classification: toward detecting high-risk ALL and implementing precision medicine. *Blood*. Jun 2015;125(26):3977-87. doi:10.1182/blood-2015-02-580043

22. Roberts KG, Yang YL, Payne-Turner D, et al. Oncogenic role and therapeutic targeting of ABL-class and JAK-STAT activating kinase alterations in Ph-like ALL. *Blood Adv*. Sep 2017;1(20):1657-1671. doi:10.1182/bloodadvances.2017011296

23. Nikolaev SI, Garieri M, Santoni F, et al. Frequent cases of RAS-mutated Down syndrome acute lymphoblastic leukaemia lack JAK2 mutations. *Nat Commun*. Aug 2014;5:4654. doi:10.1038/ncomms5654

24. George AA, Paz H, Fei F, et al. Phosphoflow-Based Evaluation of Mek Inhibitors as Small-Molecule Therapeutics for B-Cell Precursor Acute Lymphoblastic Leukemia. *PLoS One*. 2015;10(9):e0137917. doi:10.1371/journal.pone.0137917

25. Knight T, Irving JA. Ras/Raf/MEK/ERK Pathway Activation in Childhood Acute Lymphoblastic Leukemia and Its Therapeutic Targeting. *Front Oncol*. 2014;4:160. doi:10.3389/fonc.2014.00160

26. Adjei AA, Cohen RB, Franklin W, et al. Phase I pharmacokinetic and pharmacodynamic study of the oral, small-molecule mitogen-activated protein kinase kinase 1/2 inhibitor AZD6244 (ARRY-142886) in patients with advanced cancers. *J Clin Oncol*. May 2008;26(13):2139-46. doi:10.1200/JCO.2007.14.4956

27. Jain N, Curran E, Iyengar NM, et al. Phase II study of the oral MEK inhibitor selumetinib in advanced acute myelogenous leukemia: a University of Chicago phase II consortium trial. *Clin Cancer Res*. Jan 2014;20(2):490-8. doi:10.1158/1078-0432.CCR-13-1311

28. Polak A, Kiliszek P, Sewastianik T, et al. MEK Inhibition Sensitizes Precursor B-Cell Acute Lymphoblastic Leukemia (B-ALL) Cells to Dexamethasone through Modulation of mTOR Activity and Stimulation of Autophagy. *PLoS One*. 2016;11(5):e0155893. doi:10.1371/journal.pone.0155893

29. Matheson EC, Thomas H, Case M, et al. Glucocorticoids and selumetinib are highly synergistic in RAS pathway-mutated childhood acute lymphoblastic leukemia through upregulation of BIM. *Haematologica*. 09 2019;104(9):1804-1811. doi:10.3324/haematol.2017.185975

30. Suryani S, Bracken LS, Harvey RC, et al. Evaluation of the in vitro and in vivo efficacy of the JAK inhibitor AZD1480 against JAK-mutated acute lymphoblastic leukemia. *Mol Cancer Ther*. Feb 2015;14(2):364-74. doi:10.1158/1535-7163.MCT-14-0647

31. Palacios R, Steinmetz M. Il-3-dependent mouse clones that express B-220 surface antigen, contain Ig genes in germ-line configuration, and generate B

lymphocytes in vivo. *Cell*. Jul 1985;41(3):727-34. doi:10.1016/s0092-8674(85)80053-2

32. Tasian SK, Hurtz C, Wertheim GB, et al. High incidence of Philadelphia chromosome-like acute lymphoblastic leukemia in older adults with B-ALL. *Leukemia*. Apr 2017;31(4):981-984. doi:10.1038/leu.2016.375

33. Tasian SK, Doral MY, Borowitz MJ, et al. Aberrant STAT5 and PI3K/mTOR pathway signaling occurs in human CRLF2-rearranged B-precursor acute lymphoblastic leukemia. *Blood*. Jul 2012;120(4):833-42. doi:10.1182/blood-2011-12-389932

34. Wu SC, Li LS, Kopp N, et al. Activity of the Type II JAK2 Inhibitor CHZ868 in B Cell Acute Lymphoblastic Leukemia. *Cancer Cell*. Jul 2015;28(1):29-41. doi:10.1016/j.ccell.2015.06.005

35. Rodrigues DA, Sagrillo FS, Fraga CAM. Duvelisib: A 2018 Novel FDA-Approved Small Molecule Inhibiting Phosphoinositide 3-Kinases. *Pharmaceuticals (Basel)*. May 2019;12(2)doi:10.3390/ph12020069

36. Ryan SL, Matheson E, Grossmann V, et al. The role of the RAS pathway in iAMP21-ALL. *Leukemia*. 09 2016;30(9):1824-31. doi:10.1038/leu.2016.80

37. Lee P, Bhansali R, Izraeli S, Hijiya N, Crispino JD. The biology, pathogenesis and clinical aspects of acute lymphoblastic leukemia in children with Down syndrome. *Leukemia*. Sep 2016;30(9):1816-23. doi:10.1038/leu.2016.164

38. Woo JS, Alberti MO, Tirado CA. Childhood B-acute lymphoblastic leukemia: a genetic update. *Exp Hematol Oncol*. 2014;3:16. doi:10.1186/2162-3619-3-16

39. Savino AM, Sarno J, Trentin L, et al. The histone deacetylase inhibitor givinostat (ITF2357) exhibits potent anti-tumor activity against CRLF2-rearranged BCP-ALL. *Leukemia*. Apr 2017;doi:10.1038/leu.2017.93

40. van Bodegom D, Zhong J, Kopp N, et al. Differences in signaling through the B-cell leukemia oncoprotein CRLF2 in response to TSLP and through mutant JAK2. *Blood*. Oct 2012;120(14):2853-63. doi:10.1182/blood-2012-02-413252

41. Weigert O, Lane AA, Bird L, et al. Genetic resistance to JAK2 enzymatic inhibitors is overcome by HSP90 inhibition. *J Exp Med*. Feb 2012;209(2):259-73. doi:10.1084/jem.20111694

42. Chou TC. Drug combination studies and their synergy quantification using the Chou-Talalay method. *Cancer Res*. Jan 2010;70(2):440-6. doi:10.1158/0008-5472.CAN-09-1947

43. Choong ML, Pecquet C, Pendharkar V, et al. Combination treatment for myeloproliferative neoplasms using JAK and pan-class I PI3K inhibitors. *J Cell Mol Med*. Nov 2013;17(11):1397-409. doi:10.1111/jcmm.12156

44. Gianfelici V, Messina M, Paoloni F, et al. IL7R overexpression in adult acute lymphoblastic leukemia is associated to JAK/STAT pathway mutations and identifies patients who could benefit from targeted therapies. *Leuk Lymphoma*. 03 2019;60(3):829-832. doi:10.1080/10428194.2018.1499906

45. Kim SK, Knight DA, Jones LR, et al. JAK2 is dispensable for maintenance of JAK2 mutant B-cell acute lymphoblastic leukemias. *Genes Dev*. 06 2018;32(11-12):849-864. doi:10.1101/gad.307504.117

Supplementary Materials

Dual targeting of JAK and MEK is effective against *CRLF2*+ Acute Lymphoblastic Leukaemia

Elyse C Page[1, 2], Susan L Heatley[1, 3, 4], Paul Q Thomas[3, 5], and Deborah L White[1, 2, 3, 4, 6, 7]

Table SI: Materials		
Antibodies		
Protein	**Conjugate**	**Manufacturer**
TSLPR	APC	Invitrogen # 17-5499-41
IgG2a	APC	Invitrogen # 17-4724-81
IgG2a	PE	BD # 556653
IgG1	APC	BD # 551019
IgG XP	AF647	CST # 2985
pSTAT5	PE	BD # 612567
pERK	PE	BD # 612566
pS6 kinase	APC	CST # 665426
pJAK2	AF647	Abcam # ab200340
Total H3	AF647	CST # 12230
H3K9ac	AF647	CST # 4484
H3K27me3	AF647	CST # 12158
H3K9me2	AF647	CST # 66070
Annexin V	PE	BD # 556421
7-AAD		ThermoFisher # A1310
Primer Sequences – Sigma-Aldrich		
CRLF2 F232C F	5′ -CTGTCCAAAT**G**TATTTTAATTTCCAGCC- 3′	
CRLF2 F232C R	5′ -CTTTGGTTTGGGAGGCGT- 3′	
CRLF2 qPCR F	5′ -TGGATCACAGACACCCAGAA- 3′	
CRLF2 qPCR R	5′ -TCTTGGCCAACTGGACTACC- 3′	
mVEGFA_qPCR_F	5′ -AGCACAGCAGATGTGAATGC- 3′	
mVEGFA_qPCR_R	5′ -TTTCTTGCGCTTTCGTTTTT- 3′	
mBCL2_qPCR_F	5′ -AAGCTGTCACAGAGGGGCTA- 3′	
mBCL2_qPCR_R	5′ -CAGGCTGGAAGGAGAAGATG- 3′	
mMCL1_qPCR_F	5′ -GCTCCGGAAACTGGACATTA- 3′	
mMCL1_qPCR_R	5′ -CCCAGTTTGTTACGCCATCT- 3′	
mMYC_qPCR_F	5′ -CCAGATCCCTGAATTGGAAA- 3′	
EP_mMYC_qPCR_R	5′ -TCGTCTGCTTGAATGGACAG- 3′	
mGATA3_qPCR_F	5′ -CTTATCAAGCCCAAGCGAAG- 3′	
mGATA3_qPCR_R	5′ -CATTAGCGTTCCTCCTCCAG- 3′	
mCDKN1A_qPCR_F	5′ -CGGTGGAACTTTGACTTCGT- 3′	
mCDKN1A_qPCR_R	5′ -CAGGGCAGAGGAAGTACTGG- 3′	
mSOCS1_qPCR_F	5′ -CCTCCTCGTCCTCGTCTTC- 3′	
mSOCS1_qPCR_R	5′ -AAGGTGCGGAAGTGAGTGTC- 3′	
Vectors		
CLC20-MSCV-P2RY8-CRLF2-GFP		
pRufIRES-CRLF2-F232C-mCherry		
pEQ-ECO		

This page has been intentionally left blank

Chapter 5:

Discussion and Future Directions

Many genes in the Down Syndrome critical region of chromosome 21 are involved in cancer-associated or gene activation pathways and have potential involvement in leukaemogenesis[1,2]. Genes including the dual specificity tyrosine phosphorylated and regulated kinase 1A (*DYRK1A*), ETS related gene (*ERG*), ETS variant transcription factor 6 (*ETV6*) and RUNX family transcription factor 1 (*RUNX1*) have been studied in ALL so far[3-8]. This thesis builds upon the investigation of *HMGN1* in the development and persistence of *CRLF2r* ALL. Critical initial studies conducted by Lane and Mowery et al[1,2] defined genes in the Down Syndrome critical region of chromosome 21 and highlight the involvement of *HMGN1* in transcriptional activation. Deciphering the role of chromosome 21 in leukaemogenesis is imperative to determine the predisposition DS-ALL patients have to leukaemia development, as well as non-DS ALL patients who harbour polysomy 21 or intrachromosomal amplification of chromosome 21[9,10].

The articles presented in this thesis investigate the cooperation between *P2RY8-CRLF2* and chromosome 21 gene, *HMGN1*, to understand its role, and develop targeted therapeutic approaches urgently needed for DS-ALL patients. Together, the data from chapters 2 and 3 identify *HMGN1* as a critical leukaemic gene, and potential target in DS-ALL. This is because of its important functions in nucleosome remodelling, proliferation, survival and cooperation with *P2RY8-CRLF2*. In chapters 2 and 4, different combination therapies have been identified for cells harbouring the *P2RY8-CRLF2* gene fusion or the *CRLF2* p.F232C activating mutation to target their different signalling patterns. The role of HMGN1 identified here, provides significant insight into the predisposition of DS-ALL patients harbouring *P2RY8-CRLF2* and demonstrates mechanisms for the persistent nature of these cells.

Chapter 2 of this thesis demonstrates, for the first time, that *HMGN1* has driver potential similar to that of *JAK2*, in the proliferation and survival of trisomy 21 leukaemic cells. *JAK2* has been well characterised as a driver gene in haematological malignancies[11-13]. Driver potential of HMGN1 was identified using a CRISPR/Cas9 knockout of *HMGN1,* and its role was explored in a trisomy 21 *CRLF2* xenograft model. Bioluminescent imaging was used to track engraftment and also the reduction in leukaemic burden when the inducible *HMGN1* knockout was activated. When *HMGN1* was knocked out of the trisomy 21 *CRLF2*+ murine model, not only was leukaemic cell proliferation perturbed, but also a significant survival advantage was gained. Furthermore, known leukaemia associated pathologies including anaemia, thrombocytopaenia and hepatosplenomegaly were mitigated. These findings are particularly significant as the trisomy 21 cells expressed the aggressive *CRLF2* p.F232C activating mutation that constitutively activates cell signalling[10,14]. Based on this data, targeting *HMGN1* in patients harbouring *CRLF2* p.F232C, would have the potential to significantly decrease treatment related toxicity. This is clinically relevant, as patients harbouring *CRLF2* p.F232C currently have limited therapeutic options and are at high risk of relapse. Repeating this model using DS-ALL patient derived xenografts would further validate the leukaemic role of *HMGN1* in ALL, however, the low transduction efficiencies of primary ALL material may limit this study.

To support the findings from the *in vivo* model in Chapter 2, I demonstrate for the first time, cooperation between *P2RY8-CRLF2* and *HMGN1* in leukaemic transformation. This link between *P2RY8-CRLF2* and *HMGN1* was identified using two *in vitro* models described in chapters 2 and 3. Using the pro-B Ba/F3 cell line, I demonstrate that neither gene (*HMGN1* or *P2RY8-CRLF2*) was alone transformative[15,16], thus clearly

elucidating the critical synergistic role of *HMGN1* in proliferation and factor independent transformation when co-expressed with *P2RY8-CRLF2*. Further, the endogenous CRISPR/Cas9 *P2RY8-CRLF2* model described in chapter 3, provides additional mechanistic insight into the role of HMGN1 in this process. By creating the *P2RY8-CRLF2* gene fusion endogenously, the pre-leukaemic state of a cell can be explored. It has previously been demonstrated that overexpression of *HMGN1,* as a result of trisomy 21 changes the transcriptional activation patterns of a cell[17]. Expressing *HMGN1* in Jurkat cells for 72 hours prior to inducing the CRISPR/Cas9 gRNAs to generate *P2RY8-CRLF2* resulted in increased efficiency of *P2RY8-CRLF2* formation and as a result, surface expression of TSLPR. This suggests that *HMGN1* is likely a predisposing factor to the *P2RY8-CRLF2* fusion gene formation and may explain why this fusion is prevalent among patients with DS-ALL. Supporting the results identified in chapter 2, the endogenous *P2RY8-CRLF2* and *HMGN1* expressing cells demonstrate the same trends in cell signalling and histone activation as the Ba/F3 model, further validating *HMGN1* as an important leukaemic gene. HMGN1 also plays a role in DNA repair[18], and therefore, it may have a role in facilitating the 320 KB deletion and ligation event that results in the formation of *P2RY8-CRLF2* at the PAR1 locus.

To confirm this mechanism, further experiments are required to determine HMGN1 action at the *P2RY8* promotor. This will be done using ATAC seq (Assay for Transposase-Accessible Chromatin using sequencing) in the endogenously expressing *P2RY8-CRLF2* cell lines generated in chapter 3. This method exposes DNA to a highly active transposase (Tn5). Open chromatin sites will preferentially bind Tn5 which will fragment the DNA and add sequencing primers to identify regions of active chromatin. As ATAC seq assesses chromatin accessibility, an endogenously expressing *P2RY8-*

CRLF2 cell line will be a favourable option compared to virally overexpressing the fusion gene such as in the Ba/F3 cells developed in chapter 2. While *HMGN1* will be virally overexpressed, it can be determined whether the protein produced acts on the endogenous *P2RY8* promotor at PAR1 in a human cell line. The Ba/F3 cells, however, may express *P2RY8-CRLF2* at random insertion sites in the genome and are a murine cell line rather than of human origin. ATAC seq has been used to determine if HMGN1 is responsible for transcriptional activation in B-cells, however, this was not in the context of *CRLF2r*[2]. In addition to ATAC seq, chromatin immunoprecipitation (ChIP) will provide valuable information on HMGN1 binding sites and targets. Using ChIP for HMGN1 and H3K27me3 will validate the flow cytometry methylation and acetylation data generated in chapter 2, as well as demonstrate its role in cell signalling.

The endogenous *P2RY8-CRLF2* cell line model provides a useful research tool as a physiological level of gene expression is achieved, in contrast to the overexpression observed in the context of retroviral vectors[19,20]. An endogenously expressing *P2RY8-CRLF2* cell line is a valuable research tool as there are currently only cell lines harbouring the *IGH-CRLF2* fusion, not *P2RY8-CRLF2*. This model, which recapitulates a pre-leukaemic state, will also be valuable for the identification of new cooperating genes or investigation of other chromosome 21 genes in DS-ALL. As *P2RY8-CRLF2* is not a transforming fusion gene alone, but a leukaemia initiating event, the co-expression of other potential leukaemic genes can be assessed prior to inducing the CRISPR/Cas9 *P2RY8-CRLF2* fusion generation. For example, *DYRK1A*, which has been demonstrated to promote DS megakaryoblastic leukaemia in a murine model[4] can be expressed to determine its cooperation with *P2RY8-CRLF2* for leukaemic transformation and changes in cell signalling.

Evidence for the cooperation between *P2RY8-CRLF2* and *HMGN1* has been established in Chapters 2 and 3 through the achievement of cytokine independence in Ba/F3 cells and increased efficiency in the development of *P2RY8-CRLF2* in the novel CRISPR/Cas9 model cell line. To further characterise this relationship, the development of a cooperative bone marrow transplant mouse will be of value. Murine bone marrow transplants have been used to identify cooperative genes in leukaemic transformation[21]. In this experiment, lineage negative haemopoietic precursors will be harvested from male C57BL/6 mice and transduced with *P2RY8-CRLF2*, *CRLF2* p.F232C and *HMGN1* individually, as well as *P2RY8-CRLF2* and *HMGN1*, *CRLF2* p.F232C and *HMGN1* or *P2RY8-CRLF2* and *DYRK1A* as a control. Transduced cells will be injected into syngeneic C57BL/6 female mice and monitored to determine leukaemia latency and to confirm *P2RY8-CRLF2* and *HMGN1* are cooperating to develop leukaemia. Leukaemic cells harvested from these mice could later be used in a pre-clinical model to validate targeted therapies for DS-ALL, including the combination therapies identified in chapters 2 and 4. The application of CRISPR/Cas9 for *P2RY8-CRLF2* fusion generation could also be used in murine haematopoietic precursors to demonstrate leukaemic driver capabilities. Combinations of chromosome 21 genes with endogenous expressing *P2RY8-CRLF2* murine haematopoietic cells could be injected into recipient mice to determine engraftment, leukaemic potential and cooperation.

Using the cooperative *in vitro* Ba/F3 *CRLF2* model developed in chapter 2, the function of *P2RY8-CRLF2* and *HMGN1* was further elucidated. Dual expression of *P2RY8-CRLF2* and *HMGN1* lead to increased *CRLF2* mRNA production and surface TSLPR when compared to cells expressing *P2RY8-CRLF2* alone. This finding was unique to *P2RY8-*

CRLF2 cells as *HMGN1* expression did not upregulate *CRLF2* in WT *CRLF2* or *CRLF2* p.F232C cells. This supports the endogenous *P2RY8-CRLF2* model described in Chapter 3 and provides insight into the role of *HMGN1* expression in cells predisposed to *P2RY8-CRLF2* fusion formation. The *CRLF2* p.F232C mutation does not require additional lesions for leukaemic transformation[10,22] and has high constitutive expression of TSLPR. With *HMGN1* expression, *P2RY8-CRLF2* cells also have upregulated TSLPR, akin to that observed in cells harbouring *CRLF2* p.F232C. This finding raises mechanistic questions as to whether HMGN1 has a direct role binding to the *P2RY8* promotor, as it has been demonstrated to bind to promotor regulatory elements[23]. Alternatively, it may have an indirect role activating other transcription factors that can then activate *P2RY8-CRLF2*[2,17]. This warrants further investigation such as ATAC seq previously described. In addition, chromatin immunoprecipitation for HMGN1 would identify the genes HMGN1 binds to, that result in activation. This will determine if HMGN1 binding patterns change in the presence of the *P2RY8-CRLF2* fusion, and identify genes becoming active via HMGN1 demethylation that may cooperate with *P2RY8-CRLF2*.

Co-expression of *P2RY8-CRLF2* and *HMGN1* in the Ba/F3 model also identified upregulated cell signalling, postulating a mechanism for the observed cooperation. In non-DS *CRLF2r* ALL patients, 50% present clinically with *JAK2* mutations and upregulated JAK/STAT signalling[13,24]. In the models generated herein, upregulated JAK/STAT, PI3K and Ras signalling was observed when *HMGN1* was co-expressed with *P2RY8-CRLF2* cells. This signalling profile is similar to that identified in *CRLF2r JAK2* mutated patients[9,25-28]. These cells also had increased acetylation of the gene activation mark, H3K9ac, and decreased methylation of the gene silencing marks, H3K9me2 and

H3K9me3, which is indicative of *HMGN1* expression[2,17]. Therefore, *P2RY8-CRLF2* and *HMGN1* cells may cooperate via nucleosome remodelling to activate cell signalling pathways resulting in leukaemic transformation and cell survival. Interestingly, cells co-expressing *HMGN1* and *CRLF2* p.F232C did not share these signalling and epigenetic patterns. The *CRLF2* p.F232C mutation results in maximal TSLPR expression and as a result, constitutive JAK/STAT cell signalling[3,10], and therefore do not require additional cancer associated lesions. While cells harbouring the *CRLF2* p.F232C mutation exhibited increased gene activation marks upon co-expression with *HMGN1*, this did not impact signalling pathways, and no increase in PI3K or RAS signalling was observed. This further highlights the need for a precision medicine approach for DS-ALL patients, including those within the same subset of *CRLF2* rearrangements, as the fusion and mutant have different signalling patterns, and therefore, are highly unlikely to be targetable with the same therapies.

To determine which genes are activated in the Ba/F3 *CRLF2* p.F232C cell line when *HMGN1* is co-expressed, ChIP or ATAC seq will once again be beneficial. Furthermore, mass spectrometry profiling and RNA sequencing will be useful to determine signalling patterns and the gene expression profile of *CRLF2* p.F232C *HMGN1* cells to better target with small molecule inhibitors. In chapter 2, an increase in the gene activation mark, H3K9ac, was observed in Ba/F3 cells co-expressing *CRLF2* p.F232C and *HMGN1*, but not an increase in cell signalling or *CRLF2* expression. Using RQ-PCR, an increase in *BCL2* and *MYC* expression was identified in this line, however, this was a targeted experiment rather than a whole genome approach. Given the upregulation of *BCL2* and *MYC*, it will also be worthwhile to trial BCL2 and BET inhibitors such as venetoclax and

JQ1 in a cell death assay against the *CRLF2* p.F232C cells. These agents are currently being trialled in double hit lymphoma[29].

To address the need for precision medicine treatment for patients with *P2RY8-CRLF2* or the *CRLF2* p.F232C mutation due to their differing cell signalling profiles, I assessed two combination therapies for each *CRLF2* subset. Both therapies centred around the use of fedratinib, a specific JAK2 inhibitor recently approved for the treatment of myelofibrosis[30] as both *CRLF2* subsets upregulate JAK/STAT signalling. Cells expressing *HMGN1* have been demonstrated to respond to the demethylase inhibitor GSK-J4[1] which I have confirmed using Ba/F3 cells. Therefore, in chapter 2, when a combination of fedratinib and GSK-J4 was trialled against cells co-expressing *P2RY8-CRLF2* and *HMGN1*, a significant decrease in cell viability was observed, indicating the two compounds act in synergy and validating HMGN1 as a therapeutic target in *CRLF2r* DS-ALL. This drug combination also proved synergistic against cells co-expressing *CRLF2* p.F232C and *HMGN1*, however, to a much lesser extent. Therefore, in chapter 4, my focus was on targeting cells harbouring *CRLF2* p.F232C with small molecule inhibitors. The MEK inhibitor, selumetinib, was first trialled alone due to the upregulation of pERK in *CRLF2* p.F232C cells. A modest level of cell death was achieved when selumetinib was used alone. Interestingly, the combination of fedratinib and selumetinib acted in synergy to target *CRLF2* p.F232C cells. Surprisingly, a similar result was identified in an AML study[31] with selumetinib exhibiting modest single agent efficacy but a low toxicity profile suitable for combination therapies. The fedratinib and selumetinib combination was also identified to act synergistically in cells expressing the *IGH-CRLF2* fusion and *JAK2* activating mutation. Therefore, a combination therapy effective for the *CRLF2* p.F232C mutation may also be successful

in targeting *CRLF2* fusions and will be trialled in cells harbouring *P2RY8-CRLF2*. The development of targeted therapies is important for *CRLF2r* patients, in particular DS-ALL patients who experience treatment toxicity to chemotherapy, as well as poor survival outcomes and high relapse rates[7,32].

Concluding Remarks

In this thesis I have established novel roles for *HMGN1* in the proliferation and survival of *CRLF2+* cells as well as cooperation with *P2RY8-CRLF2* for leukaemic transformation. The findings presented have identified several potential mechanisms including the upregulation of *CRLF2* and TSLPR, in addition to nucleosome remodelling resulting in increased cell signalling and gene activation. Finally, for clinical translation, assessment of therapeutic interventions has revealed two synergistic combination therapies for either the *P2RY8-CRLF2* fusion co-expressing *HMGN1*, or the *CRLF2* p.F232C mutation. Importantly, taken together, these data provide much needed evidence on the predisposition of DS-ALL patients developing *P2RY8-CRLF2*, suggest potential mechanisms to this cooperation, and propose a therapeutic option that would reduce the toxicity DS-ALL patients experience from current chemotherapy regimens. This is important as the role of chromosome 21 is largely unknown in leukaemogenesis, and DS-ALL patients have a poor prognosis and need targeted therapies to improve their treatment tolerability. To add complete clarity of the role of *HMGN1* in leukaemic development and persistence, further investigations including ATAC seq and additional cooperative *in vivo* models will be valuable.

1. Lane AA, Chapuy B, Lin CY, et al. Triplication of a 21q22 region contributes to B cell transformation through HMGN1 overexpression and loss of histone H3 Lys27 trimethylation. *Nat Genet*. Jun 2014;46(6):618-23. doi:10.1038/ng.2949

2. Mowery CT, Reyes JM, Cabal-Hierro L, et al. Trisomy of a Down Syndrome Critical Region Globally Amplifies Transcription via HMGN1 Overexpression. *Cell Rep*. Nov 2018;25(7):1898-1911.e5. doi:10.1016/j.celrep.2018.10.061

3. Lee P, Bhansali R, Izraeli S, Hijiya N, Crispino JD. The biology, pathogenesis and clinical aspects of acute lymphoblastic leukemia in children with Down syndrome. *Leukemia*. Sep 2016;30(9):1816-23. doi:10.1038/leu.2016.164

4. Malinge S, Bliss-Moreau M, Kirsammer G, et al. Increased dosage of the chromosome 21 ortholog Dyrk1a promotes megakaryoblastic leukemia in a murine model of Down syndrome. *J Clin Invest*. Mar 2012;122(3):948-62. doi:10.1172/JCI60455

5. Zhang J, McCastlain K, Yoshihara H, et al. Deregulation of DUX4 and ERG in acute lymphoblastic leukemia. *Nat Genet*. Dec 2016;48(12):1481-1489. doi:10.1038/ng.3691

6. Chatterton Z, Morenos L, Mechinaud F, et al. Epigenetic deregulation in pediatric acute lymphoblastic leukemia. *Epigenetics*. Mar 2014;9(3):459-67. doi:10.4161/epi.27585

7. Izraeli S, Vora A, Zwaan CM, Whitlock J. How I treat ALL in Down's syndrome: pathobiology and management. *Blood*. Jan 2014;123(1):35-40. doi:10.1182/blood-2013-07-453480

8. Kubota Y, Uryu K, Ito T, et al. Integrated genetic and epigenetic analysis revealed heterogeneity of acute lymphoblastic leukemia in Down syndrome. *Cancer Sci*. Oct 2019;110(10):3358-3367. doi:10.1111/cas.14160

9. Mullighan CG, Collins-Underwood JR, Phillips LA, et al. Rearrangement of CRLF2 in B-progenitor- and Down syndrome-associated acute lymphoblastic leukemia. *Nat Genet*. Nov 2009;41(11):1243-6. doi:10.1038/ng.469

10. Hertzberg L, Vendramini E, Ganmore I, et al. Down syndrome acute lymphoblastic leukemia, a highly heterogeneous disease in which aberrant expression of CRLF2 is associated

with mutated JAK2: a report from the International BFM Study Group. *Blood*. Feb 2010;115(5):1006-17. doi:10.1182/blood-2009-08-235408

11. Bercovich D, Ganmore I, Scott LM, et al. Mutations of JAK2 in acute lymphoblastic leukaemias associated with Down's syndrome. *Lancet*. Oct 2008;372(9648):1484-92. doi:10.1016/S0140-6736(08)61341-0

12. Bose P, Verstovsek S. JAK2 inhibitors for myeloproliferative neoplasms: what is next? *Blood*. Jul 2017;130(2):115-125. doi:10.1182/blood-2017-04-742288

13. Harvey RC, Mullighan CG, Chen IM, et al. Rearrangement of CRLF2 is associated with mutation of JAK kinases, alteration of IKZF1, Hispanic/Latino ethnicity, and a poor outcome in pediatric B-progenitor acute lymphoblastic leukemia. *Blood*. Jul 2010;115(26):5312-21. doi:10.1182/blood-2009-09-245944

14. Yoda A, Yoda Y, Chiaretti S, et al. Functional screening identifies CRLF2 in precursor B-cell acute lymphoblastic leukemia. *Proc Natl Acad Sci U S A*. Jan 2010;107(1):252-7. doi:10.1073/pnas.0911726107

15. Russell LJ, Capasso M, Vater I, et al. Deregulated expression of cytokine receptor gene, CRLF2, is involved in lymphoid transformation in B-cell precursor acute lymphoblastic leukemia. *Blood*. Sep 24 2009;114(13):2688-98. doi:10.1182/blood-2009-03-208397

16. Nikolaev SI, Garieri M, Santoni F, et al. Frequent cases of RAS-mutated Down syndrome acute lymphoblastic leukaemia lack JAK2 mutations. *Nat Commun*. Aug 2014;5:4654. doi:10.1038/ncomms5654

17. Rochman M, Taher L, Kurahashi T, et al. Effects of HMGN variants on the cellular transcription profile. *Nucleic Acids Res*. May 2011;39(10):4076-87. doi:10.1093/nar/gkq1343

18. Birger Y, West KL, Postnikov YV, et al. Chromosomal protein HMGN1 enhances the rate of DNA repair in chromatin. *EMBO J*. Apr 2003;22(7):1665-75. doi:10.1093/emboj/cdg142

19. Vargas JE, Chicaybam L, Stein RT, Tanuri A, Delgado-Cañedo A, Bonamino MH. Retroviral vectors and transposons for stable gene therapy: advances, current challenges and perspectives. *J Transl Med*. 10 2016;14(1):288. doi:10.1186/s12967-016-1047-x

20. Sayin VI, Papagiannakopoulos T. Application of CRISPR-mediated genome engineering in cancer research. *Cancer Lett*. Feb 28 2017;387:10-17. doi:10.1016/j.canlet.2016.03.029

21. de Bock CE, Demeyer S, Degryse S, et al. HOXA9 Cooperates with Activated JAK/STAT Signaling to Drive Leukemia Development. *Cancer Discov*. 05 2018;8(5):616-631. doi:10.1158/2159-8290.CD-17-0583

22. van Bodegom D, Zhong J, Kopp N, et al. Differences in signaling through the B-cell leukemia oncoprotein CRLF2 in response to TSLP and through mutant JAK2. *Blood*. Oct 2012;120(14):2853-63. doi:10.1182/blood-2012-02-413252

23. Zhu N, Hansen U. HMGN1 modulates estrogen-mediated transcriptional activation through interactions with specific DNA-binding transcription factors. *Mol Cell Biol*. Dec 2007;27(24):8859-73. doi:10.1128/MCB.01724-07

24. Mullighan CG, Zhang J, Harvey RC, et al. JAK mutations in high-risk childhood acute lymphoblastic leukemia. *Proc Natl Acad Sci U S A*. Jun 2009;106(23):9414-8. doi:10.1073/pnas.0811761106

25. Maude SL, Dolai S, Delgado-Martin C, et al. Efficacy of JAK/STAT pathway inhibition in murine xenograft models of early T-cell precursor (ETP) acute lymphoblastic leukemia. *Blood*. Mar 2015;125(11):1759-67. doi:10.1182/blood-2014-06-580480

26. Roberts KG, Li Y, Payne-Turner D, et al. Targetable kinase-activating lesions in Ph-like acute lymphoblastic leukemia. *N Engl J Med*. Sep 11 2014;371(11):1005-15. doi:10.1056/NEJMoa1403088

27. Tasian SK, Doral MY, Borowitz MJ, et al. Aberrant STAT5 and PI3K/mTOR pathway signaling occurs in human CRLF2-rearranged B-precursor acute lymphoblastic leukemia. *Blood*. Jul 2012;120(4):833-42. doi:10.1182/blood-2011-12-389932

28. Tasian SK, Teachey DT, Li Y, et al. Potent efficacy of combined PI3K/mTOR and JAK or ABL inhibition in murine xenograft models of Ph-like acute lymphoblastic leukemia. *Blood*. Jan 2017;129(2):177-187. doi:10.1182/blood-2016-05-707653

29. Li W, Gupta SK, Han W, et al. Targeting MYC activity in double-hit lymphoma with MYC and BCL2 and/or BCL6 rearrangements with epigenetic bromodomain inhibitors. *J Hematol Oncol*. 07 2019;12(1):73. doi:10.1186/s13045-019-0761-2

30. Talpaz M, Kiladjian JJ. Fedratinib, a newly approved treatment for patients with myeloproliferative neoplasm-associated myelofibrosis. *Leukemia*. Jul 2020;doi:10.1038/s41375-020-0954-2

31. Jain N, Curran E, Iyengar NM, et al. Phase II study of the oral MEK inhibitor selumetinib in advanced acute myelogenous leukemia: a University of Chicago phase II consortium trial. *Clin Cancer Res*. Jan 2014;20(2):490-8. doi:10.1158/1078-0432.CCR-13-1311

32. Izraeli S, Shochat C, Tal N, Geron I. Towards precision medicine in childhood leukemia--insights from mutationally activated cytokine receptor pathways in acute lymphoblastic leukemia. *Cancer Lett*. Sep 2014;352(1):15-20. doi:10.1016/j.canlet.2014.02.009

This page has been intentionally left blank

Appendix

Statement of Authorship

Title of Paper	A novel role for *HMGN1* in Down Syndrome Acute Lymphoblastic Leukaemia
Publication Status	☐ Published ☒ Accepted for Publication ☐ Submitted for Publication ☐ Unpublished and Unsubmitted work written in manuscript style
Publication Details	**Page EC**, Heatley S L, Yeung DT, Thomas PQ, & White DL, 2019. A novel role for *HMGN1* in Down Syndrome Acute Lymphoblastic Leukaemia. *Blood*, 134, 1462 – 1462. Doi: 10.1182/blood-2019-126244.

Principal Author

Name of Principal Author (Candidate)	Elyse Page		
Contribution to the Paper	Conceived, designed and performed experiments, analysed results and wrote abstract		
Overall percentage (%)	95%		
Certification:	This paper reports on original research I conducted during the period of my Higher Degree by Research candidature and is not subject to any obligations or contractual agreements with a third party that would constrain its inclusion in this thesis. I am the primary author of this paper.		
Signature		Date	3/3/21

Co-Author Contributions

By signing the Statement of Authorship, each author certifies that:

i. the candidate's stated contribution to the publication is accurate (as detailed above);

ii. permission is granted for the candidate in include the publication in the thesis; and

iii. the sum of all co-author contributions is equal to 100% less the candidate's stated contribution.

Name of Co-Author	Susan Heatley		
Contribution to the Paper	Supervised, and edited the manuscript		
Signature		Date	23 2 21

Name of Co-Author	David Yeung		
Contribution to the Paper	Edited the manuscript		
Signature		Date	24 FEB 2021

Name of Co-Author	Paul Thomas		
Contribution to the Paper	Supervised, and edited the manuscript		
Signature		Date	24/2/2021

Name of Co-Author	Deborah White		
Contribution to the Paper	Supervised, and edited the manuscript		
Signature		Date	25/2/2021

618.ACUTE LYMPHOBLASTIC LEUKEMIA: BIOLOGY, CYTOGENETICS, AND MOLECULAR MARKERS IN DIAGNOSIS AND PROGNOSIS | NOVEMBER 13, 2019

A Novel Role for *HMGN1* in Down Syndrome Acute Lymphoblastic Leukemia

Elyse C Page, BSc , Susan L Heatley, PhD MD ,
David T Yeung, PhDBSc,FRACP,FRCPA,MBBS , Paul Q Thomas, PhD ,
Deborah L. White, PhD FFSc (RCPA)

Blood (2019) 134 (Supplement_1): 1462.

https://doi.org/10.1182/blood-2019-126244

Volume 134, Issue Supplement_1
November 13 2019

Background

Down Syndrome (DS) Acute Lymphoblastic Leukemia (ALL) patients have extremely poor outcomes with mortality rates four times greater than non-DS ALL patients within their first two years of diagnosis. They are more suspectible to treatment related toxicities and experience higher relapse rates compared to other ALL patients. Approximately 60% of DS-ALL patients harbor rearrangement of cytokine receptor like factor 2 (*CRLF2r*), specifically *P2RY8-CRLF2*, and/or the *CRLF2* F232C activating mutation. These lesions are considered poor risk and currently no targeted therapy exist. How increased chromosome 21 gene dosage affect disease phenotype is not yet fully elucidated. However, the high mobility group nucleosome-binding domain-containing protein 1 (*HMGN1*) on chromosome 21, which competes with histone H1 to bind the nucleosome and results in gene activation may be a candidate for targeted therapy in DS-ALL.

Methods

We aimed to determine the role of *HMGN1* in *CRLF2r* DS-ALL. To model *CRLF2r* DS-ALL, the trisomy 21 cell line, SET-2, was transduced with a retroviral vector encoding the *CRLF2* F232C activating mutation. Gene knockdown of *HMGN1* using CRISPR/Cas9 was performed in the SET-2 *CRLF2r* line and the non-trisomy-21, non-*CRLF2* expressing Jurkat line. Individual knockdowns of another two genes on chromosome 21, *DYRK1A* and *ERG* were also performed. Knockdown of *JAK2* was used as a control as it is critical for CRLF2 signaling. CellTiter-Glo was used to investigate proliferation

of knockdown lines to test the hypothesis that *HMGN1* is essential for *CRLF2r* DS-ALL cell proliferation.

Lentiviral vectors encoding the *P2RY8-CRLF2* fusion gene, *CRLF2* F232C activating mutation or an overexpression construct of *HMGN1* were transduced into BaF3 cells individually or in combination to test the hypothesis that overexpressing *HMGN1* is associated with activation of *CRLF2*. Quantitative PCR (qRTPCR) for *CRLF2* and flow cytometry for the CRLF2/IL7Rα receptor (TSLPR) were used to determine the effect of increased *HMGN1* on *CRLF2* expression. AnnexinV/7-AAD cell death assays were performed to determine if the effects of HMGN1 could be reduced by the demethylase inhibitor GSK-J4.

Results

Knockdown of *HMGN1* resulted in an 80-90% decrease in HMGN1 protein expression in SET-2 *CRLF2* and Jurkat lines compared to the Cas9 controls. While knockdowns of *DYRK1A* and *ERG* did not impair the proliferation of SET-2 *CRLF2* cells, *HMGN1* and *JAK2* knockdowns led to a complete proliferation arrest over a period of 120hrs ($p=<0.001$, $n=3$), demonstrating their effect on cell division. However, no change in proliferation was observed in the Jurkat knockdown lines.

Overexpression of either *HMGN1* or *P2RY8-CRLF2* alone in BaF3 cells did not result in cytokine independent transformation. However, cytokine independence was triggered in BaF3 cells when *HMGN1* and *P2RY8-CRLF2* were co-expressed ($p=<0.001$, $n=3$); demonstrating a role for *HMGN1* in leukemic transformation. Importantly, the overexpression of *HMGN1* in the BaF3 *P2RY8-CRLF2* line increased the mRNA expression of *CRLF2* by 5.8-fold compared to the BaF3 *P2RY8-CRLF2* line without *HMGN1* ($p=0.034$, $n=3$) and increased the mean fluorescence intensity of TSLPR by flow cytometry from 42 to 308 ($p=0.008$, $n=3$) (figure 1.a-c) indicating a novel role for *HMGN1* in *P2RY8-CRLF2* activation.

While there are no pharmacological inhibitors for HMGN1, Lane *et al.* (2014) have shown that the restoration of H3K27 methylation using the demethylase inhibitor GSK-J4 was able to prevent DS-ALL cells from repassaging. Therefore, we have employed the inhibitor GSK-J4 to determine if it can reduce cell survival in *HMGN1* overexpressed BaF3 cells. Specific inhibition of BaF3 *P2RY8-CRLF2 HMGN1* cells was evident by decreased cell viability at a concentration of 3.8μM compared to BaF3 *P2RY8-CRLF2* or BaF3 *HMGN1* lines ($p=<0.001$, $n=3$) (figure 4.d). Thus, demonstrating a role for HMGN1 in the modification of the *P2RY8-CRLF2* methylome and suggesting HMGN1 as a potential therapeutic target.

Conclusion

These data support the hypotheses that *HMGN1* has a significant role in DS-ALL cell proliferation and that overexpression of *HMGN1* results in activation of *P2RY8-CRLF2*. This is the first report of a novel role for *HMGN1* in *P2RY8-CRLF2* activation and leukemic transformation in *CRLF2r* DS-ALL. Additionally, we show that HMGN1 is a potential candidate for the

development of a pharmacological inhibitor for *CRLF2r* DS-ALL.

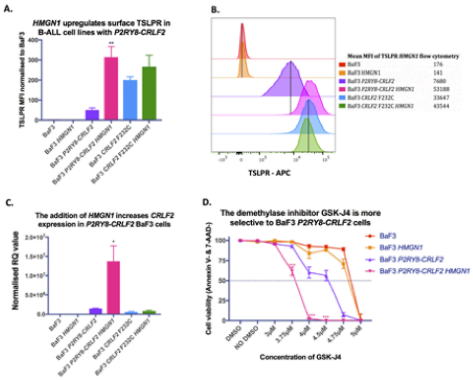

***Figure 1:** HMGN1 upregulates CRFL2 and can be targeted by the small molecule inhibitor, GSK-J4. **A&B)** HMGN1 overexpression in BaF3 P2RY8-CRLF2 cells leads to an increase in surface expression of TSLPR demonstrated by flow cytometry. **C)** An increase of CRLF2 expression is observed when HMGN1 is overexpressed in CRLF2r BaF3 cell lines. RQ values determined using housekeeper actin expression and compared to the parental BaF3 control cell line. **D)** The demethylase inhibitor GSK-J4 decreases the viability of the BaF3 P2RY8-CRLF2 cell line overexpressing HMGN1. All graphs represent n=3 with SEM error bars. Students T test was used to determine significance (*p<0.05, **p<0.01, ***p<0.001).*

VIEW LARGE DOWNLOAD SLIDE

Disclosures

Yeung:*Novartis:* Honoraria, Research Funding; *BMS:* Honoraria, Research Funding; *Pfizer:* Honoraria; *Amgen:* Honoraria. **White:***BMS:* Honoraria, Research Funding; *AMGEN:* Honoraria, Speakers Bureau.

Topics: acute lymphocytic leukemia, down syndrome, hmgn1 protein, cytokine, flow cytometry, molecular targeted therapy, histones, mobility, polymerase chain reaction, receptors, cytokine

Author notes

* Asterisk with author names denotes non-ASH members.

Statement of Authorship

Title of Paper	Inducible Knockout of *HMGN1* in an *In Vivo* xenograft Model Reduces Down Syndrome Leukemic Burden and Increases Survival Outcomes
Publication Status	☐ Published ☒ Accepted for Publication ☐ Submitted for Publication ☐ Unpublished and Unsubmitted work written in manuscript style
Publication Details	**Page EC**, Heatley SL, Thomas PQ, White DL, 2020. Inducible Knockout of *HMGN1* in an *In Vivo* xenograft Model Reduces Down Syndrome Leukemic Burden and Increases Survival Outcomes. *Blood*, 136. Doi: 10.1182/blood-2020-138620

Principal Author

Name of Principal Author (Candidate)	Elyse Page		
Contribution to the Paper	Conceived, designed and performed experiments, analysed results and wrote abstract		
Overall percentage (%)	95%		
Certification:	This paper reports on original research I conducted during the period of my Higher Degree by Research candidature and is not subject to any obligations or contractual agreements with a third party that would constrain its inclusion in this thesis. I am the primary author of this paper.		
Signature		Date	3/3/21

Co-Author Contributions

By signing the Statement of Authorship, each author certifies that:

i. the candidate's stated contribution to the publication is accurate (as detailed above);

ii. permission is granted for the candidate in include the publication in the thesis; and

iii. the sum of all co-author contributions is equal to 100% less the candidate's stated contribution.

Name of Co-Author	Susan Heatley		
Contribution to the Paper	Supervised, and edited the manuscript		
Signature		Date	23.2.21

Name of Co-Author	Paul Thomas		
Contribution to the Paper	Supervised, and edited the manuscript		
Signature		Date	24/2/2021

Name of Co-Author	Deborah White		
Contribution to the Paper	Supervised, and edited the manuscript		
Signature		Date	25/2/2021

603.ONCOGENES AND TUMOR SUPPRESSORS | NOVEMBER 5, 2020

Inducible Knockout of *HMGN1* in an *In Vivo* xenograft Model Reduces Down Syndrome Leukemic Burden and Increases Survival Outcomes

Elyse C Page, BSc , Susan L Heatley, PhD MD , Paul Q Thomas, PhD , Deborah L White, PhDFFSc(RCPA)

Blood (2020) 136 (Supplement 1): 25.

https://doi.org/10.1182/blood-2020-138620

Volume 136, Issue Supplement 1
November 5 2020

Introduction

Down Syndrome (DS) patients are at high risk of developing hematological malignancies and ~10% are born with a pre-leukemic disorder characterised by the overproduction of immature megakaryoblasts. Children with DS have a 20-fold increased risk of developing acute lymphoblastic leukemia (ALL) of which 60% are associated with high expression of cytokine receptor like factor 2 (*CRLF2*) and of these, ~9% acquire the aggressive *CRLF2* p.F232C mutation. DS-ALL children also experience high treatment toxicity and high relapse rates compared to non-DS leukemia patients. Genes on chromosome 21 including the high mobility group nucleosome-binding domain-containing protein 1 (*HMGN1*) are likely to play a role in DS leukemogenesis and may be targets for a personalized treatment approach. We aimed to determine if *HMGN1* is necessary for leukemic cell proliferation using an inducible CRISPR/Cas9 guide (g)RNA murine xenograft model.

Methods

A DS leukemic cell line model was created using the human trisomy 21 megakaryoblastic SET-2 cell line harboring *JAK2* p.V617F; the only trisomy 21 leukemic cell line currently available. SET-2 cells were transduced with *CRLF2* p.F232C to model an aggressive DS-ALL mutation. NOD.Cg-Prkdcscid,Il2rgtm1Wjl/Szj (NSG) mice were each injected with $3x10^5$ SET-2 *CRLF2* p.F232C CRISPR/Cas9 cells expressing luciferase in 3 groups; Cas9 only control, *HMGN1* gRNA, or *JAK2* positive control gRNA.

Doxycycline was administered post leukemic engraftment to induce the

gRNAs and create a knockout (KO) and leukemic burden was monitored by bioluminescent imaging (BLI) twice weekly for the remainder of the experiment. Once Cas9 control mice became moribund, they were culled along with 50% of the *JAK2* or *HMGN1* KO mice and complete blood counts were performed. Bone marrow (BM), spleen and liver sections were stained with hematoxylin and eosin (H&E) and survival analysis was carried out for remaining *JAK2* or *HMGN1* KO mice. RQ-PCR was used to detect *HMGN1* expression levels in KO mice organs at endpoint and DNA was extracted from cells harvested from each organ to undertake a gene editing analysis.

Results

Leukemic engraftment in mouse BM was observed 10 days post transplant with a radiance signal of ~1 x 10^4p/s/cm^2/sr, therefore gRNAs were induced on day 11. On day 20, a significant reduction in tumor burden was detected in *JAK2* and *HMGN1* KO mice compared to Cas9 control mice (Fig. 1, Cas9: $8.4x10^5$±$1.7x10^5$; *JAK2* KO: $2.7x10^4$±$8.9x10^3$; *HMGN1* KO: $1.5x10^5$±$1.7x10^4$ p/s/cm2/sr, prone: p<0.001, supine: p=0.005).

Blood counts at day 35 indicated similar white cell counts across Cas9, *JAK2* and *HMGN1* KO mice, however, the Cas9 mice demonstrated thrombocytopenia and anemia (platelet count: 705±43 K/µL, HCT: 22.5±2%) which was rescued in *JAK2* and *HMGN1* KO mice (*JAK2* KO platelet count: 3046±775 K/µL, p<0.001; HCT: 47±6.8%, p=0.002; *HMGN1* KO platelet count: 1503±83 K/µL, p<0.001; HCT: 38±3.4%, p=0.004). *JAK2* and *HMGN1* KO mice had reduced spleen weight (*JAK2* KO: 46±2 mg, p=0.019; *HMGN1* KO: 51±6 mg, p=0.046; Cas9: 81±7 mg) and liver weight compared to Cas9 control mice.

Megakaryoblast infiltration identified with H&E staining was evident in the BM, spleen and liver of Cas9 control mice, whereas megakaryoblasts were not observed in *JAK2* or *HMGN1* KO mice organs. Similarly, RQ-PCR demonstrated a 24% decrease in *HMGN1* expression in the BM, 99% in the spleen and 92% in the liver; and a 38% decrease in *JAK2* expression in the BM, 99% in the spleen and 70% in the liver of *HMGN1* and *JAK2* KO mice respectively compared to Cas9 control mice.

Significantly, survival analysis of the remaining *JAK2* and *HMGN1* KO mice indicated a substantial survival advantage from 35 days (Cas9) to 62 and 56 days respectively for *JAK2* and *HMGN1* KO mice (p=0.0009).

Conclusion

Our CRISPR/Cas9 DS leukemic xenograft *HMGN1* KO model demonstrates the important role of *HMGN1* in *CRLF2* p.F232C DS leukemia. Significantly, *HMGN1*KO decreased the leukemic burden of mice to the same extent as the *JAK2* (SET-2 driver gene) KO. The *HMGN1* KO mitigated ALL phenotypes including hepatosplenomegaly, anemia and thrombocytopenia, preventing leukemic progression and resulting in a significant survival advantage over Cas9 control mice. As *HMGN1* has a distinct role in proliferation and survival of DS leukemic cells, it is a potential candidate for targeting with a pharmacological inhibitor as a personalized treatment for DS leukemia

patients.

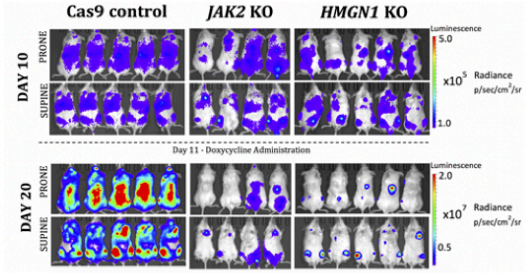

Figure 1: Bioluminescent Imaging of NSG mice engrafted with SET-2 *CRLF2* p.F232C cells with Cas9 vector only, or with a gRNA targeting *JAK2* or *HMGN1*. Doxycycline was administered on day 11 to induce KO. Images taken using a Perkin Elmer IVIS Imager and analysed using Living Image® Software.

VIEW LARGE DOWNLOAD SLIDE

Disclosures

White: *Bristol-Myers Squibb:* Honoraria, Research Funding; *Amgen:* Honoraria.

Author notes

* Asterisk with author names denotes non-ASH members.